THE RAD24 CHECKPOINT PROTEIN OF *SACCHAROMYCES CEREVISIAE*: A COMPLEX PROBLEM

A thesis submitted to the University of London
for the degree of Doctor of Philosophy
by

CATHERINE MARY GREEN

UNIVERSITY COLEGE LONDON
(Imperial Cancer Research Fund)

September 2000

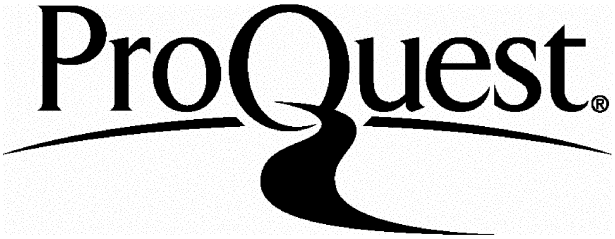

ABSTRACT

Rad24 functions in the DNA damage-dependent checkpoint pathway of *Saccharomyces cerevisiae.* Polyclonal antibodies were raised against Rad24 and other components of this pathway in order to investigate their biochemical functions. Studies demonstrated that Rad24, Mec3 or Rad17 did not interact with each other and did not appear to be modified after DNA damage treatment or during the cell cycle. Analysis of Rad24 in whole cell extracts demonstrated that its mass was considerably greater than its predicted molecular weight, suggesting that Rad24 is a component of a protein complex. A protocol was developed to purify the Rad24 complex to homogeneity. In addition to Rad24, the complex included polypeptides of 40kDa and 35kDa. The 40kDa species was found to contain Rfc2 and Rfc3 by mass spectrometry. Rfc2 and Rfc3 are subunits of Replication Factor C (RFC), a five subunit protein which is required for the loading of polymerases onto DNA during replication and repair. We hypothesised that other RFC subunits, all of which share sequence homologies with Rad24, might also be components of the Rad24 complex. Reciprocal co-immunoprecipitation studies were performed using extracts prepared from strains constructed containing epitope tagged RFC genes. These experiments showed that the small RFC proteins, Rfc2, Rfc3, Rfc4 and Rfc5 interact with Rad24, whereas the Rfc1 subunit does not. We suggest that this RFC-like Rad24 complex may function as a structure-specific sensor in the DNA damage checkpoint pathway. In order to address this hypothesis, conditional mutants of small Rfc subunits were tested for intact DNA damage responses outside of S phase. The biochemical activities of the Rad24 complex were investigated using a variety of techniques including gel mobility shift and ATP hydrolysis assays.

ACKNOWLEDGEMENTS

My thanks go to Debbie Morrison, Jorge Vialard, Sherilyn Goldstone, Maria Angeles de la Torre-Ruiz, David Lee, Jean Soulier, Jose Ramon Murguia, Chris Gilbert and Muriel Grenon who have made up the CDC lab during my time there. You all taught me much, but more than that, you all made coming to work a pleasure, I was privileged to work with all of you. To Noel for being all demanding, all encouraging, all persuasive, all supportive, and all the time a good friend as well as a good boss. To others at Clare Hall, whom I pestered for advice, John Diffley, Jesper Svejstrup, Tim Hunt, Steve West, Rick Wood and Alain Verreault, their depth of experience has taught me huge amounts – and inspired me more. To everyone else at Clare Hall whom I have worked with and laughed with: Betty, Brenda, Frank, Sue and all my friends both students and post-docs, the past four years will always be remembered as happy ones. And finally to Matt, who has put up with the downs, celebrated the ups in style, and never failed to believe in me. Thanks to you all.

TABLE OF CONTENTS

LIST OF FIGURES

LIST OF TABLES

ABBREVIATIONS AND NOMENCLATURE

AP site	Apurinic / Apyrimidinic site
A-T	*Ataxia telangiectasia*
ATM	Gene mutated in A-T
ATR	Gene related to that mutated in A-T
BER	Base excision repair
BRCA1	Gene mutated in hereditary breast cancer
BRCT	C terminal domain of BRCA1
C. elegans	*Caenorhabditis elegans*
CS	Cockaynes syndrome
DSBR	Double strand break repair
dsDNA	Double-stranded DNA
DNA	Deoxyribonucleic acid
DDR	DNA damage regulon
E. coli	*Escherichia coli*
EMS	Ethyl methane sulphonate
FHA	Fork head associated
γ irradiation	Gamma irradiation, wavelength 10^{-10} – 10^{-13}m
G1 checkpoint	Delay in G1 phase after DNA damage
G2 checkpoint	Inhibition of mitosis after DNA damage
GENE1	WT *S. cerevisiae* gene
gene1	*S. cerevisiae* or *S. pombe* gene with a loss of function mutation
gene1$^+$	WT *S. pombe* gene
Gene1	The protein encoded by *GENE1*
HNPCC	Hereditary nonpolyposis colorectal cancer
HU	Hydroxyurea
Intra-S checkpoint	Slowing of DNA synthesis after DNA damage
IR	Ionising radiation
MNNG	N-methyl-N'-nitro-N-nitrosoguanidine
MMR	Mismatch repair
MMS	Methyl methane sulphonate
NBS	Nijmegen breakage syndrome
NHEJ	Non homologous end joining
PCNA	Proliferating cell nuclear antigen
RFC	Replication factor C
ROS	Reactive oxygen species
S. cerevisiae	*Saccharomyces cerevisiae*
S. pombe	*Schizosaccharomyces pombe*
S/M checkpoint	Inhbition of mitosis if DNA synthesis is incomplete
ssDNA	Single-stranded DNA
TTD	*trichothiodystropy*
UV	Ultra violet
WT	Wild type
XP	*Xeroderma pigmentosum*

CHAPTER 1 - INTRODUCTION

Damage to DNA not only affects the viability of a damaged cell but also the success of its progeny. Cells have therefore evolved complex mechanisms to ensure that such damage is efficiently detected and correctly repaired. This introduction will present an overview of DNA damage, and the response to it, in cells ranging from *Escherichia coli* to human. This will be followed by an in depth analysis of the DNA damage-dependent checkpoint response in *Saccharomyces cerevisiae*, which is the focus of the experimental work presented in this thesis. A comparison of the DNA damage-dependent checkpoint pathways in *S. cerevisiae*, *Schizosaccharomyces pombe* and human cells will also be presented, followed by a discussion of other cell cycle checkpoint controls. Finally, the consequences of checkpoint pathway failure, and possible roles for checkpoint proteins in carcinogenesis will be discussed.

1.1 – THE CAUSES OF DNA DAMAGE

DNA is an intrinsically unstable molecule, subject to spontaneous chemical alterations as well as to attack by reactive species occurring within cells. In this section, the commonly occurring types of damage to DNA will be briefly summarised.

DNA is a complex molecule, at physiological pH and temperature some of the bonds undergo rare but important spontaneous changes (Friedburg *et al.*, 1995). One such event is the deamination event that can occur at adenine, cytosine or guanidine residues. The resulting altered bases do not base pair correctly, leading to a block in replication or the incorporation of an incorrect base. This mechanism is especially important if the deaminated base was cytosine, or the naturally occurring analogue methylcytosine, as deamination of these bases results in uracil or thymine respectively, hence a C >T mutation. The bases can also spontaneously tautomerise (a term used to describe the transition between two isomers, in this case enol and keto forms), in their alternate forms mispairing can occur during DNA replication, leading to point mutations, or mismatches if the tautomer reverts. One other spontaneous change is base loss. The glycosidic bond between sugar and base is labile at physiological conditions and will spontaneously hydrolyse, resulting in apurinic or apyridimic (AP) sites. The loss of coding information at these sites is a problem during DNA synthesis, and AP sites are

also prone to backbone cleavage, resulting in single-strand breaks. DNA synthesis progression through a single-stand break will result in the production of a double-stand break (DSB) in one of the newly synthesised molecules.

As well as these spontaneous chemical changes to the DNA other alterations can occur during DNA synthesis. No DNA polymerase is 100% accurate, and even with the inclusion of a proof-reading step mismatches will occur. Such DNA damage can occur not only during DNA replication, but also during any other process where DNA is synthesised, such as repair or recombination.

DNA is not only subject to spontaneous change but can be altered due to the effects of other agents. Some reactive species originate inside the cell, such as reactive oxygen species (ROS), which are formed during mitochondrial respiration. Hydroxyl radicals can be created as a side product of this process and these are chemically very reactive, causing many types of base changes in DNA as well as inducing strand crosslinks and strand breaks (Friedburg *et al.*, 1995). ROS are also created by external agents, the most notable being ionising radiation (IR) from both natural and man-made sources. DNA damage caused by IR is largely a result of the radiolysis of intracellular water to give hydroxyl radicals, as well as the direct ionisation of the DNA, which often results in strand breakage (Ward, 1998; Shackelford *et al.*, 2000). The lethal effects of IR are thought to be due to the production of DSBs which may form as a result of clustering of damage sites together or from transfer of reactive radical products between strands after cleavage of the initial sugar phosphate backbone. Due to the chemistry of cleavage, the termini of these breaks often lack 3' hydroxyl groups and 5' phosphate groups and hence cannot be simply repaired by ligation. Base losses at these sites may also result. It should be noted that the formation of ROS also results in damage to other cellular macromolecules such as carbohydrates and lipids that may also act as triggers of response pathways.

Base changes and replication blocks can also result from the action of other chemicals on DNA. One major class of DNA damaging compounds arising from natural sources as well as man-made pollutants are termed alkylating agents. These carbon based chemicals cause the addition of bulky adducts to the nucleophilic sites within DNA as

well as inter or intra-strand and protein-DNA crosslinks, often resulting in prevention of replication and transcription (Friedburg *et al.*, 1995).

Another major source of DNA damage that is ever present in the environment is irradiation at ultra violet (UV) wavelengths. UV light causes a variety of physical changes to DNA structure due to the absorption of photons, which leads to excited, reactive states. The most notable lesions produced by far UV light are cyclobutane pyrimidine dimers and 6 – 4 photoproducts. These helix distorting base modifications prevent DNA replication and transcription. Other chemical changes such as the UV dependent hydration of cytosine to uracil can result in important mutagenic changes, and UV irradiation can also cause DNA-protein crosslinks (Friedburg *et al.*, 1995).

In the laboratory several treatments are used to produce DNA damage. Commonly, UV irradiation is performed using a 254nm UV lamp. Alkyaltion damage is created by incubation with methyl methane sulphonate (MMS), ethyl methane sulphonate (EMS), N-methyl-N'-nitro-N-nitrosoguanidine (MNNG) and other such chemicals. IR damage is produced by exposure to a caesium 137 gamma source. Other treatments such as bleomycin (which is a radiomimetic drug) and cisplatin (which causes bulky platinum intra-stand crosslinks) can also be used.

1.2 – THE RESPONSE OF *E. COLI* TO DNA DAMAGE

Initial studies into the response of living organisms to DNA damage using the *E.coli* model system have provided the basis for much of the current understanding of the processes involved. The repair capability of *E. coli* cells is divided into 5 main groups of repair pathways, direct damage reversal, mismatch repair (MMR), base excision repair (BER), nucleotide excision repair (NER) and double strand break repair (DSBR). Repair by direct reversal of damage is catalysed by a host of specialised enzymes. A major group is the DNA-alkyltransferases, which can recognise and remove specific base alkylation damage (Friedburg *et al.*, 1995), another direct reversal is that of pyrimidine dimers catalysed by photolyase in a light-dependent reaction (Yasui and Eker, 1998). The other repair pathways comprise of multiple protein components, which catalyse the steps of damage recognition, lesion processing and repair synthesis.

Errors that occur during DNA synthesis, as a result of misincorporation by polymerases are recognised and repaired by MMR (Rasmussen *et al.*, 1998). A mismatch sensing protein directs a strand specific cleavage and resection, the resulting gap is repaired by polymerases and ligase. BER is utilised for the removal of alkylation-damaged bases (Wilson *et al.*, 1998). As implied by the name, the process involves removal of a damaged or incorrect base to leave an AP site, which is then repaired by a mechanism involving an exonuclease, DNA polymerase and DNA ligase. NER is a conceptually similar process, except that after recognition of a DNA lesion such as an UV photoproduct or bulky adduct, specific endonucleases excise a length of DNA rather than a single base (Grossman *et al.*, 1998). Polymerases and ligase repair the resulting single stranded region. Recombinational repair is a process of double strand break repair (Smith, 1998; Kowalczykowski, 2000). Rapidly growing *E. coli* generally contain more than one copy of the chromosome, which is used as a template to accurately replace the damaged region, by a process of single stranded resection, strand invasion and Holliday junction resolution. In the absence of a chromosome copy, sequence micro homologies in the vicinity of the break can be utilised in an single stranded annealing reaction, which results in repair of the break at the expense of loss of the intervening DNA sequence.

The detection of DNA damage by an *E. coli* cell not only results in DNA repair, adaptive responses are also triggered. These transcriptionally and post-transcriptionally regulated pathways result in the up-regulation of repair capability for the particular type of damage sensed. One such system is termed the SOS response (Koch and Woodgate, 1998; Smith and Walker, 1998) the activating trigger for which appears to be single stranded DNA. The co-ordinated expression of many genes involved in damage repair and damage tolerance is regulated by RecA single stranded DNA binding protein and LexA transcriptional repressor after replication arrest or DNA damage is sensed. A conceptually similar adaptive response to alkylation damage is controlled by the Ada methyl transferase protein (Friedburg *et al.*, 1995).

1.3 – THE RESPONSE OF EUKARYOTES TO DNA DAMAGE

As with prokaryotic cells the optimal end result from detection of DNA damage in an eukaryotic cell is the accurate repair of that damage. The DNA repair capability of

eukaryotic cells can be divided into the same groups as in *E. coli* (Friedburg *et al.*, 1995). Although in eukaryotic cells the individual repair pathways tend to comprise many more polypeptides than the prokaryotic versions, this is often due to an increase in the complexity of control of the processes, with the core enzymatic functions being strikingly similar in all organisms. These pathways are generally highly conserved, for example the NER process is virtually identical in human cells compared to *S. cerevisiae*, some of the mammalian genes will even complement repair deficiencies due to loss of the homologous gene in yeast and *vice versa* (Lambert *et al.*, 1988; Sung *et al.*, 1993). Loss of any of these pathways leads to a cellular DNA damage sensitivity phenotype (Friedburg *et al.*, 1995). In higher eukaryotes such loss can have complex consequences, there are many severe disorders caused by a lack of repair capability including: *xeroderma pigmentosum* (XP), t*richothiodystrophy* (TTD) and Cockaynes syndrome (CS) for NER defects (Thompson, 1998); Nijmegen breakage syndrome and immune system disorders for defects in the non homologous end joining (NHEJ) pathway for DSBR (Khanna *et al.*, 1998) and hereditary nonpolyposis colorectal cancer (HNPCC) for MMR defects (Prolla *et al.*, 1998).

A more recently identified component of the DNA damage response in eukaryotic cells is the DNA damage-dependent checkpoint pathway. Checkpoints have been defined as mechanisms that exist within cells to ensure that later events in the cell cycle are not initiated until earlier events are complete (Hartwell and Weinert, 1989). These universally conserved signal transduction pathways are involved in the preservation of genome integrity (for a recent review see Clarke and Gimenez-Abian, 2000). Activated when the normal cell cycle is perturbed, checkpoints halt cell cycle progression until the problem is resolved and then regulate co-ordinated re-entry into the cell cycle. In order to assure maintenance of genetic information and ploidy, checkpoints act to prevent mitosis if DNA is damaged or replication is incomplete (the DNA damage-dependent checkpoint and the S/M checkpoint), and to prevent chromosome segregation if the spindle machinery is not properly assembled (the spindle checkpoint).

The DNA damage-dependent checkpoint pathway was the first to be identified (Weinert and Hartwell, 1988). This pathway prevents the initiation of S phase, causes the slowing of S phase, and prevents the initiation of mitosis, if DNA damage is detected in the G1,

S or G2 phases respectively. The proteins required for the functioning of this pathway were first identified in *S. cerevisiae*, but have since been shown to be highly conserved. The checkpoint pathway not only regulates progression through the cell cycle, but also results in the activation of transcription of DNA damage responsive genes. It may also have a direct role in the up-regulation of repair processes after DNA damage is detected. This pathway is described in detail in Sections 1.4 – 1.13, (for recent reviews see Clarke and Gimenez-Abian, 2000; Lowndes and Murguia, 2000; O'Connell *et al.*, 2000).

Higher eukaryotes have a further response to DNA damage, the process of apoptosis, which is also triggered as a response to many other stimuli and is part of the developmental programme (Song and Steller, 1999). The apoptotic response is thought to be a protective mechanism, removing cells that may be carrying harmful mutations from the population (Evan and Littlewood, 1998). Although such a protective mechanism is less evolutionarily sound for a unicellular organism, a response which shows some of the characteristics of apoptosis seen in higher eukaryotes can be triggered in yeast (Madeo *et al.*, 1997; Madeo *et al.*, 1999). Hence the machinery used to illicit the response appears to be conserved, though adapted throughout evolution.

1.4 – THE IDENTIFICATION OF GENES REQUIRED FOR THE DNA DAMAGE–DEPENDENT CHECKPOINT IN *S. CEREVISIAE*

The phenomenon of cycling cells undergoing temporary cell cycle arrest in response to DNA damaging agents was noted as early as 1956 for yeast cells (Burns, 1956). In 1975, it was hypothesised that this may result from a negative feedback mechanism controlling cell cycle progression (Tobey, 1975). However, it was not until 1988 that the genetic basis for this delay in *S.cerevisiae* was discovered, with the realisation that the *RAD9* gene was necessary for budding yeast cells to temporarily halt proliferation after treatment with X-ray irradiation (Weinert and Hartwell, 1988). The term checkpoint was coined by the same authors a year later (Hartwell and Weinert, 1989). Once the lack of checkpoint delay in a *rad9-1* strain had been characterised, genetic screens were performed to identify mutations in other genes which resulted in similar phenotypes. The first reported screen utilised a temperature sensitive *cdc13* allele (Weinert *et al.*, 1994), which was subsequently shown to accumulate single stranded DNA in telomeric regions after incubation at 37°C (Garvik *et al.*, 1995). Genes were

identified which, when mutated, resulted in synthetic lethality with *cdc13-1* after a short incubation at this restrictive temperature, and that also failed to arrest in G2 phase after such treatment. This screen was used to test the known *RAD* (radiation sensitive) mutants, hence identifying *RAD24* and *RAD17* as being involved in this pathway. The novel genes identified were named *MEC1* (for mitotic entry checkpoint), *MEC2* (found to be equivalent to *RAD53*) and *MEC3* (Weinert *et al.*, 1994). A more recent screen was performed for mutations that were synthetically lethal with a temperature sensitive mutation of DNA primase (*pri1-2*), which is also likely to produce single stranded DNA at the restrictive temperature. This identified two novel genes, *DDC1* (for DNA damage checkpoint) and *DDC2* (Longhese *et al.*, 1997; Paciotti *et al.*, 2000). Although the DNA damage-dependent checkpoint pathway has been extensively investigated in *S. cerevisiae*, it is unlikely that the full complement of genes involved is truly known. Recently for example, investigation into possible functions for unidentified transcripts lead to the discovery of *HUG1* – a gene which may be involved in the checkpoint pathway (Basrai *et al.*, 1999) as it is up-regulated after DNA damage and has genetic interactions with the checkpoint gene *MEC1*. There is also evidence that there may be *MEC1*-independent pathways for example expression of the human cDNA *CHES1* produced checkpoint function that did not require *MEC1* (Pati *et al.*, 1997). Very recently the phosphatase Ptc2 has been implicated in the checkpoint pathway (Marsolier *et al.*, 2000) via the identification of genetic interactions between *PTC2* and known checkpoint genes, and biochemical approaches have identified a checkpoint role for the chaperone proteins Ssa1 and Ssa2 (Gilbert *et al.*, 2000), see Section 1.10.

1.5 – DNA DAMAGE IS THE ACTIVATING SIGNAL FOR THIS CHECKPOINT PATHWAY

As well as sensitivity to X-irradiation and synthetic lethality with *cdc13*, the checkpoint genes were also shown to have synthetic phenotypes with other mutants that result in the accumulation of damaged DNA. For example strains containing *rad9Δ*, *rad17-1*, *rad24-1*, *mec1-1*, *mec2-1* or *mec3-1* in combination with *cdc9-8* are much less viable than the equivalent single mutants and fail to arrest in G2 at the restrictive temperature (Weinert and Hartwell, 1993). *CDC9* encodes the DNA ligase required for the joining of Okasaki fragments during DNA replication. Cell cycle arrest and survival after DNA

damage induced by incubation with MMS or UV irradiation is also dependent on the checkpoint genes, strongly suggesting that it is DNA damage that initiates the pathway. This hypothesis was confirmed by observations that expression of HO or EcoRI endonucleases also activates this pathway (Lewis *et al.*, 1998; Gardner *et al.*, 1999).

1.6 – RESPONSES TO DNA DAMAGE UNDER CHECKPOINT PATHWAY CONTROL

The initial studies of checkpoint pathway function focussed on the delay of the cell cycle in the G2 phase. In yeast, this delay is of the longest duration and is hence the most apparent in asynchronously cycling cells. However, a delay at the G1/S boundary in response to DNA damage (G1 checkpoint) can be observed if the cells are first arrested in G1 and subjected to DNA damaging treatment before synchronous release into the cell cycle. This delay is dependent upon a functional checkpoint pathway (Siede *et al.*, 1993; Siede *et al.*, 1994), and also upon a functional system of NER (Neecke *et al.*, 1999). A further DNA damage-dependent checkpoint was more recently identified that operates to slow the progression of S phase in response to DNA damage (intra-S checkpoint). This is most easily observed upon release of G1 arrested cells into media containing MMS. Under these conditions WT cells progress very slowly through S-phase when compared to a culture released into media without MMS. However, checkpoint mutant strains progress rapidly through S phase even in the presence of MMS (Paulovich and Hartwell, 1995; Paulovich *et al.*, 1997). The checkpoint pathway also controls the normal timing of replication origin firing (Shirahige *et al.*, 1998). The operation of DNA damage-dependent checkpoint pathways during stages of the cell cycle when DNA synthesis is occurring is complex. Although Rad9, Rad24, Rad17 and Mec3 are required for normal activation of the DNA damage-dependent checkpoint throughout the cell cycle, other proteins are involved in this pathway specifically in S phase. These include polymerase ε(Navas *et al.*, 1995; Navas *et al.*, 1996), RFC (Sugimoto *et al.*, 1996; Noskov *et al.*, 1998), Dpb11 (Araki *et al.*, 1995) and Drc1 (Wang and Elledge, 1999). The intra-S checkpoint pathway also activates a damage tolerance mechanism, by which DNA containing lesions can be replicated, at a cost of mutagenesis. This induced mutagenesis is dependent upon the checkpoint pathway (Paulovich *et al.*, 1998).

Initially it was assumed that the checkpoint pathway induced delay was sufficient to account for the increased survival of WT strains compared to the checkpoint mutant strains. The delay was presumed to allow time for repair processes to be completed. This hypothesis was supported by the fact that an artificially induced delay (using the microtubule inhibitor methyl benzamyl carbamide (MBC)) after X-irradiation of cells in G2 phase suppressed the survival defect of a *rad9*Δ strain (Weinert and Hartwell, 1988). However, numerous experiments have demonstrated that the survival defect of checkpoint mutant strains after UV irradiation is not fully rescued by the imposition of artificial delay in G2 (Aboussekhra *et al.*, 1996; Longhese *et al.*, 1997). Recently, a novel gene, *CHK1*, has been identified, by its homology to a previously identified checkpoint gene in *S. pombe* (Sanchez *et al.*, 1999). A yeast strain which lacks this gene has a pronounced defect in the cell cycle delay after exposure to DNA damaging agents, but is not more sensitive to killing by such treatments (Sanchez *et al.*, 1999). Taken together, this suggests that the role of the checkpoint pathway in ensuring survival in the presence of damage must extend to effects other than cell cycle delays. Two mechanisms by which this may be achieved have been identified. Firstly, the checkpoint pathway has been shown to be required for the transcriptional induction of a number of genes with roles in DNA metabolism, defined as the DNA damage regulon (DDR). The genes of the DDR include components of all the major repair pathways, as well as ribonucleotide reductase subunits and some components of the checkpoint pathway itself (Aboussekhra *et al.*, 1996; Kiser and Weinert, 1996; de la Torre-Ruiz *et al.*, 1998). The latter observation suggests that there may be an element of positive feedback in the operation of the checkpoint pathway reminiscent of the SOS response of *E. coli*. The contribution of this transcriptional regulation to survival after DNA damage has yet to be determined. The second mechanism by which the checkpoint pathway may contribute to viability after DNA damage is by the direct induction of DNA repair processes. The checkpoint genes are required for the efficient repair of DNA double strand breaks (de la Torre-Ruiz and Lowndes, 2000). The binding of Ku protein to DNA ends is likely to be the initial sensing reaction for repair by NHEJ (Haber, 1999). Ku is normally sequestered at telomeres, and its relocation to damage sites is dependent upon an intact DNA damage-dependent checkpoint pathway (Martin *et al.*, 1999; McAinsh *et al.*, 1999; Mills *et al.*, 1999). The NHEJ pathway however, appears to be unique in this regulation. There is currently no evidence, for example, that the checkpoint pathway

controls NER in a similar manner. The overall rate of removal of pyrimidine dimers is no slower in a checkpoint mutant strain compared to a WT strain, although there is a defect in the removal of pyrimidine dimers from non-transcribed genes in a *rad24Δ* or *rad9Δ* strain compared to WT (Terleth *et al.*, 1990).

Recent evidence has also suggested that checkpoint genes are involved in telomeric events. Checkpoint mutants have shorter telomeres than the corresponding WT strains (Ritchie *et al.*, 1999; Longhese *et al.*, 2000), a phenotype which is suppressed by the *sml1* mutation that restores cell viability to *rad53Δ* or *mec1Δ* strains. The repression of genes located near to telomeres is enhanced in *rad53* mutants, but is reported to be reduced in *mec1* mutant strains (Craven and Petes, 2000). The mechanism of action of the checkpoint genes in these telomeric processes are unknown. The checkpoint genes are also required for normal progress through meiosis (Grushcow *et al.*, 1999), although again, their biochemical role in this process has not been determined. Mec3 has also been found to interact with Set1, a protein involved in telomere metabolism (Corda *et al.*, 1999). The true functional relevance of this interaction has not been determined but the fact that it is specific to Mec3, and not also found for other members of the RAD24 epistasis group, suggests that Mec3 must have some role outside of that group.

1.7 – GENETIC APPROACHES TO DETERMINE AN ORDER OF FUNCTION FOR BUDDING YEAST CHECKPOINT GENES

An initial working model for the operation of the DNA damage-dependent checkpoint pathway was developed from genetic studies, and is depicted in Figure 1.7. The model categorised genes as encoding either sensors (*RAD9*, *RAD17*, *RAD24*, *MEC3* and *DDC1*), transducers (*MEC1*, *RAD53*, *CHK1*, and *DUN1*) or effectors (*PDS1*, *CDC5*). This section will present the experimental evidence which led to this model with regard to the sensor and transducer checkpoint genes. The identification of the pathway effectors will be described in Section 1.9. Recent biochemical analysis and the identification of the *DDC2* gene has questioned the accuracy of this model, particularly in regard to the positioning of *MEC1*, but this will be discussed in Section 1.10.

RAD24 is in the same epistasis group as *RAD17* and *MEC3*. Double or triple mutants from the genes in this group have the same sensitivity to DNA damaging agents and the

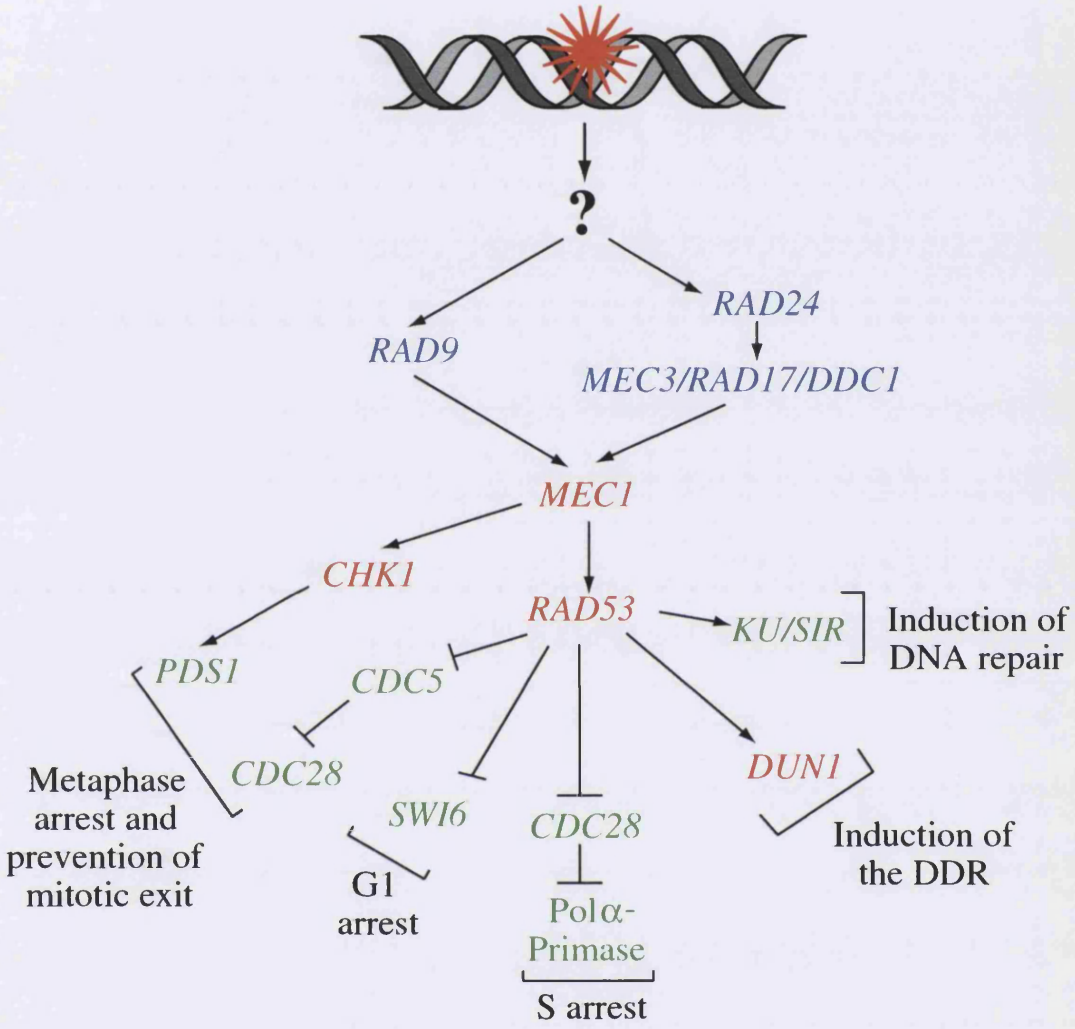

Figure 1.4. An initial working model for the DNA damage-dependent checkpoint pathway of *S. cerevisiae*. A DNA lesion is symbolised at the top of the flow chart. It is probable that this requires processing, either by a replication fork, or a repair pathway before the checkpoint pathway is activated. The activation of Rad9 and the Rad24 group (genes historically termed "sensors" are in blue) act to transmit the signal, to the "transducers" (in red) Mec1 and Rad53. Mec1-dependent phosphorylation and activation of Chk1 results in the stabilisation of Pds1 and hence prevention of anaphase. Mec1-dependent activation of Rad53, perhaps by direct phosphorylation leads to arrest in G1, G2 and intra-S, transcriptional induction and enhanced repair via the "effectors" shown (in green).

same checkpoint defects as the single mutants (Lydall and Weinert, 1995; de la Torre-Ruiz *et al.*, 1998). More recently the *DDC1* gene had been identified and also assigned to this group (Longhese *et al.*, 1997). *RAD24* is positioned genetically upstream in the pathway from *RAD17*, *MEC3* and *DDC1*. Overexpression of *RAD24* cannot rescue the defects in survival and checkpoint of the *rad17*Δ, *mec3*Δ or *ddc1*Δ strains, whereas overexpression of *RAD17*, *MEC3* or *DDC1* can partially suppress these defects in a *rad24*Δ strain (de la Torre-Ruiz *et al.*, 1998).

RAD9 is in a distinct epistasis group to *RAD24* (Eckardt-Schupp *et al.*, 1987; Lydall and Weinert, 1995; de la Torre-Ruiz *et al.*, 1998). The *rad24*Δ*rad9*Δ double mutant is more sensitive to DNA damaging agents and than either single mutant. Each single mutant has a reduced checkpoint delay after UV irradiation, and this checkpoint is further reduced in the double mutant. Overexpression of *RAD9* will rescue the survival and checkpoint defects of a *rad24*Δ strain, and overexpression of *RAD24* will rescue these defects in a *rad9*Δ strain. Hence, *RAD9* is placed in a parallel branch to *RAD24* in the model. Interestingly overexpression of *RAD24* in a *RAD9* delete strain (or *vice versa*) results in an unusually high activation of some checkpoint responses after DNA damage (de la Torre-Ruiz *et al.*, 1998). This interaction between Rad24 and Rad9 is not fully characterised or explained, but probably represents some negative feedback controls within the checkpoint pathway. Based on these genetic analyses *RAD9* and the *RAD24* group of genes were proposed to encode the DNA damage sensors of the checkpoint pathway, a role further supported by their homology to proteins with DNA metabolic functions, see Section 1.8.

The *RAD53* and *MEC1* genes were proposed to be the signal transducers within this pathway. Overexpression of *RAD53* rescued the survival and checkpoint defects of a *rad9*Δ or *rad24*Δ strain, but neither *RAD9* nor *RAD24* overexpression rescued *rad53-11* or *rad53*Δ (de la Torre-Ruiz *et al.*, 1998). Overexpression of any of the genes of the two upstream groups also failed to suppress the defects of a *mec1-1* strain. However, during these studies it was not possible to produce a strain overexpressing *MEC1* and so the reciprocal experiments were not performed. *MEC1* was shown to be upstream of *RAD53* as overexpression of *RAD53* suppressed the survival and checkpoint defects of *mec1-1* (de la Torre-Ruiz *et al.*, 1998). Unlike *RAD9* and the *RAD24* epistasis group

both *RAD53* and *MEC1* are essential genes. Also unique to these two among the checkpoint genes is the fact that they are required not only for the checkpoint responses to DNA damage, but also for the checkpoint that prevents mitosis if DNA replication is incomplete (the S/M checkpoint – see Section 1.13). It seems that the essential nature of these genes is due to their involvement in maintaining replication proficiency if S phase progression is hindered, for example due to lack of dNTPs (Desany *et al.*, 1998; Merrill and Holm, 1999). Hence an increase in cellular dNTPs levels suppresses the essential defects of *mec1* or *rad53* strains. This increase can be achieved by overexpression of subunits of ribonucleotide reductase (Desany *et al.*, 1998) or by deletion of the *SML1* gene, which encodes an inhibitor of ribonucleotide reductase (Zhao *et al.*, 1998), both allow the production of *mec1Δ* or *rad53Δ* strains.

1.8 – CLONING AND SEQUENCE ANALYSIS OF CHECKPOINT GENES REVEALED HOMOLOGIES TO OTHER GENES

The *RAD9* gene was cloned in 1989, it encodes a protein with a predicted molecular mass of 148kDa (Schiestl *et al.*, 1989). The gene was reported to have no sequence homology with other known genes. Since that time the BRCT motif has been characterised as a domain involved in protein-protein interactions, often found in proteins with DNA metabolic functions (Bork *et al.*, 1997; Callebaut and Mornon, 1997). Rad9 has two BRCT domains, located at the carboxy terminal end of the polypeptide chain. These domains are required for the function of the protein, and mediate a salt resistant Rad9-Rad9 interaction after DNA damage (Soulier and Lowndes, 1999). Outside from the BRCT motifs *RAD9* has no homology to other known genes in any organism. It has been proposed that the human *BRCA1* gene, after which the BRCT domain is named, may be a functional *RAD9* homologue, because the position of BRCT domains within these proteins are similar and the BRCT domains are related in sequence. Also, there are similarities in the regulation of phosphorylation of these proteins and they are both involved in DNA damage-dependent checkpoint pathways. However, to date no biochemical functions have been described for either protein that would confirm or refute this proposal.

The *S. cerevisiae RAD24* gene encodes a protein with a predicted molecular mass of 78kDa. More recently, it has become clear that there are homologues of *RAD24* not

only in *S.pombe* (Griffiths *et al.*, 1995), but in many species, including mouse (Bao *et al.*, 1998; Bluyssen *et al.*, 1999; von Deimling *et al.*, 1999), humans (Parker *et al.*, 1998b; Li *et al.*, 1999), *Drosophila melanogaster* (Dean *et al.*, 1998) and *Arabidopsis thaliana* and *Caenorhabditis elegans* (J. R. Murguia, personal communication). In each case the homologue is most closely related to the fission yeast gene and so is named Rad17. Figure 1.8.1 shows an alignment of these Rad24 homologues. The homology is distributed throughout the proteins. Each of these genes also has homology to the subunits of replication factor C (RFC). RFC is a highly conserved five subunit protein complex essential for DNA replication (Mossi and Hubscher, 1998). The biochemical function of RFC is the ATP-dependent loading of the trimeric replication clamp PCNA (proliferating cell nuclear antigen) for processive DNA synthesis (Jonsson and Hubscher, 1997). A model for the interaction between RFC and PCNA at the replication fork is depicted in Figure 5.6. In *S. cerevisiae* the five essential genes that encode RFC are designated *RFC1*, *RFC2*, *RFC3*, *RFC4* and *RFC5*, each are highly homologous to each other. An alignment of Rad24 with the *S. cerevisiae* RFC subunits is shown in Figure 1.8.2, the homology is largely confined to the so called RFC boxes which are indicated on the figure. Each RFC subunit is more homologous to the other RFC subunits than to Rad24. The positions of the RFC boxes are also indicated in Figure 1.8.1, to make it clear that the similarities between the *RAD24* homologues in the different species is not confined to these motifs. It is noticeable that Rfc1 has amino and carboxyl terminal regions that are not related to the other RFC subunits. Rad24 also has an extended carboxyl terminal region, but this is not related to the Rfc1 domain.

Genetic and physical interactions have been identified between components of RFC and Rad24. A genetic interaction was identified between *CDC44* (which encodes Rfc1) and *RAD24* (Lydall and Weinert, 1997), overexpression of *RAD24* in *cdc44-1* cells resulted in lethality. Strains carrying the *rfc5-1* mutation arrest with fragmented chromosomes at the restrictive temperature but not with a terminal G2 morphology, suggesting that the *RFC5* gene is also required for checkpoint function (Sugimoto *et al.*, 1996). The viability defect of this strain was suppressed by the over expression of *RAD53*. To confirm that *RFC5* is involved in the S phase checkpoint it was demonstrated that the checkpoint pathway activation (as measured by Rad53 phosphorylation) was impaired in an *rfc5-1* strain after DNA damage (Sugimoto *et al.*, 1997). Further studies showed

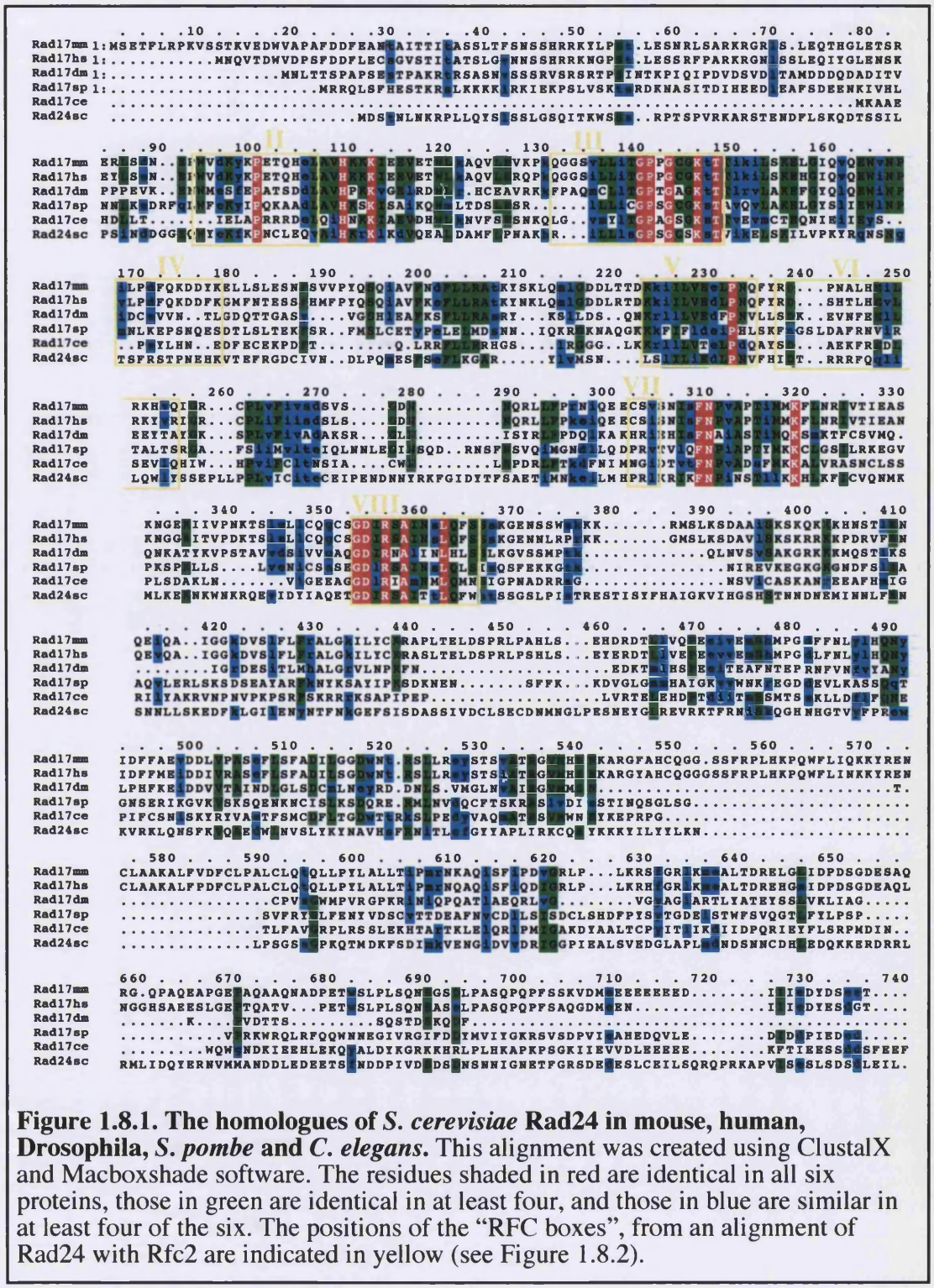

Figure 1.8.1. The homologues of *S. cerevisiae* Rad24 in mouse, human, Drosophila, *S. pombe* and *C. elegans*. This alignment was created using ClustalX and Macboxshade software. The residues shaded in red are identical in all six proteins, those in green are identical in at least four, and those in blue are similar in at least four of the six. The positions of the "RFC boxes", from an alignment of Rad24 with Rfc2 are indicated in yellow (see Figure 1.8.2).

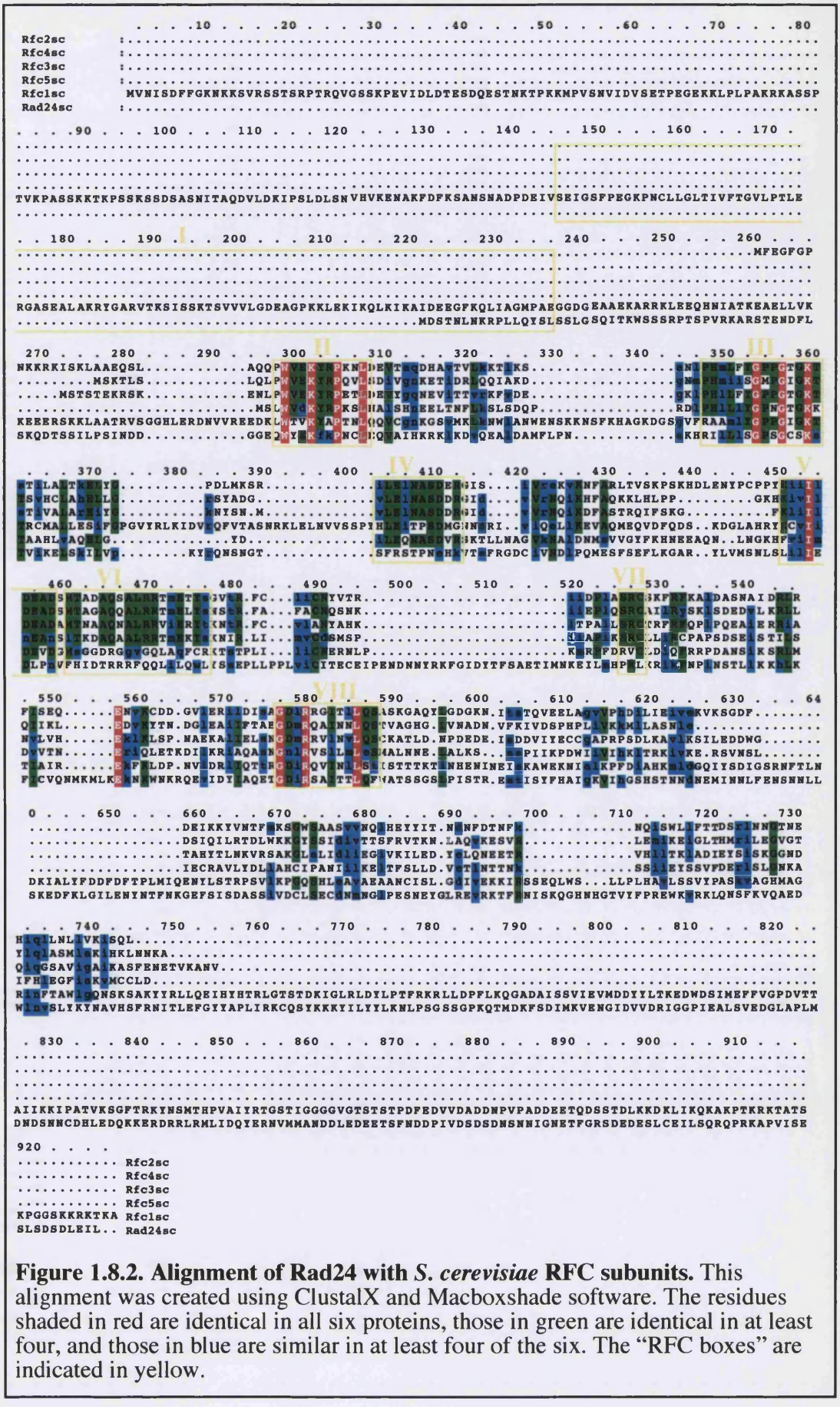

Figure 1.8.2. Alignment of Rad24 with *S. cerevisiae* RFC subunits. This alignment was created using ClustalX and Macboxshade software. The residues shaded in red are identical in all six proteins, those in green are identical in at least four, and those in blue are similar in at least four of the six. The "RFC boxes" are indicated in yellow.

that Rfc5 and Rfc2 could be detected in immunoprecipitations with Rad24 (Shimomura *et al.*, 1998), and it was suggested that Rad24 associated with the RFC complex. Work presented in this thesis demonstrates that this is not the case, and that Rad24 forms a complex with Rfc2, Rfc3, Rfc4 and Rfc5 that is distinct from replication factor C (Green *et al.*, 2000), and see Figure 5.6. A very recent paper identifies a role for *RFC5* in checkpoint responses outside of S phase (Naiki *et al.*, 2000), supporting the work presented here.

Like Rad24, there are homologues of the 45kDa Rad17 protein in many other species including *S. pombe* (Lydall and Weinert, 1995), mouse, humans (Freire *et al.*, 1998; Udell *et al.*, 1998), *C. elegans* and Drosophila (J. R. Murguia, personal communication). Also like Rad24 the homologues are most similar to the *S. pombe* protein and so are named Rad1. One of the original homologies identified to sc*RAD17* (and sp*Rad1*) was of the *Ustilago maydis* Rec1 gene, which encodes a 3'-5' exonuclease and is a checkpoint gene (Thelen *et al.*, 1994; Onel *et al.*, 1996). However, in the primary sequence of the Rad17 protein there is a change from the consensus sequence in the region of the predicted exonuclease domain that would disrupt the putative nucleotide binding salt bridges (J. R. Murguia, personal communication). It therefore seems unlikely that the *S. cerevisiae* Rad17 protein would have this enzymatic function, even if other members of the family do. Recently it has been shown that Rad17 has homology to the other checkpoint proteins Mec3 and Ddc1 as all these proteins are predicted to have PCNA-like folds (Venclovas and Thelen, 2000). It has been suggested that these proteins may associate with each other into a trimeric toroidal complex resembling PCNA (Thelen *et al.*, 1999). Indeed physical interaction between these proteins has been identified (Paciotti *et al.*, 1998; Kondo *et al.*, 1999). A similar physical interaction has been identified between the S. pombe proteins Rad1, Rad9 and Hus1 (Kostrub *et al.*, 1998; Caspari *et al.*, 2000), and the human homologues (St. Onge *et al.*, 1999; Volkmer and Karnitz, 1999; Hang and Lieberman, 2000; Rauen *et al.*, 2000). A comparison between the protein sequences of the *S. cerevisiae* and *S. pombe* checkpoint genes has demonstrated that scDdc1 has homology to spRad9, and scMec3 has homology to spHus1 (Caspari *et al.*, 2000).

In order for any response to be coupled to the presence of DNA damage, that damage must first be detected, and signals sent to engage the protein machinery that effects the response. In the case of the repair pathways of BER, NER, NHEJ and recombinational repair, the damage is sensed by proteins that recognise and bind to particular DNA structures. These recognition proteins then recruit the enzymatic components of the pathway to the damage site. In the case of the DNA damage-dependent checkpoint pathway the response to the sensing of DNA damage is spatially removed from the site of the damage to distant parts of the cell, namely the central cell cycle controlling machinery and promoter regions of target genes. Hence in addition to sensors, this pathway must include a signal transduction component to transfer the information to the effectors of the downstream responses. The signalling component of the checkpoint pathway consists of the kinases Rad53, Chk1 and Mec1. The Dun1 kinase acts downstream of Rad53 to transmit the checkpoint pathway signal to the transcriptional effectors (Zhou and Elledge, 1993; Allen *et al.*, 1994; Sun *et al.*, 1996). There are conflicting reports regarding whether Dun1 is required for checkpoint delay (Pati *et al.*, 1997).

The *RAD53* gene was independently isolated in a number of different studies. The other names that have historically been given to this gene are *SAD1* (Allen *et al.*, 1994), *SPK1* (Stern *et al.*, 1991) and *MEC2* (Weinert *et al.*, 1994). As well as a protein kinase domain, the 97kDa Rad53 protein contains two forkhead-associated (FHA) domains (Hofmann and Bucher, 1995; Hammet *et al.*, 2000), which differ in sequence, although both act as phosphopeptide binding domains (Durocher *et al.*, 1999). The *S. pombe* homologue of Rad53 is Cds1 (Murakami and Okayama, 1995), which is only required for the S/M and intra-S checkpoints, and the human version is hCds1, also called hCHK2 (Blasina *et al.*, 1999). The *S. cerevisiae CHK1* gene was identified by its homology to *S. pombe* Chk1 (Sanchez *et al.*, 1999), the primary sequence includes a classic protein kinase domain, but has no other notable domains. The human homologue is known as hChk1 (Sanchez *et al.*, 1997).

The *MEC1* gene was cloned and sequenced (it was also called *ESR1*), and its gene product of 273kDa was found to have homology to a family of proteins related to phosphatidyl inositol 3 kinases (PI-3 kinases) (Kato and Ogawa, 1994). Other PI-3

kinase-like proteins have been identified, including the human proteins DNA-PK and ATM, and shown to have protein kinase rather than lipid kinase activities (Carr, 1997). These proteins are involved in DNA repair and signal transduction processes. The initial model therefore presumed that Mec1 received the signal from the sensors and its kinase activity then enabled the activation of the Rad53 protein kinase. Mec1 is homologous to another budding yeast protein Tel1 (Greenwell *et al.*, 1995), which is required for normal telomere maintenance (Lustig and Petes, 1986). The *TEL1* gene is not a *bona fide* checkpoint gene, as *tel1Δ* strains are not DNA damage sensitive and have intact cell cycle checkpoint responses (Morrow *et al.*, 1995). However, in the absence of *MEC1*, *TEL1* is able to compensate for some *MEC1* functions (Sanchez *et al.*, 1996). For example the DNA damage-dependent phosphorylation of Rad9 is dependent on *MEC1*, but in a *mec1Δ* strain some phosphorylation of Rad9 is detected. This residual modification is completely abrogated in a *mec1Δtel1Δ* double mutant strain (Vialard *et al.*, 1998). Homologues of Mec1 in other systems have also been identified: ATR and ATM in humans (Keegan *et al.*, 1996), Rad3 in *S. pombe* (Kato and Ogawa, 1994), and Mei-41 in Drosophila (Hari *et al.*, 1995). Table 1.8 lists the checkpoint genes of *S. cerevisiae* and their homologues in *S. pombe* and humans.

S. cerevisiae	*S. pombe*	Human
RAD9	*crb2⁺/rhp9⁺*	BRCA1
RAD24	*rad17⁺*	hRad17
RAD17	*rad1⁺*	hRad1
MEC3	*hus1⁺*	hHus1
DDC1	*rad9⁺*	hRad9
MEC1	*rad3⁺*	ATR
TEL1	*tel1⁺*	ATM
DDC2	*rad26⁺*	?
RAD53	*cds1⁺*	hCds1/Chk2
CHK1	*chk1⁺*	Chk1

Table 1.8. Structural or functional homologues of *S. cerevisiae* checkpoint genes. See Section 1.8 for references.

1.9 – THE EFFECTOR GENES WHICH CONTROL THE RESPONSES TO DNA DAMAGE IN *S. CEREVISIAE*

The Pds1 gene was identified as a target of the checkpoint pathway in 1996 (Yamamoto *et al.*, 1996; Cohen-Fix and Koshland, 1997) and the anaphase promoting complex (APC) was also implicated in checkpoint control (Lim and Surana, 1996). More recently it was shown that the G2 checkpoint inhibits mitosis via two parallel mechanisms (Sanchez *et al.*, 1999). The kinases Rad53 and Chk1 are activated in a checkpoint pathway-dependent manner. Rad53 acts to maintain high Clb2-Cdc28 kinase activity at the arrest point, thereby preventing exit from mitosis and initiation of the next cell cycle. This is likely to be achieved through the inhibition of Cdc5, which is required both for exit from mitosis but also for the initiation of anaphase. Interestingly Cdc5 is phosphorylated during the G2 checkpoint arrest in a checkpoint pathway-dependent manner (Cheng *et al.*, 1998). Chk1 acts to inhibit mitosis through the stabilisation of the anaphase inhibitor Pds1 (Sanchez *et al.*, 1999). Pds1 is phosphorylated after damage, and this is dependent upon the checkpoint pathway but not Rad53 (Cohen-Fix and Koshland, 1997). It has not been confirmed whether these phosphorylations of Pds1 and Cdc5 cause the stabilisation and inhibition of function respectively, which this model proposes. This redundancy of pathways to maintain arrest prior to anaphase in the presence of DNA damage suggests that there was strong evolutionary pressure for such an arrest, and that it is likely to contribute significantly to the survival fitness of budding yeast.

Currently only one mechanism has been suggested by which the checkpoint pathway might initiate a G1 arrest. MMS treatment of cells in G1 causes a down regulation in the transcription of the *CLN1* and *CLN2* cyclins which are required for entry into S phase. This down-regulation is dependent upon Rad53 and Swi6 which is required for the G1 specific transcription of *CLN1* and *CLN2*. Swi6 is phosphorylated by Rad53 *in vivo* and *in vitro* after MMS treatment (Sidorova and Breeden, 1997). Again, it has not been demonstrated that this modification results in an inactivation of Swi6.

A mechanism has also been suggested by which the checkpoint pathway can slow the progression of S phase in response to DNA damage. Rad53 and Mec1 are required to inhibit the initiation of late firing origins of replication when the replication from early

firing origins is stalled due to damage (Shirahige *et al.*, 1998). The primase complex responsible for the initiation of DNA synthesis is normally modified by phosphorylation in a cell cycle dependent manner (Foiani *et al.*, 1995). This polymerase α/primase complex has been shown to be required for the G1 and intra-S checkpoints (Marini *et al.*, 1997). The phosphorylation of this primase complex is inhibited by active Rad53 (Pellicioli *et al.*, 1999), hence this could be the mechanism by which S phase is inhibited by the checkpoint pathway. However, the mechanism by which Rad53 might inhibit this phosphorylation has not been identified.

Another downstream response for which the effectors have been determined is the transcriptional induction of the *RNR3* gene. The Crt1 transcriptional repressor binds DNA and recruits the Ssn6 and Tup1 co-repressors to the promoters of damage inducible genes. After DNA damage Crt1 is phosphorylated in a *DUN1* and checkpoint-dependent manner, so that it no longer binds DNA and the repression is alleviated. This was identified because a *crt1* mutation suppresses the lethality of *rad53*, via the resulting increase in RNR levels (Huang *et al.*, 1998). Interestingly the *CRT1* transcript itself is up regulated after DNA damage, allowing a potential negative feedback system to operate.

The modulation of the efficiency of NHEJ is also achieved by the DNA damage-dependent checkpoint pathway (de la Torre-Ruiz and Lowndes, 2000). This is mediated by the checkpoint-dependent re-localisation of Ku and Sir proteins to the vicinity of the break after induction of DSB damage (Martin *et al.*, 1999; McAinsh *et al.*, 1999; Mills *et al.*, 1999). These proteins are required for repair of the break, and they are normally sequestered at the telomeres. Recently, the DNA repair protein Rad55 has been shown to be phosphorylated in a checkpoint dependent manner after MMS and HU treatments, particularly in the G2 phase of the cell cycle (Bashkirov *et al.*, 2000). If this phosphorylation is an activating modification, this could be a mechanism which preferentially activates recombinational repair activity in the stage of the cell cycle when there are sister chromatids available. It has not yet been demonstrated however, that the recombinational repair capacity of yeast cells is indeed enhanced after DNA damage. Interestingly checkpoint deficient cells are defective in meiotic recombination, a process which also requires Rad55 (Kato and Ogawa, 1994, Grushcow, 1999 #122).

1.10 – TOWARDS A BIOCHEMICAL UNDERSTANDING OF THE BUDDING YEAST DNA DAMAGE-DEPENDENT CHECKPOINT PATHWAY

It is clear that the activation of the checkpoint pathway can occur as a response to the sensing of a wide range of DNA damage lesions. The mechanism by which such a broad range of lesion types can activate a single pathway has been the subject of much speculation. One hypothesis is that processing of lesions could convert a myriad of different lesions to a single DNA structure, which a single sensor protein could recognise. An intriguing study analysing the production of ssDNA at telomeres in the *cdc13-1* strain suggested that checkpoint genes could be involved in such a processing reaction (Lydall and Weinert, 1995). The rate of accumulation of ssDNA at the restrictive temperature was decreased in *rad24Δcdc13-1*, *rad17Δcdc13-1* and *mec3Δcdc13-1* mutants and increased in a *rad9Δcdc13-1* strain compared to the *cdc13-1* rate. This correlated with an increased survival at 37°C of the *rad24Δcdc13-1* strain over WT, and a decreased survival of *rad9Δcdc13-1*. The authors presented a model in which *RAD24*, *RAD17* and *MEC3* control the activity of an exonuclease, and *RAD9* acts antagonistically to these genes. The model was supported by the observation that *RAD17* has homology to genes encoding 3'-5' exonucleases (Lydall and Weinert, 1995), although the processing reaction observed would require a 5'-3' exonuclease. No such enzymatic activity has been demonstrated for Rad17 although recently the human homologue of Rad17, hRad1 has been reported to have 3'-5' exonuclease activity when expressed in *E. coli* (Parker *et al.*, 1998a). However this report did not conclusively rule out the possibility that this activity was due to a contaminating *E. coli* enzyme. A more convincing paper recently reported that recombinant human Rad9 protein, which is the homologue of Ddc1 has a similar exonuclease activity (Bessho and Sancar, 2000), this study determined that the exonuclease activity was abolished by a mutation in the active site of hRad9.

In an alternative hypothesis DNA lesions are initially recognised and processed by the specific DNA repair pathways. During the repair process, the different repair pathways might all produce a common structural intermediate and it is this intermediate which is recognised by the sensor apparatus of the DNA damage-dependent checkpoint pathway. A possible DNA structure that could be common to all repair pathways is a transition between dsDNA and ssDNA. ssDNA has been suggested to be the signal that triggers

checkpoint pathway activation in *cdc13* mutants (Garvik *et al.*, 1995). Interestingly, the DNA structure that is recognised by RFC during replication is just such a ssDNA to dsDNA transition at the primer-template junction. Rad24 interacts with subunits of RFC, presumably to form an RFC-like complex specialised for checkpoint pathway activation. It is thus tempting to speculate that this Rad24 complex could initiate a checkpoint pathway signal arising from the processing of primary lesions by repair enzymes.

This hypothesis has been strengthened further by the observation that a protein complex containing Mec3, Rad17 and Ddc1 operates downstream of the Rad24 protein in the checkpoint pathway (Paciotti *et al.*, 1998; Kondo *et al.*, 1999), and that this complex is predicted to be structurally related to PCNA (Aravind *et al.*, 1999; Thelen *et al.*, 1999; Venclovas and Thelen, 2000). It is postulated that the Rad24 complex could catalyse the loading of this Rad17 complex onto DNA for the transmission of the DNA damage signal by an unknown mechanism. In support of this model it has been possible to demonstrate a physical interaction between the homologues of Rad17 and Rad24 from *S. pombe* (Caspari *et al.*, 2000) and human cells (Rauen *et al.*, 2000).

As further support for this model in which lesions must be processed by repair pathways before they can activate the checkpoint pathway, it has been demonstrated that in the G1 phase of the cell cycle UV induced lesions do not initiate the checkpoint response in the absence of a functional NER pathway (Neecke *et al.*, 1999). Furthermore, in human cells processing of alkylating agent-induced lesions by MMR is required to activated the G2 checkpoint (Hawn *et al.*, 1995; Aquilina *et al.*, 1999) also the MMR sensor proteins hmsh2 and hmsh6 are required for the checkpoint-dependent activation of p53 (see Section 1.13) after MNNG treatment (Duckett *et al.*, 1999). In a variation of this model it is not DNA damage processing *per se*, but the assembly of repair proteins at the damage site that is the initiating step for checkpoint pathway activation. This activation is then mediated by protein-protein interactions between checkpoint and repair complexes (Lowndes and Murguia, 2000). To date no experimental data is available to distinguish between the validity of these related models. This will require analysis of checkpoint pathway activation in yeast strains which assemble non-functional repair complexes at sites of DNA damage. It should be noted that the three

models: processing by checkpoint proteins, processing by repair proteins, and protein-protein interaction mediated activation of the checkpoint pathway are not mutually exclusive. All of these mechanisms could be employed in the initiation of the DNA damage-dependent pathway signal.

The Rad53 kinase is an essential, nuclear protein that can phosphorylate proteins on serine, threonine and tyrosine (Zheng *et al.*, 1993). The kinase activity of Rad53 is activated by phosphorylation, which occurs in response to DNA damage in a *MEC1*-dependent manner (Sanchez *et al.*, 1996; Sun *et al.*, 1996). A study of different point mutations in the *RAD53* gene revealed that high levels of Rad53 kinases activity are required for checkpoint activity but less is required for the essential function of Rad53 (Fay *et al.*, 1997). The phosphorylation of Rad53 after treatment with DNA damaging agents in G1 or G2 phases is also dependent upon a functional *RAD9* gene (as well as the *RAD24* group) (de la Torre-Ruiz *et al.*, 1998). When activated, Rad53 has autophosphorylation activity, but the protein can be phosphorylated *in trans* by Mec1 (Sun *et al.*, 1996; Pellicioli *et al.*, 1999). After DNA damage an interaction can be detected between Rad9 and Rad53, both of which are phosphorylated (Emili, 1998; Sun *et al.*, 1998; Vialard *et al.*, 1998). This interaction is stable as a complex containing Rad53 and Rad9 can be purified to homogeneity from whole cell extracts (Gilbert *et al.*, 2000). Analysis of protein complexes containing Rad9 have allowed us to develop a model for the mechanism by which Rad9 and Mec1 may enable the activation of Rad53 in response to DNA damage.

We have recently purified Rad9 from whole cell extracts as a component of a large molecular mass protein complex (Gilbert *et al.*, 2000). In undamaged cells the protein is associated with Ssa1 and/or Ssa2, two of the Hsp70 family of chaperone proteins. The complex is of a mass consistent with it containing multiple copies of both Rad9 and the chaperones. When purified from damaged cells the complex was also shown to contain the Rad53 protein, and the hydrodynamic properties of the complex were altered, suggesting a conformational change had occurred. The Ssa1 and Ssa2 proteins were found to be required for a normal checkpoint response after DNA damage and for normal phosphorylation of Rad9 and Rad53. This leads us to suggest a model in which chaperone protein-dependent re-modelling of Rad9 occurs after DNA damage and this

is required for the checkpoint function of Rad9. The checkpoint function of Rad9 may be to act as a scaffold to recruit the Rad53 protein. It is possible that the Mec1-dependent phosphorylation of Rad9 produces docking sites for the FHA domains of Rad53. This docking then allows phosphorylation and activation of Rad53, by bringing Rad53 into close proximity with other molecules of Rad53. In this way Rad9 is acting analogously to a solid phase catalyst, increasing the local concentration of Rad53 (Figure 1.10). This interaction of Rad53 with Rad9 could also mediate the direct phosphorylation of Rad53 by Mec1. The chaperone-dependent re-modelling of the Rad9 complex could be required for any stage of this mechanism, from phosphorylation of Rad9, recognition or binding of Rad9 by Rad53, phosphorylation of Rad53 or release of activated Rad53 from the Rad9 complex. Importantly, deletion of the amino terminal FHA domain significantly impairs the kinase activity of Rad53 (Fay *et al.*, 1997), suggesting that this domain is important for the activation of the protein. It is not known how the *RAD24* branch of the pathway might contribute to the activation of Rad53. The Chk1 kinase is also activated by *MEC1* and *RAD9*-dependent phosphorylation after DNA damage, but the mechanism by which this occurs is unknown. Interestingly Chk1 has been reported to interact with Rad9, even though Chk1 does not contain FHA domains (Sanchez *et al.*, 1999). However Chk1 is not required for transcriptional induction of the DDR or for the intra-S checkpoints. It appears that the only role of Chk1 is to prevent anaphase by the stabilisation of the Pds1 anaphase inhibitor (Sanchez *et al.*, 1999; Liu *et al.*, 2000b), (see Section 1.9).

As with the work described above, many other recent studies have questioned the genetic positioning of *MEC1* as a downstream transducer. After Rad9 was identified as a phospho-protein the DNA damage-dependent modifications were found to be dependent on *MEC1*, supporting a model in which *MEC1* function is upstream of a so called sensor protein (Emili, 1998; Vialard *et al.*, 1998). Similar dependence on *MEC1* was demonstrated for the DNA damage-dependent modification of Ddc1, another protein supposedly upstream of *MEC1* (Paciotti *et al.*, 1998). The identification of the Mec1-interacting checkpoint protein Ddc2, which is phosphorylated by Mec1 independently of the other checkpoint proteins (Paciotti *et al.*, 2000) further supports a model placing Mec1 as an upstream component of the checkpoint pathway. This study is in agreement with an earlier report that the *S. pombe* Rad3 protein interacts with and

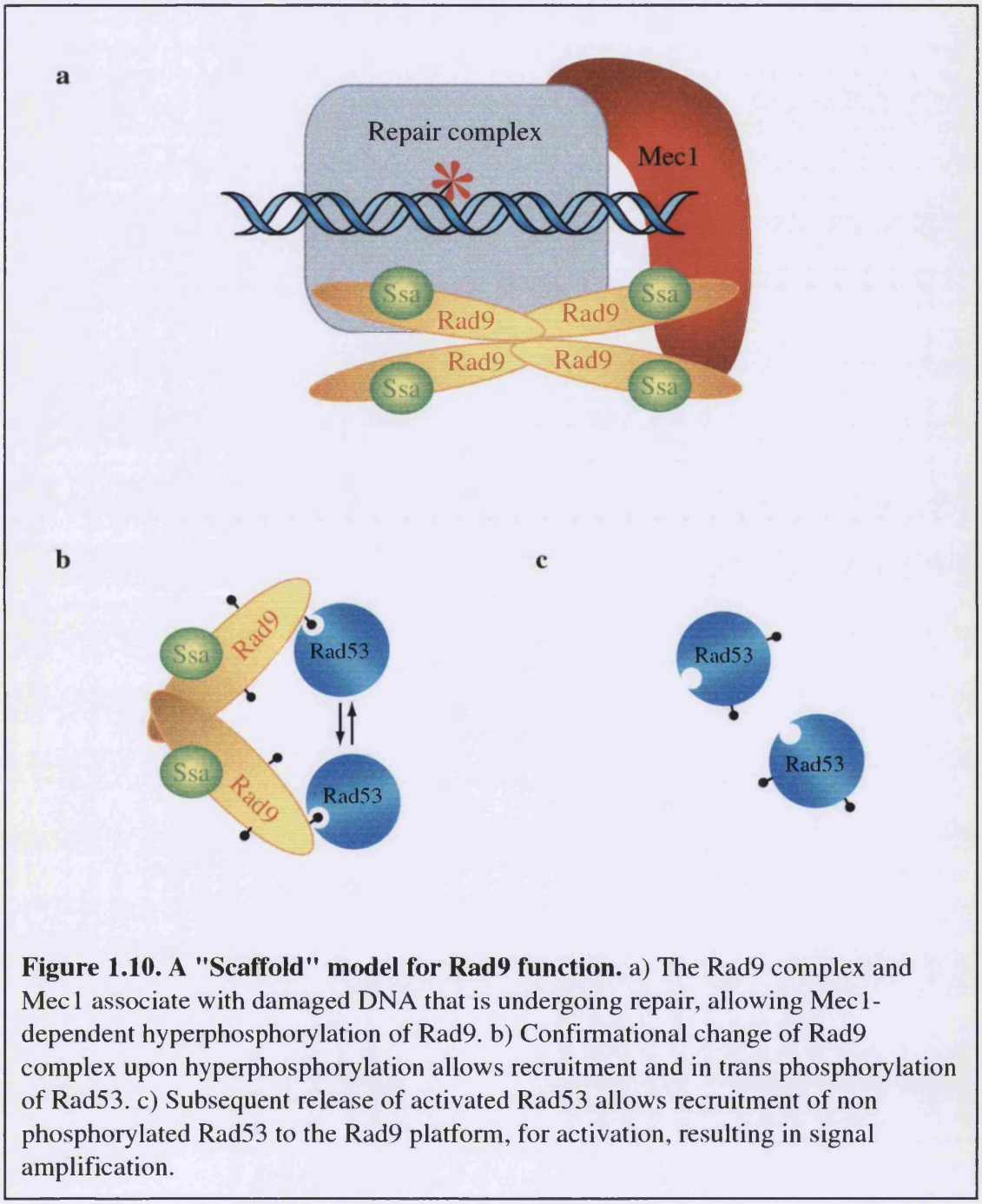

Figure 1.10. A "Scaffold" model for Rad9 function. a) The Rad9 complex and Mec1 associate with damaged DNA that is undergoing repair, allowing Mec1-dependent hyperphosphorylation of Rad9. b) Confirmational change of Rad9 complex upon hyperphosphorylation allows recruitment and in trans phosphorylation of Rad53. c) Subsequent release of activated Rad53 allows recruitment of non phosphorylated Rad53 to the Rad9 platform, for activation, resulting in signal amplification.

phosphorylates Rad26 independently of the other fission yeast checkpoint proteins, placing the fission yeast homologue of Mec1 in an upstream position (Edwards *et al.*, 1999). However, because it has not been demonstrated that any of these phosphorylation events are required for checkpoint pathway activation, it is conceivable that they represent feedback mechanisms, which could be either positive or negative, with Mec1 remaining in downstream, signal transduction role. Another possibility is that the recognition and signal initiation requires the activity of *RAD9* or the *RAD24* group in concert with *MEC1* rather than in a linear pathway. On the other hand, analysis of the human homologues of Mec1 lends further support to the idea that Mec1 may be an upstream component of the checkpoint pathway, indeed even suggests that Mec1 could be a direct sensor of DNA damage, or a DNA structure produced by ongoing repair processes. The ATM protein has DNA binding activity, and localises specifically at DNA ends, suggesting that it may recognise double strand breaks (Smith *et al.*, 1999). ATR also has kinase activity which is stimulated in vitro by DNA (Hall-Jackson *et al.*, 1999).

1.11 – RECOVERY FROM OR ADAPTATION TO THE DNA DAMAGE-DEPENDENT CHECKPOINT

Once a cell has activated the DNA damage-dependent checkpoint pathway there are two possible outcomes. The damage that initiated the checkpoint signal may be repaired, in which case the pathway is shut off, and the cell cycle resumed – a process known as recovery. Alternatively the repair may not be successful, which can either result in permanent arrest if the pathway is not shut off, the activation of damage toleration mechanisms such as mutagenesis, or the cell cycle may be re-entered in the continued presence of irreparable damage, a process known as adaptation. All of these phenomenon have been observed in *S. cerevisiae*.

In *S. pombe* different pathways operate to initiate the DNA damage-dependent checkpoint signal (Rad3-dependent) and to maintain the signal while damage is still present (Rad3-independent) (Martinho *et al.*, 1998). However, in *S. cerevisiae* Mec1 is required for maintenance as well as initiation of the signal (Gardner *et al.*, 1999). This implies that there must be phosphatases or other inactivation mechanisms which prevent the continued signalling from the Rad53 kinase if it is not continually being activated by

Mec1. Indeed the activity of Rad53 is decreased during the recovery process (Pellicioli *et al.*, 1999). Therefore in budding yeast the process of recovery can occur solely via the inactivation of the Mec1 kinase after repair of damage. A simple mechanism by which this could occur would be that Mec1 is only in an activated state while associated with damaged DNA. Such a hypothesis has yet to be tested. Because in fission yeast Rad3 is not required for arrest maintenance, there must be some other means by which the signal is propagated during arrest, which would have to be inactivated for recovery to occur. This recovery in *S. pombe* requires the Cdc2-dependent phosphorylation of the Rad9 homologue, Crb2/Rhp9 (Esashi and Yanagida, 1999), and also possibly requires Slp1 (a Cdc20 homologue) (Matsumoto, 1997). Interestingly, overexpression of *CDC20* in *S. cerevisiae* abrogates the DNA damage-dependent checkpoint, suggesting that a similar process of recovery may be occurring in the two yeasts (Lim and Surana, 1996). However although Rad9, like Crb2, is regulated by Cdk-dependent phosphorylation, the lack of this phosphorylation in *S. cerevisiae* does not lead to a recovery defect (J. Soulier and N. Lowndes, personal communication).

The phenomenon of adaptation to the DNA damage-dependent checkpoint was first described in 1993. It was found that *S. cerevisiae* cells containing an irreparable double strand break underwent *RAD9*-dependent arrest which was maintained for approximately ten hours, but then resumed the cell cycle even though the break was not repaired (Sandell and Zakian, 1993). This adaptation was found to require WT *CDC5*, as a *cdc5* allele was identified (*cdc5-ad*) which failed to adapt, but remained permanently arrested under conditions in which WT cells resumed cycling (Toczyski *et al.*, 1997). In the same study a specificity subunit of casein kinase II was also identified as being required for this adaptation, but the biochemical basis for this is not understood. Cdc5 is a kinase required for the completion of anaphase. The activity of Cdc5 is modulated through the cell cycle, being high at the G2/M transition. During the DNA damage-dependent checkpoint arrest the Cdc5 kinase activity is high but the protein becomes phosphorylated in a checkpoint-dependent manner (Cheng *et al.*, 1998). This suggests that checkpoint pathway modulation of the kinase activity of Cdc5 is not a mechanism for ensuring arrest, rather that Rad53 must inactivate Cdc5 in some other manner (Sanchez *et al.*, 1999), possibly via this phosphorylation. The defect of the

cdc5-ad strain in adaptation could be explained if the encoded Cdc5 protein can be inactivated by Rad53, but is not re-activated when the checkpoint signal is attenuated.

Other proteins recently shown to be involved in the adaptation of *S. cerevisiae* to persistent DNA damage are Ku and the ssDNA binding protein RPA. A yeast strain without Ku70 protein (*hdf1*) was unable to adapt to an irreparable break and was arrested permenently in G2. It was hypothesised that this effect was due to the production of ssDNA in this strain at the break site, as *mre11* or *rad50* deletions, which prevent the accumulation of such ssDNA, suppressed this permanent arrest. It was also suggested that the ssDNA binding protein RPA could be involved in the signalling of this arrest, as mutation of the large subunit of RPA also suppressed the adaptation defect of *hdf1* (Lee *et al.*, 1998). Interestingly in human cells the catalytic subunit of DNAPK, which interacts with Ku has been implicated in adapation to the replication inhibition observed after DSB induction (Guan *et al.*, 2000).

1.12 – THE DNA DAMAGE-DEPENDENT CHECKPOINT PATHWAY IN *S. POMBE*

One of the most striking aspects of the investigations into DNA damage-dependent checkpoint pathways in recent years has been the remarkable conservation of this pathway in different organsisms. The initial identification of a genetic basis for the cell cycle delays observed after X-irradiation or HU treatment of *S. cerevisiae* led to the identification of similar responses in other organisms. It was quickly realised that there was a very similar DNA damage response to that in *S. cerevisiae* in the fission yeast *Schizosaccharomyces pombe*, (for a recent review see Caspari and Carr, 1999). Initial analysis of the known radiation sensitive mutants of *S. pombe* revealed that six of these (*rad1, rad3, rad9, rad17, rad26* and *rad27*) failed to delay the cell cycle in G2 after UV irradiation, hence defining the first checkpoint genes outside of *S. cerevisiae* (al-Khodairy and Carr, 1992; Jimenez *et al.*, 1992; Rowley *et al.*, 1992; al-Khodairy *et al.*, 1994). Unlike in *S. cerevisiae*, in *S. pombe* it was found that many of the initial Rad checkpoint genes were sensitive to hydroxyurea (HU) because they are also defective in the S/M checkpoint. Other screens to identify checkpoint genes utilised this phenotype, resulting in the identification of *hus1*$^{+}$ which is also required for the DNA damage-dependent checkpoint (Enoch *et al.*, 1992). As in budding yeast, new screens continue

to identify novel components of checkpoint pathways in *S. pombe*, recently *rad18*$^+$ was shown to be required for maintenance of checkpoint arrest after DNA damage although its function is unknown (Verkade *et al.*, 1999).

In recent years studies of the checkpoint pathways in the two yeasts have often paralleled each other. Hence in a similar manner to the budding yeast homologues it has been shown that Crb2 is phosphorylated in a Rad3-dependent manner after DNA damage (Saka *et al.*, 1997). Hus1 associates with Rad1 and Rad9, in what is predicted to be a PCNA-like complex (Caspari *et al.*, 2000). Rad17 is associated with RFC subunits and RFC subunits are implicated in checkpoint function (Shimada *et al.*, 1999). The Rad3 protein is proposed to act in an upstream position as it interacts with and phosphorylates Rad26 independently of other checkpoint proteins (Edwards *et al.*, 1999).

The kinase Cds1 (for checking DNA synthesis) was identified as a key component of the checkpoint pathway for sensing incomplete replication but not for DNA damage-dependent arrest (Murakami and Okayama, 1995), except in S phase (Lindsay *et al.*, 1998), a different role to that of its homologue Rad53. The *rad27*$^+$ gene was independently identified as the checkpoint gene *chk1*$^+$ (for checkpoint) (Walworth *et al.*, 1993), this gene is only involved in the checkpoint response to DNA damage, and is not required for the S/M hydroxyurea initiated checkpoint except under sub-optimal growth conditions or if *cds1*$^+$ is deleted (Francesconi *et al.*, 1997; Boddy *et al.*, 1998). More recently a further checkpoint gene required only for the DNA damage checkpoint, *crb2*$^+$ (for Cut5-repeat binding) was identified (Saka *et al.*, 1997), which because it has some homology to *S. cerevisiae* Rad9 has also been named Rhp9 (for Rad9 homologue in *S. pombe*) (Willson *et al.*, 1997). Like Chk1, this gene does have a role in the S/M checkpoint when cells are grown under sub-optimal conditions (Grenon *et al.*, 1999). *cut5*$^+$ (for cell untimely torn) was identified as only being required for the replication checkpoint and responses to gamma-irradiation, and not for correct checkpoint responses to UV damage (Saka *et al.*, 1994; McFarlane *et al.*, 1997), although mutations in this gene (which is identical to *rad4*$^+$), are sensitive to UV light. Cut5 has an essential role in the initiation of DNA synthesis (Saka and Yanagida, 1993), and is homologous to *S. cerevisiae* Dpb11 (Araki *et al.*, 1995).

Like *S. cerevisiae*, *S. pombe* also has an intra-S checkpoint, which slows S-phase in the presence of damage, Cds1 and Rad3 are required for this pathway (Lindsay *et al.*, 1998; Rhind and Russell, 1998b). Interestingly Cds1 can interact with Rad26, it has yet to be investigated whether the newly identified *S. cerevisiae* Ddc2 has a similar interaction with Rad53. Some *S. pombe* RNA transcripts are up-regulated by DNA damage (Degols and Russell, 1997), but the dependence of this on the checkpoint pathway is not well studied. The induction of repair processes by the fission yeast checkpoint pathway has also not been reported.

When a comparison is made between the sensing and signal transduction components of the checkpoint pathways in *S. cerevisiae* and *S. pombe*, although the similarities are very great some differences can be identified. One of the most apparent differences is that in budding yeast the upstream genes *RAD9*, *RAD24*, *RAD17*, *MEC3* and *DDC1* are not involved in the S/M checkpoint that prevents mitosis in the presence of unreplicated DNA that is activated by HU. In fission yeast the homologous genes *rad17*$^+$, *rad1*$^+$, *hus1*$^+$ and *rad9*$^+$ are absolutely required for this arrest, and the *crb2*$^+$ gene is required under some conditions. This may suggest that there are slight differences in the DNA structures that activate the pathways in the different yeasts, or perhaps that HU treatment modulates the processing polymerases in slightly different ways in the two species. A further difference can be identified in the kinases that are used to transduce the signal from the DNA damage. In *S. pombe* Cds1 only has a role in the S/M checkpoint and signalling from DNA damage in S phase and Chk1 is involved in both S/M and DNA damage-dependent checkpoint activation. In *S. cerevisiae*, the Cds1 homologue, Rad53 is absolutely required for the activation of both pathways, while the Chk1 protein has not been demonstrated to be involved in the HU-dependent checkpoint.

The major difference between the *S. cerevisiae* and *S. pombe* checkpoint pathways lies not in the sensing and signal transduction components, but in the mechanisms by which cell cycle arrest is achieved (Figure 1.12) and see (Murakami and Nurse, 2000) for a review. While the budding yeast pathway impinges on Pds1 and the anaphase promoting complex via Cdc5 in order to prevent cell cycle progression, the fission yeast pathway achieves the same result via the maintenance of inhibitory tyrosine 15

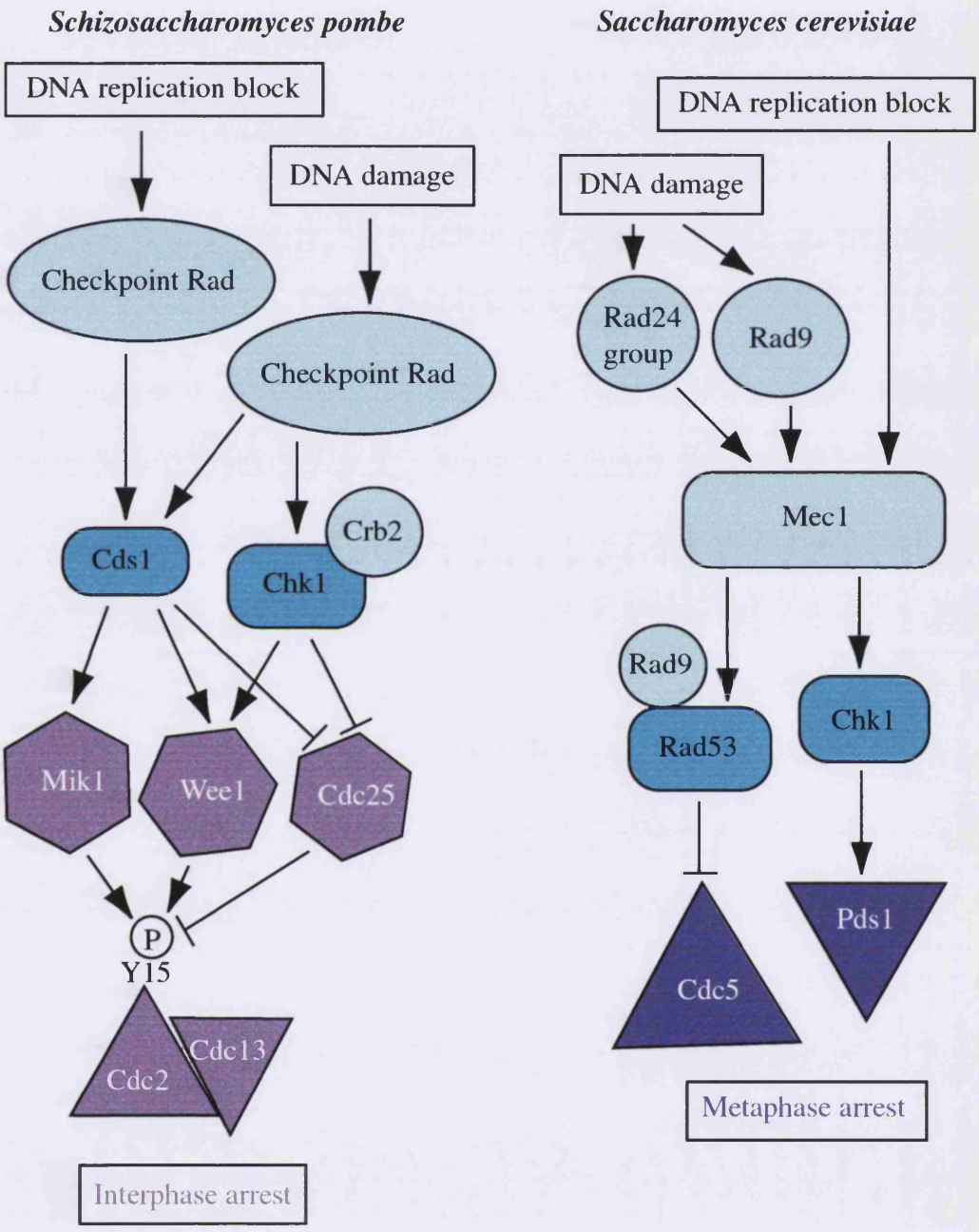

Figure 1.12. Similarities and differences in budding and fission yeast checkpoint pathways. Adapted from Murakami and Nurse (2000). See text for further details.

phosphorylation of Cdc2 (Rhind *et al.*, 1997; Rhind and Russell, 1998c). The mechanism by which this occurs has been well characterised, see below and Weinert, 1997; Rhind and Russell, 1998a; Murakami and Nurse, 2000 and O'Connell *et al.*, 2000 for reviews.

The Cdc2 protein kinase plays a central role in the regulation of cell cycle progression (Nurse, 1990). Its activity is regulated by interactions with cyclins, and by phosphorylation. Loss of the activity of Cdc2 arrests cells either in G1 or before mitosis (Nurse and Bissett, 1981). Inhibitory phosphorylation of Cdc2 occurs at tyrosine-15, which must be removed in order to activate the kinase, before mitosis can occur. This phosphorylation event is controlled by the Wee1 and Mik1 kinases (Lundgren *et al.*, 1991), and the Cdc25 phosphatase (Millar and Russell, 1992). The G2 DNA damage-dependent checkpoint and the S/M checkpoint in *S. pombe* prevent mitosis by acting on Wee1, Mik1 and Cdc25. Neither *wee1Δ* or cells lacking *cdc25*$^{+}$ function are checkpoint defective, but a double mutant strain does not arrest the cell cycle in response to DNA damage (Raleigh and O'Connell, 2000). *In vitro* Chk1 is able to phosphorylate both Wee1 and Cdc25 (Furnari *et al.*, 1997; O'Connell *et al.*, 1997) and Cds1 also phosphorylates Cdc25 (Zeng *et al.*, 1998; Furnari *et al.*, 1999) and Wee1 (Boddy *et al.*, 1998). The phosphorylation of Cdc25 is thought to create binding sites for the 14-3-3 protein Rad24. Such binding of Rad24 to Cdc25 may result in the exclusion of Cdc25 from the nucleus, and hence prevents the dephosphorylation of Cdc2 (Zeng and Piwnica-Worms, 1999). Chk1 itself also associates with Rad24 and another 14-3-3 protein Rad25 in a damage-dependent manner, although the function of this interaction is unknown (Chen *et al.*, 1999). It seems that there is significant redundancy in this mechanism of mitotic inhibition, involving two signalling kinases, Chk1 and Cds1, that can both achieve arrest via Cdc25 or Wee1 mediated inhibition of Cdc2. This suggests that an effective G2 checkpoint pathway must be a very important survival mechanism for fission yeast, to have evolved such a fail safe means to ensure mitosis is not initiated in the presence of DNA damage or unreplicated DNA.

1.13 – THE DNA DAMAGE-DEPENDENT CHECKPOINT PATHWAY IN HUMAN CELLS

In human cells the DNA damage-dependent checkpoint pathway conserves many of the protein components found in the yeast model systems, from sensors to effectors. One major difference in the pathway in human cells is the evolution of a novel effector – the p53 protein, which is responsible for achieving and maintaining arrest at G1 and G2 and also for the regulation of apoptosis. These responses are mediated by a complex and redundant network of signalling pathways, again suggesting that such arrest mechanisms are important for cellular fitness. The most upstream components of the checkpoint pathway are the kinases ATM and ATR, which are structurally and functionally related to the yeast proteins Mec1 and Rad3. ATM was identified as the gene mutated in individuals with A-T (Savitsky *et al.*, 1995), which is characterised by neurodegeneration, cancer, immunodeficiencies, radiation sensitiviy and genetic instability (Meyn, 1999). ATM is activated after treatment of cells with IR or radiomimetic drugs, whereas ATR is activated after UV irradiation. This suggests that a function which is supported by a single protein in the yeast model systems has diverged to two proteins in the human system. The ATM protein has DNA binding activity, and localises specifically at DNA ends, suggesting that it may recognise double strand breaks (Smith *et al.*, 1999). ATR has kinase activity which is stimulated *in vitro* by DNA (Hall-Jackson *et al.*, 1999; Lakin *et al.*, 1999). All this evidence points to these kinases as the sensors of DNA damage in this pathway, that and the fact that there are no known proteins whose functions are required for ATM or ATR activation after DNA damage.

Once activated, the ATM and ATR kinases must signal through a signal transduction pathway to the downstream effectors. The conserved kinases hChk1 and hCds1 (*S. cerevisiae* homologues Chk1 and Rad53) are components of this signal transduction pathway. Other human homologues of yeast proteins involved in the DNA damage-dependent checkpoint pathway have recently been identified, through analysis of EST databases and sequences published by the human genome project. The existence of a signal transduction cascade that operates in a similar manner to that in yeast is expected, but to date the human proteins hRad9, hRad17, hHus1 or hRad1 have not been shown to be required downstream of ATM and ATR for hCds1 or hChk1 activation after DNA

damage. Interestingly however, overexpression of hRAD9 has recently been shown to activate apoptosis (Komatsu *et al.*, 2000).

One of the major effectors of DNA damage-dependent responses in human cells is the tumour supressor p53 (Levine, 1997). It is likely that the most significant contribution of the p53 protein to the prevention of tumorigenesis is through its role in the initiation of apoptotic events when cells have received DNA damage or hypoxic stress. p53 is activated directly in an ATM-dependent manner after ionising radiation, and in an ATR-dependent manner after UV by phosphorylation on serine 15 (Lakin *et al.*, 1999). This post translational modification is thought to lead to the activation of p53-dependent apoptotic responses. This apoptotic role of p53 will not be discussed here, (for reviews see Bates and Vousden, 1996; Levine, 1997; May and May, 1999; Song and Steller, 1999).

However p53 also has a well defined role as an effector of cell cycle checkpoint pathways, both in G1 and G2, and this may also contribute to genome stability. In this way loss of p53 function is very detrimental: loss of checkpoint function may increase genomic instability and the frequency of mutagenic events, and loss of apoptotic responses prevent these unstable cells from being removed from the population, allowing clonal expansion and tumorigenesis. This may account for the observation that p53 function is impaired in 50% of all sporadic tumours (and this proportion is likely to be higher if loss of normal function of p53 regulators such as ARF or MDM2 are included (Matlashewski, 1999)), as it is a nodal point for the integration of many genome stability maintenance pathways (Chan *et al.*, 2000).

The mechanism by which the p53 protein controls arrest in the G1 phase of the cell cycle is well documented. p53 is a sequence specific transcriptional activator and one of its most important transcriptional targets, in terms of the G1 arrest, is the cyclin dependent kinase inhibitor $p21^{CIP1/WAF1}$. In unperturbed cells p53 levels are low, as the protein has a short half life, and so there is little p53-dependent transcriptional activity. In addition p53 may be maintained in an inactive form. DNA damage (in particular, double strand breaks (Nelson and Kastan, 1994)) causes the stabilisation of p53, via the prevention of p53 interaction with Mdm2 which normally targets p53 for destruction

(for reviews see Ashcroft and Vousden, 1999; Lakin and Jackson, 1999). It is likely that this stabilisation is mediated by phosphorylation of p53 on serine 20, in an ATM/ATR and checkpoint pathway-dependent manner (Chehab *et al.*, 1999). The resulting increased levels of p21 prevent the activation of the kinase cyclinD-CDK4 which would normally phosphorylate the Rb protein. Phosphorylation of pRb prevents it from the binding to and inactivating trancriptional activators of the E2F family and hence induces E2F-dependent genes, resulting in passage through the restriction point and S phase initiation (Donjerkovic and Scott, 2000). Therefore the p53-dependent inactivation of CDK prevents this pRB phosphorylation, hence preventing E2F dependent transcriptional induction and arrests cells in G1 (for reviews see Bates and Vousden, 1996; May and May, 1999). The p53-dependent induction of other proteins, for example *GADD45* may also mediate arrest, although the mechanism by which this might be achieved is presently unknown. GADD45 is however known to interact with PCNA (Smith *et al.*, 1994), and so could feasibly affect both repair and replication. p21 has also been demonstrated to interact with PCNA, and to inhibit replication *in vitro* (Li *et al.*, 1994; Waga *et al.*, 1994). Interestingly another of the genes which is transcribed in a p53-dependent manner is *MDM2*, which is a negative regulator of p53 both by direct inhibition of its transcriptional function and also by targeting p53 for degradation (Wu *et al.*, 1993). This implies that the p53 pathway includes an element of negative feedback regulation, which might be important for recovery from the G1 arrest once damage is repaired. p53 may also be involved in the activation of repair pathways (Hwang *et al.*, 1999; Tanaka *et al.*, 2000).

In addition to the p53 mediated cell cycle delay in G1 activated by DNA damage, human cells in culture also delay at the G2 phase of the cell cycle after such treatment (Piette and Munoz, 2000). This G2 delay is in part mediated by two different p53 dependent mechanisms, involving 14-3-3σ and p21 (Chan *et al.*, 2000). The 14-3-3σ protein is transcriptionally regulated by p53 after ionising radiation. 14-3-3σ binds to cyclin B1/cdc2 and sequesters it in the cytoplasm, where it is inactive (Chan *et al.*, 1999). A further p53 dependent contribution to G2 arrest is via p21. p21 inhibits cyclin B/Cdc2 by preventing the CAK (cdk activating kinase)-mediated phosphorylation of Thr 161 which is required for CDK activity (Smits *et al.*, 2000). CyclinB/Cdc2 levels also decrease throughout the G2 arrest via transcriptional repression in a p53, p21 and

pRb dependent manner. This mechanism is particularly important for the maintanence of the G2 checkpoint (Flatt *et al.*, 2000). A second mechanism for G2 arrest involves the kinases hChk1 and hCds1, which are activated after DNA damage in an ATM or ATR-dependent manner (Tominaga *et al.*, 1999; Liu *et al.*, 2000a). When activated these kinases prevent mitosis via the 14-3-3-dependent inhibition of Cdc25C, in a manner analogous to the fission yeast proteins (see Figure 1.12) (Peng *et al.*, 1997; Sanchez *et al.*, 1997; Blasina *et al.*, 1999). Caffeine treatment of cells results in an increased sensitivity to DNA damaging agents, which results from the inhibition of ATM and ATR-dependent activation of hCds1 (Hall-Jackson *et al.*, 1999; Zhou *et al.*, 2000). Both hChk1 and hCds1 can also phosphorylate p53 *in vitro* at Ser20, which *in vivo* results in p53 activation via inhibition of Mdm2 binding (Hirao *et al.*, 2000; Shieh *et al.*, 2000) and this will contribute to the p53 dependent G2 arrest described above. It has also been reported that hCds1 is required for the stabilisation of p53 during G1 arrest (Chehab *et al.*, 2000), and that p53 negatively regulates hCds1, perhaps indicating the presence of a feedback control (Tominaga *et al.*, 1999). For a recent review of this pathway see (Dasika *et al.*, 1999). A schematic for the operation of DNA damage-dependent checkpoint controls in human cells is shown in Figure 1.13.

Two further components of the DNA damage-dependent response are also of interest to studies of the checkpoint field, but for clarity they have been omitted from Figure 1.13. The Nbs protein (also called nibrin or p95) was recently identified as being encoded by the gene mutated in patients with the A-T-like disorder Nijmegen breakage syndrome (Carney *et al.*, 1998; Varon *et al.*, 1998). Nbs is a component of a three subunit protein complex also containing Mre11 and Rad50. The homlogous complex in *S. cerevisiae* is required for the DNA repair pathways that respond to double strand breaks, and also for the initiation of homologous recombination during meiosis (Haber, 1998). The human complex may have similar roles (Petrini, 1999), but is less well characterised. Mutations in hMre11, another component of this complex also results in clinical symptoms similar to NBS and A-T (Stewart *et al.*, 1999). The phenotypes of cells deficient in Nbs or hMre11 function suggest that as well as repair, these proteins are also required for initiation of the DNA damage-dependent checkpoint signal after IR. Recent studies have demonstrated that Nbs is phosphorylated after IR in an ATM-dependent manner and that this phosphorylation is required for the downstream responses to this damaging

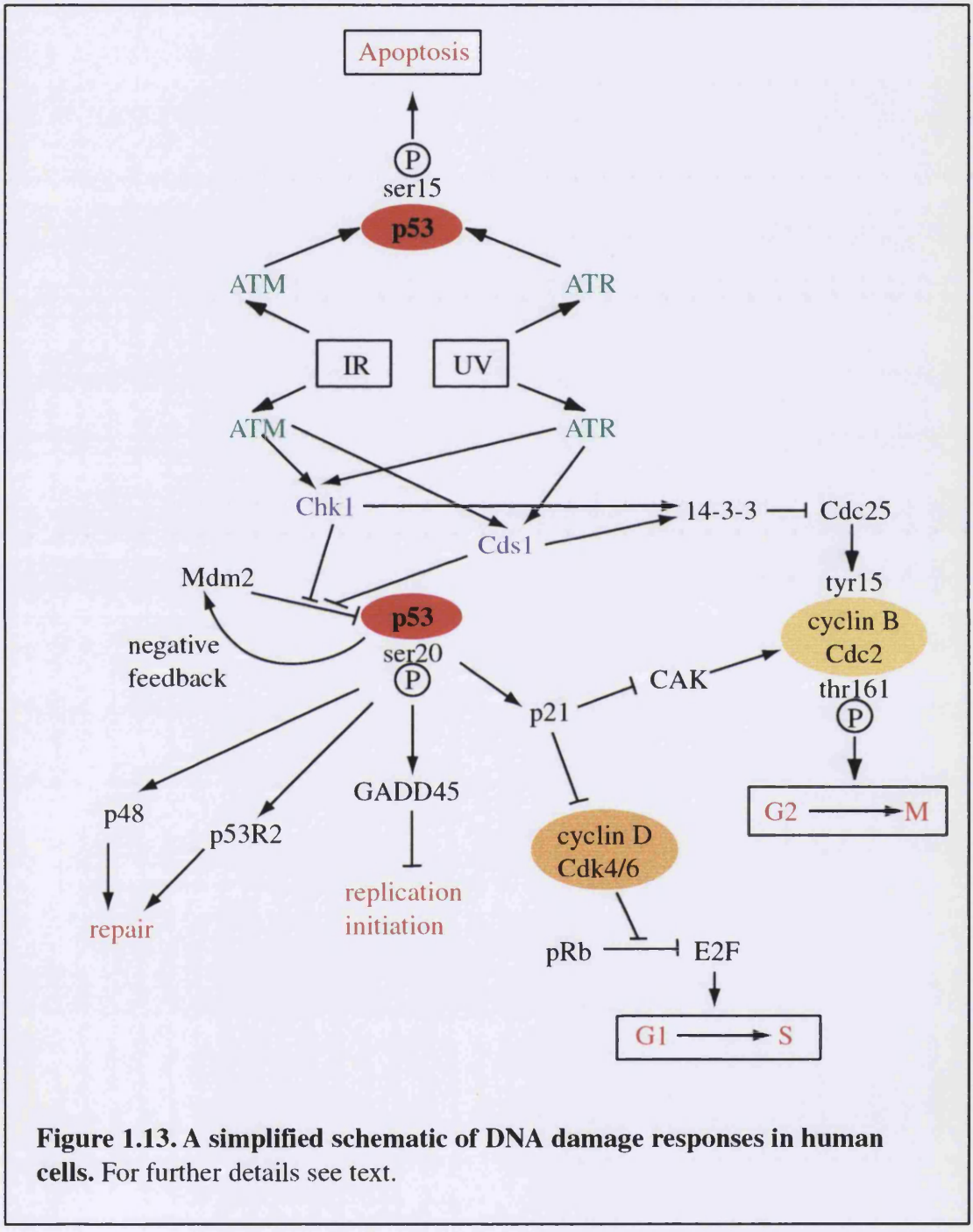

Figure 1.13. A simplified schematic of DNA damage responses in human cells. For further details see text.

agent (Lim *et al.*, 2000; Wu *et al.*, 2000; Zhao *et al.*, 2000). ATM is normally activated in NBS cells, suggesting that the Nbs/Mre11/Rad50 complex is part of a signal transduction pathway operating downstream of ATM after IR. Nbs is also phosphorylated after UV, it has yet to be determined whether this modification is ATR-dependent. The question of whether the yeast homologues of this complex have a similar role in the *S. cerevisiae* DNA damage response is currently under investigation in our laboratory. A second protein found to have multiple roles in the response of human cells to DNA damage is BRCA1. The *BRCA1* gene is mutated in families with hereditary breast cancer predisposition (Miki *et al.*, 1994). The protein is implicated in DNA repair (Scully *et al.*, 1997; Gowen *et al.*, 1998; Zhong *et al.*, 1999) and is required for normal induction of GADD45 and p21 after DNA damage (Li *et al.*, 2000) (for a recent review see Welcsh *et al.*, 2000). BRCA1 is often reported to be a homologue of the *S. cerevisiae* Rad9 protein, as both contain BRCT motifs at their carboxyl termini, and both are regulated after DNA damage in an ATM (Mec1 for Rad9) dependent manner (Cortez *et al.*, 1999). Recent reports demonstrate that BRCA1 is also phosphorylated by Cds1 (Lee *et al.*, 2000), required for a normal G2 checkpoint (Xu *et al.*, 1999), and that it may co-ordinate the cellular response to DNA damage via a large protein complex including proteins involved in MMR, DSBR and repair synthesis (Wang *et al.*, 2000). No similar biochemical activities have been described for Rad9 and BRCA1 that would confirm them as functional homologues.

1.14 – OTHER CELL CYCLE CHECKPOINT PATHWAYS

Since the discovery of the DNA damage-dependent checkpoint in yeasts many other feedback control mechanisms that regulate cell cycle progression have been identified, (A number of these are reviewed in Clarke and Gimenez-Abian, 2000). The checkpoint that prevents the initiation of mitosis if DNA replication is incomplete (S/M checkpoint) is well characterised in both budding and fission yeasts. As mentioned above the S/M checkpoint in *S. pombe* is controlled by the same proteins that operate the DNA damage-dependent checkpoint. This pathway is activated during exposure to hydroxyurea, although the exact nature of the initiating signal is unknown. The mechanisms by which mitosis is prevented are as for the DNA damage response and are reviewed in (Boddy and Russell, 1999). In *S. cerevisiae* the S/M checkpoint requires *MEC1* and *RAD53*, but not the so called "sensor class" of checkpoint genes, *RAD9* and

the *RAD24* group. One effector of the S/M checkpoint in budding yeast is the Dbf4 protein which controls the activity of the Cdc7 kinase required for the initiation of origin firing. Dbf4 is phosphorylated and inactivated in a Rad53-dependent manner after HU treatment (Weinreich and Stillman, 1999). This may be the mechanism by which the checkpoint pathway prevents the firing of late replicating origins during HU mediated arrest (Santocanale and Diffley, 1998). It is possible that the Dbf4/Cdc7 kinase affects the activity of the polα/primase complex, as it is known to directly phosphorylate this protein (Weinreich and Stillman, 1999), and polα/primase has been implicated as an effector or S phase arrest (Foiani *et al.*, 1995; Pellicioli *et al.*, 1999). As the replication checkpoint clearly does not involve *RAD9* or *RAD24* other proteins are presumably able to initiate and transduce a signal to Rad53. The helicase Sgs1 in required upstream of Rad53 for this pathway to operate (Frei and Gasser, 2000), as is the BRCT containing protein Dpb11 (Araki *et al.*, 1995). It is possible that the roles of these proteins in sensing HU are equivalent to those of Rad24 and Rad9 respectively in sensing DNA damage.

An unrelated checkpoint, the spindle checkpoint, ensures that anaphase is not attempted until the sister chromatids of each chromosome are attached to spindle microtubules from opposite poles. This pathway was originally identified in the budding yeast, but as for the DNA damage and replication checkpoints has been found to be highly conserved throughout evolution, (for a recent review see Burke, 2000). In *S. cerevisiae* this checkpoint pathway is controlled by a complex network of *MAD* and *BUB* genes. These were identified by the sensitivity of mutants to the microtubule depolymerising drug nocodazole. Much like the DNA damage-dependent checkpoint these genes form parallel pathways responding to such treatment and the downstream effector of the pathway in *S. cerevisiae* is the Pds1 protein.

Pertubations to the actin cytoskeleton also lead to a cell cycle checkpoint in *S. cerevisiae*, the morphogenesis checkpoint, for a review see (Lew, 2000). Interestingly this checkpoint prevents the initiation of mitosis in a manner analogous to that utilised by human cells and *S. pombe* in response to DNA damage. The Wee1 kinase Swe1 is stabilised upon actin depolymerisation, via the negative regulators Hsl1 and Hsl7

(McMillan *et al.*, 1999). This results in the Swe1 mediated inhibitory phosphorylation of Cdc28 on tyrosine-19 (analogous to Tyr15 of Cdc2) and hence prevention of mitosis.

Checkpoint pathways also operate to ensure a correct order of events during progression through the meiotic cell cycle. A pathway has been identified in *S. cerevisiae* which prevents meiotic division if recombination events are not complete (Lydall *et al.*, 1996), and in *S. pombe* that halts meiotic division if replication is inhibited (Murakami and Nurse, 1999). In both organisms these pathways involve genes involved in the DNA damage-dependent checkpoint pathway in mitosis. The human homologue of the *S. cerevisiae* Rad17 protein, hRad1 also localises to meiotic chromosomes (Freire *et al.*, 1998), as do ATM and ATR (Keegan *et al.*, 1996) suggesting that these responses might have been conserved through evolution.

1.15 – CONSEQUENCES OF CHECKPOINT PATHWAY FAILURE

The fact that A-T patients are prone to cancer development, that mutation of BRCA1 is linked to familial breasr cancer susceptibility and that p53 function is abrogated in at least 50% of sporadic human tumours suggests that there may be a link between a loss of checkpoint pathway function and the onset of tumouigenesis. The onset of cancer is a result of the accumulation, within one somatic cell, of sufficient mutations in genes that normally regulate proliferation to allow the progeny of that cell to multiply unrestrained by normal control (Vogelstein and Kinzler, 1993). It is hypothesised that one of the principle mechanisms by which these mutations can accumulate is an increase in the genomic instability of a cell (Lengauer *et al.*, 1998; Cahill *et al.*, 1999). Such instability would allow rapid evolution within a population and the eventual clonal expansion of those cells which have lost sensitivity to the controlling mechanisms in place to prevent unrestrained growth. Checkpoint pathways are mechanisms by which genetic stability is maintained, and therefore it is likely that the abrogation of these pathways could result in initiation of tumourigenesis (Hartwell and Kastan, 1994).

Cells from A-T patients do indeed show genomic instability, and a loss of function of P53 and BRCA1 also results in loss of checkpoint activity and increased genomic instability. However the high incidence of tumourigenesis that results from inactivation

of these genes may not be entirely due to checkpoint pathway defects as the loss of these gene functions also results in impaired repair and apoptotic responses.

More recently human homologues of yeast spindle checkpoint genes have been found to be mutated in human cancer cell lines displaying chromosomal instabilities (Cahill *et al.*, 1998) and mutations in the human *CHK2* gene has been implicated in a familial cancer susceptibility condition, Li-Fraumeni syndrome (Bell *et al.*, 1999). The Tax oncoprotein, encoded by the virus that causes adult T cell leukemia (ATL), targets the Mad1 checkpoint protein and hence inactivates the spindle checkpoint. This lack of checkpoint function may explain the karyotypic abnormalites that are detected in ATL cells, and that may be the initiating events for oncogenesis (Jin *et al.*, 1998). It therefore seems likely that the inactivation of cellular checkpoint pathways may indeed be a contributing factor to the onset of tumourigenesis. The newly identified human homologous of the yeast DNA damage-dependent checkpoint pathway genes are likely to be involved in pathways that contribute to the maintenance of genomic stability. Hence they are candidates for inactivation during the multistep process that is oncogenesis. Therefore studies of the yeast homologues of these genes are valuable, not only for their interest as a basic biological phenomenon, but also because information obtained from the yeast system may be valuable in understanding the complex regulatory processes in human cells that must be rendered inoperative if a tumour is to form. In time we may even understand how we can exogenously regulate these control pathways in order to prevent their inactivation, or utilise them for therapeutic purposes.

CHAPTER 2 – MATERIALS AND METHODS

Many of the methods given here are taken, or adapted from Sambrook *et al.*, 1989.

2.1 – COMMONLY USED BUFFERS

Materials used were generally obtained from Sigma and were of the highest purity available, unless otherwise stated.

10x Blue Juice: 0.25% bromophenol blue, 0.25% xylene cyanol FF, 30% glycerol in deionised water (dH_2O).

Coomassie Stain: For 1litre; 450ml dH_2O, 450ml methanol, 100ml glacial acetic acid, 1g coomassie blue.

Destain solution: 10% methanol, 10% acetic acid in dH_2O.

Elution Buffer: 10mM Tris in dH_2O, pH 8.5.

10x Gel running Buffer (GRB): 30g Tris base, 144g glycine, 10g SDS, dH_2O to 1l.

3x Laemmli sample buffer (Laemmli buffer): For 10ml; 2ml glycerol, 1.5ml ß-mercaptoethanol, 4.5ml 20% SDS, 1.875ml 1M Tris.HCl pH 6.8, 125µl 1% bromophenol blue.

LB: 10g bacto-tryptone, 5g bacto-yeast extract, 10g NaCl in 1litre dH_2O, pH to 7.0 with NaOH. Sterilise by auotclaving.

LB/Amp: LB with 50µg/ml ampicillin and 50µg/ml methicillin.

2x Native lysis buffer (lysis buffer): 300mM KCl, 100mM Hepes pH 7.5, 20% glycerol, 8mM ß-mercaptethanol, 2mM EDTA, 0.1% Tween20, 0.01% NP-40, 2mM NaF, 2mM ß-glycerophosphate, 0.4mM Na_3VO_4, 2mM EGTA, 5mM sodium pyrophosphate, 1.3mg/ml benzamidine, 0.7mg/ml PMSF, 5µg/ml pepstatinA, 1µg/ml leupeptin, 5µg/ml antipain and 4µg/ml chymostatin (i.e. final concentration 4x Pis, 2xPpis).

Oligo Buffer: 0.3M $NaCH_3CO_2$, 10mM $MgCl_2$.

PBS: 8g NaCl, 0.2g KCl, 1.44g Na_2HPO_4, 0.24g KH_2PO_4 in 1litre dH_2O, pH to 7.4 with HCl. Sterilise by autoclaving.

PBST: PBS with 0.02% Tween20.

50x Phosphatase Inhibitors (Ppis): 0.105g NaF, 0.540g ß-glycerophosphate, 0.092g Na_3VO_4, 0.951g EGTA, 5.579g sodium pyrophosphate in 50ml dH_20.

Ponceau S stain: 1g Ponceau S, 15g Trichloroacetic acid, 15g Sulphosalicylic acid, dH_20 to 500ml.

100x Protease Inhibitors (Pis): 1.42mg leupeptin, 6.85mg pepstatin A, 0.85g PMSF, 1.65g benzamidine, 6.25mg antipain, 4mg chymostatin (dissolved in DMSO), ETOH to 50ml.

5x TBE: 54g Tris base, 27.5g boric acid, 20ml 0.5M EDTA (pH 8.0), in 1litre dH_20.

TE: 10mM Tris.HCl (pH 8.0), 1mM EDTA (pH 8.0).

Transfer buffer: 5.82g Tris base, 2.93g glycine, 1.875ml 20% SDS, 200ml methanol, dH_2O to 1litre.

YPD: 1% yeast extract, 2% peptone, 2% glucose.

YNB: 0.67% Yeast nitrogen base without amino acids (Difco), 2% glucose, appropriate amino acids at 40μg/l final concentration.

2.2 - BASIC DNA METHODS

PREPARATION OF COMPETENT *E. COLI* CELLS

E. coli strain DH5α was used for all routine cloning procedures. Heat shock competent cells were prepared from 125ml cultures grown overnight at 25°C, until the A_{600} spectrophotometer reading was 0.6. The culture was chilled on ice for 10 minutes, harvested, and washed in ice cold TB buffer (10mM PIPES, 15mM $CaCl_2$, 250mM KCl, 55mM $MnCl_2$ (all components except $MnCl_2$ mixed, pH adjusted to 6.7 with KOH, then $MnCl_2$ added and solution filter sterilised)). After a second centrifugation, cells were resuspended in TB with 7% DMSO, aliquoted and snap frozen in liquid nitrogen. Alternatively subcloning efficiency competent cells were purchased from Life Technologies.

E. COLI TRANSFORMATIONS

An aliquot of competent cells was thawed on ice. 1-5μl ligation reaction or miniprep DNA was added to chilled Eppendorf tubes and 100μl cells were added. After mixing the transformation mixture was incubated on ice for 30 minutes, then at 42°C for 90s, then replaced on ice for 2 minutes. 400μl LB without ampicillin was added and the cells incubated for 30 minutes at 37°C, after which time samples were plated onto LB/amp plates and incubated overnight at 37°C.

PLASMID STOCK STORAGE

All plasmids were stored as *E. coli* glycerol stocks (850μl overnight *E. coli* culture plus 150μl glycerol) at –80°C. Records were maintained in the lab database (4D-first). Throughout this thesis, vectors are referred to by stock numbers EXXX and name. The DNA sequence files for plasmids used here are given in Appendix II on the attached CD-ROM.

DNA PREPARATION

Mini-preps were performed to obtain up to 10μg plasmid DNA from overnight cultures inoculated from a single colony into 5ml LB/Amp and grown at 37°C. The cells were harvested, resuspended in 100μl lysis solution (25mM Tris.HCl pH 8.0, 10mM EDTA pH 8.0, 50mM D-glucose, 2mg/ml lysozyme) and incubated on ice for 30 minutes. The lysed cells were transferred to an Eppendorf tube on ice, containing 200μl alkaline/SDS solution (0.2M NaOH, 1% SDS) and incubated for a further 5 minutes. 150μl high salt solution was added (for 5ml add 575μl glacial acetic acid to 4.425ml 3.39M $NaCH_3O_2$) the tubes were inverted to mix and left on ice for 60 minutes. After centrifugation at 14000rpm for 5 minutes the supernatant was retained, and the DNA precipitated by the addition of 1ml ethanol (previously cooled to –20°C). The DNA was recovered by centrifugation at 14000rpm for 15 minutes, the pellet washed with 250μl 70% ethanol then dried in a speed-vac (Savant). The pellet was resuspended in 50μl EB containing 20μg/ml RNAse A (previously boiled to remove DNAse). Alternatively, a Qiaprep Spin miniprep kit (Qiagen) was used according to manufacturers protocols. Larger quantities of plasmid DNA were obtained using the Qiafilter Midi Kit (Qiagen), according to manufacturers protocols.

ENZYMATIC REACTIONS

Restriction digests, ligations and dephosphorylations were performed with buffers and protocol supplied with the enzymes. Restriction enzymes and T4 DNA ligase were from NEB, calf intestinal alkaline phosphatase was from Boeringher Mannheim. Enzymes and small DNA fragments were removed after reactions with Qiaquik Nucleotide Removal Kit (Qiagen) according to manufacturers protocol.

OLIGONUCLEOTIDE PREPARATION

Oligonucleotides were obtained from the ICRF synthesis service. The pellet was dissolved in 200μl oligo buffer and 600μl cold ethanol was added. The solution was placed on dry ice for 15 minutes then centrifuged at 14000rpm for 20 minutes at 4°C.

The pellet was washed in 80% ethanol in H_2O then dried in a speed-vac. The oligo was dissolved in EB at a final concentration of 1mg/ml.

YEAST GEMOMIC DNA PREPARATION

Genomic DNA was prepared from 5ml yeast cultures in YPD or selective media, grown overnight at 30°C, using the Kristal Yeast Genomic Mini Kit (Stratech Scientific) according to the manufacturers protocol.

POLYMERASE CHAIN REACTION (PCR)

PCR was used for 2 main purposes, *Pfu* enzyme (Stratagene) was used for cloning purposes, while *Taq* enzyme (ICRF protein production) was used for diagnostic PCR. A typical PCR reaction contained 200μM dATP, dCTP, dGTP and dTTP, 1.5mM $MgCl_2$, 10mM Tris.HCl pH 8.4, 50mM KCl, 0.25μM each primer and 2.5 units *Taq* polymerase in 100μl final volume. 1-100μg plasmid or 100-250μg genomic DNA were used as template. Reactions were incubated in a DNA engine thermocycler (GRI), an example program is:

1 min @ 94°C
25x (30 sec @ 94°C, 30 sec @ 50°C, 2 min @ 72°C)
10 min @ 72°C
cool to 4°C and END.

Programs varied depending on Tm of primers used and whether template used was plasmid or genomic DNA. The sequences of all oligonucleotides used are given in Appendix I, all other sequences necessary are in Appendix II on the attached CD-ROM. Extension times were longer when Pfu polymerase was used. If PCR products were to be cloned, primers were designed with non-complimentary tails containing the required restriction sites for direct cloning into the target vector. An additional 5 cycles using a lower annealing temperature was included before the main chain reaction cycle when such primers were used. PCR products were purified on agarose gels before cloning.

AGAROSE GELS

Agarose gels of 0.7-2% were prepared (Gibco BRL) and run in 1xTBE. Ethidium Bromide was added to the gel to a final concentration of 0.5μg/ml. Blue Juice was used as loading buffer at a final 2x dilution. Markers used were ϕxBstEII, λHindIII, (NEB) or 100bp and1kb ladders (Life Technologies) in the same buffer as the samples. 250ng were generally loaded. Gel running equipment was BioRad mini (50ml gel) or wide mini (100ml gel) sub cells, which were run at 80V until the required separation was

achieved. Gels were visualised on a transilluminator (Ultra Violet Products), photographs were taken on Kodak polaroid 57 film with a Polaroid camera. If necessary DNA bands were excised from gel and purified using Qiaquik Gel Extraction kit (Qiagen) according to manufacturers protocol.

DNA SEQUENCING

DNA sequencing was performed to ensure that cloning of PCR fragments yielded correct vector constructs. PCR based sequencing was performed, using the ABI Prism BigDye Terminator Cycle Sequencing Ready Reaction Kit according to the manufacturers protocol. After precipitation of the labelled products the reactions were loaded onto the automated sequencer by the ICRF sequencing service (Lincolns Inn Fields).

2.3 - BASIC PROTEIN METHODS

PROTEIN CONCENTRATION DETERMINATION

1μl sample extract was added to 800μl dH_2O in an Eppendorf tube, and vortexed. 200μl BioRad protein assay reagent was added and mixed. The samples were transferred to plastic cuvettes (Elkay) and the absorbance at 595nm determined using a Shimadzu spectrophotometer. A standard curve was prepared using this method and known concentrations of bovine serum albumin (BSA). From this the concentration of protein in the samples was interpolated (Figure 2.3).

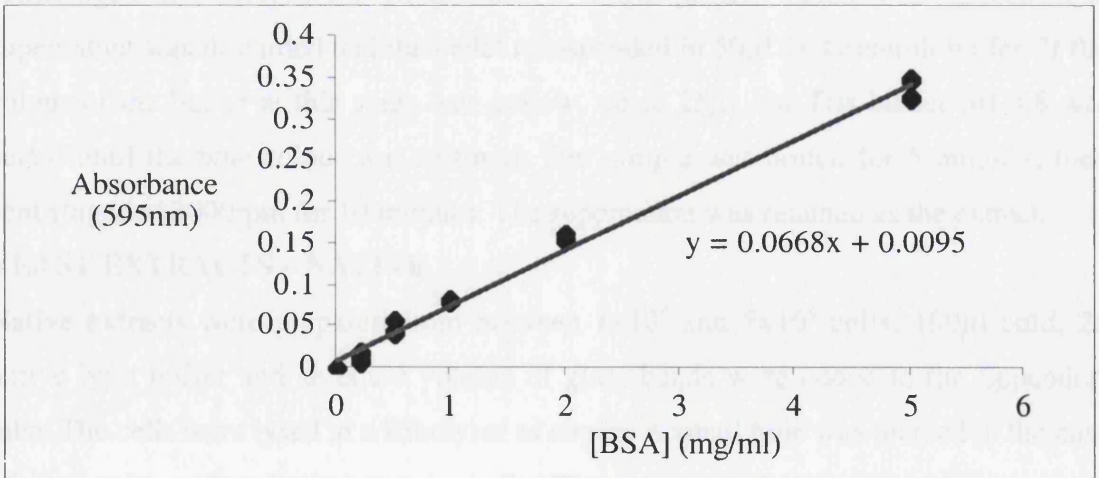

Figure 2.3. Standard curves from bradford protein reagent using known amounts of BSA. The samples were prepared as described above.

DENATURED *E. COLI* EXTRACTS

1ml of an *E. coli* culture of known A_{600} was centrifuged at 14000rpm at room temperature for 1 minute. The cell pellet was resuspended in 100μl 3x Laemmli buffer per 1 unit of absorbance at 600nm. This was boiled for 5 minutes, centrifuged and the supernatant retained. 10μl of this extract was sufficient for visualising by Coomassie staining after SDS-PAGE.

DENATURED YEAST EXTRACTS

A known amount of cells (approximately $2x10^8$) was harvester and transferred to a 1.5 ml screw-capped tube. 50μl Laemmli buffer was added and the cells lysed by five, 30s bursts at setting 5.0 in a Hybaid ribolyser. The beads and buffer were heated to 95°C for 5 minutes, then the beads were pelleted by centrifugation and all the buffer removed. This was used as the extract for determination of cellular copy number.

YEAST EXTRACTS – TCA

Denatured extracts were prepared using a trichloroacetic acid (TCA) precipitation method. Between $1x10^8$ and $5x10^8$ cells were harvested and transferred to a 1.5ml screw-capped Eppendorf tube. The pellet was resuspended in 100μl 20% TCA (prepared from 100% TCA solution – Sigma) and glass beads (0.4mm, BDH) added up to the meniscus. The cells were lysed in a Hybaid Ribolyser (setting 5.0 for 2x 20 seconds) at 4°C. The liquid was removed to a new tube and the beads washed with 100μl 5% TCA which was added to the initial suspension. The suspension was centrifuged at 3000rpm for 10 minutes, a white protein pellet was formed. The supernatant was discarded and the pellet resuspended in 50μl 1x Laemmli buffer. If the colour of the buffer at this stage was yellow, up to 25μl 1M Tris buffer pH 8.8 was added until the blue colour was restored. The sample was boiled for 5 minutes, then centrifuged at 3000rpm for 10 minutes. The supernatant was retained as the extract.

YEAST EXTRACTS – NATIVE

Native extracts were prepared from between $1x10^8$ and $5x10^8$ cells. 100μl cold, 2x native lysis buffer and an equal volume of glass beads were added to the Eppendorf tube. The cells were lysed in a Ribolyser as above. A small hole was pierced in the base of each tube with a hot mounted needle. The tube was the placed inside a second Eppendorf tube, and the tubes spun in a swing out rotor (Beckman JS-6) at 1000rpm for 2 minutes. This forced the supernatant through to the lower tube while the beads were

kept in the upper tube, which was discarded. The lower tube was centrifuged at 14000rpm for a further 10 minutes at 4°C and the supernatant retained as the extract.

SDS PAGE PROTEIN GELS

Protein gels were run using either the BioRad mini protean system, for up to 15 samples or the Anachem SV2010 system for up to 36 samples. The table below gives recipes for common gels used (Table 2.3.1). Resolving gels were allowed to set for 30 minutes, with a layer of water on the surface to ensure a sharp interface between the resolving and stacking layers.

Gel %	6.5	7.5	8.5	10
Protogel	1083	1250	1417	1666
dH_20	3237	3070	2903	2654
3M Tris pH 8.8	620	620	620	620
20% SDS	25	25	25	25
10% APS	25	25	25	25
Temed	6	6	6	6

Table 2.3.1. Preparation of SDS-PAGE gels (Resolving). All volumes are in μl, giving a total of 5ml. Protogel (National Diagnostics) contains 30% acrylamide, 0.8% bis-acrylamide (37.5:1).10% APS was made weekly. The BioRad system requires 5ml/gel, the Anachem requires 10ml/gel.

Stacking gels were poured (Table 2.3.2) and the comb added immediately. All combs and plates were thoroughly washed before use in hot water and detergent, and handled only with gloves to reduce contamination by skin keratins. Samples of up to 25μl were loaded, the gels were run at 200V for 45 minutes to 1 hour in 1x GRB. Molecular weight markers used were Sigma SDS-6H or SDS-7B, made up according to manufacturers instructions or Novex Multimark, 5μl was loaded. Gels were either stained with Coomassie blue or transferred to nitrocellulose.

COOMASSIE STAINING OF GELS

For staining, the gel was transferred into a clean plastic box and Coomassie stain added to cover the gel. This was incubated at room temperature with agitation for 30 minutes. The stain was removed and kept for re-use. The stain was removed by three 30 minute

Protogel	330
dH_20	1575
1M Tris pH 6.8	313
20% SDS	12.5
10% APS	25
Temed	2.5

Table 2.3.2. Preparation of SDS-PAGE gels (stacking). All volumes are in μl, sufficient for 1 BioRad gel, for Anachem twice as much is required.

washes in destain solution, with the inclusion of a sponge piece to help absorb the excess dye. After the stain was sufficiently removed the gel was soaked in 5% glycerol in dH_20 before air dying between 2 porous cellophane sheets (BioRad).

SILVER STAINING OF GELS

During this procedure all containers were either new or scrupulously cleaned with hot water and detergent. All solutions were made with freshly drawn water that was not stored in glassware and filtered through 0.2μm cellulose nitrate filters. The gel was handled as little as possible, and only with low protein, powder free gloves. The gel was soaked in 50% methanol, 12% acetic acid, 0.5ml/litre 37% formaldehyde (HCOH) in dH_2O for 1 hour, followed by soaking in 50% ethanol in dH_2O for 30 minutes. Both soaks were at room temperature with agitation. The gel was then placed in 0.2g/litre sodium thiosulphate ($Na_2S_2O_3$) in dH_2O for 1 minute, followed by 3 washes in dH_2O of 20 seconds each. Next, the gel was soaked in 2g/litre silver nitrate ($AgNO_3$), 0.75ml/litre 37% HCOH in dH_2O for 45 minutes at room temperature with agitation. After 2 washes in dH_2O of 30 seconds each the stain was developed in 60g/litre sodium carbonate (Na_2CO_3), 4mg/litre $Na_2S_2O_3$, 0.5ml/litre 37% HCOH in dH_2O. The staining was stopped by soaking the gel in 1% glacial acetic acid (CH_3CO_2H) in dH_2O just prior to reaching the required intensity. The gel was then air dried between porous cellophane.

SEMI-DRY TRANSFER

The SDS-PAGE gel was rinsed with transfer buffer then placed onto cut to size Hybond C-extra membrane (Amersham) which had been previously soaked in transfer buffer. This was sandwiched between two sheets of extra thick blotting paper (Schleicher &

Schuell) soaked in transfer buffer and placed between the plates of a BioRad semi-dry transfer apparatus with the membrane closest to the anode. 13V was applied for 35 minutes. The efficiency of transfer was monitored by comparing the amount of prestained markers remaining in the gel to the amount transferred. The filter was soaked in Ponceau S solution for 5 minutes then rinsed in water. This allowed marking of the non-stained molecular weight standards in pencil, and also provided an approximate loading control. The stain was removed by washing in PBST.

WESTERN BLOTTING

The conditions for antibody incubations depended on the antibody being used. The optimised conditions for polyclonal antibodies are given in Table 3.1.2. The conditions for monoclonal antibodies are given below (Table 2.3.3).

Antibody	Epitope name and sequence	Block	Primary
12CA5	HA (YPYDVPDYA)	1%, 10min	1 in 750, 1% milk
9E10	Myc (EQKLISEEDL)	3%, 20min	1 in 250, 1% milk
α-FLAG (Sigma)	FLAG (DYKDDDDK)	3%, 10min	1 in 20000, 1% milk
α-T7 (Novagen)	T7 (MASMTGGQQMG)	3%, 10min	1 in 10000, 3% milk

Table 2.3.3. Optimised conditions for western blotting using monoclonal antibodies.

The blocking step was performed using 20ml block at room temperature with agitation. Primary antibody incubation was in 10ml to 20ml, for 2 hours to overnight, at room temperature with agitation. Overnight incubations were used either to maximise the signal or for reason of convenience. After removal of the primary antibody with at least 5 washes in 100ml PBST, the filter was incubated with secondary antibody. 20ml of 1 in 10000 dilution in PBST with no milk was used for 45 minutes at room temperature with agitation. After 5 washes as before the filter was developed using an ECL kit (Amersham), according to the manufacturers protocol, except only 25% of the recommended volumes of each reagent were found to be necessary. The developed filter was exposed to Kodak X-Omat film for 1 to 20 minutes, the films were processed in a Fuji developer.

2.4 - ANTIBODY PRODUCTION

ELECTRO-COMPETENT CELL PREPARATION

A 1litre culture of the strain was grown at 37°C until an absorbance of 0.8 at 600nm was reached. The culture was chilled on ice for 15 minutes, then harvested by centrifugation in a cold rotor. The pellet was resuspended in 1litre cold dH_2O, re-centrifuged and resuspended in 500ml cold dH_2O, re-centrifuged and resuspended in 20ml cold water and finally re-centrifuged and resuspended in a final volume (including cell pellet) of 2ml containing 10% final glycerol. These cells were aliquoted and frozen in liquid nitrogen.

TRANSFORMATION BY ELECTROPORATION

For transformation, 0.2cm electroporation cuvettes (Flowgen) were chilled on ice. To a cold Eppendorf tube was added up to 0.5ng transforming DNA and 20μl competent cells, which were mixed and incubated on ice for 1 minute. The cells were transferred to the cuvette, avoiding bubbles, and a pulse charge was applied using a BioRad electroporator (settings: 25μF, 400Ω, 2.5kV, resulting in a pulse of 12.5kV/cm with a time constant of 8 to 10ms). Immediately the cells were resuspended in 400μl LB without ampicillin and the cells plated onto the appropriate selective media (up to 200μl/plate).

ANTIBODY PRODUCTION

Briefly, fragments from the genes *RAD17*, *RAD24*, *RAD53* and *MEC3* were amplified by PCR and cloned into the pET21-b vector (Novagen) (See section 3.1.). The vectors were transformed into *E. coli* strain FB810, a gift from Fiona Benson, using the electroporation method. An entire colony from a fresh transformant was transferred to a large scale culture, typically 400ml. Expression of the recombinant fragments was induced by the addition of IPTG. The cells were lysed under denaturing conditions, the proteins purified using an NTA-nickel agarose (Qiagen) column according to the manufacturers protocol and used to immunise rabbits (ICRF antibody production unit – Clare Hall). The resulting polyclonal sera were tested for specificity in western blot analysis using yeast extracts from WT or the appropriate delete strain, and western blotting conditions were optimised.

2.5 - YEAST METHODS

NORMAL CULTURE CONDITIONS

Yeast cultures were grown in conical flasks in YPD liquid medium at 30°C, with agitation at approximately 200rpm. The volume of culture did not exceed one quarter of the nominal flask volume to ensure adequate aeration. Solid media was YPD plus 2% agar. Plates were allowed to set for 24 hours at room temperature before use. Diluted liquid yeast cultures were plated for single colonies using 5 to 10 sterile 4mm glass balls (Fisher) per plate. Yeast colonies were streaked out to give single colonies using sterile, sealed 50μl glass capillaries. Plates were incubated at 30°C in the dark, colonies were approximately 1mm diameter after 40 hours.

SELECTIVE MEDIA

Solid selective media was YNB with 2% agar and the required amino acids (W303 requires histidine, leucine, tryptophan and uracil as well as adenine). The carbon source was normally 2% glucose. If galactose based media was required 2% sucrose was used in addition to 2% galactose was added, to increase cell growth rate.

ARREST OF CULTURES AT DIFFERENT CELL CYCLE STAGES

To arrest cells in G1 phase α-factor was added to the growth medium at 10μg/ml, the culture was left for at least 2 hours. Arrest was confirmed by microscopy, a fully arrested culture contained at least 95% unbudded cells. For S-phase arrest cells were first arrested in G1 as above, then the α-factor containing medium was washed off and replaced with medium containing 0.2M hydroxyurea. This was maintained for a further hour, resulting in a uniform arrest in early S phase. Arrest was confirmed by microscopy, a fully arrested culture contained at least 90% budded cells. For arrest in G2, nocodazole was added to the media at 5μg/ml, the culture was left for at least 2 hours. Arrest was confirmed by microscopy, a fully arrested culture contained at least 85% large budded cells. If the nocodazole arrest was initially unsuccessful this was likely to be because the population contained a large proportion of petite mutants, as mitochondrial function appears to be required for efficient nocodazole arrest, for reasons that are unclear. To overcome this problem, strains that were to be arrested in this manner were first propagated on media with glycerol as the sole carbon source, in order to remove cells lacking mitochondrial function from the population.

CELL CYCLE BLOCK AND RELEASE EXPERIMENTS

A mid-logarithmic yeast culture was arrested in G1 phase with the addition of 5μg/ml α-factor. When >90% cells were unbudded the cells were quickly washed three times in saline, then resuspended in pre-warmed medium without mating pheromone. Samples were taken immediately before the first centrifuge step (-0 minutes), immediately after the cells were returned to medium (+0 minutes), and at five minute intervals thereafter. For analysis of cell morphology samples were sonicated briefly then fixed with formaldehyde. For western blot analysis samples were snap frozen on dry ice before processing. For analysis of the G1 checkpoint cells were irradiated in saline immediately before releasing from the alpha factor block.

GAMMA IRRADIATION

An asynchronous mid-log yeast culture was harvested and washed into a 50ml falcon tube. The cells were pelleted and irradiated in a ^{137}Cs irradiator (CIS bio international) as a dose rate of 2.75Gy/minute. After irradiation the cells were resuspended in medium and allowed to recover for 30 minutes before harvesting for analysis. For analysis of strain sensitivity to gamma irradiation on solid media yeast cultures were applied to YPD plates, and the plates irradiated as above.

MMS TREATMENT

MMS treatment was performed by the addition of MMS to mid logarithmic cultures at a final concentration of 0.05-0.2%. Cells were incubated for up to 1 hour with the chemical, then harvested for analysis. All media solutions containing MMS, and contaminated glasswear was treated with concentrated NaOH solution to inactivate the MMS before disposal. For analysis of strain sensitivity to MMS on solid media, YPD plates were prepared containing 0.01% MMS.

UV IRRADIATION

Asynchronous cultures, or those which had been arrested, were harvested, washed into saline and irradiated using a prewarmed Philips 254nm UV-C lamp (Ultra Violet Products). The distance from the lamp was adjusted to give a fluence rate of 3J/m^2/s, measured on a UVP dosimeter. The cells were irradiated in large surface area containers, at a cell density of no more than 1x10^7 cells/ml. 10cm square petri dishes were used to irradiate up to 20ml samples, 30cm square cell culture dishes for up to 100ml, and larger volumes in stainless steel baking trays. After irradiation, the cells were poured from the trays into centrifuge bottles, the tray was rinsed with saline and

this wash added to the previous cells. The cells were pelleted by centrifugation and resuspended in YPD. Recovery was for 30 minutes at 30°C, before the cells were harvested for analysis. For analysis of strain sensitivity to UV on solid media cultures were applied to the appropriate plates, which were allowed to dry before irradiating as for saline suspension.

SURVIVAL ANALYSIS

Yeast cultures were grown to a density of $1x10^7$ cells/ml in YPD at 30°C. A dilution series was prepared in YPD and known numbers of cells, between 30000 and 300, depending on the anticipated dose were plated onto YPD plates. These plates were exposed to UV light (254nm wavelength) at a fluence rate of $3J/m^2/s$ for calculated times. The plates were then incubated at 30°C for two days and the number of colonies counted. This number was corrected to the 0J dose and the percentage survival relative to this dose was determined.

MICRO COLONY ANALYSIS

For the determination of the fate of a single yeast cell dilute cultures were streaked at one side of a dry, flat plate of appropriate medium. Using a Singer tetrad dissector single cells in G1 phase were transferred to known co-ordinates of the plate. After 4-48 hours growth under the appropriate conditions the fate of the single cell was determined by microscopic analysis of the cells at each set of coordinates.

2.6 - YEAST GENETIC MANIPULATION

TRANSFORMATION

A culture of the strain to be transformed was grown to mig-logarithmic growth phase. $1x10^9$ cells were harvested by centrifugation, washed twice in TE then resuspended in 1ml LA solution (0.1M $LiCH_3CO_2$ pH 7.5 in TE). The transforming DNA (up to 15μg restriction digest reaction) and 50μg single stranded herring sperm carrier DNA (10mg/ml) were added to an Eppendorf tube on ice. 200μl cells were added to each tube, followed by 1.2ml LAP solution (0.1M $LiCH_3CO_2$ pH 7.5, 40% Polyethylene glycol Mw 3350). The cells were incubated with agitation for 30 minutes at 30°C followed by 15 minutes at 42°C, then aliquots plated directly onto the appropriate selective media.

HTH-RAD24 STRAIN CONSTRUCTION

Complementary oligonucleotides encoding the tag required were synthesised, annealed and directionally cloned into the multiple cloning site of the pRS303 vector. 1kb of sequence upstream of the *RAD24* ORF was amplified by PCR and cloned 5' to this tag. The first 400bp of the open reading frame was amplified and cloned 3' to the tag. Linearisation of this construct with BsgI enzyme and subsequent yeast transformation resulted in integration of the construct at the *RAD24* locus. This was confirmed by PCR from genomic DNA.

RFC-FLAG STRAIN CONSTRUCTIONS

Complementary oligonucleotides encoding three FLAG epitopes were annealed and cloned into the multiple cloning site of the pRS304 and pRS306 vectors. 400 base pairs from the 3' end of each RFC ORF were amplified by PCR and cloned 5' to the tag sequences. For RFC1, RFC3 and RFC4 pRS306 was used, pRS304 was used for RFC2 and RFC5. Linearisation (with StuI, Eco47III, NsiI, BclI or BclI for RFCs 1-5 respectively) and subsequent transformation of yeast resulted in the integration of the tagging construct at the RFC loci, replacing the endogenous 3' end of the genes. Integration was confirmed by PCR from genomic DNA.

DIPLOID PRODUCTION

One diploid strain was produced, the product of W3031b (α-type) and *HTH-RAD24* (a-type). The two strains were spread in adjacent sectors on a YPD plate, then part of each streak was mixed with a sterile spreader. The diploids were selected by replica plating to a selective media lacking histidine and including α-factor at 10μg/ml. This prevents the growth of both haploids while the diploid is viable. Individual isolates were confirmed to be diploid by western blot analysis using the anti-Rad24 polyclonal, but their diploid nature could be easily verified using the Coulter multisizer II, as the mean cell diameter of a diploid population was 5.8μm compared to 4.6μm for either haploid.

STORAGE OF YEAST STOCKS

To prepare yeast for freezing at –80°C a 100ml culture of the strain was gown to approximately $3x10^7$ cells/ml in rich medium. The cells were pelleted by centrifugation, the pellet resuspended in congelation medium (1% yeast extract, 1% bacto-tryptone, 2% glucose, 25% glycerol) and immediately snap frozen on dry ice.

2.7 - YEAST WHOLE CELL EXTRACTS

SMALL SCALE

See Section 2.3

MEDIUM SCALE

Yeast cultures were grown to a density of $1x10^7$ cells/ml in YPD at 30°C. An additional 2% glucose was then added and the cells grown until the density reached $3x10^7$ cells/ml. The cells were harvested by centrifugation, washed twice in ice cold water and the mass of the pellet determined. An equivalent volume of 2x lysis buffer was used to resuspend the pellet, which was then dropped into liquid nitrogen to form beads. These beads were ground in a pestle and mortar at liquid nitrogen temperature, for approximately 20 minutes, until a very fine powder was obtained. The powder was defrosted and the resulting extract was then centrifuged at 14000rpm at 4°C to remove cellular debris. The protein concentration was determined with BSA as a standard.

LARGE SCALE

Large scale yeast cultures (100l) were grown in YPD in a fermenter and harvested at a density of 4 $x10^7$ cells/ml. The cell pellets were washed twice in ice cold water, then piped into liquid nitrogen through a bag to form frozen "spaghetti" (Schultz, 1999). Two of these cultures were pooled (a total of 1.3kg yeast) for the large scale purification. The cells were lysed by grinding at liquid nitrogen temperature in 150g batches in a 1 litre capacity mortar until a fine powder was achieved. An equal volume of 2x lysis buffer relative to yeast wet weight was added slowly so that it froze immediately. This buffer was ground until incorporated into the yeast powder. The frozen powder was transferred to a beaker and allowed to thaw at room temperature. The extract was centrifuged at 42000rpm in a Beckman Ti45 rotor. The supernatant from this spin was the load for the heparin column

2.8 – IMMUNOPRECIPITAION AND GST PULL DOWN

IMMUNOPRECIPITATION

All immunoprecipitations were performed from 500μg total yeast proteins made by the medium scale liquid nitrogen method. In each case the volume of the precipitation was adjusted to 500μl with 1x lysis buffer. The extracts were precleared using 20μl protein A or G slurry, for 1 hour, which was then removed by centrifugation through a vectaspin filtration device (Whatman) The precipitating antibody was added to the

samples (at a dilution of 1 in 50 for 12CA5, 1 in 100 for polyclonal antibodies and 1 in 300 for anti-Flag), and incubated at 4°C for 1 hour. The extracts were then centrifuged at 14000rpm at 4°C for 20 minutes to remove aggregated material, this results in lower background signals (Sherilyn Goldstone, personal communication). 20μl protein A or G slurry was added to the supernatants. The precipitation was allowed to continue for 2 hours at 4°C. The samples were centrifuged at 3000rpm for 1 minute to pellet the beads, the supernatant was retained as flow through sample, and the beads washed 5 times in 1x lysis buffer containing up to 500mM KCl. The last traces of buffer were removed using a pipetman fitted with an Eppendorf gel loader tip. The precipitated proteins were removed from the beads by heating to 95°C in 2x Laemmli loading buffer for 4 minutes, and analysed by western blot.

PREPARATION OF GST-RAD17

An *E. coli* expression vector was constructed, based on the pGEX system, in order to produce a fusion protein comprising full length Rad17 and Glutathione S-Transferase (GST) (Theresa Fitzpatrick). This construct was transformed into FB810 cells by electroporation. 50ml cultures were grown and expression of the protein induced by the addition of 0.5mM IPTG for 3 hours. The *E. coli* were harvested and resuspended in 5ml NETN buffer (20mM Tris pH 8.0, 100mM NaCl, 1mM EDTA, 0.5% NP40, 2x Pis). 100μl lysozyme solution (50mg/ml) was added and the cells left on ice for 15 minutes. The cell suspension was then sonicated 3 times for 15s, with a 2 minute cooling period between bursts, at setting 30 with a fine probe. The debris was removed by centrifugation at 14000rpm and 4°C, the supernatant was retained as soluble extract, and stored at –80°C. An extract expressing GST alone was prepared in parallel to the GST-Rad17 extract, to be used as a control for the pull down step.

PREPARATION OF GST-RAD17 BEADS

100μl glutathione sepharose beads were washed four times in NETN buffer plus 0.5% milk powder. These beads were then added to the soluble *E. coli* extract and binding allowed to occur for 1 hour at 4°C. After this time the beads were washed three times with 5ml NETN, then resuspended as a 50% slurry in NETN. The amount of GST-Rad17 bound to the beads was quantitated compared to beads produced from the GST alone expression extract by SDS-PAGE after boiling in Laemmli buffer, and coomassie staining. The total concentration of each protein relative to bead volume was adjusted

by the addition of glutathione sepharose beads, so that the two bead preparations were equivalent.

GST PULL DOWN

Yeast extracts were diluted to 1mg/ml protein concentration with 1x lysis buffer. GST and GST-Rad17 beads were washed with lysis buffer. Extracts were precleared by the addition of 20μl GST beads per 500μl extract for 1 hour. These beads were then removed by passing the extract through a vectaspin micro filtration device (Whatman). The GST-Rad17 beads were then added to yeast extract (20μl beads to 500μl extract). Binding was for 1 hour at 4°C, after which time the beads were washed three times in 1x lysis buffer, then resuspended in Laemmli buffer, heated to 95°C for 3 minutes and analysed by western blotting.

2.9 – MOLECULAR SIZE ANALYSIS

GEL FILTRATION CHROMATOGRAPHY

All gel filtration analysis was performed using a Superose6 PC3.2/30 column connected to a Smart chromatography system (Pharmacia Biotech). 250μg total protein from yeast extract was loaded in a volume of 50μl. The buffer used was 1x lysis buffer. The column was run at a flow rate of 30μl/min and the protein containing fractions (8-20) were analysed by western blotting. Size markers (Pharmacia) were dissolved in the same buffer and run under the same conditions, immediately before and after each sample.

GLYCEROL GRADIENT SEDIMENTATION

5ml gradients of 20-35% glycerol in 1x lysis buffer were poured using a Jencons gradient former and peristaltic pump (Gilson) with the flow rate at 1ml/min, then allowed to settle at 4°C for 2 hours before loading. This method had been used previously in the lab, and found to give good separation over the range 50-600kDa (Sandra Healy, personal communication). 250μg protein samples were carefully applied to the top in a volume of 100μl. The gradients were centrifuged for 16 hours at 42000rpm in a SW55 rotor in a Beckman ultracentrifuge at 4°C. 250μl aliquots were carefully removed starting at the top of the tube using a pipette. The sedimentation position of standard proteins was determined by coomassie blue staining of fractions from an identical gradient loaded with a mixture of known proteins and centrifuged with the samples.

2.10 - PURIFICATION METHODS

HEPARIN SEPHAROSE COLUMN

A 400ml heparin sepharose column on a BioRad econosystem was equilibrated into 1x lysis buffer. The extract, up to 1litre, was loaded at a flow rate of 6 ml/minute. The column was washed with 600ml 1x lysis buffer, followed by 600ml 1x lysis buffer containing 300mM KCl. The HTH-Rad24 protein was eluted with 1x lysis buffer containing 500mM KCl, but without EDTA. 15ml fractions were collected, and analysed by western blot for the presence of HTH-Rad24. The desired fractions were pooled, and imidazole added to a final concentration of 20mM. Heparin Sepharose was regenerated after use according to the manufacturers protocol (Pharmacia Biotech).

NTA-NICKEL COLUMN

An NTA-nickel superflow column, 10ml, was equilibrated into 1x lysis buffer containing 300mM KCl and no EDTA. The pooled fractions from the heparin, approximately 200ml, were loaded onto this column at a flow rate of 1ml/min. The column was washed with 1x lysis buffer containing 300mM KCl, 50mM imidazole and no EDTA. The HTH-Rad24 protein was eluted in 1x lysis buffer containing 300mM KCl, 250mM imidazole. 1ml fractions were collected, and EDTA added to a final concentration of 5 mM to avoid nickel mediated oligomerisation (Sprules *et al.*, 1998). The HTH-Rad24 containing fractions were identified by western blot analysis and pooled.

ANTIBODY COUPLING TO PROTEIN G BEADS

The method used was a modification of those described in (Schneider *et al.*, 1982) and on pages 522-523 of (Harlow E and D., 1988). 400μl 50% protein G slurry (Pharmacia) was resuspended in 15ml PBS, centrifuged at 3000rpm and washed a further two times in PBS. The beads were then transferred to an 1.5ml Eppendorf tube. 0.625ml purified 12CA5 antibody solution (stock concentration 1.6mg/ml, a final ratio of 5mg antibody to 1ml beads) was added and binding allowed to occur for 30 minutes at 4°C with agitation. After centrifugation at 3000rpm the supernatant was discarded and the beads washed into 15ml PBS, and then with a further 2x 15ml PBS. A borate buffer was prepared from 0.1M boric acid and 0.1M sodium borate solutions, which were mixed in a ratio of 7:4, to give a buffer with pH 9.0. The beads were washed twice in 15ml of this buffer. 0.5g dimethylpimelimidate (stored dessicated at –20°C) was dissolved in 50ml

0.1M sodium borate. The resulting solution was checked to ensure the pH was above 8.5, then 15ml was added to the washed beads and coupling was allowed to occur for 1 hour at room temperature in a tube fixed onto a rotating wheel. After this time the beads were washed three times in pH 9.0 borate buffer, then once with Tris buffer pH 9.0 (0.76g Tris-HCl, 5.47g Tris base, in 50ml dH_2O), then the beads were incubated in 15ml Tris buffer pH 9.0 for 15 minutes at room temperature to block unreacted coupling sites. Finally the beads were washed twice in PBS and resuspended in PBS as a 50% slurry. Sodium azide was added at 0.02% and the beads stored for up to two weeks at 4°C.

IMMUNOAFFINITY PURIFICATION

The pooled peak fractions from the nickel column were added to 200μl 12CA5 beads previously equilibrated into 1x lysis buffer with 300mM KCl. Batch binding proceeded for 2 hours at 4°C. The supernatant was then removed, and the beads washed in five washes of lysis buffer containing 300mM KCl. Elution was achieved by incubating the beads in 200μl 1x lysis buffer containing 300mM KCl and 2mg/ml competitor peptide (sequence KKKRILKMYPYDVPDYARIL) at 30°C for 15 minutes. This elution step was then repeated. In order to concentrate the samples for loading onto an SDS-PAGE gel 20μl nickel resin was added to the sample for 1 hour, the beads were collected by centrifugation and the proteins eluted by heating at 95°C in 2x Laemmli loading buffer.

2.11 - MASS SPECTROGAPHIC METHODS

The preparatory gel was coomassie-stained and destained as normal, protein bands were excised, washed three times in 50% methanol, and dried in a speedvac. Identification was done by digesting the material with 0.2μg trypsin (Hellman *et al.*, 1995). The resulting peptide mixture was then loaded onto 2μl bed volume of Poros 50 R2 (Perseptive, Framingham, MA) reversed-phase beads (packed into an Eppendorf gel-loading tip) and stepwise eluted with 4μl of 16% (and then with 4μL 30%) acetonitrile / 0.1% formic acid (Erdjument-Bromage *et al.*, 1998). The "16%" and "30%" peptide pools were each analysed twice by matrix-assisted laser-desorption / ionization (MALDI) time-of-flight (TOF) mass spectrometry (MS), in the presence and absence of peptide calibrants, using a REFLEX III (Brüker-Franzen, Bremen, Germany) instrument equipped with a gridless pulsed-extraction ion source and a 2GHz digitizer, and operated in reflectron mode. Spectra were obtained by averaging multiple signals. For more details see (Webb *et al.*, 1999; Wisniewski *et al.*, 1999). After recalibration with

internal standards, monoisotopic masses were assigned for the most prominent peaks and a peptide mass list generated to search a protein non-redundant database (nr; National Center for Biotechnology Information, Bethesda, MD) using the PeptideSearch algorithm with an accuracy requirement of 30ppm (Mann *et al.*, 1993). For the identification of the 80kDa band, 10 of 20 experimental masses (random matches ≤4/20) matched yeast RAD24 (SwissProt P32641). For the identification of the 40kDa band, 11 of 33 experimental masses (random matches≤5/33) matched yeast RFC2p (SwissProt P40348) and a non-overlapping set of 10 out of 33 masses matchedRFC3p (SwissProt P38629).

2.12 - ACTIVITY ASSAYS

RAD53 KINASE ASSAY

An anti-Rad53 immunoprecipitation was performed from small scale extracts as described above, except that the final precipitating beads were not boiled in Laemmli buffer. Instead, the beads were washed a further three times in kinase buffer (25mM MOPS pH 7.2, 5mM EGTA, 15mM $MgCl_2$, 60mM ß-glycerophosphate, 0.1mM Na_3VO_4, 1mM DTT, 1x Pis). All the buffer was then removed using an Eppendorf gel loading tip, the beads resuspended in 10μl prewarmed kinase buffer, and 10μl reaction buffer was added (Reaction buffer for 10 samples: 100μl kinase buffer, 10μl [γ^{32}P]ATP (NEB 6000Ci/mmol, 10μCi/μl), 2.5μl histone HI (type III-S, from a 10mg/ml stock solution)). The reaction was incubated for 30 minutes at 30°C, then stopped by the addition of 10μl 3xLaemmli buffer. For analysis the samples were separated on 12% acrylamide SDS-PAGE, the gel was dried on a BioRad gel drier, and exposed to Kodax Biomax MS film, using a Biomax screen, at –80°C for 30 minutes to two days (de la Torre-Ruiz *et al.*, 1998).

ATPASE ASSAY

ATP hydrolysis in reaction mixtures containing Rad24 complex and [γ^{32}P]ATP was analysed by thin layer chromatography (TLC). 20μl reactions contained 25mM Tris.HCl pH 7.5, 1mM DTT, 3mM $MgCl_2$, 50μg/ml BSA, 50μM [γ^{32}P]ATP (NEB $1.5x10^4$cpm/pmol), 12.5μM DNA nucleotide equivalents and 1μl purified Rad24 complex. DNA substrates used were ssM13, dsM13, ssM13 annealed to a short complimentary primer (-21 M13 control primer (Perkin-Elmer Applied Biosystems)), or dsM13 that had been irradiated at a concentration of 50μg/ml with a dose of 450J/m^2.

The reactions were incubated at 30°C for 30 minutes, then 5μl each was spotted 2cm from the base of a polyethyleneimine cellulose TLC plate (Polygram Cel 300 PEI/UV_{254}- Camlab). The chromatography was performed in 1M formic acid, 0.5M LiCl for 45 minutes. The released phosphate group migrates more quickly than the ATP in this system. The plate was dried and exposed to BioMax MS film for 1 hour to 2 days.

BANDSHIFT ASSAY- PROBE PREPARATION

A 96mer hairpin DNA (oligonucleotide 805 – see Appendix I), (Tsurimoto and Stillman, 1991) was purified by denaturing gel electrophoresis through a 12% acrylamide gel. The position of the major product was determined by UV shadowing, and the band containing this was excised. The DNA was eluted from this slice by crushing the acrylamide in oligonucleotide elution buffer (0.1% SDS, 0.5M ammonium acetate, 10mM magnesium acetate) and incubating at 37°C for 12 hours with agitation. The oligonucleotide was preciptated from this solution using cold ethanol. A hairpin structure was ensured by resuspending the purified oligo in 1xNEB buffer 2, heating it to 100°C in a boiling bath, and allowing the entire bath to cool slowly to room temperature. The purified probe was labelled with [γ^{32}P]ATP using T4 Polynucleotide Kinase (NEB), in the following reaction; 1μl NEB kinase buffer, 1μl T4 PNK, 1μl [γ^{32}P]ATP, 1μl purified oligo and 6μl H_20, for 30 minutes at 30°C. The reaction was stopped with 5μl 0.5M EDTA and 35μl H_2O. The unincorporated nucleotide was removed by loading the reaction onto a Quick Spin G-25 Sephadex column (Boehringer Mannheim) and centrifuging at 3000rpm for 4 minutes. The column, and retained nucleotide was disposed of, and the elution was used as the labelled probe for the bandshift assays.

BANDSHIFT ASSAY

A non denaturing polyacrylamide gel was poured in a GibcoBRL V16-50 gel apparatus, the gel mixture consisted of 3.67ml 40% acrylamide, 1.63ml 2% bis-acrylamide, 2.25ml 10xTBE, 29.5ml dH_2O, 37.5μl TEMED and 150μl 10% APS. This was allowed to set for at least 2 hours, with a 20 well comb. Bandshift reactions were performed in a 96 well microtitre plate. The following components were mixed on ice; 1μl 10x bandshift buffer (300mM Hepes pH 7.8, 70mM $MgCl_2$, 5mM DTT, 1mg/ml BSA), 0.25μl 20mM ATP or 200μM ATPγS or dH_2O, 1μl appropriate dilution of poly(dI-dC)· poly(dI-dC) and 5μl purified Rad24 complex preparation. dH_2O was added to a final 9.6μl volume.

The plate was removed from the ice bath, and 0.4μl of a 1 in 10 dilution (2.5fmol total) of the labelled probe was added to each. The reaction was incubated at 30°C for 15 minutes. If crosslinking was required 1μl 5% gluteraldehyde was added for 5 minutes at room temperature, then 1μl loading buffer (40% sucrose, 1mg/ml bromophenol blue) was added. The samples were loaded onto the gel, which had previously been pre-run for 45 minutes at 4°C. The gel was run for approximately 2 hours at 250V at 4°C, then dried and exposed to Biomax MS film with a Biomax screen at –80°C for 30 minutes to 2 days.

PLASMID BINDING SIZE SHIFT ASSAY

WT yeast extract was made by the medium scale liquid nitrogen method. pRS313 plasmid DNA was irradiated at a concentration of 50μg/ml with UV light at 450J/m^2, a procedure resulting in approximately 2 pyrimidine dimers per kb (R. Wood pers comm.). 500μg extract was either incubated at 30°C for ten minutes, or 10μg plasmid (either untreated or UV irradiated) was added prior to the incubation. The reactions were fractionated on a superose 6 gel filtration column. Aliquots were analysed by western blot analysis for the fractionation position of Rad24, and by ethidium bromide staining of agarose gels for the fractionation position of the plasmid.

PLASMID BINDING STUDIES- PLASMID BEADS PREPARATION

The plasmids used for this assay were a gift from K. Hartland, they contain either a WT or mutant version of a yeast replication origin. This allowed the binding of origin recognition complex subunits to be used as a control for extract quality, as this system in currently being used successfully in the laboratory of Dr. John Diffley to monitor such activity (K. Hartland, personal communication). Large quantities of the two plasmids were prepared using a Qiagen Maxi prep DNA purification kit. 1mg each plasmid was diluted in dH_2O to a concentration of 50μg/ml. 10ml of each plasmid was irradiated at 450J/m^2 at a fluence rate of 6J/m^2/s. The irradiated and control DNAs were recovered by precipitation with isopropanol; the solution was adjusted to 1.25M NaCl, 50mM Tris.HCl pH 8.5 and 15% isopropanol then 0.7 volumes isopropanol was added to precipitate the plasmids. The solution was centrifuged for 30 minutes in an SS-34 rotor at 11000rpm and 4°C. The pellets were washed in 5ml 70% EtOH, then centrifuged, air dried, resuspended in 200μl dH_2O then the concentration adjusted to 1mg/ml in dH_2O. The plasmids were crosslinked to photoprobe (S-S) biotin (Vector laboratories). The newly opened biotin was reconstituted with 500μl dH_2O, and stored

in 50μl aliquots protected from light at –80°C. 240μl each plasmid (four in total) was mixed with 100μl of a 1 in 100 dilution of photoprobe (S-S) biotin and 140μl dH_2O in a 4 well culture dish. These samples were covered with a petri dish lid, placed on ice and irradiated with a 365nm UV light source 2cm above the samples for 30 minutes. To stop the reaction 480μl 0.1M Tris pH 9.0 was added, followed by 960μl butanol. The mixture was vortexed vigorously, then the butanol layer discarded. This was repeated until the aqueous phase was reduced to 400μl. The plasmids were precipitated by the addition of 96μl 10M ammonium acetate and 1.2ml ethanol at –20°C. After incubation at –20°C for 15 minutes the DNA was pelleted by centrifugation at 13000rpm and 4°C for 15 minutes, then washed with 70% ethanol, dried and resuspended in 240μl dH_2O. 600μl streptavidin dynabeads (Dynal) in an Eppendorf 1.5ml tube, which was placed onto the specially designed Dynal magnet to hold the beads while the supernatant was removed. The beads were washed twice in buffer 1 (10mM Tris.HCl pH 7.6, 1mM EDTA, 2M NaCl), then resuspended in 200μl buffer 1. 200μl biotinylated DNA was added to the beads, which were incubated overnight on a rotating wheel at room temperature. Next morning the beads were washed with twice with buffer 2 (10mM Hepes-KOH pH 7.6, 1mM EDTA, 1M KCH_3CO_2), twice with buffer 3 (10mM Hepes-KOH pH 7.6, 1mM EDTA) and resuspended in 200μl buffer 2 for storage.

PLASMID BINDING STUDIES

In each case, binding reactions contained 80μl beads, 40μl dH_2O, 100μl reaction buffer (80mM Hepes pH 7.6, 1M sorbitol, 32mM $Mg(CH_3CO_2)_2$, 8mM EGTA, 3.2mM DTT, 10mM ATP, 64mM Creatine phosphate, 0.065U/μl creatine phosphokinase, 1xPis, 2.5mg/ml poly (dI:dc)· poly (dI:dc)) and 160μg yeast extract made by the medium scale lysis method (20mg/ml protein concentration). This was incubated at room temperature for 30 minutes, then the supernatant removed and the beads washed three times with 1ml wash buffer (6:5:8 volume ratio of dH_2O:reaction buffer:lysis buffer).The beads were boiled in 60μl 3x Laemmli buffer for 4 minutes to remove the bound proteins. 10μl samples of each bead prep and 10μg samples of load and supernatant samples were loaded for SDS-PAGE, which was analysed by western blot .

2.13 – COMPUTER METHODS

NIH IMAGE

For densitometric analysis of western blots, ECL detection was used, and the filter exposed to pre-flashed Kodak X-Omat film. The film was scanned using Vistascan software and a Umax scanner, the image was reduced to less than 300Kb in Adobe Photoshop and saved as a non compressed TIFF file. This image was opened in NIH Image. The included gel loading macro was used to define each lane, then a densitometry plot was prepared using internal calibration. The area under each peak corresponding to the appropriate bands on the film was allocated using the wand tool. The data set was exported as a delimited text file to Microsoft excel for analysis.

MICROSOFT EXCEL

This program was used for numerical analysis and graph production. Best fit lines were fitted to graphed data using the TRENDLINE function. In order to export graphs to Adobe Photoshop, images were cut and pasted into ClarisDraw, then saved in CGM format, which can be read by Photoshop.

THESIS PRODUCTION

This document was created on an Apple Macintosh iMac, using Microsoft Word 98 with Endnote 3.1. Figures were created in Adobe Illustrator 7.0, with data imported as Adobe Photoshop files from Vistascan capture using a Umax scanner. DNA sequence files in Appendix II are in DNA Strider 3.1 format, the spreadsheet for calculation of protein partial specific volumes on the same disk is a Microsoft Excel 98 document. Protein sequence alignments were created using BoxShade, and are presented as ClarisDraw images.

2.14 - WWW USEFUL SITES

http://www.ncbi.nlm.nih.gov/PubMed/ - A search site for the NCBI PubMed database of scientific publications.

http://www.public.iastate.edu/~pedro/research_tools.html - A comprehensive site listing the tools available on the web for biologists.

http://www.sacs.ucsf.edu/home/hdeacon/stokesradius.html – A clear introduction to the principles and practices of molecular size analysis.

http://www.mamma.com/ - A meta search engine.

http://cellcycle-www.stanford.edu/ - The site for information from the Stanford cell cycle project, analysing cell cycle stage transcription of all the *S. cerevisiae* ORFs.

http://www.neb.com/rebase/rebase.html - The NEB database for restriction enzyme information.

http://www.proteome.com/YPDhome.html – A comprehensive site cataloging the available information of all described *S. cerevisiae*, *S. pombe* and Drosophila proteins.

http://www.biosupplynet.com/ - A commercial site for locating laboratory supplies.

http://vectordb.atcg.com/vectordb/vector.html – A resource for downloading sequence files of published vectors.

http://www-sequence.stanford.edu/group/yeast_deletion_project/deletions3.html – The Stanford resource for obtaining information from the project to systematically delete all *S. cerevisiae* ORFs.

http://genome-www.stanford.edu/Saccharomyces/ - The Saccharomyces Genome Project sequence database.

http://www.abe.msstate.edu/fto/calculator/convert5/html – A resource for the interconversion of scientific units.

http://www.ebi.ac.uk/clustalw/ - Software for the production of multiple alignments.

http://www.shareware.com - A resource for the downloading of shareware and freeware programs.

CHAPTER 3 – INITIAL CHARACTERISATION OF *S.CEREVISIAE* CHECKPOINT PROTEINS

At the initiation of this study a number of groups had previously performed genetic screens in *S. cerevisiae* in order to identify the genes involved in the DNA damage responsive checkpoint pathway. The genes *RAD9*, *RAD24*, *RAD17*, *MEC3*, *RAD53* (also called *SPK1*, *SAD1* or *MEC2*) and *MEC1* (also called *ESR1*) had been identified and cloned (Weinert and Hartwell, 1988; Schiestl *et al.*, 1989; Allen *et al.*, 1994; Kato and Ogawa, 1994; Weinert *et al.*, 1994; Griffiths *et al.*, 1995; Siede *et al.*, 1996; Lydall and Weinert, 1997). The genetic interactions between these genes were beginning to be investigated, leading to the model that Rad9, Rad24, Rad17 and Mec3 function upstream of the presumptive signal transducers Mec1 and Rad53, possibly as sensors of damage (Lydall and Weinert, 1995; Elledge, 1996). The presence of multiple cell cycle checkpoints had been identified, in G1, intra-S and S/M as well as G2 (Siede *et al.*, 1993; Weinert *et al.*, 1994; Paulovich and Hartwell, 1995). It had also been observed that these checkpoint pathways controlled the DNA damage-dependent transcription of a number of genes (Allen *et al.*, 1994; Aboussekhra *et al.*, 1996; Kiser and Weinert, 1996).

In terms of the biochemistry of the known checkpoint proteins, only Rad53 had been intensively studied. It had been determined that Rad53 is a dual specificity protein kinase (Zheng *et al.*, 1993) that is activated by DNA damaging agents in a *MEC1*-dependent manner (Sanchez *et al.*, 1996; Sun *et al.*, 1996). It was also shown that the Rad53 protein is phosphorylated in a cell cycle dependent manner (Sun *et al.*, 1996). Biochemical information about the other components of the pathway was however much more limited. Sequence alignments revealed domains within the proteins with homology to proteins involved in DNA metabolism (Griffiths *et al.*, 1995; Lydall and Weinert, 1995), strengthening the hypothesis that they act as sensors in the pathway. It was therefore decided to initiate a study of these proteins, to attempt to determine whether they are involved in the biochemical processes of DNA damage recognition, and if so how this occurs and the signal is transmitted to the downstream effectors.

3.1 – PRODUTION OF CHECKPOINT PROTEIN SPECIFIC ANTIBODIES

Because the biochemical functions of the checkpoint proteins were unknown, it was necessary to use a method other than an enzymatic activity to begin to study them. Initial attempts in our laboratory to produce epitope tagged versions of the proteins, using a vector encoding a carboxyl terminal His_6-MYC tag were unsuccessful (Jorge Vialard, personal communication). However, a polyclonal antibody raised against a fragment of the Rad9 protein was producing initially promising results (Vialard *et al.*, 1998), and so it was decided that the same approach should be followed for the other known checkpoint proteins. Fragments of the genes *RAD17*, *RAD24*, *RAD53*, *MEC1*, and *MEC3* were amplified by PCR from yeast genomic DNA (primers used are given in Table 3.1.1, see appendix I for sequences) and cloned in frame into the *E. coli* expression vector pET21-b (Novagen) (Figure 3.1.1). pET21-b encodes an amino terminal T7 epitope tag and a carboxyl terminal His_6 tag under the control of a T7 promoter (Figure 3.1.1). The *DDC1* gene has recently been shown to be required for the checkpoint response (Longhese *et al.*, 1997), but because this was not identified at the time, it was not included at this stage.

The expressed polypeptides were purified using NTA-Nickel Agarose (Qiagen) affinity chromatography. Expression and purification conditions were optimised using the anti-T7 antibody (Novagen) for detection by western blot or coomassie blue staining after SDS-PAGE (Figure 3.1.2 and Tables 3.1.1, 3.1.2). Purified polypeptides were used to immunise rabbits at the ICRF polyclonal antibody production facility.

Although successful induction and purification schemes were developed for the majority of pET vector constructs, in some cases there were problems. In the case of the Mec1 fragment and the full length Rad17 constructs no induced product was ever observed by Coomassie staining or western blot using the anti-T7 antibody. Although DH5αcells containing plasmid E00313 (containing full length Rad53) grew with normal kinetics, BL21(λDE3) cells transformed with this plasmid grew very slowly. If IPTG was added to the culture, cell number did not increase further, suggesting that expression of Rad53 is toxic to *E. coli*. The low level of production of the protein under non-inducing conditions probably accounts for the slow growth of this strain. Purification of the small amount of Rad53 produced under non-inducing conditions was

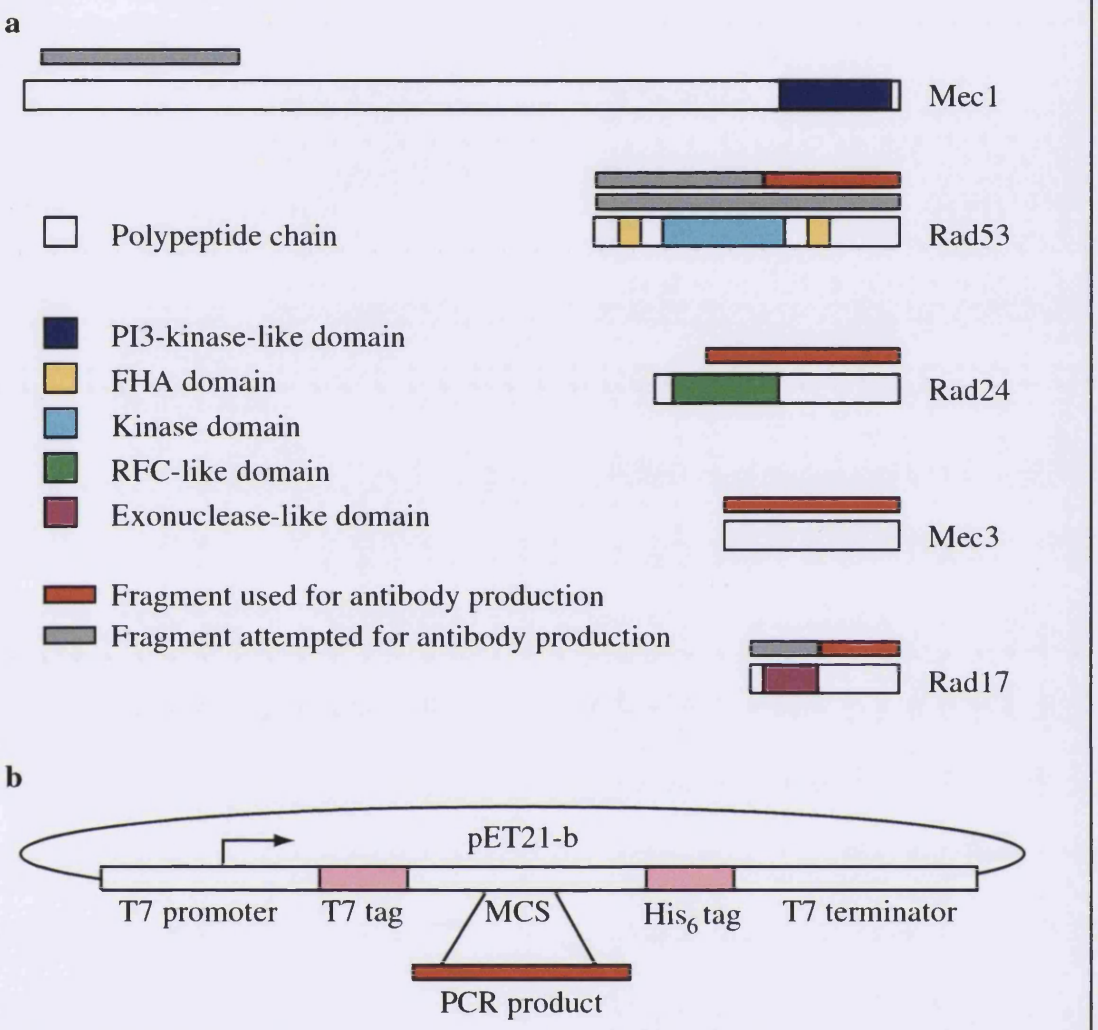

Figure 3.1.1. Schematic representation of checkpoint protein fragments used for antibody production. a) The proteins are depicted as open boxes, with amino termini to the left. Proteins are drawn to scale according to length of amino acid chain. Coloured boxes within the proteins represent the main domains of each protein. Grey or red bars above represent the fragments used, unsuccessfully or successfully, for antibody production. b) The pET21-b vector used for expression of the fragments, which were cloned into the multiple cloning site (MCS) as indicated. Transformation of the constructs into *E. coli* strain BL-21(λDE3) allows IPTG induced expression of the T7 RNA polymerase which results in expression of the required fragment.

attempted. Although the amount of Rad53 produced was readily detectable using the anti-T7 antibody for western blot analysis, it was not possible to produce sufficient material for antibody production purposes.

FRAGMENT	VECTOR	PRIMERS	IPTG (mM)	Time (hours)	Temp (°C)
Rad24	E00347	N00442/443	2	3	37
Mec3	E00312	N00362/363	2	3	37
Rad17NE	E00354	N00441/509	1	2	30
Rad17E	E00353	N00510/358	1	2	30
Rad53FL	E00313	N00360/361	none	Harvest when A600 = 1.0	25
Rad53NK	E00344	N00487/361	2	4	37
Rad53K	E00343	N00360/488	2	1	37

TABLE 3.1.1. Optimised induction conditions for recombinant fragments. *E. coli* strain BL-21 was freshly transformed with the appropriate plasmid for each induction, (the primers used in the cloning are given in the table – sequences can be found in appendix I). A single colony was picked into 10 ml LB/Amp and grown to stationary phase overnight. This starter was used to inoculate a 500ml culture, which was grown until the absorbence of the culture at 600nm was 0.6. IPTG was added to the concentration given in this table and if required the flasks were removed to the induction temperature given above. Induction was for the times shown in this table, after which cells were harvested by centrifugation and the expressed proteins purified (Table 3.1.2). Rad17NE and Rad17E – fragments of Rad17 not containing or containing the exonuclease domain respectively, Rad53FL, NK and K – Full length Rad53 or fragments not containing or containing the kinase domain respectively.

The resulting polyclonal sera were tested for specificity against the recombinant polypeptides and yeast whole cell extracts in western blots. Sera that were able to recognise a specific band in wild type yeast extracts but not in extracts made from yeast strains with the corresponding gene deleted were obtained for *RAD17*, *RAD24*, *RAD53*, and *MEC3* (Figure 3.1.3). The western blotting conditions for these sera were optimised (Table 3.1.3).

FRAGMENT	Solubilisation	Binding	Washes	Elution
Rad24	A	A (no I)	B, C	C (+250mM I)
Mec3	A	A (no I)	B	C
Rad17NE	B	B (no I)	none	B (+250mM I)
Rad17E	B	B (no I)	none	B (+250mM I)
Rad53NK	A	A (+2mM I)	B	Beads injected
Rad53K	A	A (+2mM I)	B	Beads injected

TABLE 3.1.2. Optimised conditions for purification of recombinant fragments using NTA-Nickel agarose chromatography. Cell pellets from 400ml cultures after induction (Table 3.1.1) were solublised by resuspension in buffer containing either 6M guanidine (A) or 8M urea (B) for 2 hours at room temperature with stirring. Extracts were clarified by centrifugation and imidazole (I) added to the specified binding concentration. The extract was batch bound to 2ml pre-equilibrated NTA-Nickel resin at room temperature for 1 hour and the resin loaded onto a column. The resin was washed and the protein eluted as specified in this table.

Buffers: A – 6M Gu·HCl; 0.1M NaH2PO4; 0.01M Tris·Cl, pH 8.0.

B – 8M urea; 0.1M NaH2PO4; 0.01M Tris·Cl, pH 8.0.

C - 8M urea; 0.1M NaH2PO4; 0.01M Tris·Cl, pH 6.3.

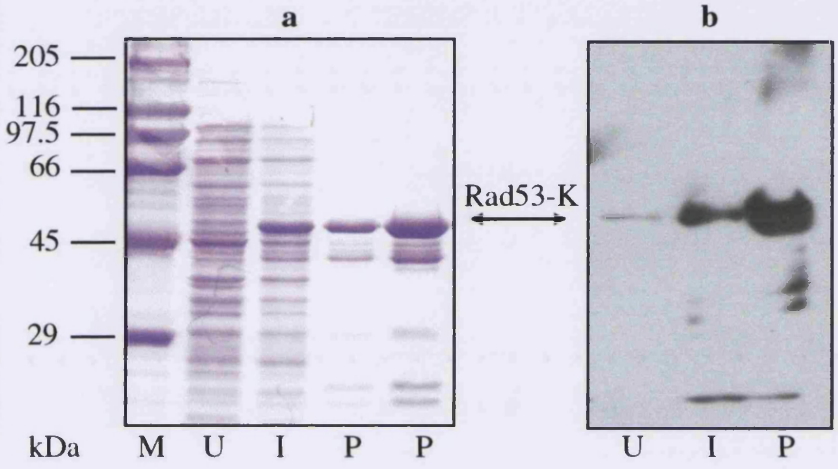

Figure 3.1.2. An example of the production of recombinant checkpoint protein fragments. E. coli BL21(λDE3) strain was transformed with vector E00343. Recombinant protein was induced and purified as in Tables 3.1.1 and 3.1.2.
a) Coomassie blue stained 10% SDS-PAGE with M-Molecular weight markers (Sigma SDS-6H), U-Uninduced whole cell lysate, I-Induced lysate, P-Purified recombinant protein boiled from Ni-NTA agarose beads.
b) Western blot from a similar gel using the anti-T7 monoclonal antibody (Novagen).

ANTIBODY	EPITOPE	GEL (%)	BLOCK	PRIMARY
NLO16	Rad52NK	6.5 - 8.0	1% (w/v)	1/5000 o/n 1% milk
NLO25	Mec3	8 - 10	3% (w/v)	1/3000 o/n 3% milk
NLO28	Rad24	7.5 - 10	3% (w/v)	1/3000 o/n 1% milk
NLO32	Rad17NE	8.5 – 10	1% (w/v)	1/1000 o/n 3% milk

TABLE 3.1.2. Optimised conditions for detection of checkpoint proteins in yeast whole cell extracts using new rabbit polyclonal sera. Yeast extracts were separated through SDS-PAGE. The percentage of acrylamide in the gel was as in this table, all were prepared using the protogel system (National Diagnostics). Mini-gels (BioRad) were run at 200Vuntil the bromophenol blue (included in the loading buffer) was off the bottom. Gels were transferred to Hybond C-extra nitrocellulose filters (Amersham) using a semi-dry transfer system (BioRad). Transfer was at 13V for 35 minutes. Filters were blocked with milk powder dissolved in PBS-T at the concentrations given in this table. Primary antibodies were incubated with the filters overnight at the dilutions given here. Primary antibody was removed with five washes in PBS-T and secondary anti-rabbit-HRP-linked antibody (Amersham) was used at a dilution of 1/10000 for 30 minutes with no milk in all cases. After a final five washes in PBS-T the proteins were detected using ECL reagents (Amersham) according to the manufacturers protocol (1-2ml total reagent per filter) and exposure to X-Omat film (Kodak). Exposures of 1-20 minutes were usually sufficient.

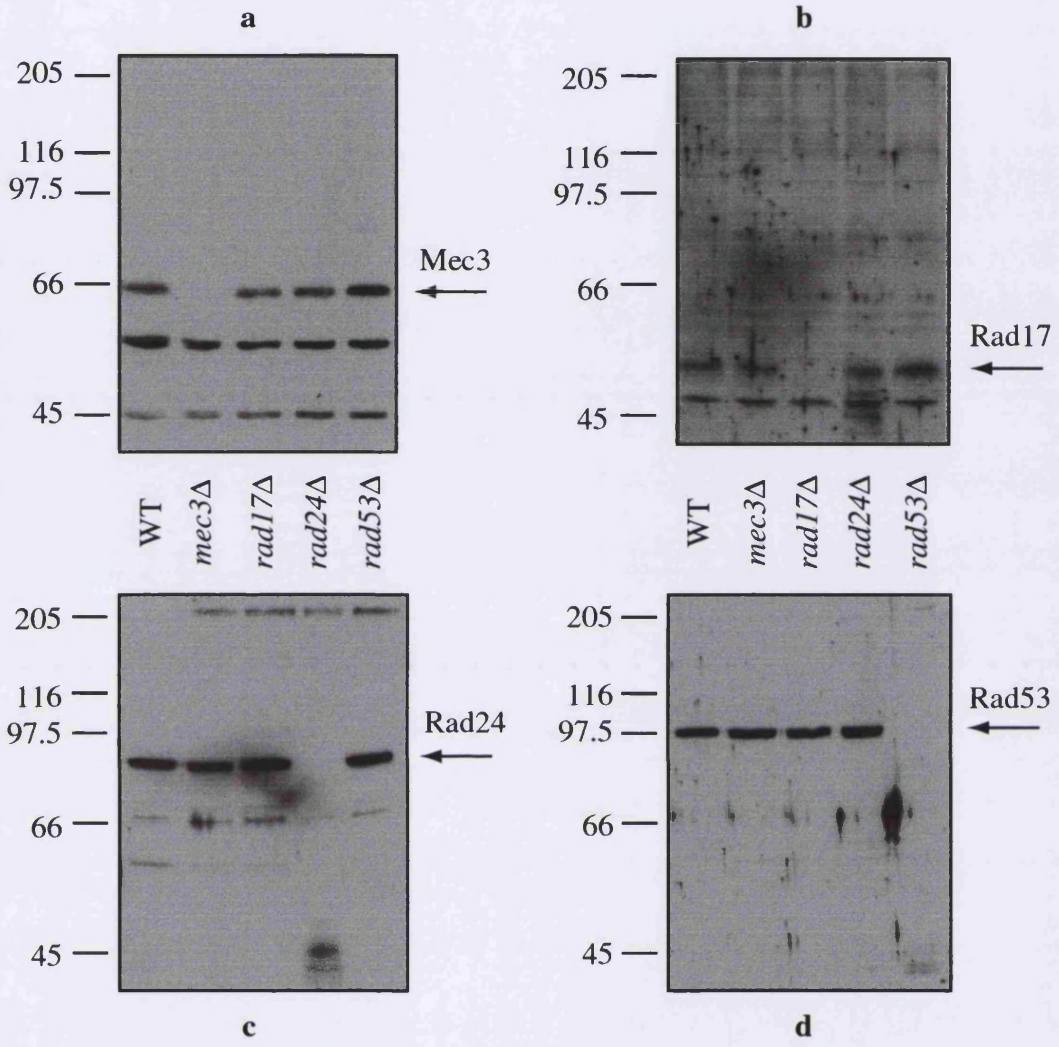

Figure 3.1.3. Western blot confirmation of antibody specificity. Whole cell yeast extracts from the strains indicated were analysed by western blot using the conditions given in table 3.1.3.
a) NLO25 serum.
b) NLO32 serum.
c) NLO28 serum.
d) NLO16 serum.
All gels were 8.5% acrylamide in this case. The migration positions of standard markers, in kDa (Sigma SDS-6H), is indicated to the left.

3.2 – ANALYSIS OF CHECKPOINT PROTEINS DURING THE CELL CYCLE

The Rad9, Rad53 and Ddc1 proteins have been reported to undergo cell cycle stage dependent phosphorylation (Sun *et al.*, 1996; Longhese *et al.*, 1997; Vialard *et al.*, 1998). A block and release cell cycle experiment was performed to determine if the other checkpoint proteins undergo such regulation. WT yeast cultures in mid logarithmic growth phase were arrested in the G1 phase of the cell cycle by addition of 10mg/ml α factor mating pheromone. Cell morphology was analysed until at least 95% of cells were unbudded. This took approximately 2.5 hours. The α factor was removed by washing the cells and resuspending them in fresh, pre-warmed media. Samples were taken over the next 3 hours and prepared for western blot analysis (Figure 3.2). In this experiment the Rad9 protein was modified as previously described. No differences in the quantity of Rad24, Rad17 or Mec3 or their migration through SDS-PAGE were observed as the cells progressed through the cell cycle. The reported cell cycle dependent modifications of Rad53 were not observed. This is likely due to differences in the SDS-PAGE conditions used, and to the fact that the NLO16 serum used here recognises the unphosphorylated forms of Rad53 more efficiently than the phosphorylated forms (Muriel Grenon, personal communication).

3.3 – ANALYSIS OF CHECKPOINT PROTEINS AFTER DNA DAMAGE

The checkpoint proteins Rad9, Rad53 and Ddc1 are also modified by phosphorylation after yeast cells are treated with DNA damaging agents (Sun *et al.*, 1996; Longhese *et al.*, 1997; Emili, 1998; Vialard *et al.*, 1998). In order to investigate whether similar modification of Rad24, Rad17 or Mec3 occurred, DNA damage exposure experiments were performed. Yeast cultures in mid logarithmic growth phase were either treated with MMS, exposed to UV irradiation or mock treated as described in the materials and methods section. Samples were removed after 30 and 60 minutes and prepared for western blot analysis (Figure 3.3). No differences in the quantity of Rad24, Rad17 or Mec3 or in their migration through SDS-PAGE were observed after any of the treatments performed. The positive control blot for Rad53 showed that the treatments had been effective as this protein was modified.

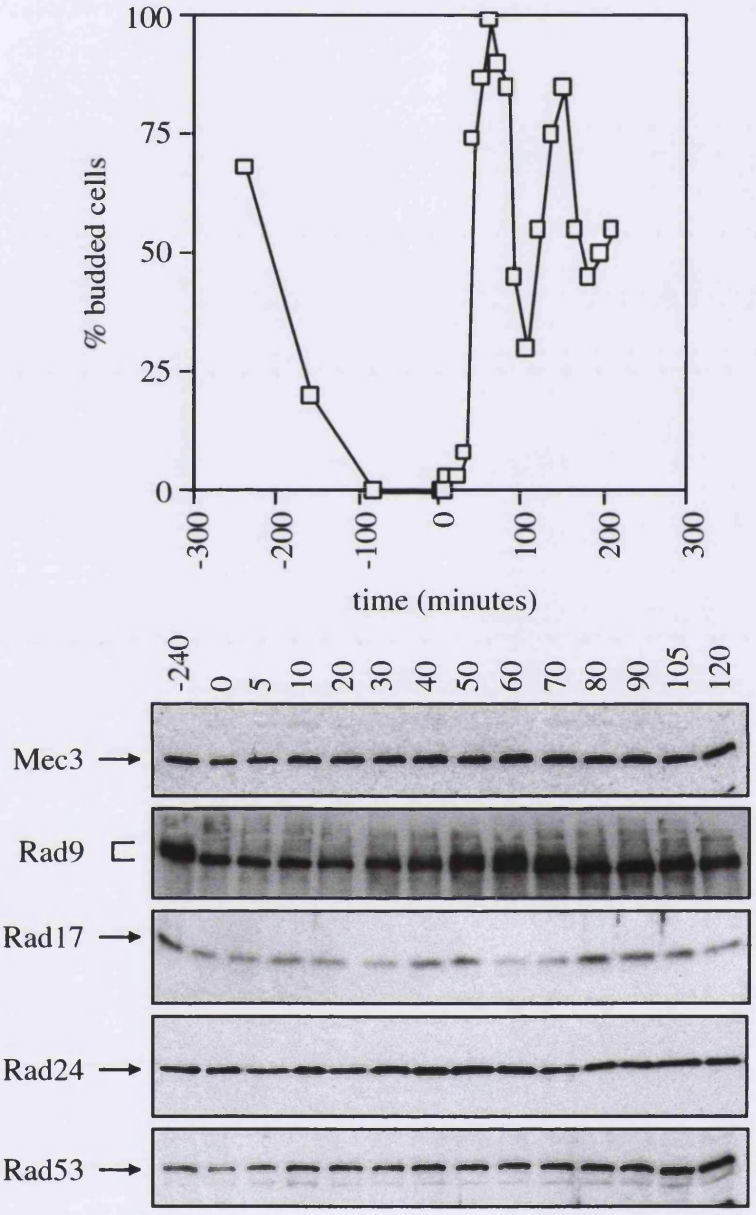

Figure 3.2. Analysis of the checkpoint proteins during the cell cycle. A culture of WT yeast was arrested in G1 phase by the addition of α factor at -240 minutes. At time 0 the α factor was removed by washing and the cells allowed to re-enter the cell cycle. Samples were taken for morphology analysis (graph) and western blot analysis (panels below) at the time points indicated.

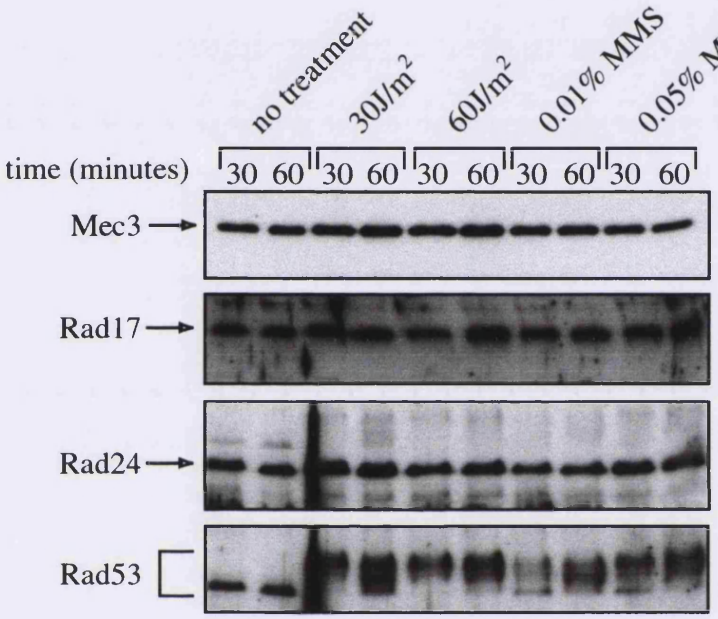

Figure 3.3. Analysis of checkpoint proteins after DNA damage. In each case mid logarithmic cultures were treated with the indicated doses of UV or MMS as described in the materials and methods section. Small scale ribolyser extracts were prepared and 10µg total protein was loaded in each lane for SDS-PAGE. Immuno-blotting was performed as described in the materials and methods section.

3.4 – DETERMINATION OF THE QUANTITY OF EACH CHECKPOINT PROTEIN PER CELL

To conclude the basic characterisation of the checkpoint proteins the number of molecules of each protein present in a logarithmically growing haploid cell was determined. This had previously been estimated for Rad9 as approximately 500 copies per cell (Jorge Vialard personal communication). To determine whether the other checkpoint proteins were also of low copy number it was necessary to perform quantitative western blot analyses. Recombinant checkpoint protein fragments were prepared as previously (Tables 3.1.1 and 3.1.2) and quantitated against BSA standards (for examples see Figure 3.4.1). Known amounts were subjected to western blot analysis alongside total denatured yeast extracts made from a fixed quantity of cells. The ECL developed filters were exposed to pre-flashed film, and a standard curve of optical density against amount of recombinant protein was produced. From this curve, the quantitative amount of checkpoint protein in the yeast sample was interpolated (for examples see Figure 3.4.2), and hence copy number per cell was determined. (Table 3.4)

Protein	Mass(pg) per µl yeast extract	Mass per cell (x 10^{-17}g)	Molecular mass (Da)	Moles per cell (x10^{-22})	Molecules per cell
Rad17	20	1	46000	2.2	130
Rad24	50	2.5	76000	3.3	200
Rad53	400	20	92000	22	1300
Mec3	200	10	53000	19	1100

Table 3.4.1. Estimation of the number of molecules of each checkpoint protein per haploid yeast cell. See figures 3.4.1 and 3.4.2 for experimental details.

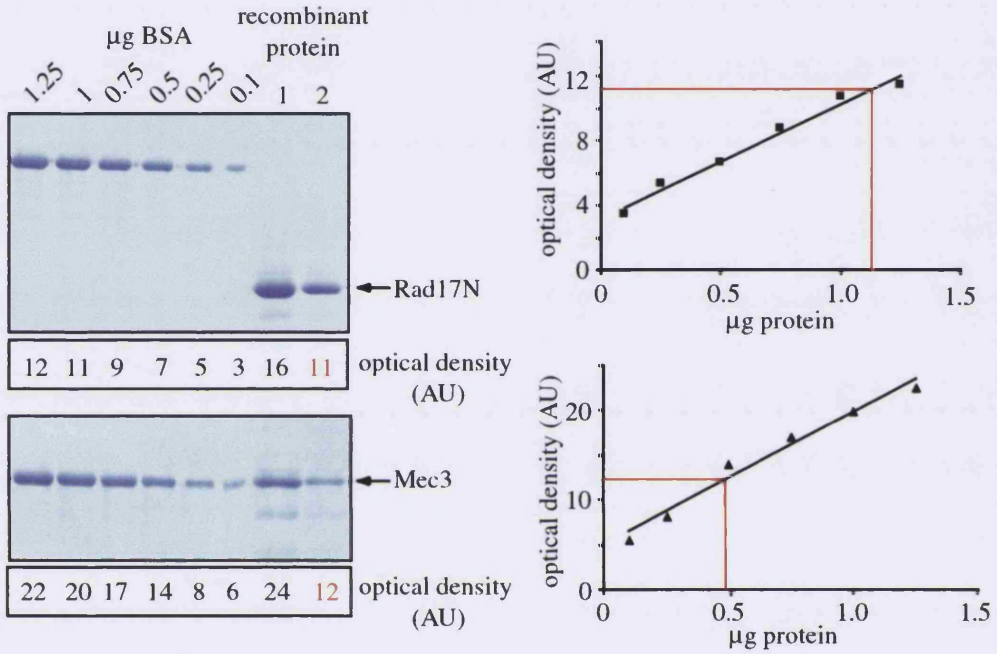

Figure 3.4.1. Production and quantitation of recombinant fragments for copy number estimation. Rad17 and Mec3 are shown as examples. The recombinant proteins were induced and purified as described in Tables 3.1.1 and 3.1.2. For quantitation the Coomassie stained gel was scanned and optical density of each band determined using the NIH Image software. The density of the BSA standards was plotted against amount loaded to give a standard curve, from which the quantity of recombinant protein was interpolated. The optical density and inferred protein quantity of the number 2 sample in each case is marked in red on the graphs. AU = arbitrary units.

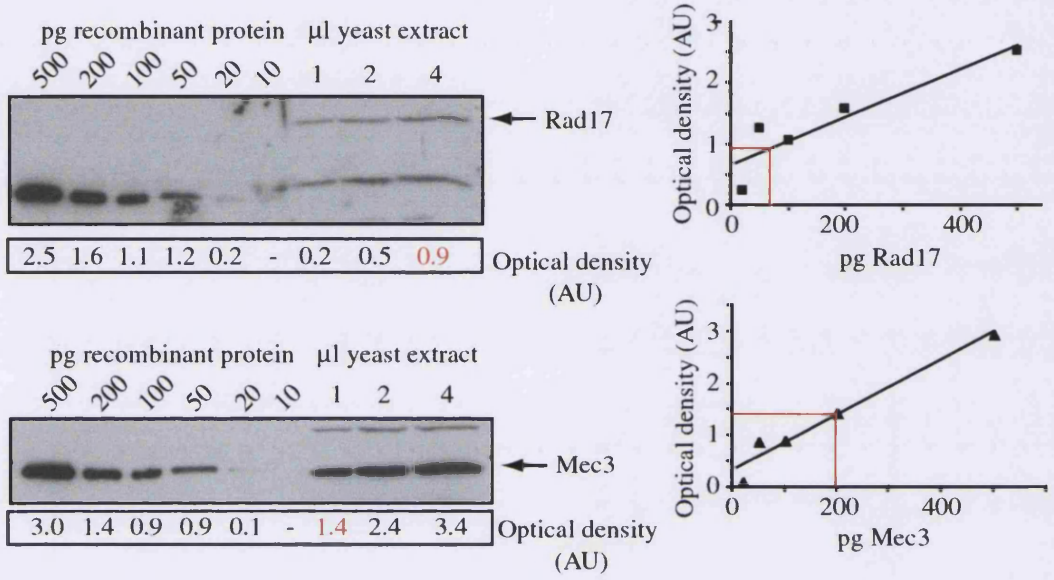

Figure 3.4.2. Estimation of amount of Mec3/Rad17 per cell. Quantitative western analysis to compare the signal from known amounts of recombinant proteins with that from known numbers of yeast cells. Amounts were loaded as shown, and exposed to pre-flashed film. Optical density of the standards were determined using the NIH Image software after scanning, and plotted against amount loaded to give a standard curve from which the amount of Mec3 or Rad17 in each sample was interpolated. The optical density and inferred amount of each protein in the lanes indicated in red are depicted on the graphs. $1x10^8$ cells resulted in 50µl yeast extract as described in the materials and methods section. From the interpolated quantity the number of molecules of each protein per cell was calculated (Table 3.4). AU = arbitrary units.

3.5 – INVESTIGATION OF CHECKPOINT PROTEINS INTERACTIONS

Many of the initial studies into the genetics of the checkpoint pathway in *S. cerevisiae* concluded that the genes *RAD24*, *RAD17* and *MEC3* are in the same epistasis group (Lydall and Weinert, 1995; Lydall and Weinert, 1997; de la Torre-Ruiz *et al.*, 1998). Often models for checkpoint pathway function proposed that the protein products of these genes may interact in protein complex. In order to investigate whether these proteins associate with each other and whether such interactions are regulated, co-immunoprecipitation and co-purification studies were initiated.

For the co-immunoprecipitation analysis extracts were prepared from WT cells either untreated (Figure 3.5.1) or irradiated with UV light (Figure 3.5.2). The immunoprecipitations were performed as described in the materials and methods section. With the exception of the anti-Rad17 antibody, all the precipitations resulted in good depletion of the target protein from the extracts (compare Load and Supernatant lanes in Figures 3.5.1 and 3.5.2). In the un-irradiated samples the only interaction detected was between Rad17 and Mec3. The anti-Rad17 antibody precipitation resulted in the co-precipitation of Mec3 (Figures 3.5.1). This co-immunoprecipitation data also does not imply a direct physical interaction, as there could be other, bridging proteins involved. One of the difficulties with these co-immunoprecipitation studies was that the antibodies used for the precipitation stages were of the same origin as the antibodies used for the detection stage, both being rabbit polyclonals. After the precipitation the associating proteins were removed from the protein A beads by boiling in Laemlli buffer before SDS-PAGE. This process also removes the precipitating antibodies from the beads, which are resolved with the precipitated proteins during the gel run. Antibodies are comprised of 2 heavy (approx. 50kDa) and 2 light (approx. 30kDa) chains, held together by di-sulphide bridges. These di-sulphide bonds are cleaved by reduction in laemlli buffer so the 2 chains migrate independently. The HRP-linked secondary antibody used is a donkey anti-rabbit antibody, which also recognise the chains of the precipitating antibody which are resolved in the gel. This results in a very dark signal at 30kDa and 50kDa, masking any signal from proteins of these sizes, this is a particular problem for Rad17 which migrates at approximately 50kDa. It was therefore not possible to analyse whether the Mec3 antibody co-precipitated Rad17. A second problem with this analysis was the continued difficulties with the anti-Rad17

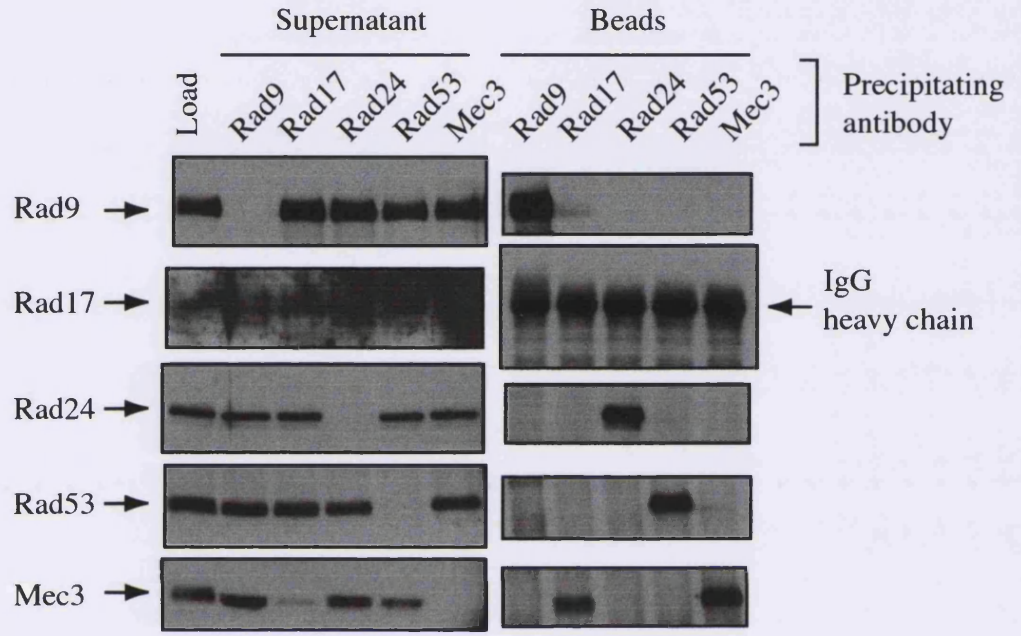

Figure 3.5.1. Co-immunoprecipitations of the checkpoint proteins from extracts made from logarithmically growing cells. In each case 500µg was used for the precipitations in a final volume of 500µl, and antibody was added to a final dilution of 1 in 50. The antibodies used for the precipitations are indicated above the images, the antibodies used for the western blot analyses are indicated to the left. For the western blot analyses 10µl of each starting extract and supernatant was loaded. The total proteins bound to the precipitating beads were removed by boiling in 50µl Laemmli buffer, 20µl of this was loaded onto the gel for western analysis. In this case the signal was much stronger from the beads than the loads or supernatants, and so lighter exposures are shown here (20 seconds versus 5 minutes).

antibody. The quality of western blots obtained using this antibody was variable and often very poor. This was one of the reasons that later studies focussed on the Rad24 protein. It should be noted that this experiment is not fully controlled, as it is possible that the Rad17 antibody is precipitating Mec3 in a Rad17 independent manner. To fully establish that this Rad17-Mec3 interaction is occurring it would be necessary to demonstrate that Mec3 is not precipitated by this antibody from extracts made from *rad17Δ* cells. However, interactions between Mec3, Rad17 and Ddc1 have been described recently by other groups (Paciotti *et al.*, 1998; Kondo *et al.*, 1999) and see Section 3.6 - Discussion.

When the co-immunoprecipitation studies were performed from extracts made from UV irradiated cells slightly different results were obtained. The interaction between Rad17 and Mec3 was still observed and a DNA damage-dependent interaction was observed between Rad53 and Rad9 (Figure 3.5.2). Precipitation with the anti-Rad53 antibody resulted in the co-precipitation of some Rad9 protein. It appeared that only the phosphorylated (slower migrating) forms of Rad9 were precipitated. Clearly only a fraction of the cellular Rad9 was precipitated as there was no observable depletion of Rad9 in the supernatant sample after anti-Rad53 precipitation. In the reciprocal precipitation it appeared that some Rad53 protein was precipitated by the anti-Rad9 antibody. This was very difficult to detect from this quantity of extract. The anti-Rad53 antibody is approximately ten time less sensitive in western blot analysis than the anti-Rad9 polyclonal (data not shown), it is therefore possible that using more starting material might improve this signal. It appeared that the phosphorylated form of Rad53 was precipitated by the anti-Rad9 antibody. The amount of Rad53 in the supernatants from the anti-Rad9 precipitation was not appreciably lower than in the load sample, suggesting that only a small fraction of the total Rad53 was precipitated. As mentioned above these results do not demonstrate a direct interaction between Rad9 and Rad53, and they are not conclusive due to the lack of the appropriate deletion strain controls. However, this DNA damage-dependent Rad9-Rad53 interaction has recently been shown by other methods (Emili, 1998; Sun *et al.*, 1998; Vialard *et al.*, 1998) and we

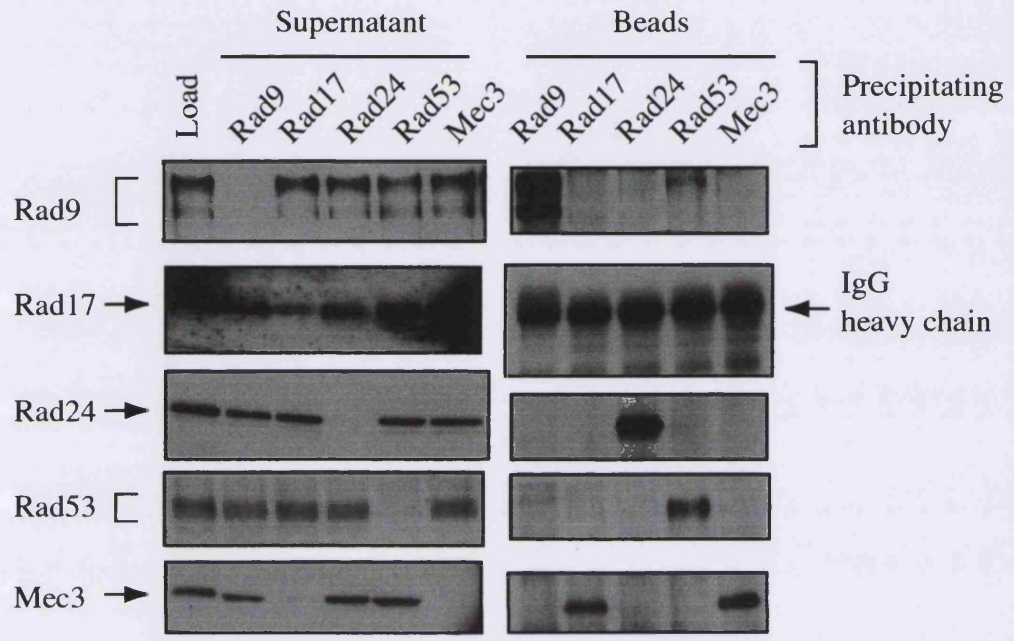

Figure 3.5.2. Co-immunoprecipitations of the checkpoint proteins from extracts made from cells treated with UV (40J/m^2). In each case 500µg was used for the precipitations in a final volume of 500µl, and antibody was added to a final dilution of 1 in 50. The antibodies used for the precipitations are indicated above the images, the antibodies used for the western blot analyses are indicated to the left. For the western blot analyses 10µl of each starting extract and supernatant was loaded. The total proteins bound to the precipitating beads were removed by boiling in 50µl Laemmli buffer, 20µl of this was loaded onto the gel for western analysis. In this case the signal was much stronger from the beads than the loads or supernatants, and so lighter exposures are shown here (20 seconds versus 5 minutes).

have purified the Rad9 complex to homogeneity and demonstrated that it contains Rad53 after DNA damage (Gilbert *et al.*, 2000).

Under no conditions tested was an interaction observed between Rad24 and any other checkpoint protein, even if only very low stringency washes were used. It is possible however, that the interaction between an antibody and its antigen, which is usually of a high affinity, can perturb the normal interaction of that antigen with other molecules. For this reason, the results presented here were not sufficient to draw the conclusion that there are no interactions between Rad24 and Mec3, Rad17, Rad9 or Rad53. In order to further investigate the possibility that Rad24 interacts with other checkpoint proteins some non-immunological techniques were used. Firstly it was observed that Rad24 and Mec3 behaved very differently when extracts were precipitated with polyethylenimine (PEI) (Figure 3.5.3). PEI selectively precipitates chromatin, although some non-chromatin proteins may also be precipitated. This data suggests that at least the majority of these proteins are not associated with each other in a stable manner.

Because of the difficulties resulting from the unreliable anti-Rad17 antibody it was decided to approach the question of whether Rad24 interacts with Rad17 in a different manner. Two separate approaches were used. Firstly an *E. coli* expression vector was constructed that expressed a fusion protein comprising of Rad17 and a glutathione S-transferase (GST) moiety. The expressed product and a GST control were purified from *E. coli* extracts using glutathione sepharose beads as described in the materials and methods section. These beads were used as affinity reagents to investigate whether Rad24 from yeast whole cell extracts would specifically associate with GST-Rad17. In the original experiment the results appeared promising, a band that was recognised by the anti-Rad24 antibody was bound with high affinity to the Rad17 column (Figure 3.5.4). This band was observed independent of whether the yeast extracts were made from cultures that had been UV irradiated or not (data not shown). However further analysis revealed that this band was in fact a contaminant polypeptide, the band was still present if the yeast extract used for the affinity pull down was made from a *rad24Δ* strain (Figure 3.5.4). This contaminant was found to be an *E.coli* protein that co-purified with the recombinant GST-Rad17 on the glutathione sepharose column, as it was detected if the beads alone were analysed by western blot (Figure 3.5.4). Attempts

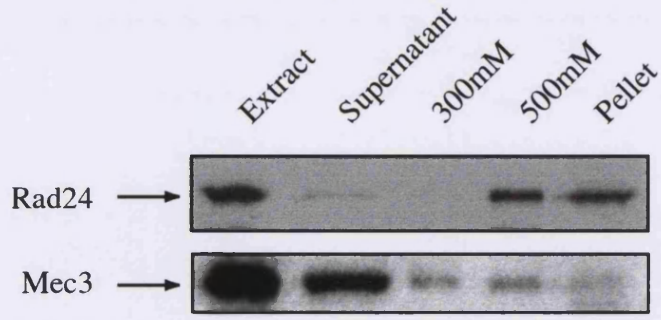

Figure 3.5.3. 0.1% PEI precipitation from native extracts. The precipitation was performed from 500µg small scale extracts at a protein concentration of 1mg/ml. Polyethylenimine (PEI) was added to 0.1% from a stock 10% pH7.0 solution and precipitation was for 30 minutes at 4°C. The resulting pellet was washed with 1x lysis buffer containing 300mM then 500mM KCl then resuspended in Laemmli buffer and boiled. 10µg starting extract and equivalent fractions of each step were loaded for western blot analysis.

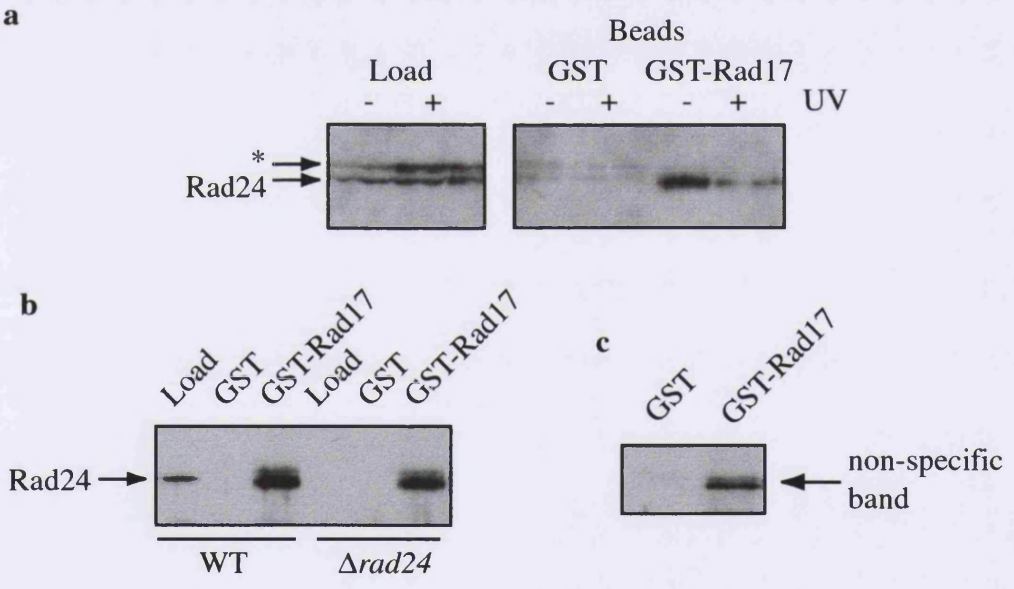

Figure 3.5.4. Pull-down analysis using GST-Rad17 beads. Beads were prepared as described in Materials and Methods. a) Pull downs from extracts made from a diploid yeast strain expressing tagged (*) and native Rad24, either with or without UV treatment (see Fig 5.1.1 and 5.1.2). The pull down was from 500µg extract, 10µg was used for western analysis of the load fraction. The beads were washed in lysis buffer then boiled in Laemmli buffer and half the total released protein was used for analysis. b) As part a, except the extracts used were from WT or Δ*rad24* strains without UV treatment. c) The GST or GST-Rad17 beads were prepared then washed in lysis buffer and boiled in Laemmli buffer. The released proteins were analysed by western blot using the anti-Rad24 polyclonal.

were made to purify the recombinant protein under more stringent conditions, but with no success. This contaminating band made it impossible to use this technique to investigate possible interactions between Rad17 and Rad24.

A final attempt to demonstrate an interaction between Rad24 and Rad17 utilised an epitope tagged version of the Rad17 protein (for a description of the production of such an epitope tagged protein see Section 5.1). The epitope tag used in this case consisted of ten histidine residues and was located at the amino terminus of the protein. The epitope tagged version of *RAD17* (designated *H-RAD17*) replaced the endogenous *RAD17* gene at the *RAD17* locus. The survival of the *H-RAD17* strain after UV irradiation was not significantly different from a WT strain, indicating that the H-Rad17 protein is functional (data not shown). A similar strain was produced with a ten histidine tagged version of *RAD24* – designated *H-RAD24*. Whole cell extracts were made from these strains, and passed through an NTA-Nickel agarose column, which has a high affinity for histidine residues.The bound proteins were eluted from the column using imidazole and analysed by western blotting using the anti-Rad24 antibody (Figure 3.5.5). H-Rad24 efficiently bound and was eluted from the column, but no Rad24 was detected in the elution from the H-Rad17 containing extract, suggesting that Rad17 and Rad24 do not stably interact. However, using the anti-Rad17 to analyse the eluted material was not successful so it is possible that the H-Rad17 was not efficiently bound to the column.

3.6 – DISCUSSION

The production of polyclonal antibodies specific to the checkpoint proteins has proven to be a valuable tool for investigating the biochemistry of this pathway. Unfortunately the set of reagents described here is not complete. Due to difficulty expressing the recombinant fragments in *E. coli* no antibody was raised against the Mec1 protein. This protein is still largely unstudied. Our laboratory has recently developed a polyclonal sera raised against a different fragment of this protein (Chris Gilbert, unpublished data). Similar studies to those described here are therefore being initiated to attempt to dissect the role of Mec1 in the checkpoint pathway. Because the Ddc1 checkpoint protein had not been identified at the initiation of this study we did not raise antibodies against it. It

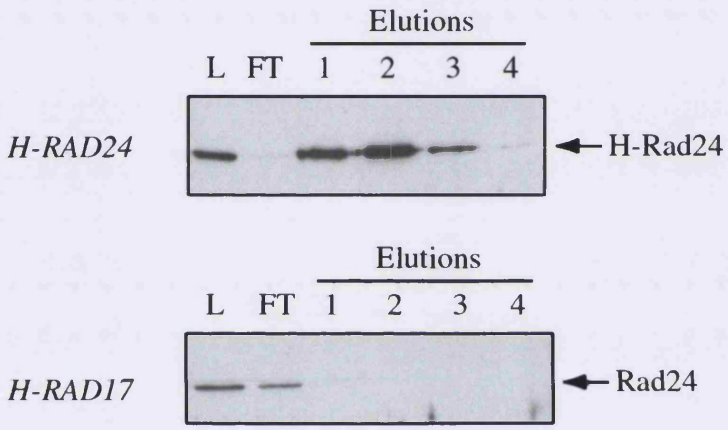

Figure 3.5.5. Purification of yeast extracts on NTA-Ni agarose columns. Extracts were prepared from the strains indicated to the left, expressing either Rad17 or Rad24 with a six histidine epitope tag at the amino terminus. 5mg was bound to a 100µl NTA-Ni agarose column. Proteins were eluted in lysis buffer containing 200mM imidazole. 10µg each of load (L) and flow through (FT) and 1/20 the each elution fraction were analysed by western blot using the anti-Rad24 polyclonal.

would be useful to produce these, and a more effective sera against Rad17 in order to have a full complement of reagents in the laboratory.

Unlike the Rad53, Ddc1 and Rad9 proteins no modifications to Rad17, Rad24 or Mec3 were detected by SDS-PAGE either during a cell cycle or after DNA damage treatments. It is always possible that modifications do occur but do not result in a change in mobility through SDS-PAGE. Isoelectric focussing or radiolabelling could be used to resolve this issue. If these proteins are not modified, it is possible that their activities are regulated by some other mechanism. One such mechanism could be cellular localisation. The site of activation of the DNA damage-dependent checkpoint pathway is presumed to be lesions in DNA in the nucleus. Regulation of the cellular position of the checkpoint proteins would allow checkpoint activation to be modulated. It should be possible to investigate the subcellular localistion of the checkpoint proteins using the polyclonal antibodies described here for *in vivo* immunofluorescence.

The finding that the checkpoint proteins are expressed at such a low copy number was surprising, as if these proteins are acting as a general sensor of global genomic DNA damage it might be expected that more molecules are needed to constantly survey the entire genome. This is another indication that a basic model, in which Rad9 and the other upstream checkpoint proteins are the direct sensors of DNA damage may be an over simplification. The higher quantity of Mec3 per cell compared to Rad17 and Rad24 may be due to the participation of Mec3 in pathways other than checkpoint activation. It has recently been demonstrated that Mec3 interacts with the Set1 protein, and has a role in telomere function, independent of the other checkpoint proteins (Corda *et al.*, 1999).

Many groups have recently begun to investigate possible interactions between the proteins of the DNA damage-dependent checkpoint pathways in *S. cerevisiae*, *S. pombe* and human systems. After sequence analysis of Rad17 homologues revealed that this protein has homology to PCNA (Thelen *et al.*, 1999), the hypothesis that Rad17 should interact with Rad24, in a manner analogous to PCNA with RFC, was strengthened. Interactions between Rad17, Mec3 and Ddc1 were identified (Paciotti *et al.*, 1998; Kondo *et al.*, 1999). All the members of this complex were subsequently found to share

sequence homology with PCNA (Venclovas and Thelen, 2000), and similar interactions were identified between the human and *S. pombe* homologues (Kostrub *et al.*, 1998; St. Onge *et al.*, 1999; Volkmer and Karnitz, 1999; Caspari *et al.*, 2000; Hang and Lieberman, 2000). No groups have successfully identified interactions between *S. cerevisiae* Rad24 and the Rad17 PCNA-like complex, however very recently, interactions have been identified between *S. pombe* and human Rad17 and Rad1 complexes (Caspari *et al.*, 2000; Rauen *et al.*, 2000), the homologues of *S. cerevisiae* Rad24 and Rad17 respectively. Therefore is seems likely that there is an interaction between *S. cerevisiae* Rad24 and Rad17. The failure to detect this interaction could be due to a number of factors, for example it is possible that the interaction is very transient, or weak, or that only a small proportion of the cellular population of these proteins interact at any one time, or that the interaction only occurs on the DNA. It may therefore be possible to demonstrate such an interaction using different techniques to those tried here, perhaps two hybrid analysis or immunoprecipitation after crosslinking.

CHAPTER 4 – HYDRODYNAMIC PROPERTIES OF *S.CEREVISIAE* CHECKPOINT PROTEINS

Although no interaction had been detected between the checkpoint proteins using immunoprecipitation, nickel purification or GST pull-down approaches, because of the limitations of these techniques, it was still possible that such interactions did occur. It was also possible that these proteins interacted with other, as yet unidentified components of the checkpoint pathway. In order to investigate whether the checkpoint proteins do exist as components of multi-protein complexes, molecular size analyses were performed.

4.1 - STOKES RADIUS DETERMINATION BY GEL FILTRATION

Gel filtration chromatography, also called size exclusion chromatography, utilises differences in the size of molecules to separate them. The physical property that correlates best with separation by gel filtration is the Stokes radius of a molecule (where the Stokes radius describes a sphere with a hydrodynamic behaviour equivalent to that of a particular irregularly shaped particle) (Siegel and Monty, 1966; Scopes, 1993). The chromatography principles are simple, the sample is passed through a column containing an inert resin of homogeneous beads, with defined and regular pore size. The porous nature of the resin allows small molecules to diffuse into the beads much more efficiently than larger molecules, due to steric and frictional effects. Hence small molecules are retarded by the column to a greater extent, and emerge later in the column run. The sample must be loaded in a small volume relative to the column volume. The column is run isocratically (in a constant buffer), and is calibrated by running proteins of known Stokes radius either mixed with the samples of interest, or in a separate run under identical conditions. Figure 4.1.1 shows the elution profile of a mixture of standard proteins from a Superose 6 gel filtration column run using a Smart system (Pharmacia) as described in Materials and methods.

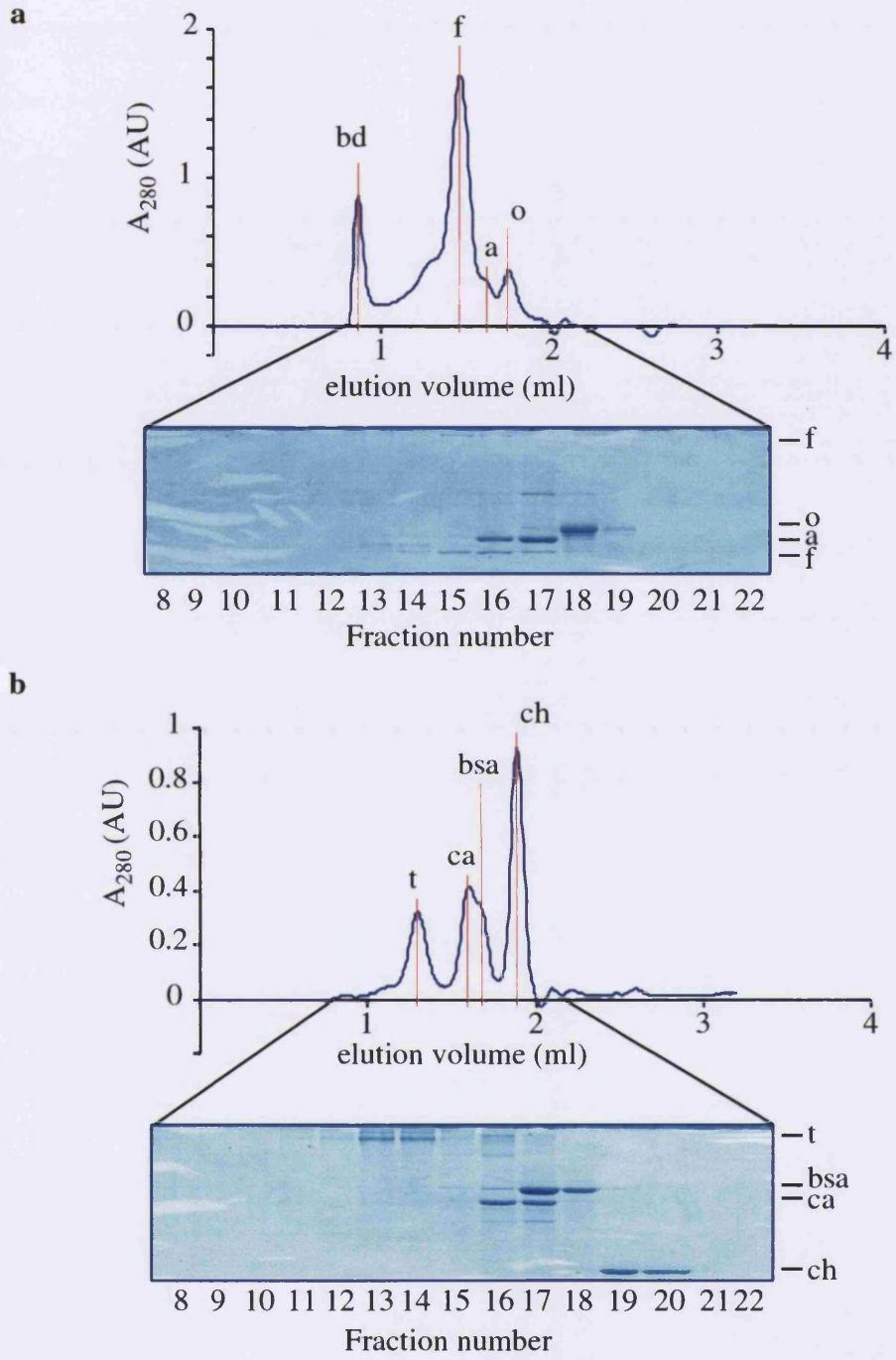

Figure 4.1.1. Separation of standard size marker proteins by gel filtration using a Superose 6 column. 50µl of a mixture containing 1mg/ml of each of four markers was loaded onto consecutive column runs. The total column volume is 3.2ml, fractions were 100µl. Part a) blue dextran (bd), ferritin (f), aldolase (a) and ovalbumin (o). The graph shows the absorbance at 280nm detected during the column run. The red lines depict the peaks. Samples from the protein containing fractions (8-22) were visualised by Coomassie staining after SDS-PAGE (below the graph) to confirm the position of peaks. Part b) as a) but thyroglobulin (t), catalase (ca), bovine serum albumin (bsa) and chymotrypsinogen (ch).

The elution position of each standard was converted to the parameter K_{av} using the equation

$$K_{av} = \frac{V_e - V_0}{V_t - V_0} \qquad \text{[Equation 4.1]}$$

where V_e = protein elution volume

V_0 = column void volume = elution volume for blue dextran

V_t = total bed volume.

(Laurent and Killander, 1964). For the Superose 6 column used in these experiments, the values for V_0 and V_t were 850µl and 3200µl respectively. The calculated values are shown in Table 4.1.1.

Protein	Mass (kDa)	Stokes radius (nm)	Elution fraction	Ve	Kav	$\sqrt{-\log(K_{av})}$
Chymo-trypsinogen	25	2.09	19/20	1900	0.45	0.59
Ovalbumin	44	3.05	18	1750	0.38	0.65
BSA	67	3.55	17/18	1675	0.35	0.67
Aldolase	158	4.81	17	1625	0.33	0.69
Catalase	232	5.22	16/17	1600	0.32	0.70
Ferritin	440	6.1	15	1450	0.26	0.77
Thyroglobulin	667	8.5	13/14	1300	0.19	0.85

Table 4.1.1. Gel filtration separation of standard protein mixtures.

A calibration curve (Figure 4.1.2) was drawn by plotting the Stokes radius of each of the standards against $\sqrt{-\log(K_{av})}$ (Laurent and Killander, 1964).

In order to determine the Stokes radius of each of the checkpoint proteins, native extracts made from undamaged, WT cells were separated in a similar manner to the standards. Fractions were analysed by western blot for the presence of Rad24, Mec3, Rad17, Rad53 and Rad9 (Figure 4.1.3). The peak fraction was determined using NIH Image analysis software. K_{av} was determined for each of the checkpoint proteins using Equation 4.1 and the Stokes radius was interpolated from the trendline (Equation 4.2) of the calibration graph (Table 4.1.2).

Protein	Elution fraction	Ve	Kav	$\sqrt{-\log(K_{av})}$	Stokes radius (nm) (interpolated)
Rad9	9/10	≤900	≤0.02	≥1.3	≥20
Rad17	18	1750	0.38	0.65	3.3±0.5
Rad24	15/16	1500	0.28	0.75	5.9±0.6
Rad53	15/16	1500	0.28	0.75	5.9±0.6
Mec3	16/17	1600	0.32	0.70	4.8±0.5

Table 4.1.2. Prediction of the Stokes radius of checkpoint proteins from gel filtration data. In each case the error margin is calculated from an estimated experimental error in Ve of ±50µl, which is the estimated variation observed between the peak elution positions of the standard proteins on different occasions. Note that due to the proximity of the Rad9 peak to the void volume, only a "greater than" estimation can be given.

To investigate whether complexes containing the checkpoint proteins were altered after DNA damage, extracts made from UV treated WT cells were separated by gel filtration, and the Stokes radius of each checkpoint protein determined as above (Figure 4.1.4 and Table 4.1.3).

Protein	Elution Fraction	Ve	Kav	$\sqrt{-\log(K_{av})}$	Stokes radius (nm) (interpolated)
Rad9 +UV	11	1050	0.09	1.0	13±1
Rad17 +UV	17/18	1725	0.37	0.66	3.6±0.5
Rad24 +UV	15/16	1500	0.28	0.75	5.9±0.6
Rad53 +UV	15/16	1500	0.28	0.75	5.9±0.6
Mec3 +UV	16/17	1600	0.32	0.70	4.8±0.5

Table 4.1.3. Prediction of the Stokes radius of checkpoint proteins after UV irradiation from gel filtration data. In each case the error margin is calculated from an estimated experimental error in Ve of ±50µl as in Table 4.1.2.

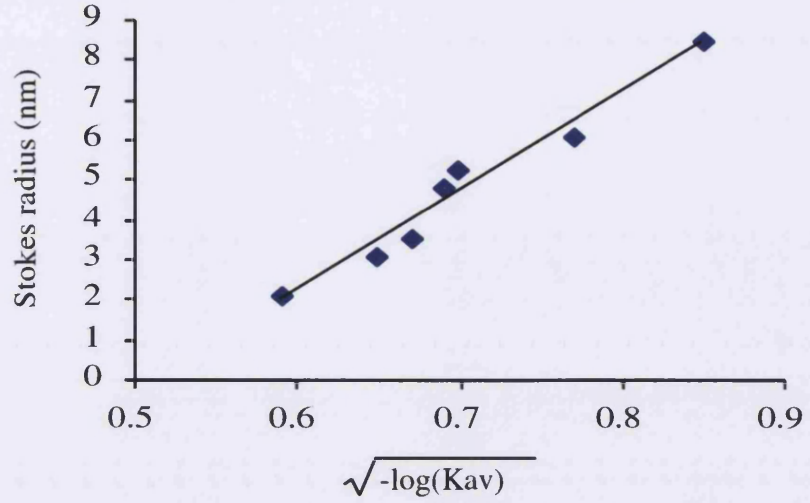

Figure 4.1.2. Calibration of gel filtration column for determination of Stokes radius. 100µl of a mixture of standard proteins of known Stokes radius (see table 4.1.1) each at 1mg/ml concentration, were loaded onto a Superose 6 column as described in the materials and methods section (Chapter 2). A trendline was fitted to the data series using Microsoft Excel software. The equation of this line is:

$$y = 24.912x - 12.75 \quad \text{[Equation 4.2]}$$

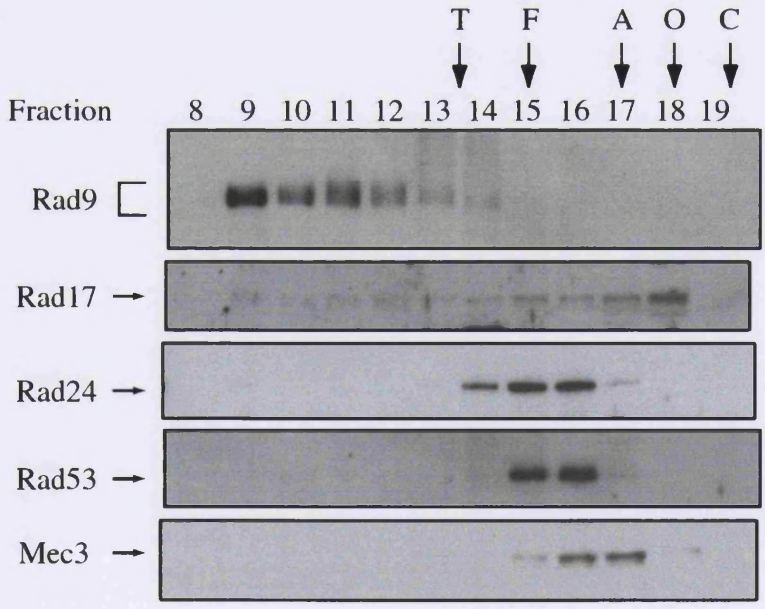

Figure 4.1.3. Western blot analysis of whole cell extracts fractionated by gel filtration. 50µl extract at 10mg/ml protein concentration was separated on a Superose 6 column. 100µl fractions were collected and 10µl of each was analysed by western blot as described in materials and methods. The peak elution position of standard proteins is depicted above the fraction numbers, T- thyroglobulin, F- ferritin, A- aldolase, O- ovalbumin, C- chymotrypsinogen.

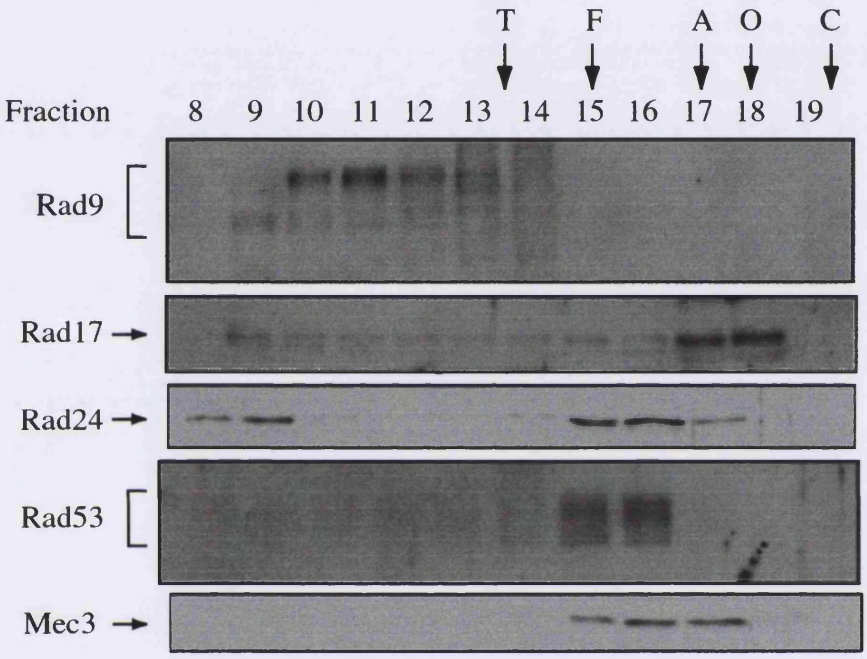

Figure 4.1.4. Western blot analysis of extracts made from UV irradiated cells fractionated by gel filtration. Extracts were made from cells grown to mid log growth phase, treated with 45J/m^2 UV in saline and then allowed to recover in rich medium for 45 minutes. 500µg total protein was loaded onto a Superose 6 column, and 10µl of the resulting 100µl fractions were analysed by western blot as described in the materials and methods section (Chapter 2). The peak elution position of standard proteins is depicted above the fraction numbers, T- thyroglobulin, F- ferritin, A- aldolase, O- ovalbumin, C- chymotrypsinogen.

4.2 – SEDIMENTATION COEFFICIENT DETERMINATION BY GLYCEROL GRADIENT SEDIMENTATION

Glycerol gradient sedimentation analysis separates molecules as a function of their mass and shape. The hydrodynamic parameter which correlates with this separation is the sedimentation coefficient, which is a measure of the terminal velocity a particle reaches under a given centrifugal acceleration (Steensgaard *et al.*, 1992). The sedimentation coefficient of an uncharacterised protein can be determined by comparing its sedimentation position to that of known standards (Martin and Ames, 1961). Glycerol gradients were poured using a gravity flow linear gradient maker. In this case the gradients used were 5ml, with 20 – 35% glycerol in standard 1x lysis buffer including phosphatase and protease inhibitors. The sample, in 100µl of a buffer less dense than the lightest buffer of the gradient, was layered gently onto the surface of each gradient. The gradients were centrifuged for 16 hours, at 42 000 rpm in a Beckman SW55 rotor. After the run 200µl fractions were manually removed from the top of each gradient, using a pipetteman. For calibration, gradients were loaded with a mixture of standard protein markers of known sedimentation coefficients. The fractions were analysed by SDS-PAGE and coomassie staining (Figure 4.2.1). The fraction containing the peak of protein was determined using NIH Image analysis software (Table 4.2.1).

Protein	Sedimentation position (Fraction number)	Sedimentation coefficient ($x10^{-13}$ sec)
Ovalbumin	4/5	3.66
BSA	5/6	4.3
Aldolase	9	7.35
Catalase	12/13	11.3
Thyroglobulin	19	18

Table 4.2.1. Glycerol gradient sedimentation analysis of standard proteins.

A calibration curve was prepared by plotting the known sedimentation coefficients against the experimental sedimentation position (Figure 4.2.2).

In order to determine the sedimentation coefficient of each of the checkpoint proteins, native extracts made from undamaged WT cells were separated in a similar manner to the standards. Fractions were analysed by western blot for the presence of Rad24, Mec3, Rad17, Rad53 and Rad9 (Figure 4.2.3). The fraction containing the peak signal was determined using the NIH Image analysis software. The sedimentation coefficient was interpolated from the trendline (Equation 4.3) of the calibration graph (Figure 4.2.2).

Protein	Sedimentation position (fraction number)	Interpolated sedimentation coefficient ($x10^{-13}$ sec)
Rad9	8/9	7.3 ± 1
Rad17	4	2.8 ± 1
Rad24	11/12	10.3 ± 1
Rad53	5/6	4.3 ± 1
Mec3	7/8	6.3 ± 1

Table 4.2.2. Sedimentation coefficients of the checkpoint proteins, interpolated from the glycerol gradient standard curve. This analysis assumes that all the proteins have the same partial specific volume. In each case the error is calculated by assuming an experimental error of ± 100µl in the peak sedimentation position.

As with the gel filtration these analyses were also performed using extracts made from UV treated WT cells, to attempt to identify changes in the checkpoint protein complexes that may occur after DNA damage (Figure 4.2.4 and Table 4.2.3). These analyses were performed on a different occasion to the extracts from untreated cells, and so the sedimentation positions cannot be directly compared. For these analyses the trendline of the calibration graph was $y = 1.2985x - 2.437$ [Equation 4.4].

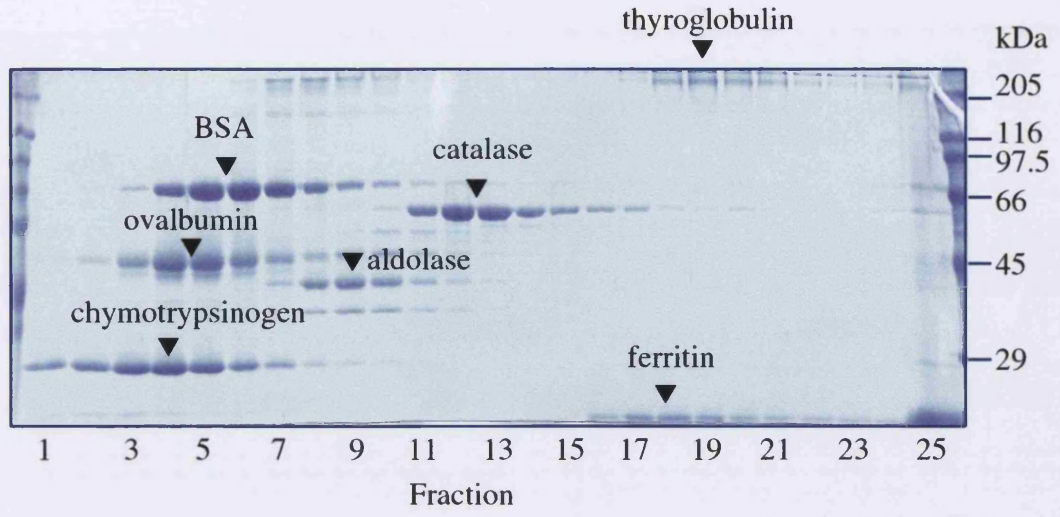

Figure 4.2.1. Separation of standard size marker proteins by glycerol gradient sedimentation. 100µl of a mixture containing 1mg/ml of each of the markers was sedimented through a 20-35% glycerol gradient as described in Materials and methods. 10µl of each 200µl fraction was analysed by SDS-PAGE and Coomassie staining. The peaks were assigned using NIH image analysis software. Each peak is highlighted by a triangle, with the protein indicated above or to the right. The bars and numbers to the right side of the image represent the migration of standard proteins through SDS-PAGE.

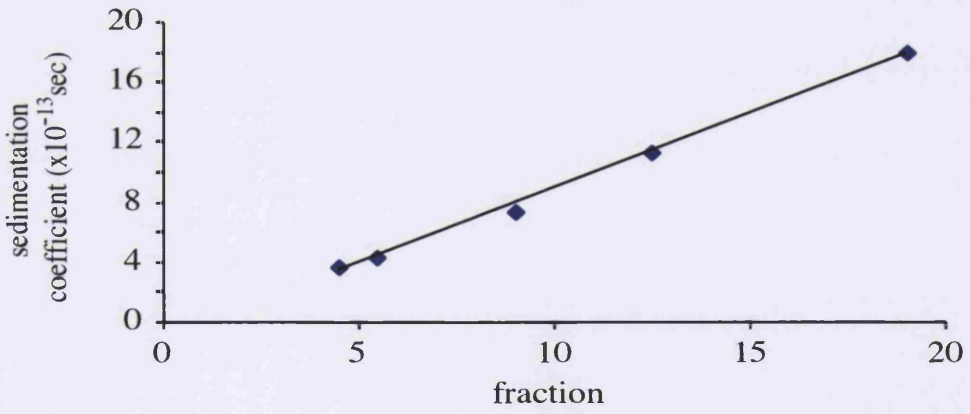

Figure 4.2.2. Calibration of glycerol gradients for determination of sedimentation coefficients. 100µl of a mixture of standard proteins of known sedimentation coefficients (see table 4.2.1) were loaded onto a 20-35% glycerol gradient as described in the materials and methods section. A trendline was fitted to the data series using Microsoft Excel software. The equation of this line is:

$$y=1.0019x - 1.1969 \qquad \text{[Equation 4.3]}$$

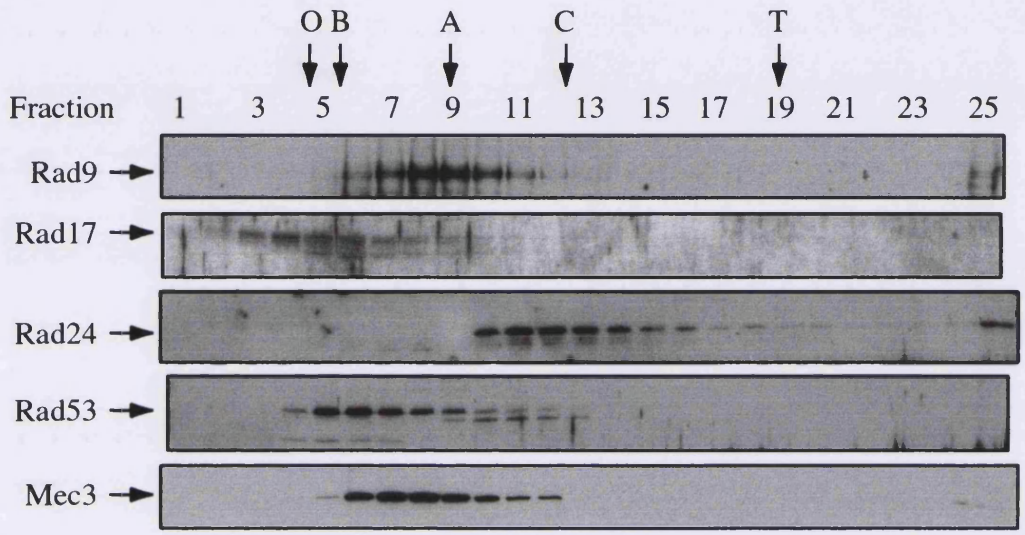

Figure 4.2.3. Western blot analysis of whole cell extracts fractionated by glycerol gradient sedimentation. 100µl extract at 10mg/ml protein concentration was sedimented through a 20-35% glycerol gradient. 200µl fractions were collected and 10µl of each was analysed by western blot as described in Materials and methods. The peak elution position of standard proteins is depicted above the fraction numbers, O- ovalbumin, B- bovine serum albumin, A- aldolase, C- catalase, T- thyroglobulin.

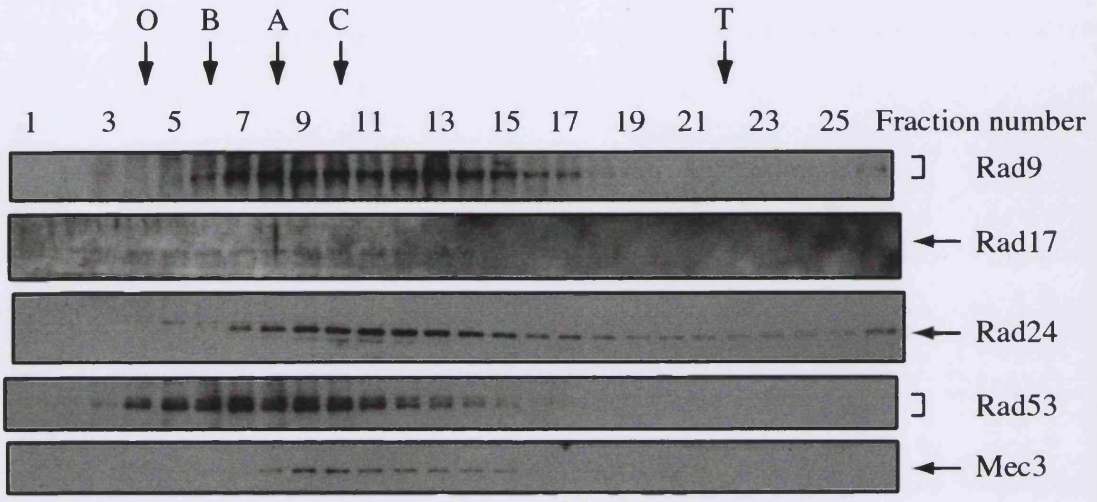

Figure 4.2.4. Western blot analysis of whole cell extracts from UV treated cells fractionated by glycerol gradient sedimentation. Cells were grown to mid log growth phase and treated with 45J/m^2 UV dose in saline. Cells were allowed to recover in rich medium for 45 minutes before harvesting and extract preparation. 100µl extract at 10mg/ml protein concentration was sedimented through a 20-35% glycerol gradient. 200µl fractions were collected and 10µl of each was analysed by western blot as described in Materials and methods. The peak elution position of standard proteins is depicted above the fraction numbers, O- ovalbumin, B- bovine serum albumin, A- aldolase, C- catalase, T- thyroglobulin. Note that because the gradients were prepared and run on separate occasions the sedimentation positions cannot be directly compared to Figure 4.2.3.

Protein	Sedimentation position (fraction number)	Interpolated sedimentation coefficient (x10^{-13} sec)
Rad9 +UV	8/9	8.6 ±1.3
Rad17 +UV	4	2.7 ±1.3
Rad24 +UV	9/10	9.9 ±1.3
Rad53 +UV	6/7	6.0 ±1.3
Mec3 +UV	9/10	9.9 ±1.3

Table 4.2.3. Sedimentation coefficients of the checkpoint proteins from extracts from UV treated cells. This analysis assumes that all the proteins have the same partial specific volume. In each case the error is calculated by assuming an experimental error of ± 100µl in the peak sedimentation position.

4.3 - ESTIMATION OF FRICTIONAL COEFFICIENTS AND MOLECULAR MASSES OF THE CHECKPOINT PROTEINS.

If the checkpoint proteins do indeed exist in complexes with other proteins then their native molecular mass would be expected to be greater than the mass of the monomeric protein. The mass of a particle can be determined if its partial specific volume, sedimentation coefficient and Stokes radius are known by using the equation:

$$M = \frac{6\pi\eta Nas}{1 - \bar{\upsilon}\rho} \qquad \text{[Equation 4.5]}$$

Where M = molecular weight, a = Stokes radius, s = sedimentation coefficient, $\bar{\upsilon}$ = partial specific volume, η = viscosity of medium, ρ = density of medium and N = Avogadro's number.

The frictional coefficient (f/f_0) of the particles can also be determined, which gives a measure of the particles asymmetry, or deviation from a spherical shape (Siegel and Monty, 1966).

$$f/f_0 = a \Big/ \left(\frac{3\bar{\upsilon}M}{4\pi N}\right)^{1/3} \qquad \text{[Equation 4.6]}$$

Although the partial specific volume for each of the checkpoint protein complexes has not been experimentally determined, for most proteins an assumption of 0.725 cm^3/g can be used as the actual densities of most proteins are very similar (Martin and Ames, 1961). The partial specific volume of a protein can be calculated from the data for the constituent amino acids (Steensgaard *et al.*, 1992). When this calculation was performed for the checkpoint proteins their calculated partial specific densities did not deviate from this assumption by more than 1.4% (Table 4.3.1). The viscosity and the density of the medium is taken to be that of water, $1.002 \times 10^{-2} g/(cm*s)$ and $0.998 g/cm^3$ respectively. Avogadro's number is $6.02 \times 10^{23}/mol$.

Using the equations given above (Equations 4.5 and 4.6) and the experimentally determined Stokes radii and sedimentation coefficients, the molecular masses and frictional coefficients for each of the native checkpoint protein complexes were determined (Table 4.3.2).

Protein	Calculated partial specific volume (g/cm^3)
Rad9	0.727
Rad17	0.735
Rad24	0.730
Rad53	0.733
Mec3	0.729

Table 4.3.1 Calculated partial specific volumes of the checkpoint proteins.

Protein	Stokes radius (nm)	Sed. coefficient ($x10^{-13}$ sec)	Molecular mass (kDa)	Frictional coefficient
Rad9 -UV	≥20	7.3±1	≥600±80	≥3.6
Rad9 +UV	13±1	8.6±1.3	460±110	2.5±0.5
Rad17 -UV	3.3±0.5	2.8±1	40±20	1.5±0.6
Rad17 +UV	3.6±0.5	2.7±1.3	40±30	1.6±1.3
Rad24 -UV	5.9±0.6	10.3±1	260±50	1.4±0.3
Rad24 +UV	5.9±0.6	9.9±1.3	240±60	1.4±0.3
Rad53 -UV	5.9±0.6	4.3±1	110±40	1.9±0.5
Rad53 +UV	5.9±0.6	6.0±1.3	150±50	1.7±0.4
Mec3 -UV	4.8±0.6	6.3±1	130±40	1.4±0.4
Mec3 +UV	4.8±0.5	9.9±1.3	200±50	1.2±0.3

Table 4.3.2. Hydrodynamic properties of the checkpoint protein complexes.

4.4 – DISCUSSION

The first striking observation upon initial analysis of the checkpoint proteins by gel filtration was the apparent lack of overlap of the peaks. The only coincident peaks were that of Rad24 with Rad53, the other proteins appear to exist, at least in the majority, as discrete complexes. Using the molecular masses of standard proteins as a guide Rad9, Rad24 and Rad53 were likely to be in protein complexes with masses greater than expected for monomeric proteins. However, because gel filtration separates molecules on the basis of radius rather than mass, accurate mass cannot be determined from this analysis alone. The peak of Rad9 protein is in or very close to

the void volume of the column, indictating that this protein has an extremely large radius, much greater than expected for a globular molecule with a mass of 148kDa. This suggests that either the Rad9 molecule is extremely non-spherical, or that Rad9 associates with other proteins in a large molecular mass complex, or both. With the exception of Rad9, which appears to reduce in radius after UV treatment, there appears to be little change to the radii of the other checkpoint proteins after UV. It was also noted that the gel filtration profile of Rad24 and Mec3 was not altered by treatment of the extracts with high salt (1M KCl) or DNAse I (data not shown). The peaks of Rad17 and Mec3 are not coincident, a surprising result given that these proteins can be readily co-precipitated (Section 3.5). However the Rad17 signal in very broad, some Rad17 can be detected in most of the elution fractions. This suggests that Rad17 may exist in the cell in more than one form, perhaps as monomer and also in protein complexes. It seems likely from the co-precipitation data, and the work of other laboratories that Mec3 and Rad17 do associate (Kondo *et al.*, 1999), and indeed the fractions containing Mec3 do contain some Rad17, but clearly not all of the cellular population of the two monomers is in this putative PCNA-like complex.

Occasionally in the extracts from UV treated cells a proportion of Rad24 was detected in the early fraction of the superose 6 column, corresponding to material with large molecular mass. It is likely that this is due to non-specific aggregation effects during extract preparation. The frequency of observation of this peak increases with decreasing extract quality, it is common in extracts made using the ribolyser, and less so in liquid nitrogen extracts. Mec3 is also sometimes in a large radius species, though less often than Rad24. These large complexes do seem to occur more often in extracts from damaged cells. A possible physiological role for them has not been investigated. For a fuller discussion of the differences in extract preparation please see Sections 5.3 and 5.6. Other groups have performed gel filtration analysis of Rad24 or the *S. pombe* homologue from crude extracts, and have presented data consistent with the size suggested here (Shimomura *et al.*, 1998; Griffiths *et al.*, 2000).

The modification of Rad53 by phosphorylation after DNA damage does not alter the elution profile from superose 6. Although it is known that some Rad53 is associated with Rad9 under these conditions, this must be a minority of the total cellular Rad53,

which remains in a smaller sized peak. This observation is consistent with the co-immunoprecipitation analysis (Section 3.5). The elution profile of Rad9 is altered in extracts from UV treated cells, the hyperphosphorylated forms are of a smaller molecular radius than the undamaged, hypophosphorylated forms. This decrease in radius could occur due to a loss of mass from the complex or a structural rearrangement.

Analysis of checkpoint protein complexes by glycerol gradient sedimentation produced results that were largely consistent with the gel filtration analysis. This technique clearly separated Rad24 from Rad53, supporting the suggestion that the majority of these two proteins do not interact, even though they co-fractionate through gel filtration. then glycerols. Similarly to the gel filtration profiles, Rad17 is present over a broad range of sedimentation positions, some of which overlap with Mec3. The separation of molecules by density gradient centrifugation is dependent upon mass and shape. If the large radius of the Rad9 complex was entirely accounted for by a large mass complex, with a roughly globular structure, then the sedimentation coefficient of Rad9 would be much larger than measured by this technique. This suggests that the Rad9 protein complex must have a non-spherical structure as well as large mass.

The data obtained from gel filtration in combination with that from glycerol gradient analysis allows the calculation of the mass and frictional coefficients of molecules.
The masses determined for the checkpoint proteins suggest that Rad9, Rad24 and Mec3 probably exist as protein complexes in whole cell extracts, whereas the majority of Rad17 and Rad53 is likely to be monomeric. Only Rad9 and Mec3 show a significant change in mass after UV treatment, the physiological relevance of a change to the Mec3 complex has not been determined. It is known that the Rad9 complex contains Rad53 after DNA damage but not before (Emili, 1998; Sun *et al.*, 1998; Vialard *et al.*, 1998), and also that Rad9 interacts with itself after damage (Soulier and Lowndes, 1999), so it was surprising to identify that this complex actually loses mass after such treatment. This must be indicative of a large structural alteration of the Rad9 complex after DNA damage. We have proposed a model for this process, in which Rad9 acts as a solid phase catalyst for the intra-molecular autophosphorylation of Rad53 (Gilbert *et al.*, 2000). The frictional coefficients determined from this analysis strongly suggests that the Rad9 complex is non globular. A perfect sphere has a frictional coefficient of 1.0,

the high coefficients for Rad9 represent an extremely elongated molecule. The frictional coefficients for the other checkpoint proteins are in the range expected for roughly globular complexes.

The majority of the Rad17 in these extracts appears to behave as a monomer. This was surprising as it is expected that Rad17 should associate with Mec3 and Ddc1 to form a complex with a mass approximately three times that of monomer. However the Rad17 signal is very broad in both gel filtration and glycerol gradient analysis. As discussed earlier this may be due to the existence of multiple complexes containing Rad17. It should be possible to identify if the large size of the Mec3 complex is due to association with Rad17 by investigating the hydrodynamic properties of this Mec3 complex in extracts made from *rad17Δ* cells.

CHAPTER 5 – PURIFICATION OF THE RAD24 CHECKPOINT PROTEIN COMPLEX

The hydrodynamic properties of the Rad24 protein in native extracts suggested that the protein may exist as a component of a multi-protein complex. Because no interactions had been identified between Rad24 and other known components of the checkpoint pathway, in order to determine absolutely the existence and composition of such a complex, it was necessary to purify it to homogeneity. As previously determined Rad24 is not an abundant protein, only present at approximately 200 copies of the protein per haploid cell, therefore such a purification had to be very efficient.

Previously, an epitope tagging procedure for many of the checkpoint proteins, including Rad24 had been attempted, but it was found that addition of an epitope tag at the carboxyl terminus led to a loss of function of Rad24 (Jorge Vialard, personal communication). It was therefore decided to engineer a yeast strain expressing an amino terminally epitope tagged version of the Rad24 protein. The aim was to use affinity purification techniques in order to rapidly purify the complex and determine its components.

5.1 – PRODUCTION AND CHARACTERISATION OF EPITOPE-TAGGED *RAD24*.

In order to produce a yeast strain containing an epitope-tagged version of *RAD24* a targeting vector had to be generated. The vector was based on pRS303, one of the yeast vectors first designed by Dr. P. Heiter (Sikorski and Hieter, 1989). This vector contains an *E. coli* replication origin and ampicillin resistance gene, as well as the yeast *HIS3* gene, which is defective in the WT strain background *W303*. The vector also contains a multiple cloning site (MCS). The vector was produced in multiple stages. Firstly, complementary oligonucleotides encoding ten histidine residues and an ATG start codon flanked by unique restriction enzyme sites were annealed and cloned into the MCS (oligos 564 and 605, see Appendix I) using XbaI and BamHI. The resulting vector was termed pRS30310His (E368). Primers were then designed in order to amplify the promoter region of the *RAD24* gene and, seperately, the 5' end of the *RAD24* ORF by PCR from genomic DNA, these primers also contained unique restriction sites to

facilitate cloning (primers 600-603, see Appendix I). The promoter was presumed to be contained within the 1kb DNA immediately 5' to the ORF. The fragment of ORF amplified was selected to be as small as possible, while containing a restriction site that will be unique in the finished vector, as the plasmid has to be linearised within the *RAD24* ORF for correct targeting of the homologous recombination event (Rothstein, 1991). The PCR products were cloned either side of the 10His tag in the pRS30310His vector using SacII/XbaI for the promoter and SmaI/ClaI for the ORF (vector designated pRS303HisRad24 (E372)). Transformation of this vector into WT yeast, after linearisation with BsgI enzyme, resulted in an epitope tagged *RAD24* under the control of the *RAD24* promoter, at the *RAD24* locus. The reaction also produced a short truncated *RAD24* ORF with a WT promoter, upstream of the epitope tagged full length ORF. It was expected that this truncated polypeptide would not interfere with the function of the full length protein. See Figure 5.1.1 for a schematic of this construction. Yeast cells which stably incorporated the vector were selected by their ability to grow on media without histidine. Integration at the correct genomic locus was ensured by dianostic PCR and western blot analysis of selected isolates. Similar vectors were also constructed to produce histidine tagged versions of *MEC3*, *RAD9* and *RAD17* (vectors E369-71 respectively, PCR primers 566-7 (*RAD9*, *RAD9* ORF fragment subcloned from vector E367 (J. Vialard) using BamHI/EcoRI), 596-9 (*RAD17*) and 592-5 (*MEC3*)). Yeast strains expressing these histidine tagged checkpoint proteins were used for analysis of checkpoint protein interactions (see Figure 3.5.5).

Due to the low abundance of Rad24 it was anticipated that a single nickel affinity step was unlikely to be sufficient to purify the protein to homogeneity. Because the yeast strain expressing *10HIS-RAD24* behaved as WT under all conditions tested (data not shown) it appeared that the protein could tolerate an amino terminal epitope tag for normal function. It was therefore decided to increase the size of this tag, with the addition of an HA epitope (Kolodziej and Young, 1991) and a cleavage site for the tobacco etch virus (TEV) protease (Parks *et al.*, 1994), in order to be able to purify the protein with greater ease (see Figure 6.3.1 for the anticipated purification strategy).

Complimentary oligonucleotides encoding both of these epitopes (651 and 652 see Appendix I) were annealed and cloned into the pRS303HisRad24 vector between the

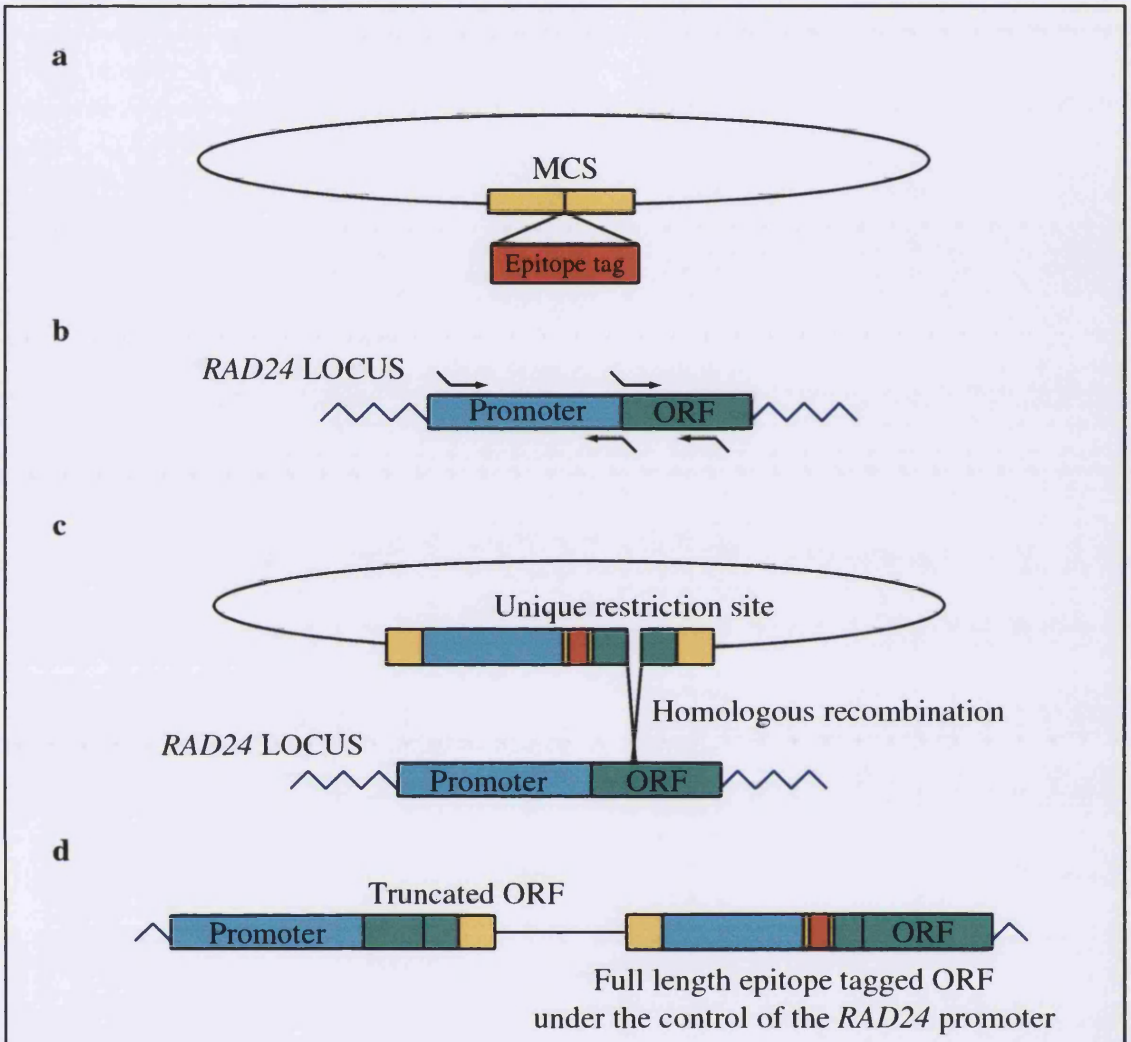

Figure 5.1.1. Integration of a vector into the yeast genome by homologous recombination to produce amino terminal epitope tagged checkpoint proteins. a) Oligonucleotides encoding the epitope tag (for example 10 histidine codons) and appropriate restriction sites were annealed and cloned into the multiple cloning site (MCS) of pRS303. The yeast auxotrophic marker on this vector is His3, it also contains an *E.coli* origin of replication and ampicillin resistance gene. b) 2 PCR were performed from yeast genomic DNA to amplify 1kb of the promoter region of the *RAD24* locus (Promoter) and a 5' fragment of the open reading frame (ORF) containing a unique restriction site. Oligonucleotide primers were designed that included appropriate restriction sites for cloning these fragments into pRS303HIS. c) The resulting vector was linearised and used to transform yeast. The DNA end will initiate a homologous recombination event. d) The resulting *RAD24* locus, a truncated ORF is produced, followed by the epitope tagged gene. Correct integration events were selected using the His3 marker, followed by PCR to confirm the structure of the locus, and western blotting to confirm the expression of a correct sized protein.

histidine codons and the beginning of the *RAD24* ORF using the NcoI enzyme. Whole cell extracts were made from isolates of successful integrations of this vector. Upon incubation with TEV protease however, it was found that the histidine residues were not cleaved from the tagged Rad24 (data not shown). In some cases it has been shown that histidine residues in close proximity to the cleavage site prevent the cleavage reaction (Life Technologies). In order to overcome this problem it was necessary to re-make the vector including spacer residues between the histidines and the cleavage sites. This new construct was created in two steps, cloning annealed oligonucleotides 720 and 721 with AflIII and NcoI (which encode a spacer and TEV site), followed by oligonucleotides 733 and 734 with NcoI and EagI (which encode an HA epitope) into pRS303HisRad24. After transformation with linearised vector, isolates were selected on plates without histidine, and correct integration checked by PCR (data not shown). The resulting strain was designated *HTH-RAD24*.

Whole cell extracts were made from *HTH-RAD24* and *W303* strains in order to check that the novel *RAD24* gene was properly expressed. Equal quantities of these extracts and a *rad24Δ* control extract were loaded for SDS-PAGE and analysed by western blotting using the anti-Rad24 polyclonal serum (Figure 5.1.2). The HTH-Rad24 migrated more slowly than Rad24 through SDS-PAGE due to the extra amino acids that comprise the tag. The level of the tagged protein in the extract was comparable to that of WT Rad24 suggesting that the novel gene was normally expressed.

In order to ensure that HTH-Rad24 retains normal biological function the survival of *HTH-RAD24* strain after UV irradiation was compared to WT. Known numbers of WT, *HTH-RAD24* and *rad24Δ* cells (from 300 to 300000) were plated onto YPD plates. The plates were irradiated with 254nm UV light at a range of doses between 0 and 75J/m^2 with a fluence rate of 3J/m^2/sec. After incubation at 30°C in the dark for two days the number of colonies on each plate was counted. The percentage survival was calculated for each strain at each dose. This percentage was adjusted relative to the survival at 0J, which was taken to be 100% (Figure 5.1.3). The *HTH-RAD24* strain survived the UV irradiation similarly to the WT strain and much better than *rad24Δ*. This implies that HTH-Rad24 retains biological function.

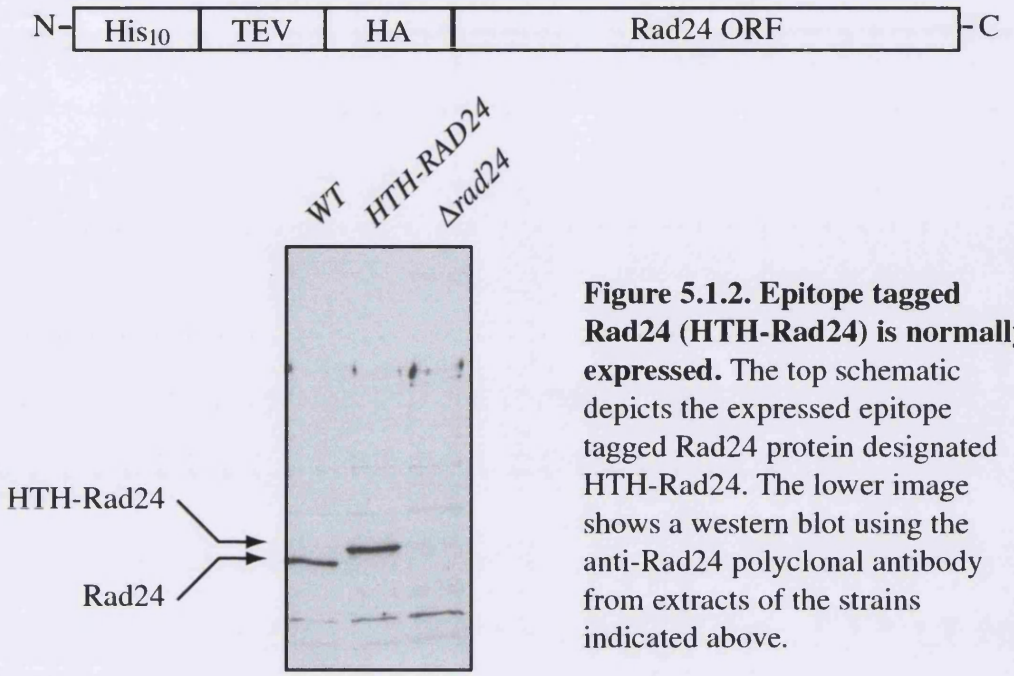

Figure 5.1.2. Epitope tagged Rad24 (HTH-Rad24) is normally expressed. The top schematic depicts the expressed epitope tagged Rad24 protein designated HTH-Rad24. The lower image shows a western blot using the anti-Rad24 polyclonal antibody from extracts of the strains indicated above.

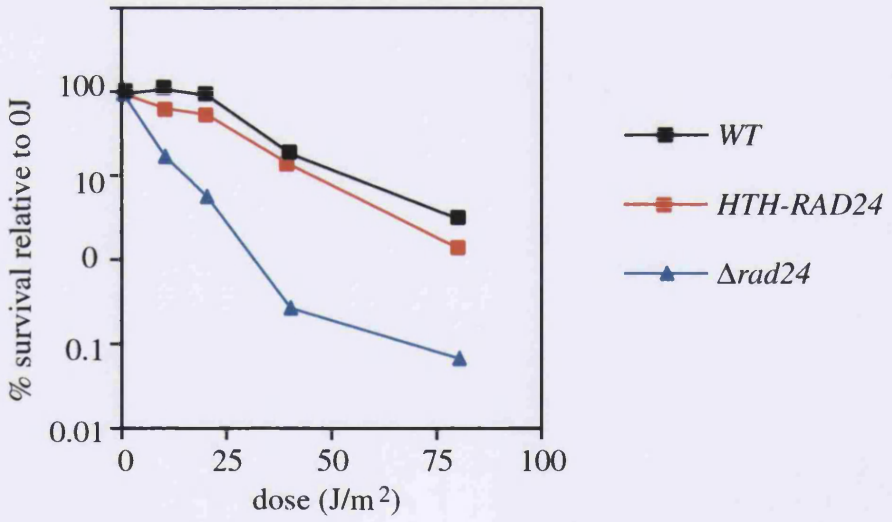

Figure 5.1.3. Survival after UV irradiation of WT, *HTH-RAD24* and *Δrad24* strains. Known numbers of cells from mid-log cultures were plated onto YPD plates. The plates were irradiated at the doses shown at a fluence rate of $3J/m^2/sec$. The plates were then incubated at 30°C for two days, and the number of colonies was counted. % survival was calculated relative to $0J/m^2$ which was taken to be 100%.

To confirm that the *HTH-RAD24* construct is a suitable reagent for the purification of the Rad24 complex it was necessary to analyse the size of the complex in this strain. Size analyses were performed as described in Chapter 5. 250μg of extract from tagged and untagged strains, that had been mock treated or UV irradiated, were fractionated by gel filtration using a superose 6 column. Fractions were analysed by western blotting using the anti-Rad24 polyclonal serum (Figure 5.1.4). The elution profile of HTH-Rad24 was very similar to that of Rad24, suggesting that the tagged protein is able to associate into the Rad24 complex. After UV irradiation some Rad24 is eluted in early fractions, as discussed in Section 5.3 this is likely to be due to aggregation artefacts from the extract preparation. As a further verification of the complex size, glycerol gradient sedimentation was performed on the same extracts. 250μg of each extract was centrifuged at 45000rpm in a 20-35% glycerol gradient at 4°C for 16hours. Fractions were removed carefully from the top of each gradient and analysed by western blotting using the anti-Rad24 polyclonal serum (Figure 5.1.5). As with the gel filtration analysis the profiles of Rad24 and HTH-Rad24 from glycerol gradient sedimentation were not significantly different. These data strongly suggest that HTH-Rad24 can substitute for Rad24, as measured by survival after UV treatment and formation of the large molecular mass complex. It was therefore decided that it was valid to use this construct to purify this complex.

5.2 – ANALYSIS OF RAD24 HOMO-OLIGOMERISATION

Thus far, it had been demonstrated that Rad24 exists as a large molecular mass complex in whole cell extracts. No interaction had been identified between Rad24 and the other checkpoint proteins. It was still possible that the observed size of Rad24 was due to the association of multiple Rad24 molecules, with no other proteins being components of the complex. In order to identify whether one molecule of Rad24 is capable of interacting with another, a diploid strain was produced expressing both Rad24 and HTH-Rad24. This was achieved by mating *W303-1b* (mating type α) with *HTH-RAD24* (mating type a). Whole cell extracts were prepared from this strain and the original haploid strains. These extracts were used for immuno-precipitation studies using the 12CA5 monoclonal antibody. Samples from the starting extracts and the proteins eluted from the immuno-precipitation beads were analysed by western blot using the anti-Rad24 polyclonal antibody (Figure 5.2). HTH-Rad24 was efficiently precipitated by the

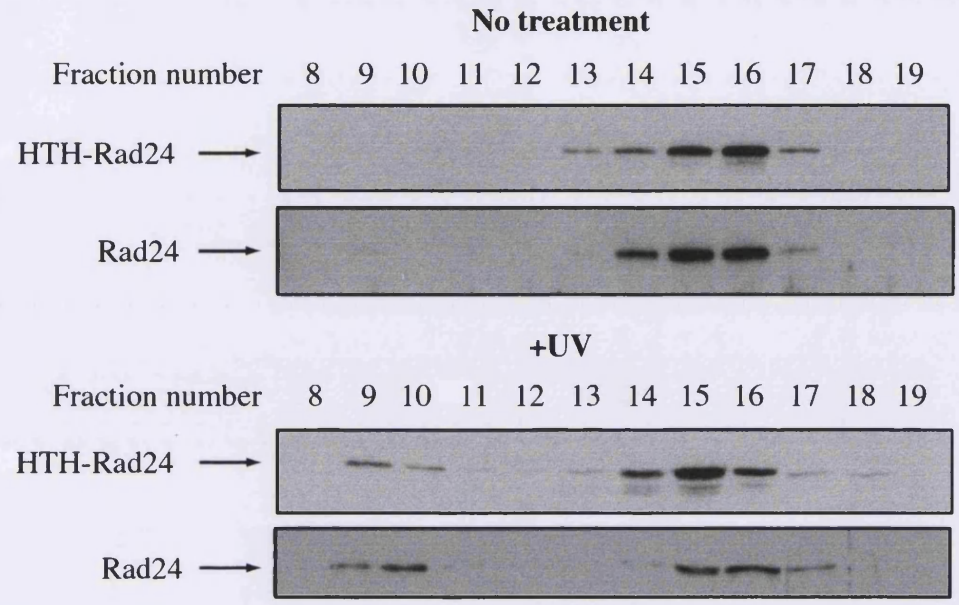

Figure 5.1.4. Gel filtration analysis of Rad24 and HTH-Rad24 proteins from whole cell extracts. Extracts were made from damaged or untreated cells. 250µg was loaded onto a Superose 6 column as before. Fractions were separated by SDS-PAGE and then analysed by western blot using the anti-Rad24 polyclonal.

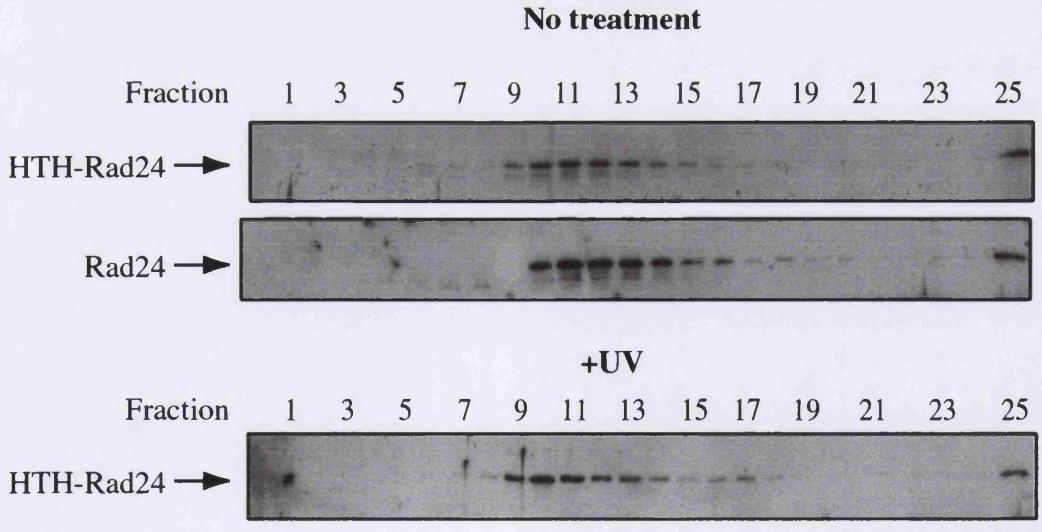

Figure 5.1.5. Glycerol gradient sedimentation analysis of Rad24 and HTH-Rad24 proteins from whole cell extracts. Extracts were made from damaged or untreated cells. 500µg was loaded onto a 20-35% gradient as before. Fractions were separated by SDS-PAGE and then analysed by western blot using the anti-Rad24 polyclonal.

12CA5 antibody. Rad24 in a WT extract was not precipitated by this method. In the extract from the diploid strain HTH-Rad24 was precipitated and Rad24 was not. This clearly demonstrated that HTH-Rad24 does not interact with Rad24 in a stable manner. Similar results were obtained if UV irradiated cells were used for the extract preparation (data not shown). It was therefore likely that the observed size of the Rad24 complex was due to the association of Rad24 with other, as yet uncharacterised proteins.

5.3 – PURIFICATION OF THE HTH-RAD24 PROTEIN COMPLEX

The epitope tag of HTH-Rad24 was designed with a particular purification scheme in mind. The anticipated strategy is depicted in Figure 5.3.1. Whole cell extract would be made from a large culture of *HTH-RAD24* yeast. This would undergo initial purification on heparin sepharose, followed by NTA-nickel agarose purification. The eluted material would be treated with TEV protease in order to remove the histidine residues. This material would then be loaded onto a new nickel column. The only molecules that would not bind to this second nickel column should be the cleaved TH-Rad24 and associated proteins, the protease itself contains a six histidine tag. These would therefore be present in a highly purified form in the flow through from the column. As a final purification step the HA epitope could be used in an immuno-purification procedure using a column of immobilised 12CA5 monoclonal antibody. The tagged Rad24 would be eluted from this column by competition using a peptide containing the HA epitope.

The first stage of the purification was the production of a large amount of whole cell extract. Large yeast cultures were grown in a fermenter, up to 100litres in a single batch. It was found that densities of up to $5x10^7$cells/ml could be achieved while maintaining the cells in mid-logarithmic growth phase by the addition of extra glucose to a final concentration of 4%w/v (data not shown). The cells were harvested using a continuous flow centrifuge. Each batch produced approximately 700g wet weight cell pellet. The harvested cells were washed with lysis buffer and then extruded into liquid nitrogen through a syringe or bag to give yeast "noodles" (Schultz, 1999). These noodles were stored at –80°C until processing. Many different methods of extract preparation were attempted, using 100g noodles in order to optimise the procedure.

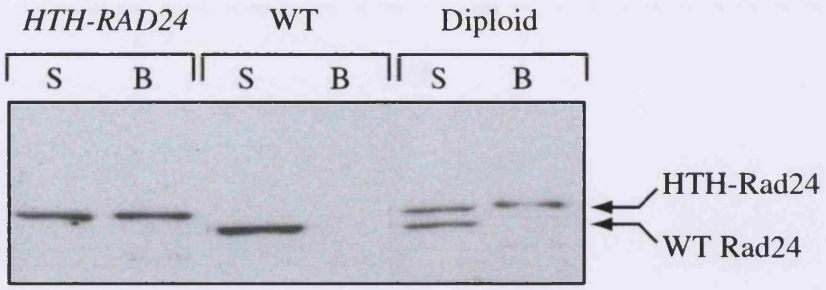

Figure 5.2. The Rad24 protein does not associate with itself. Immuno-precipitation using the 12CA5 monoclonal antibody from extracts containing Rad24, HTH-Rad24 or both. The immuno-precipitation was performed using 1mg each extract at 1mg/ml and a dilution of 12CA5 of 1 in 50.

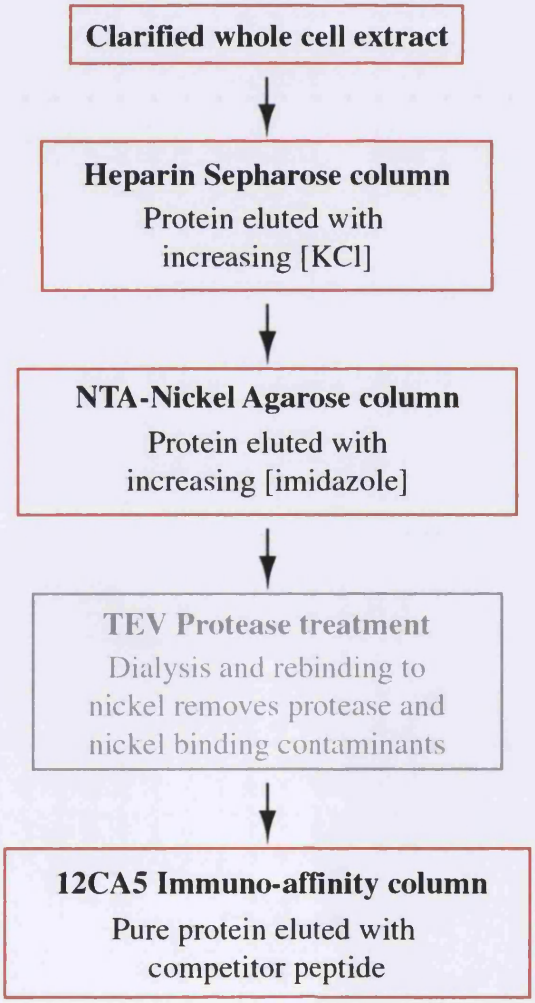

Figure 5.3.1. A strategy for purification of HTH-Rad24. The schematic shows the anticipated steps and order of the purification.

Initially the noodles were allowed to thaw, then mixed with cold lysis buffer and glass beads. The mixture was shaken vigorously in a bead beater at 4°C to produce the extract. After clarification by centrifugation the extract was loaded onto the heparin column. Using this extract preparation method more than half the HTH-Rad24 did not bind to the column (data not shown). When this extract was analysed by gel filtration using a superose 6 column HTH-Rad24 appeared to be present in all fractions (Figure 5.3.2). This was suggestive of non-specific aggregation artefacts due to the extract preparation method. A second lysis method was tested, this involved grinding the noodles in an electric blender in the presence of solid carbon dioxide. Lysis buffer was then added in frozen form and ground to a powder. The powder was thawed, the extract clarified and analysed by fractionation over a gel filtration column. The HTH-Rad24 in extracts prepared by this method also appeared to be aggregated as it was present in a wide variety of sizes (Figure 5.3.2). The method that consistently produced extracts with the least aggregation, and hence the greatest proportion of HTH-Rad24 that was competent to bind to heparin sepharose, was also the method that required considerable "elbow grease". Noodles were manually ground with a pestle under liquid nitrogen in a ceramic mortar. Once a sufficient proportion of cells (approximately 70%) were lysed, as monitored by microscopic analysis, lysis buffer was added, and ground to a powder. This powder was thawed, the majority of debris removed by a low speed spin, and then the extract was clarified by centrifuging for 45minutes at 40000rpm in a Beckman Ti45 rotor. The supernatant was the load material for the heparin column. For the successful large scale purifications cells from a total of 200litres yeast culture, grown in a fermenter were used, corresponding to approximately 1.3kg wet weight. This was ground in a mortar in 150g batches, and resulted in 1100ml clarified extracts at an initial protein concentration of 20mg/ml (data not shown).

After the extract was prepared all purification steps were performed at 4°C. Extracts and fractions were frozen in liquid nitrogen and stored at -80°C between procedures. A 400ml heparin sepharose column was equilibrated at 150mM KCl, and the extract loaded at a flow rate of 6ml/minute using an econo-system (BioRad). The column was washed with buffers containing 300mM and 500mM KCl (these buffers did not contain EDTA). 15ml fractions were collected. Samples from each fraction of the column were analysed by western blot using the anti-Rad24 polyclonal (Figure 5.3.3). HTH-Rad24

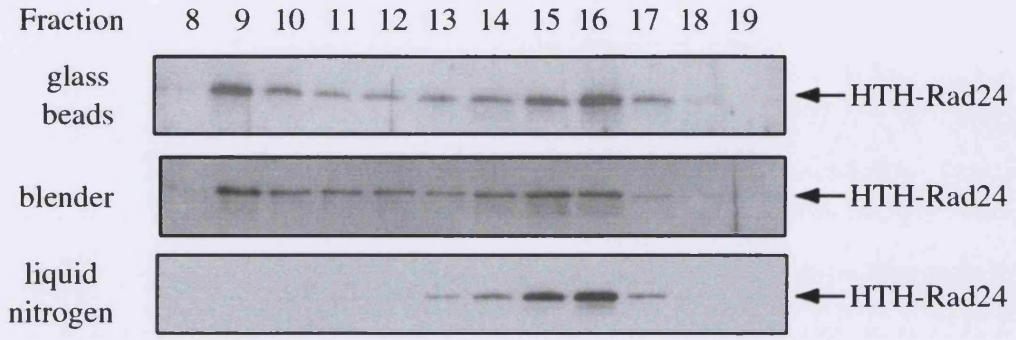

Figure 5.3.2. Comparison of different extract preparation methods. 250µg large scale extracts made in the manner indicated were fractionated on a superose 6 gel filtration column. Fractions as indicated were analysed by western blot for the presence of Rad24.

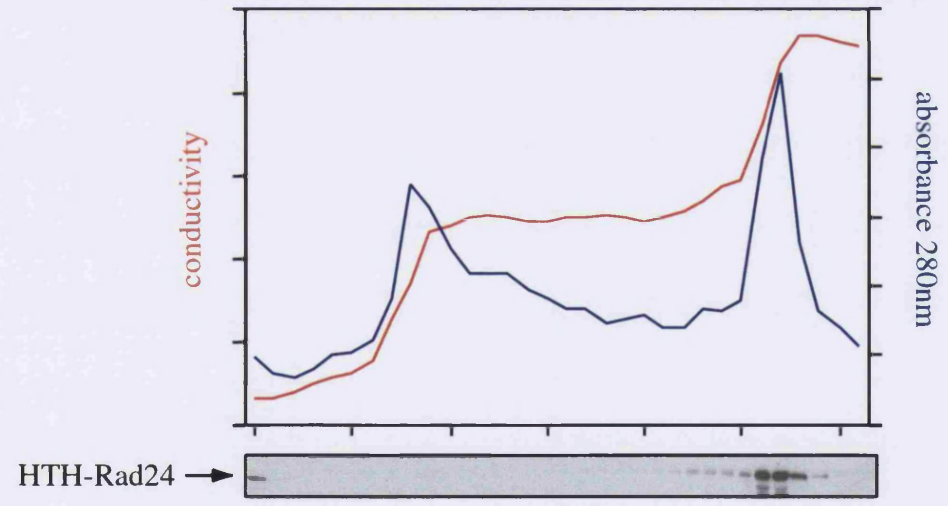

Figure 5.3.3. Purification of HTH-Rad24 on heparin sepharose. Clarified whole cell extract from a 100litre culture was applied to a 400ml heparin sepharose column in 150mM KCl using an econo-system (BioRad). The column was washed with buffers containing 300mM and then 500mM KCl. 15ml fractions were collected throughout. UV absorbance (blue) and conductivity (red) were monitored throughout the column run and plotted on the graph (units are arbitrary). The image below is of western blot analysis of 1µl each fraction using the anti-Rad24 polyclonal.

eluted in a single peak as the KCl concentration increased to 500mM. The majority of proteins did not bind to the column, and a further proportion was removed with the 300mM KCl wash. An increase in the concentration of Rad24 relative to the total protein concentration of approximately 8 fold was achieved on this column (data not shown). The fractions from the heparin column which contained the peak of HTH-Rad24 were pooled, and imidazole added to a final concentration of 10mM. This material was loaded at 0.5ml/minute onto a 10ml NTA-nickel agarose column on the econo-system. The column was washed with buffers containing 40mM and 200mM imidazole. 1ml fractions were collected. Samples from each fraction of the column were analysed by western blot using the anti-Rad24 polyclonal (Figure 5.3.4). HTH-Rad24 eluted in a single peak as the imidazole concentration increased to 200mM. The majority of proteins did not bind to the column, and a further proportion was removed with the 40mM imidazole wash. An increase in the concentration of Rad24 relative to the total protein concentration of approximately 50 fold was achieved on this column (data not shown).

The fractions from the nickel column which contained the peak of HTH-Rad24 were pooled. In order to optimise the TEV protease cleavage step, aliquots were removed and incubated with the protease under different conditions of temperature, time and enzyme concentration. The reactions were analysed by western blot using the anti-Rad24 polyclonal (Figure 5.3.5). A maximum of 50% cleavage was obtained, when the reaction was performed with 5units enzyme in a 50µl volume for 30minutes at 30°C. The presence of protease inhibitors in the reaction did not inhibit the action of the protease.

The anticipated protocol for HTH-Rad24 purification next involved the re-binding of the cleaved material to a nickel column. The most efficient small scale trial was dialysed to a buffer containing 20mM imidazole in a micro-dialysis system (Pierce). NTA-nickel beads were added, and batch binding was allowed to occur for 1 hour. The supernatant was removed, the beads washed in 20mM imidazole and proteins eluted in a buffer containing 250mM imidazole. The stages of this binding were analysed by western blot (Figure 5.3.6). Instead of the HTH-Rad24 separating into cleaved product (which was expected in the supernatant) and non-cleaved (which should have bound to

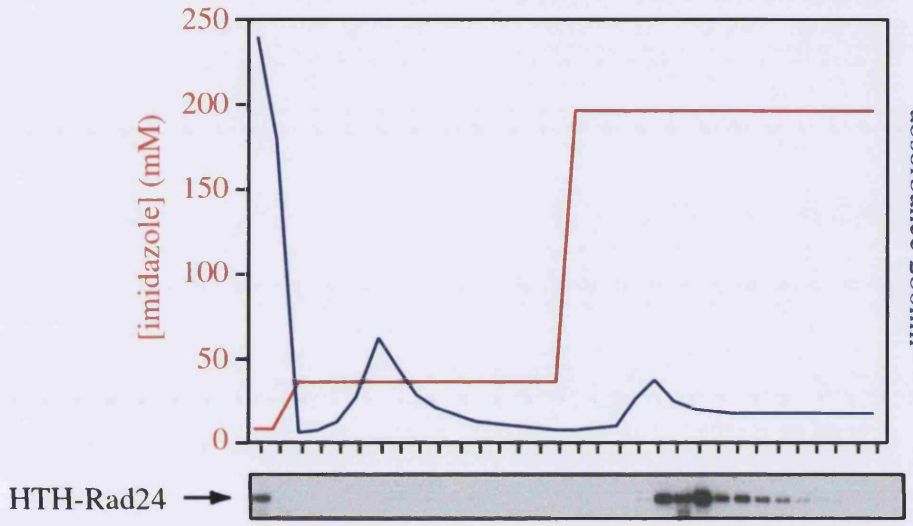

Figure 5.3.4. Purification of HTH-Rad24 on NTA-nickel agarose. Imidazole was added to the pooled fractions containing the peak of HTH-Rad24 to 10mM. This was loaded onto a 10ml NTA-nickel agarose column using an econo-system. The column was washed with buffers containing 40 and 200mM imidazole. 1ml fractions were collected. UV absorbance was monitored throughout (blue line), conductivity did not change significantly during the run, so the imidazole concentration (red line) was plotted for clarity (arbitrary units). The image below is of western blot analysis of 1µl each fraction using the anti-Rad24 antibody.

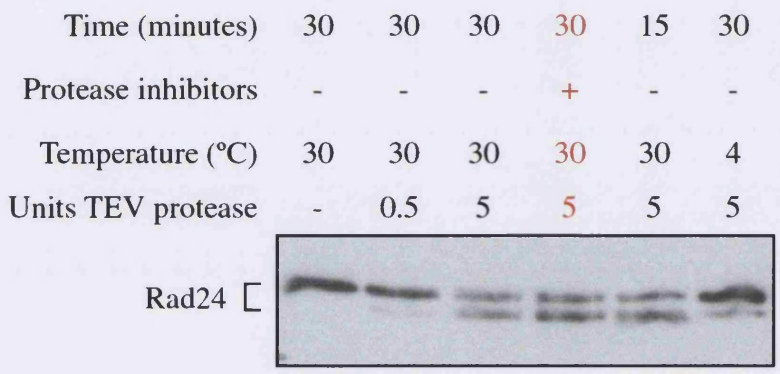

Figure 5.3.5. Cleavage of HTH-Rad24 with TEV protease. A sample from the pooled peak material eluted from the NTA-nickel agarose column was dialysed into reaction buffer, then incubated under the conditions indicated above. The Rad24 was analysed by western blot using the polyclonal antibody.

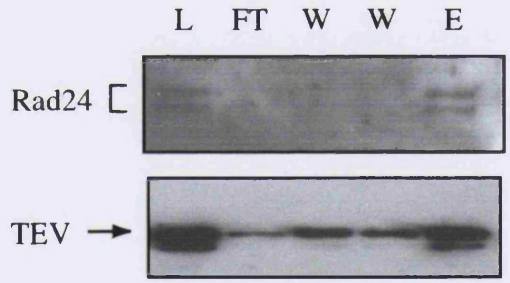

Figure 5.3.6. Analysis of cleaved products binding to NTA-nickel agarose. After treatment of samples with TEV protease, NTA-nickel agarose beads were added and binding allowed to occur for two hours at 4°C. The sample used is highlighted in red in Figure 5.3.4. The beads were washed with buffer containing 20mM imidazole (W) and bound proteins eluted with buffer containing 250mM imidazole (E).

the beads), all the Rad24 had bound to the beads and was present in the elution fraction. This suggests that Rad24 has affinity for NTA-nickel agarose even without the presence of the histidine tag. When the profile of TEV protease during this procedure was analysed by western blot using an anti-His monoclonal (Figure 5.3.6), it was found in all fractions. The protease tag is only of six histidine residues, and so at 20mM wash stringency may have been too high. Because it was not possible to find conditions in which the cleaved and non-cleaved HTH-Rad24 products were separated on the nickel column, while maintaining the binding of the protease to the column, protease cleavage was omitted from the finalised purification protocol.

It was now necessary to have a very efficient purification at the final stage. For immuno-affinity purification, 12CA5 monoclonal antibody was covalently coupled to protein G sepharose using a dimethlypimelimidate coupling reaction (Schneider *et al.*, 1982). For a trial experiment a sample from the TEV protease test reactions was used. This cleaved product was allowed to bind to the 12CA5 beads for 1 hour, then the beads were washed with buffers of increasing stringency. The buffers used contained, 500mM KCL, 1mg/ml or 5mg/ml peptides containing the HA epitope (HAPEP1 sequence CSKAFSNCYPYDVPDYASLRS and HAPEP2 sequence KKKRILKMYPYDVPDYA RIL), pH11.5, pH2.5, and finally boiling laemmli buffer. Each step of this procedure was analysed by western blot using the anti-Rad24 polyclonal antibody (Figure 5.3.7 part a). The majority of the HTH-Rad24 had bound to the column. A small amount was present in the wash containing the highest concentration of HAPEP2. Significantly more HTH-Rad24 was eluted from the beads by the high pH wash. However, a large quantity of the HTH-Rad24 was left on the beads after these elutions as can be seen from the analysis of proteins removed by boiling the beads in Laemmli buffer. It was decided to optimise the elution with the peptide wash further, as the very specific nature of this elution could result in a large purification factor from this procedure. Optimisation did indeed improve the efficiency of this elution. It was found that by incubating the beads in the presence of the elution buffer at 30°C instead of on ice a much greater proportion of the protein was released. An extra quantity of freshly made protease inhibitors were added before the elution, to give protection during the 30°C incubation. Also, the addition of KCl to a concentration of 500mM improved elution. The beads were agitated during the incubation to improve elution and a repetition of the

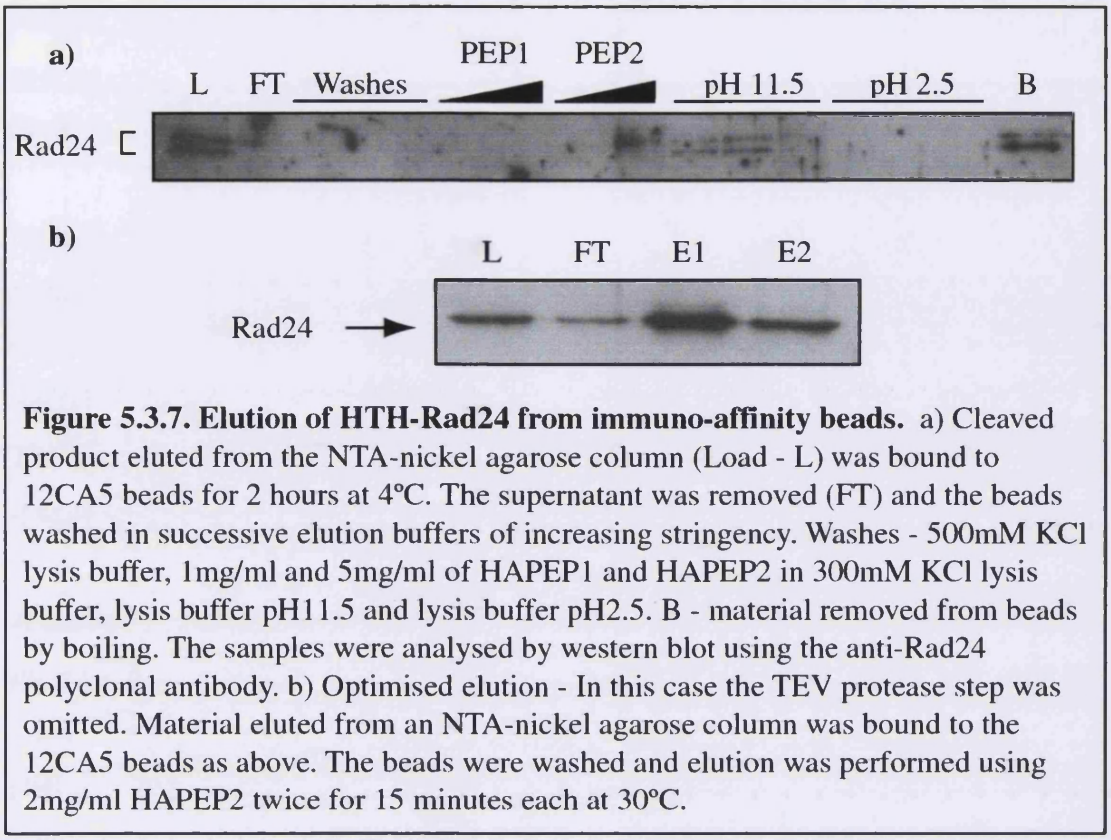

Figure 5.3.7. Elution of HTH-Rad24 from immuno-affinity beads. a) Cleaved product eluted from the NTA-nickel agarose column (Load - L) was bound to 12CA5 beads for 2 hours at 4°C. The supernatant was removed (FT) and the beads washed in successive elution buffers of increasing stringency. Washes - 500mM KCl lysis buffer, 1mg/ml and 5mg/ml of HAPEP1 and HAPEP2 in 300mM KCl lysis buffer, lysis buffer pH11.5 and lysis buffer pH2.5. B - material removed from beads by boiling. The samples were analysed by western blot using the anti-Rad24 polyclonal antibody. b) Optimised elution - In this case the TEV protease step was omitted. Material eluted from an NTA-nickel agarose column was bound to the 12CA5 beads as above. The beads were washed and elution was performed using 2mg/ml HAPEP2 twice for 15 minutes each at 30°C.

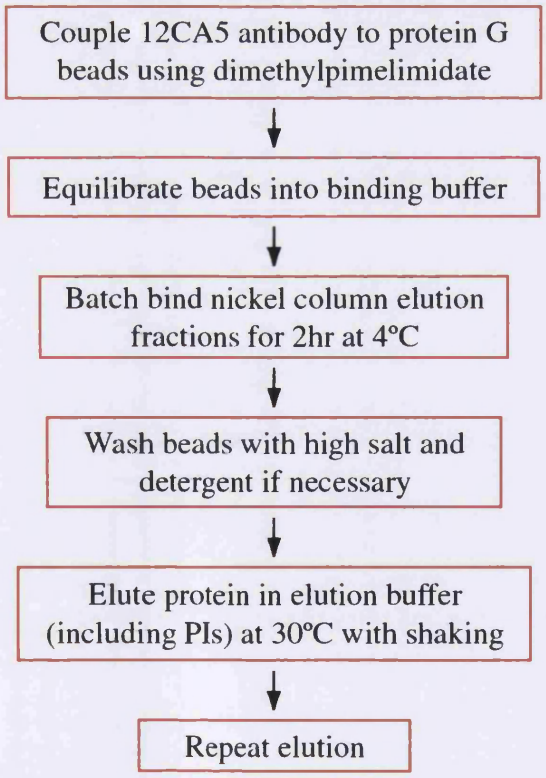

Figure 5.3.8. A strategy for the immuno-affinity purification of NTA-nickel purified HTH-Rad24. The full procedure is described in the text and in the materials and methods section.

elution step was also included to release more protein. An example of western blot analysis of an improved elution is given in Figure 5.3.7 part b. Figure 5.3.8 depicts the final optimised procedure.

In order to analyse the purified products from the immuno-affinity step samples were separated on an 8-15% SDS-PAGE gradient gel (BioRad) and analysed by silver staining (Figure 5.3.9). 100 fold less volume of the load and flow through samples were loaded relative to the eultion samples. Standard molecular markers were also loaded. The elution fraction contained three visible bands, one at the size expected for HTH-Rad24 and two smaller polypeptides of approximately 40 and 35kDa.

A sample of the purified material was fractionated on a superose 6 gel filtration column in order to ascertain if the HTH-Rad24 complex had survived the purification procedure intact. When analysed by western blot it was clear that the purified HTH-Rad24 was still a component of a large molecular mass complex. The elution profile was not significantly different from that of the stating material (heparin column load sample) (Figure 5.3.10). This suggests that the complex was purified intact, and that all of the components should be present for mass spectrographic analysis.

A large, 30ml 10% acrylamide gel was poured in order to prepare the remainder of the sample for mass spectrographic analysis. The sample was incubated for 1hour with new NTA-nickel agarose beads. This was to concentrate the sample for loading onto the gel, and also to remove some of the elution peptide which is in the buffer. The supernatant was removed and the beads boiled in Laemmli buffer which was then loaded onto the gel. After the run, the gel was stained with coomassie blue, de-stained extensively and the bands excised. The bands were washed in 50% methanol, dried, and shipped to Dr Paul Tempst in New York, who had kindly offered to collaborate with us on this project. The results of his analysis are given below, but briefly, the large band was indeed identified as containing HTH-Rad24, the 40kDa band contained both Rfc2 and Rfc3, and the p35 band could not be assigned due to high background levels of elution peptide in the sample (Figure 5.3.9).

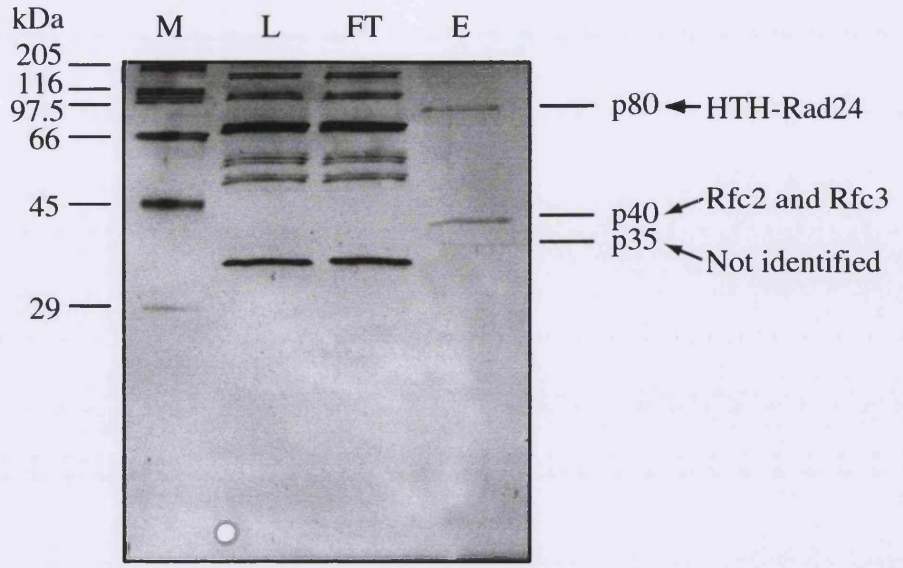

Figure 5.3.9. Silver stained SDS-PAGE gel of the final step of the purification. 0.1µl each of the load (L) and supernatant (FT) from the immuno-affinity column and 10µl of the first peptide elution fraction (E) were loaded onto a 8-15% gradient gel (Bio-Rad). Standard molecular weight markers were also loaded (M). The gel was stained as described in the materials and methods section. Above 45kDa the bands all appear as doublets, this is an artefact due to the drying of the gel. The proteins indicated to the right were deduced to be the major components of the bands indicated by mass spectrographic analysis of the remainder of sample E run on a larger gel.

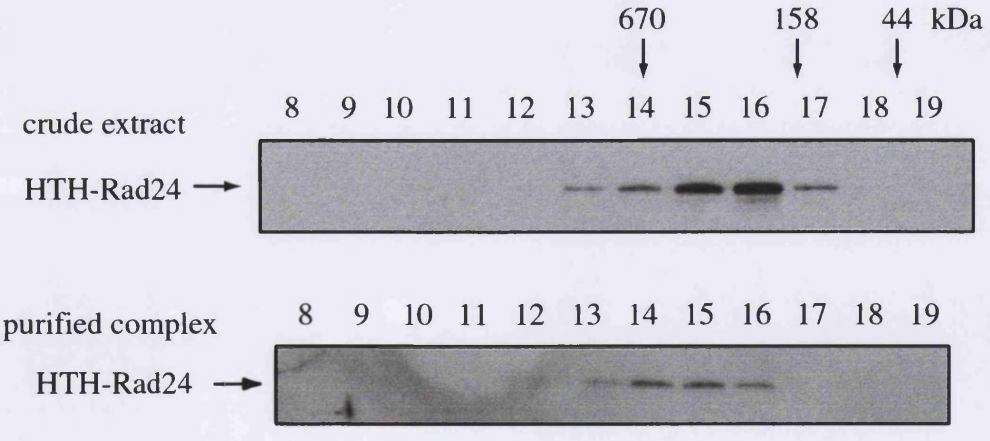

Figure 5.3.10. The purified complex has a large stokes radius. 250µg crude extract from the start of the large scale purification and 0.1µl from the most purified fraction were run independently on a superose 6 gel filtration column. The fractions were analysed by western blot using the anti-Rad24 polyclonal antibody. The elution position of standard size markers is shown above.

Upon arrival in New York the gel-bound protein bands designated p80, p40 and p35 were digested with trypsin, and the peptides purified by reversed phase chromatography (Erdjument-Bromage *et al.*, 1998). Mass spectrometry (MALDI-ReTOF) was performed on the two recovered peptide pools using a Bruker REFLEX III instrument with delayed extraction. For mass fingerprinting, top 'major' experimental masses (m/z) combined from both MALDI-ReTOF experiments were used to search a non-redundant protein database (NR; ~403000 entries; NCBI; Bethesda, MD), using the PeptideSearch algorithm (Mann *et al.*, 1993).

From peptide p80 twenty major experimental masses were used, one protein of molecular weight ~76kDa was retrieved, having 8/18 theoretical mass [MH+] matches with the masses obtained from p80. This was the *S. cerevisiae* Rad24 protein; SwissProt P32641. From peptide p40 thirty three major experimental masses were used, one protein of molecular weight ~41kDa was retrieved, having 11/33 theoretical mass [MH+] matches with the masses obtained from p40. This was the *S. cerevisiae* Rfc2 protein; SwissProt P40348. The remaining twenty two major experimental masses were used for a second search; one protein of molecular weight ~40kDa was retrieved, having 10/22 theoretical mass [MH+] matches with the masses obtained from p40. This was the *S. cerevisiae* Rfc3 protein; SwissProt P38629. The masses and calculated peptides are given in Table 5.3.

The only masses obtained from the p35 band were of 1389.59 and 1778.95, which corresponded to the HAPEP2 peptide used during the purification procedure, hence the polypeptide component of this band was not identified by mass spectrometry.

5.4 – COMPLEX ANALYSIS BY CO-IMMUNOPRECIPITATION

Rfc2 and Rfc3 are two of the five subunits of *S. cerevisiae* replication factor C (Mossi and Hubscher, 1998). Because these two had been identified as co-purifying with HTH-Rad24 is was decided to investigate whether the other RFC subunits could also be detected interacting with Rad24. It is possible, for example, that any signal from peptides arising from the other subunits was masked by the high background in the spectrographic run due to the competitor peptide, or that the other subunits had less

a) p80 peptides from Rad24				
observed (m/z)	Calculated (MH+)	ΔDa (ppm)	Residues	Sequence in Rad24
1010.464	1010.465	0.001 (1)	132-140	(R)QNSNGTSFR(S)
1067.515	1067.519	0.004 (13)	579-586	(R)MLIDQYER(N)
1115.583	1115.569	-0.014 (19)	529-538	(R)VENGIDVVDR(I)
1259.625	1259.649	0.024 (19)	26-36	(R)WSSSRPTSSPVR(K)
1352.689	1352.684	-0.005 (4)	334-345	(R)ESTISYFHAIGK(V)
1412.659	1412.682	0.023 (16)	434-445	(K)QGHNHGTVYFPR(E)
1749.833	1749.865	0.032 (18)	298-312	(R)QEVIDYIAQETGDIR(S)
1906.021	1905.966	-0.055 (28)	297-312	(K)RQEVIDYIAQETGDIR(S)
b) p40 peptides from Rfc2				
observed (m/z)	Calculated (MH+)	ΔDa (ppm)	Residues	Sequence in Rfc2
1072.581	1072.600	-0.019 (17)	220-229	(R)ILDISAGDLR(R)
1093.526	1093.552	0.026 (24)	203-211	(R)FISEQENVK(C)
1144.524	1144.530	0.006 (5)	156-165	(R)TMETYSGVTR(F)
1159.584	1159.595	0.011 (9)	92-101	(R)ILELNASDER(G)
1228.672	1228.701	0.029 (23)	220-230	(R)ILDISAGDLRR(G)
1580.739	1580.807	0.068 (43)	320-332	(K)NQISWLLFTTDSR(L)
1786.833	1786.894	0.061 (34)	55-71	(K)SANLPHMLFYGPPGTGK(T)
1933.055	1933.086	0.031 (16)	333-349	(R)LNNGTNEHIQLLNLLVK(I)
2032.979	2033.022	0.043 (21)	136-154	(K)IIILDEADSMTADAQSALR(R)
1802.814	1802.889*	0.075 (41)	55-71	(K)SANLPHMLFYGPPGTGK(T)
2048.994	2049.017*	0.023 (11)	136-154	(K)IIILDEADSMTADAQSALR(R)
c) p40 peptides from Rfc3				
observed (m/z)	Calculated (MH+)	ΔDa (ppm)	Residues	Sequence in Rfc3
1022.589	1022.599	0.010 (9)	178-186	(R)IANVLVHEK(L)
1178.685	1178.700	0.015 (13)	177-186	(R)RIANVLVHEK(L)
1218.592	1218.615	0.023 (19)	196-206	(K)ALIELSNGDMR(R)
1327.690	1327.700	0.010 (8)	166-176	(R)FQPLPQEAIER(R)

1496.755	1496.826	0.071 (47)	46-59	(K)LPHLLFYGPPGTGK(T)
1862.828	1862.892	0.064 (34)	250-265	(K)SILEDDWGTAHYTLNK(V)
2043.044	2043.054	0.010 (5)	113-131	(K)LIILDEADAMTNAAQNALR(R)
2172.096	21722.149	0.053 (24)	40-59	(K)FVDEGKLPHLLFYGPPGTGK(T)
1756.717	1756.781*	0.064 (36)	74-88	(K)NYSNMVLELNASDDR(G)
2059.037	2059.049*	0.012 (6)	113-131	(K)LIILDEADAMTNAAQNALR(R)

Table 5.3. Peptides identified from mass spectrographic analysis of purified HTH-Rad24 complex. The observed mass to charge ratio (m/z) is given in the first column. The closest theoretical mass to this value is in the second, followed by the difference between the two. Only matches within 40ppm accuracy were allowed. The fourth and fifth columns give the position and peptide sequence of matched peptides in the proteins indicated. An asterisk indicates the mass derived included an oxidised methionine residue.

cleavage sites for trypsin, which would result in their under representation in the analysis. No reagents were available for the detection of the yeast RFC subunits. In order to generate such reagents quickly it was decided to use an epitope tagging approach similar to that described in Figure 5.1.1 to integrate an epitope at the carboxyl terminal end of each RFC gene. The epitope tag chosen for this purpose consisted of three FLAG epitopes. This was chosen because a highly specific and sensitive monoclonal antibody is commercially available which recognises this motif (anti-FLAG (Sigma)). Complimentary oligonucleotides (oligos 812-3) encoding this tag were cloned into the pRS304, pRS305 and pRS306 vectors. A fragment from the 3' end of each RFC ORF was amplified by PCR from genomic DNA (primers 829-38 see Appendix I) so that it could be cloned in frame with the tag in the vector. Linearisation of the resulting constructs and integration into the yeast genome by homologous recombination resulted in the production of carboxyl-terminally FLAG-tagged RFC genes (designated RFC-F). The integrations were checked by PCR (data not shown).

To ensure that the tagging of the RFC subunits did not affect the biological function of RFC drop test survival analyses were performed. RFC is an essential activity for growth, and all RFC subunits are encoded by essential genes, therefore any perturbation

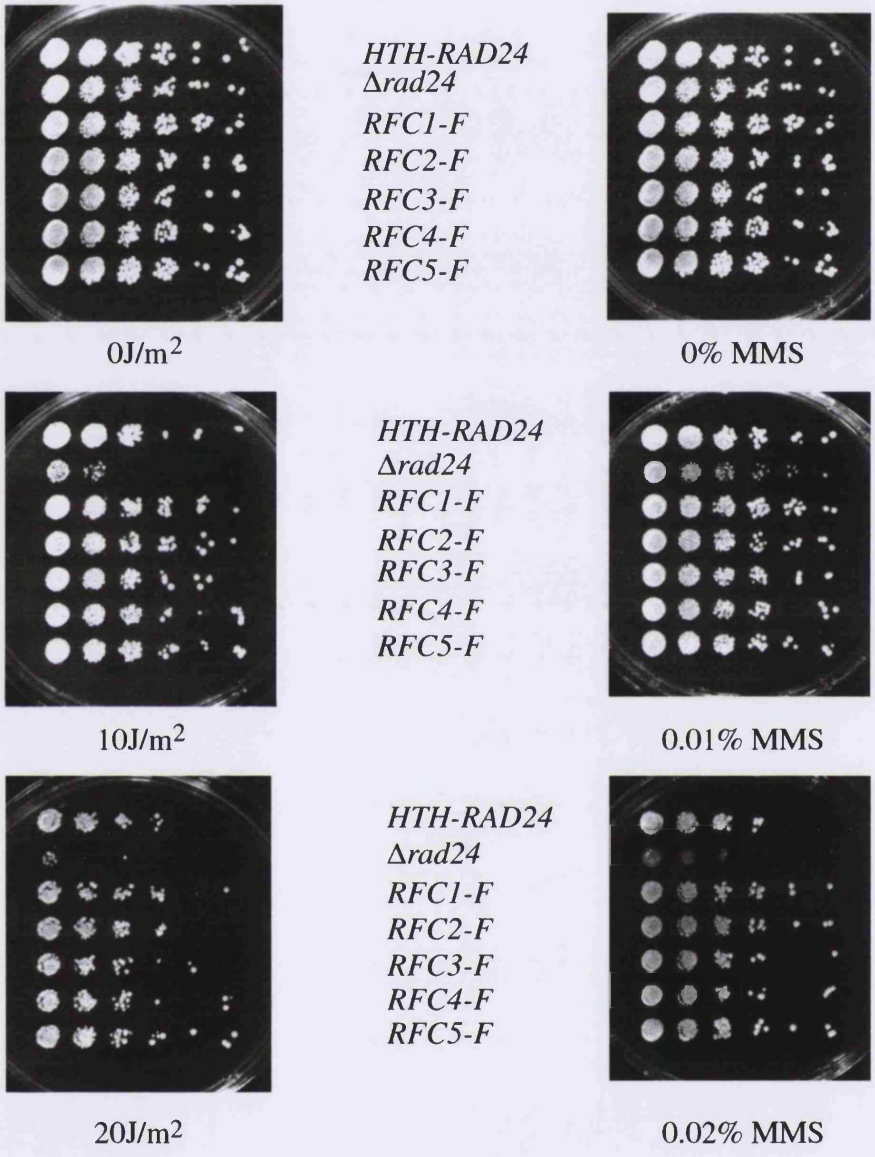

Figure 5.4.1. Drop test survival analysis after UV irradiation of strains containing FLAG-tagged RFC subunits. Ten fold dilution series from the strains indicated were plated onto YPD plates using a replica plater. The starting concentration was $1x10^7$ cells/ml. The plates either contained MMS at the concentrations indicated, or were exposed to UV light for the doses indicated. Photographs were taken after two days growth at 30°C.

of function was likely to result in a growth detect in the RFC-F strains. Ten fold dilution series were prepared from each strain in mid logarithmic growth phase, with a starting concentration of $5x10^6$cells/ml. Cells were transferred to YPD plates using a replica plater. Survival was analysed under a variety of conditions, for example UV irradiation, MMS exposure (Figure 5.4.1) and different temperatures (data not shown). In all conditions tested the RFC-F strain growth was equivalent to WT, suggesting that the tagged proteins retain normal biological function.

In order to investigate possible interactions between Rad24 and RFC subunits co-immunoprecipitation experiments were performed. Extracts were prepared by the small scale liquid nitrogen method from *RFC-F* and *rad24Δ RFC-F* strains. The anti-Rad24 polyclonal serum and protein A beads were used for the precipitation as described in Materials and Methods. The starting extracts and precipitated proteins were analysed by western blotting using the anti-Rad24 polyclonal and the anti-FLAG monoclonal antibodies (Figure 5.4.2). An anti-FLAG reactive band of the expected size for Rfc1, Rfc2, Rfc3, Rfc4 and Rfc5 was visible in the extracts from the appropriate strains (lower panel). The anti-FLAG antibody has one non-specific cross reactive band in these extracts, at approximately 90kDa, which migrates slightly faster than Rfc1 through SDS-PAGE. Immuno-precipitation of HTH-Rad24 co-precipitated Rfc2, Rfc3, Rfc4 and Rfc5. Rfc1 was not co-precipitated even though the efficiency of HTH-Rad24 precipitation was equivalent in this strain (top panel). This precipitation was specific as the small RFC subunits were not precipitated by the anti-Rad24 polyclonal in extracts made from the control *rad24Δ RFC-F* strains. This strongly suggests that HTH-Rad24 is capable of interacting with all the small RFC subunits but not Rfc1. Similar results were obtained if HTH-Rad24 was precipitated using the 12CA5 monoclonal antibody rather than the anti-Rad24 polyclonal (data not shown).

Reciprocal precipitations were performed using the anti-FLAG monoclonal antibody and protein G beads. The starting extracts and precipitated proteins were analysed by western blotting using the anti-Rad24 polyclonal and the anti-FLAG monoclonal antibodies (Figure 5.4.3). HTH-Rad24 was co-precipitated with Rfc2, Rfc3, Rfc4 and Rfc5 but not with Rfc1 (lower panel), even though the efficiency of Rfc1 precipitation

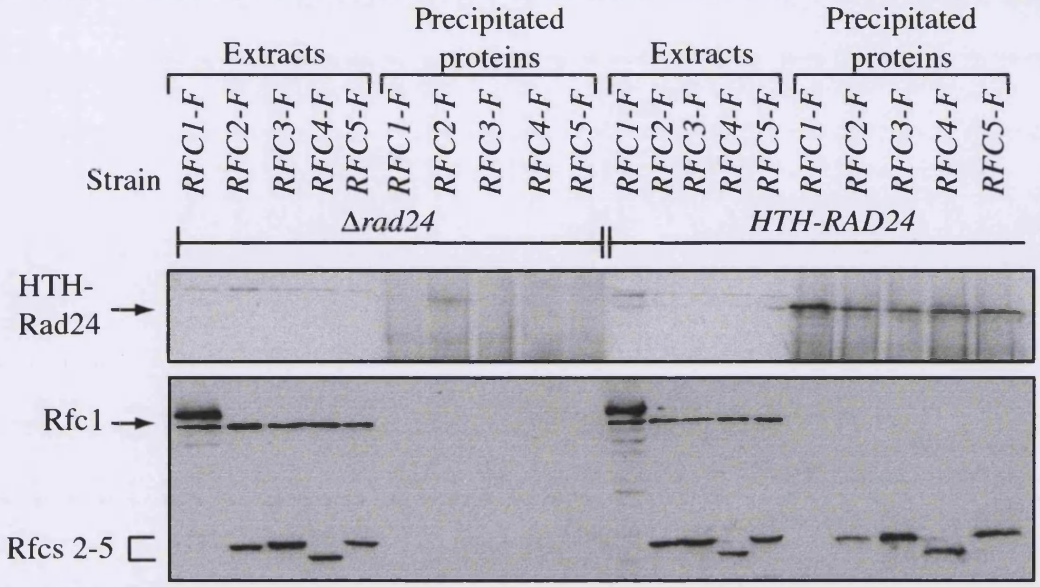

Figure 5.4.2. Immunoprecipitations from strains containing FLAG-tagged RFC subunits using anti-Rad24 polyclonal serum. Precipitations were performed from 500µg each extract using antibody at a 1 in 50 dilution and protein A beads. The starting material and proteins boiled from the beads were analysed by western blot with the anti-Flag monoclonal antibody (upper panel) and anti-Rad24 polyclonal antibody (lower panel). An F after a gene name designates the addition of a 3' FLAG epitope. The band migrating just below Rfc1-F is a non-specific anti-Flag reactive band in the yeast extracts.

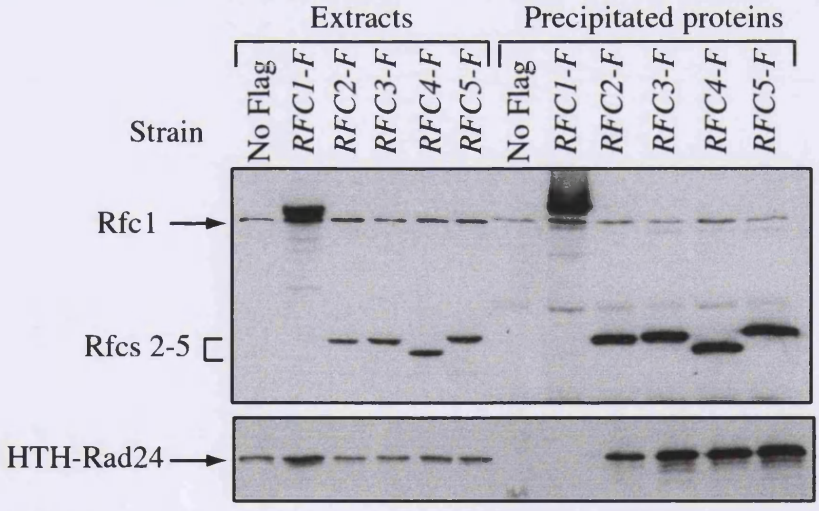

Figure 5.4.3. Immunoprecipitations from strains containing FLAG-tagged RFC subunits using anti-FLAG monoclonal antibody. Precipitations were performed from 500µg each extract using antibody at a 1 in 50 dilution and protein G beads. The starting material and proteins boiled from the beads were analysed by western blot with the anti-Flag monoclonal antibody (upper panel) and anti-Rad24 polyclonal antibody (lower panel). An F after a gene name designates the addition of a 3' FLAG epitope. The band migrating just below Rfc1-F is a non-specific anti-Flag reactive band in the yeast extracts.

was equivalent to the other RFC subunits (top panel). This precipitation was specific as the HTH-Rad24 was not precipitated by the anti-FLAG monoclonal in extracts made from the control *HTH-RAD24* strain without an epitope tagged RFC subunit. This confirms that the HTH-Rad24 complex is likely to contains Rfcs2-5 but not Rfc1.

5.5 – GEL FILTRATION ANALYSIS OF RFC SUBUNITS AND PURIFIED COMPLEX

The extracts made for the immuno-precipitation analyses were subjected to gel filtration through a superose 6 column. Fractions were analysed by western blotting using the anti-Rad24 polyclonal serum and the anti-FLAG monoclonal antibody (Figure 5.5.1). In agreement with the precipitation data the Rfc1 peak did not correspond to the size of the Rad24 peak, confirming the hypothesis that the majority of Rfc1 is not associated with Rad24. The Rfc1 protein peak was in fraction 10, suggesting that this protein has a very large stokes radius, perhaps diagnostic of a large protein complex. The small RFC subunits RFCs2-5 had a bi-phasic distribution of elution from the sizing column. Approximately 75% of the signal from these subunits co-fractionated with Rfc1 in a large complex, as was expected. The radius of this complex was larger than the Rad24 complex. This may be indicative of the association of RFC with other protein components as Rfc1 and Rad24 are similar in mass, so their direct substitution might be expected to lead to two complexes of similar sizes.

The remaining proportion of the small RFC subunits co-fractionated with each other in fractions 15 and 16. Although it would be tempting to speculate that this population of these small subunits corresponded to that fraction that is associating with Rad24, this second peak of these subunits did not exactly co-fractionate with Rad24. The HTH-Rad24 peak eluted slightly earlier than the RFC peak with the smaller Stokes radius. It is therefore likely that this second peak represents either monomeric small RFC subunits, or an RFC sub-complex.

In order to absolutely confirm the association of all four small RFC subunits with HTH-Rad24 the purification was repeated using extract from a strain expressing RFC3-FLAG. The purification was as before except the stringency of washing of the NTA-nickel agarose column was reduced to 20mM imidazole. The peptide-eluted material

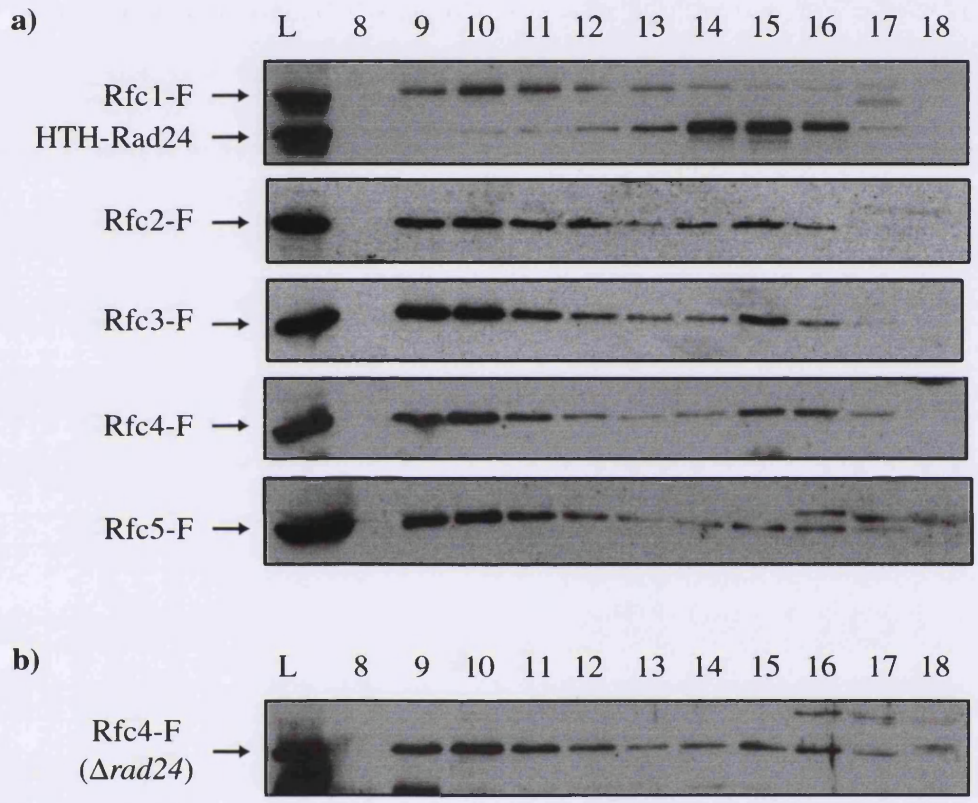

Figure 5.5.1. Gel filtration analysis of RFC subunits. a) 250mg whole cell extracts from WT strains expressing FLAG-tagged RFC subunits were fractionated on a superose 6 column. The fractions were analysed by western blotting using the anti-FLAG monoclonal or anti-Rad24 polyclonal antibodies. b) as in part a but with extract from a Δ*rad24* strain expressing *RFC4-FLAG*.

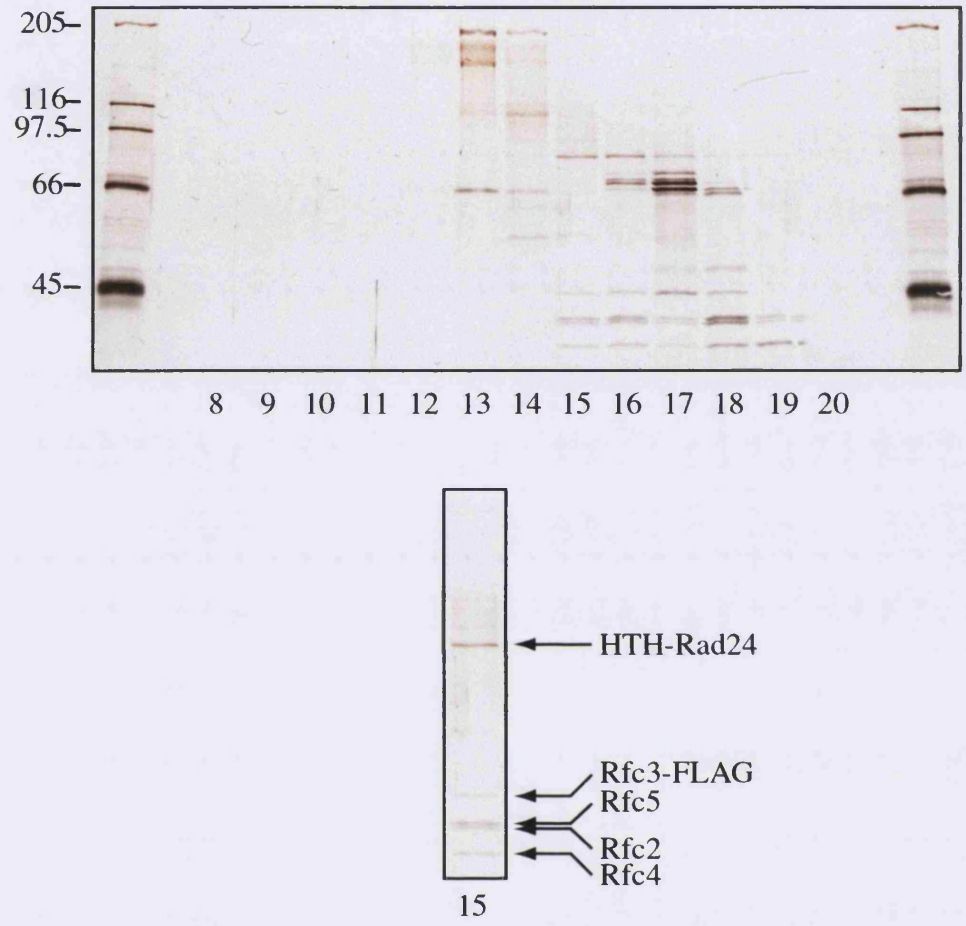

Figure 5.5.2. Purification of the HTH-Rad24 complex from a strain containing *RFC3-FLAG*. The purification was as before except a lower stringency wash was used during the nickel column. The peptide eluted sample was fractionated on a superose 6 gel filtration column, and the fractions analysed by SDS-PAGE and silver staining. The migration positions of standard size markers (SDS-6H) are indicated. The most purified Rad24 containing fraction is 15, which is shown separately below the main image. The proteins that are assumed to be the major component of each band are labelled.

from the immuno-affinity column was separated by gel filtration and the fractions analysed by silver staining (Figure 5.5.2). In this case the Rad24 complex eluted in fractions 15 and 16. In these fractions four co-fractionating polypeptides were clearly visible. The gel used for this analysis, contained 8.5% acrylamide, a much lower percentage than used for the gel of Figure 5.3.8. The Rfc3 protein in this extract contains the three FLAG epitopes, therefore it migrated more slowly than the untagged RFCs, at approximately 45kDa. The identity of this band was confirmed by western blot. Under these conditions it was possible to separate the p40 band into two species. From their relative migration under these conditions the other three co-fractionating bands are assumed to be Rfc5, Rfc2 and Rfc4, which have theoretical masses of 39.9, 39.7 and 36.2kDa respectively.

5.6 – DISCUSSION

One of the advantages of using the yeast *S. cerevisiae* as a model system is the elevated activity of the homologous recombination pathway for double strand break repair. This, along with the fully sequenced genome allow the rapid production of deletion mutants and genes with epitope tags by simple PCR based methods (Rothstein, 1991)(Figure 5.1.1). Without such technology the purification of extremely low abundance protein species such as the Rad24 complex described here would be virtually impossible.

One of the disadvantages of using budding yeast for purification studies however is the difficulty of preparing cell extracts. The cell wall of this organism is strong, and enzymatic or vigorous mechanical methods are needed to break it. On a large scale enzymatic treatment is impractical, so it was necessary to optimise a lysis procedure that efficiently broke the cells while preserving the nature of the soluble cell contents. One of the major difficulties with mechanical methods is the avoidance of localised heating during the disruption. This may be a factor affecting the quality of the extracts, particularly those produced by the classic bead disruption method. Lysis of yeast cells in a coffee grinder in the presence of solid carbon dioxide has been described as an efficient way of producing high quality extracts (Schultz, 1999). This method was found to result in aggregation artefacts for Rad24. However this appears to be a specific problem, as many other groups at Clare Hall have been using this method with

success. It is possible that this aggregation could be caused be changes in pH of the extracts due to the carbon dioxide used. The most gentle way of lysis, manual grinding at liquid nitrogen temperatures, although time consuming on this scale, was found to be the most reproducible high quality extraction method. This technique had been shown to be effective at producing NER competent yeast extracts on a large scale (Stephanie Kong, personal communication). It was even found that the choice of mortar affected the extract quality. Extracts produced in 100g batches in a 1.5 litre mortar contained less aggregated Rad24 than 600g batches in a 6 litre mortar (data not shown). This may be due to the time spent on the extraction, 40 minutes/batch versus 2 hours.

In the final purification procedure the TEV cleavage step was omitted (Figure 5.3.1). There were many problems with this step in the case of Rad24, but it may be a useful addition if this procedure is attempted for the purification of other proteins. The high concentration of protease required for efficient cleavage (Figure 5.3.5) meant that a concentration step was needed in order to use this procedure on the approximate 6ml material that was eluted from the large scale NTA-nickel agarose column. Many concentration methods were attempted, including ultra-centrifugation and polyethylene glycol compound mediated osmosis, but none were found to efficiently concentrate this very dilute protein solution without a loss of material (data not shown). Also the maximum cleavage obtained was 50% (Figure 5.3.5), which would result in a minimum 50% loss of material at this stage even if all else was optimised. However the major difficulty with this step was the failure to separate the cleaved and non-cleaved HTH-Rad24 species on the subsequent nickel column while maintaining the binding of the protease (Figure 5.3.6). Without this step, the cleavage reaction was useless, as no increase in the complex purity was obtained.

The initial purification allowed the identification of Rfc2 and Rfc3 as components of the Rad24 complex. Another group had recently published a study demonstrating that Rad24 could be co-immunoprecipitated with Rfc5 and Rfc2 (Shimomura *et al.*, 1998). It was therefore decided to engineer epitope tagged versions of all of the RFC subunits, to conclusively demonstrate which were components of the Rad24 complex. The co-immunoprecipitation studies presented here demonstrate clearly that the small

RFC subunits interact with Rad24, whereas Rfc1 does not (Figures 5.4.2 and 5.4.3). As Rfc4-F migrates more quickly than the other small subunits through SDS-PAGE it is a good candidate for the p35 band observed in the original purifcation (Figure 5.3.9). It is likely that Rfc5 is contained in the p40 band though this was not identified by mass spectrometry. The presence of three polypeptides in the p40 band would account for the stronger staining of this band relative to p35.

A model for RFC complex assembly has been presented in which the four small subunits form a stable preliminary structure, and Rfc1 then joins (Podust and Fanning, 1997). The data presented in Figure 5.5.1 supports such a model as is can be interpreted to suggest that the four small subunits exist as a stable sub-complex in crude cell extracts. The lack of co-precipitation of HTH-Rad24 with the small RFC subunits in crude extract suggests that the proportion of the total cellular RFC involved in this checkpoint complex is small, too low to be detected by this method.

The final gel filtration column resulted in the purification of a complex with apparent 1:1:1:1:1 stoichiometry, including Rad24, Rfc3, and three other subunits of precisely the sizes expected for the other small RFC subunits (Figure 5.5.2). This makes a compelling case for the existence of the Rad24 checkpoint complex depicted in Figure 5.6, especially when taken together with the previous purification and co-immunoprecipitation analysis. The theoretical mass of such a complex would be 232kDa, which agrees well with the predicted mass for the Rad24 complex of 260±50kDa, as determined in Chapter 4. The observation that overexpression of *RAD24* is synthetically lethal in a strain carrying a mutation in *cdc44* (Lydall and Weinert, 1997) can now be explained. The *CDC44* gene encodes Rfc1, it is likely that the mutant version of rfc1 is impaired either in its production or in its ability to associate with the small RFC subunits. Over-production of Rad24 would therefore exacerbate this defect by titrating available small subunits until not sufficient RFC complex was available for cell growth. The predicted interaction of this complex with DNA and the subsequent loading of the presumptive Rad17 "PCNA-like" complex (see Introduction) is a hypothesis upon which the work presented in Chapter 6 and that currently ongoing is based.

The purifications of HTH-Rad24 presented here were all from extracts made from undamaged cells. Recently protocols have been developed in the laboratory for UV and γ irradiation of large yeast cultures (Gilbert *et al.*, 2000). It would therefore be possible to undertake purification of the Rad24 complex from damaged cells. Although there is no apparent change in the complex after UV irradiation (see Chapter 4), some subtle modification or structural rearrangement could occur. This might result in activation of an enzymatic activity which has so far failed to be identified in the complex purified from undamaged cells (see Chapter 6). Work is currently under way in the laboratory to purify Mec3 from yeast extracts using a similar method to that developed here. We have also recently been successful in the purification to homogeneity of complexes containing Rad9, using similar (Gilbert *et al.*, 2000). It is likely that any soluble protein that can tolerate the addition of an epitope tag can be purified in this manner.

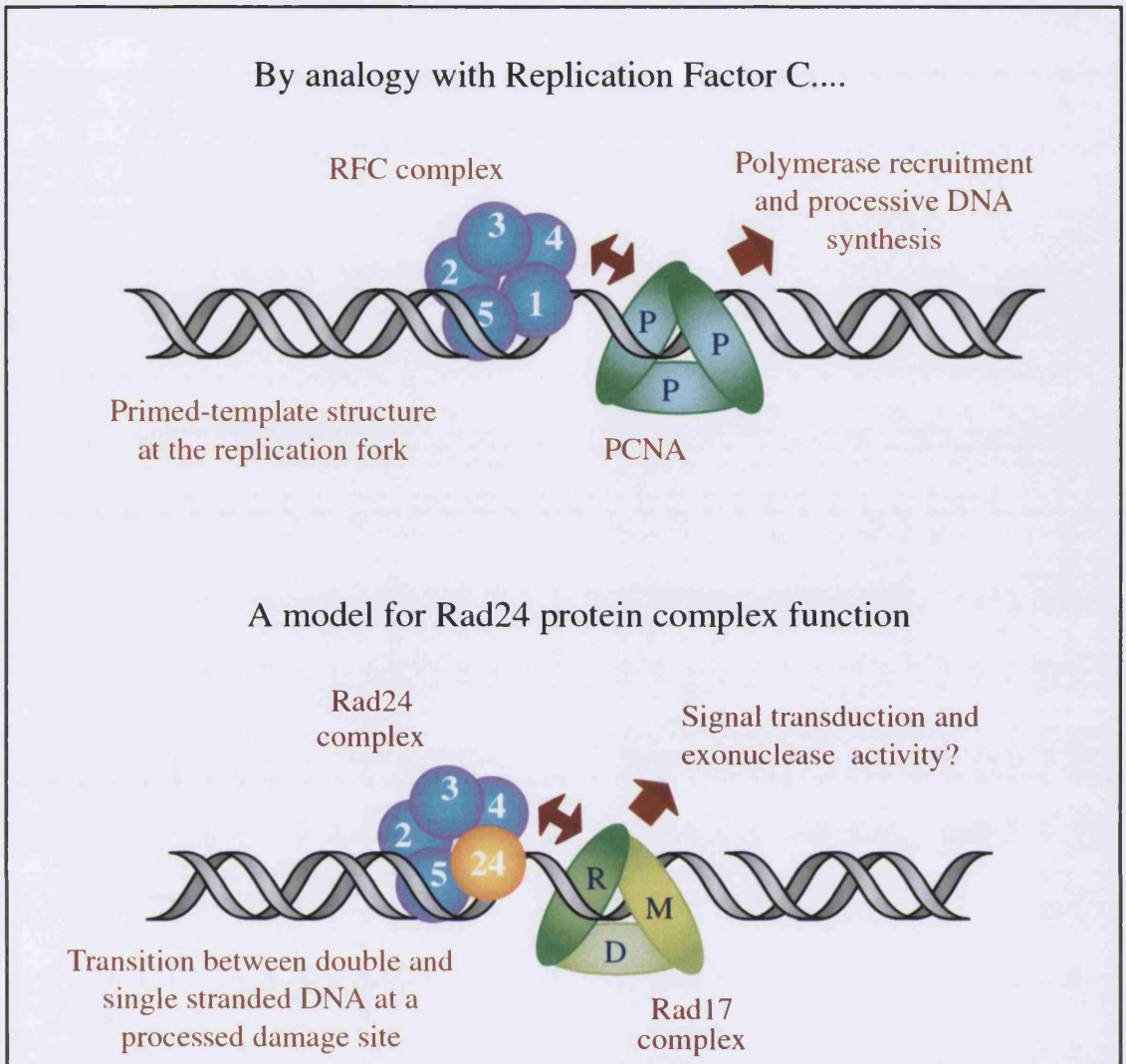

Adapted from Lowndes and Murguia. Curr Opin Gen & Dev. 2000

Figure 5.6. A model for Rad24 complex function during checkpoint pathway activation. Because of the similarity between the Rad24 complex and the RFC complex, it is likely that these two complexes have similar biochemical roles. RFC (1,2,3,4,5) functions as a clamp loader to load the trimeric PCNA (P) at a primer template junction for processive DNA synthesis (upper image). The Rad24 complex (24,2,3,4,5) might recognise a single stranded to double stranded DNA transition and load the putative PCNA-like Rad17 complex (R,M,D) which contains Rad17, Mec3 and Ddc1 (lower image). This DNA structure may result from processing of lesions by repair pathways. It is possible that Mec1 may be required for this loading to occur. The Rad17 complex, in association with DNA somehow causes the activation of Rad53, possibly via Mec1. The Rad17 complex may also possesses exonuclease activity, which could extend the single stranded DNA region, perhaps amplifying the signal.

CHAPTER 6 – PHYSIOLOGICAL AND BIOCHEMICAL ANALYSIS OF THE RAD24 COMPLEX

The Rad24 complex has been identified as comprising Rad24, Rfc2, Rfc3, Rfc4 and Rfc5, most likely as a complex containing one molecule of each of these subunits (Chapters 5 and 4), in a complex analogous to RFC. RFC is a highly conserved five subunit protein complex essential for DNA replication (Mossi and Hubscher, 1998). In *S.cerevisiae* the five essential genes that encode RFC are designated *RFC1*, *RFC2*, *RFC3*, *RFC4* and *RFC5*, each are highly homologous to each other. The complex was originally identified in extracts from human cells, the yeast genes were identified by their sequence homologies to the human subunits (Cullmann *et al.*, 1995), and also by purification of the RFC activity from yeast (Fien and Stillman, 1992). An alignment of the *S.cerevisiae* RFC genes with *RAD24* is shown in Figure 1.8.2. The RFC complex is responsible for the recognition of primed template structures at the initiation of leading strand synthesis and for each Okasaki fragment. RFC binds to PCNA at the single stranded to double stranded DNA transition during replication and recruits polymerases delta and epsilon (Burgers, 1991). The RFC complex has ATPase activity which is stimulated by single stranded DNA (Yoder and Burgers, 1991). All five RFC subunits have potential ATP binding sites, mutations in any of these binding sites in the human subunits, except that in subunit p38, inactivates the RFC complex (Cai *et al.*, 1998). Viral vectors for producing the yeast RFC in baculovirus have been constructed (Podust and Fanning, 1997), and used to analyses interactions between the subunits. It is also possible to over produce the entire complex in yeast cells, which allow an easy purification using the magnesium-dependent association of RFC to PCNA beads as a high affinity chromatography step (Gerik *et al.*, 1997).

The Rad24 protein eluted as a single peak throughout the purification in Chapter 5, hence it is likely that this represents the major form of Rad24 as exists in cells extracts. The principle genetically characterised role of *RAD24* is in activation of the DNA damage-dependent checkpoint pathway, and so it is likely that this complex has a role in this response. In order to address the question of what role the Rad24 complex has in this pathway, two directions of study were initiated. The first was a physiological approach, to attempt to identify a role for the small RFC subunits in the checkpoint

pathway. Secondly a biochemical study was initiated, using the purified material, to try and identify a biochemical function of the Rad24 protein complex.

6.1 – INVESTIGATING A ROLE FOR RFC SUBUNITS IN THE DNA DAMAGE-DEPENDENT CHECKPOINT PATHWAY

RFC5 and *RFC2* are both required for the function of the checkpoint that prevents mitosis during S-phase if replication is blocked (Sugimoto *et al.*, 1996; Noskov *et al.*, 1998), *RFC5* is also required for the checkpoint that slows S-phase in the presence of DNA damage (Sugimoto *et al.*, 1997). A similar checkpoint defect has been identified for mutants of the *S. pombe* RFC genes $rfc2^+$ and $rfc3^+$ (Reynolds *et al.*, 1999; Shimada *et al.*, 1999). Interestingly a mutation in the gene encoding Rfc1, *CDC44*, is not defective in S-phase checkpoint control (Howell *et al.*, 1994). In both yeasts, all RFC genes are essential for growth, hence these studies were performed using temperature sensitive conditional alleles. *rfc2-1* and *rfc5-1* are the only currently available conditional mutants in *S. cerevisiae* RFC genes. The model presented in Chapter 5 implies that the small RFC subunits should have a role in checkpoint activation outside of S phase. The *S. cerevisiae rfc5-1* strain, although defective in S-phase checkpoints, has a WT checkpoint response to DNA damaging agents outside of S-phase (Sugimoto *et al.*, 1997), suggesting that the checkpoint pathway which operates through *RAD24* is likely to be intact in this strain. Although *rfc2-1* is sensitive to DNA damaging agents, the effect of cell cycle position on this sensitivity has not been determined (Noskov *et al.*, 1998). It is possible that this sensitivity is due to a defect in S-phase damage sensing, as for *rfc5-1*, and/or a defect in DNA damage-dependent checkpoints outside of S-phase. In an attempt to demonstrate a requirement for an RFC subunit in a non S-phase checkpoint pathway, the response of the *rfc2-1* strain to DNA damaging agents in G2 phase was investigated.

The rfc2-1 and parental WT strains were kindly provided by Dr. Akio Sugino. The strains were grown to mid-logarithmic growth phase at 25°C in YPD medium. The doubling time of both strains was approximately 3 hours under these conditions. Nocodazole was added to a final concentration of 10μg/ml and the cells incubated for a further 2.5 hours until >80% had a dumb-bell morphology as determined by microscopy. After this time cells were resuspended in fresh YPD medium, prewarmed

to 37°C and containing 10μg/ml nocodazole. The cells were maintained at 37°C for a further 2 hours, then transferred to saline, UV irradiated at 40J/m^2 and re-suspended in YPD plus nocodazole at 37°C. After a further 30 minutes the cells were harvested and extracts prepared for western blot analysis using the anti-Rad53 antibody (Figure 6.1.1).

The phosphorylation of Rad53 is taken to be an indication that the checkpoint pathway is activated (Sun *et al.*, 1996). In the WT *RFC2* extracts Rad53 migrates as a fast migrating species in the unirradiated samples, and a more slowly migrating smear of bands in the irradiated samples, a pattern characteristic of the phosphorylation of Rad53. Although a similar pattern was observed in the *rfc2-1* extracts, there did appear to be some defect in the phosphorylation of Rad53. This may be indictative of a partial checkpoint defect in G2 in this strain. However there were some problems with this experiment. The slower growth rate of the *rfc2-1* strain relative to WT meant that the nocodazole block may not have been complete. The entire experiment involves a prolonged G2 arrest, which is not always well maintained by nocodazole, especially at 37°C. If a proportion of the cells had exited the arrest and entered S phase, the reported defect in S-phase checkpoints could explain the altered phosphorylation of Rad53. On the other hand, the *rfc2-1* strain undergoes at least three doublings at 37°C before arrest (Noskov *et al.*, 1998), suggesting that it can take up to 8 hours for the rfc2-1 protein to become inactive. The experimental design only allowed for a two hour inactivation. An incomplete inactivation of rfc2-1 could account for the observed partial Rad53 phosphorylation. Improvement of the experimental design may allow detection of a more serious checkpoint defect in this strain.

As a further investigation of the *rfc2-1* strain, extracts were made from cultures grown at 25°C overnight, then shifted to 37°C or maintained at 25°C for five hours. These extracts were fractionated by gel filtration on a superose 6 column and the fractions analysed by western blotting using the anti-Rad24 polyclonal. No differences were observed in the elution position of Rad24 in either extract, compared to that in extract prepared from an *RFC2* strain (data not shown). This suggested that the rfc2-1 protein is still able to interact with Rad24 at the non-permissive temperature.

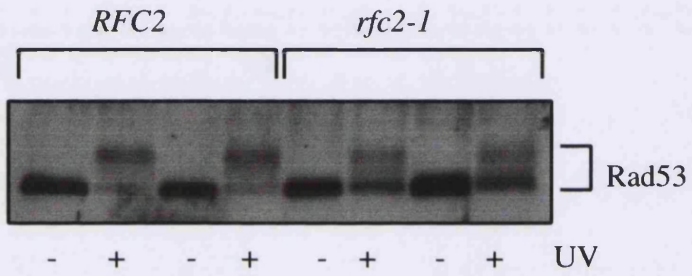

Figure 6.1.1. Analysis of Rad53 phosphorylation after UV irradiation in WT and *rfc2-1* strains. Yeast cultures were growth to mid-log phase then arrested in G2 with nocodazole. The arrest was maintained and the cultures shifted to 37°C for two hours. The cells were resuspended in saline and UV irradiated (40J/m^2) or mock treated. The cells were resuspended in prewarmed YPD with nocodazole at 37°C for a further 30 minutes then harvested and samples prepared for western blotting. The blot was analysed using the anti-Rad53 polyclonal antibody. Two independent cultures were used from each strain.

In the *rfc2-1* strain obtained from Dr. Sugino, the *rfc2-1* gene is present on a centromeric plasmid, in a yeast strain in which the genomic *RFC2* gene has been deleted. One of the phenotypes of the *rfc2-1* mutation is that of plasmid loss. The loss of the plasmid carrying the *rfc2-1* gene would result in the death of the cell. This phenomenon may account, at least in part, for the slow growth rate of this strain. This problem, and the fact that the strain background was not isogenic to that used for the remainder of this work, meant that this strain was not used for further experiments. In order to further investigate the role of RFC subunits outside of S phase it was decided to generate new reagents.

A strategy has been developed for the targeted production of conditional mutants of essential genes in *S. cerevisiae* (Dohmen *et al.*, 1994). This degron approach utilises the properties of a portion of a temperature sensitive dihydrofolate reductase (DHFR) gene. When integrated 5' to the gene of interest, this gene fragment confers temperature dependent degradation (td) on the target protein, via the ubiquitin mediated proteasome pathway. The fusion protein is expressed from a copper dependent promoter after genomic integration at the normal locus of the gene of interest. The fusion encodes an initial ubiquitin moiety, which is cleaved upon translation to leave an amino terminal arginine residue. This is necessary as the yeast cell proteosome degradation machinery recognises proteins as for destruction via such a residue. The DHFR fragment is thought to fold normally at a permissive temperature, usually 25°C. At higher temperatures, the DHFR adopts a more open conformation, which allows access of the ubiquitinating enzyme to a target lysine residue within this portion. Subsequent ubiquitination targets the protein for proteosome dependent proteolysis.

Oligonucleotide primers (792/3 and 810/1, see Appendix I) were designed in order to amplify the 5' end of the *RFC2* and *RFC3* genes by PCR from genomic DNA. A BamHI/ HindIII fragment from the pPW66R plasmid was cloned into pRS304. This fragment encodes the ubiquitin moiety, HA epitope and fragment of the DHFRts ORF, downstream of the copper inducible CUP1 promoter. The amplified RFC gene fragments were cloned in frame with the DHFR ORF in this degron vector to give $rfc2^{td}$ and $rfc3^{td}$ vectors. Linearisation of these vectors within the RFC portion and subsequent integration into the yeast genome should result in the production of conditional RFC

alleles which fail to grow at elevated temperature. Although this degron method has been effective in the production of a number of conditional mutants, the success rate of the method has been shown to be improved by the overexpression of the *UBR1* gene, which encodes the ubiquitin conjugating enzyme of the proteolytic pathway (Karim Labib, personal communication). A galactose inducible promoter was therefore integrated into the yeast genome upstream of the *UBR1* ORF using pKL59, a gift from Karim Labib, linearised with PmeI. After transformation of this *GALUBR1* strain with the rfc2^{td} and rfc3^{td} degron constructs, correct integration events were selected on the appropriate growth media and checked by PCR. However, when these isolates were analysed for growth at different temperatures no temperature sensitive phenotypes were observed (Figure 6.1.2), even if grown in galactose as the sole carbon source and in the absence of copper. This suggested that the RFC subunits were not being sufficiently degraded in these strains at elevated temperature to cause growth arrest.

The degradation of rfc2^{td} and rfc3^{td} proteins was analysed by western blot using the 12CA5 monoclonal antibody (Figure 6.1.3). No 12CA5 specific signal was obtained from extracts made from *rfc2^{td}* or *rfc3^{td}* strains grown at 37°C (data not shown). For both of these strains a specific band was observed corresponding to rfc2^{td} and rfc3^{td} respectively was observed in extracts grown at 25°C in glucose (D) medium. This band was reduced or absent if the cells were grown in galactose (G) medium. This strongly suggested that the degron construct was working to some extent, as the protein levels were depleted if the ubiquitin dependent degradation pathway was boosted by the overexpression of *UBR1*. However, this depletion of these proteins was not sufficient to cause growth arrest. Because it was still possible that a depletion of rfc2^{td} or rfc3^{td} would result in a checkpoint defect, even without affecting the essential function of these proteins extracts were prepared from UV irradiated cells from these degron strains (Figure 6.1.3). These extracts were analysed by western blot using the anti-Rad53 polyclonal antibody, to ascertain if the checkpoint pathway was activated in these cells. The observed pattern of Rad53 migration was not different in an *rfc2^{td}* strain when compared to the parental *RFC2* strain (both containing the GALUBR1 construct), under glucose or galactose conditions. Similar results were obtained using the *rfc3^{td}* strain (data not shown). This suggests that the DNA damage-dependent checkpoint pathway is functional, even in the presence of very reduced levels of Rfc2 or Rfc3.

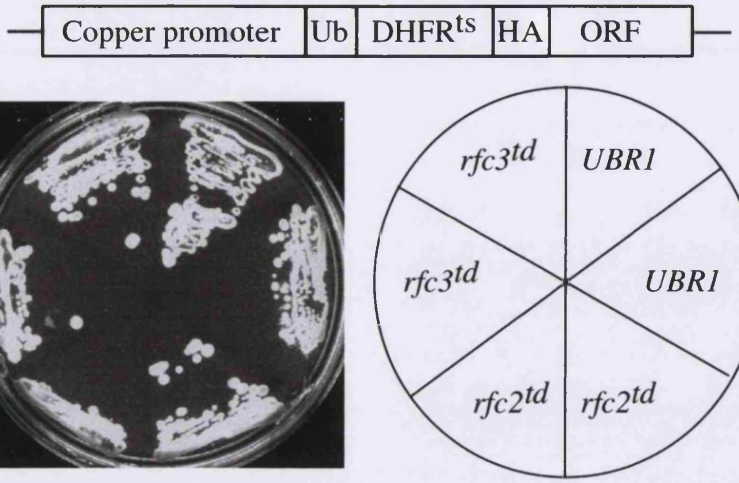

Figure 6.1.2. Production of strains expressing temperature degradable (td) RFC subunits. The specific temperature degradable alleles were created by homologous recombination of linearised vectors containing the 5' half of RFC2 or RFC3 cloned downstream of a temperature degradable DHFR ORF. The organisation of the resulting RFC2/3 locus is depicted above. Ub - ubiquitin, HA - epitope tag. The resulting strains were tested for temperature sensitivity by replica plating YPGal plates onto fresh YPGal and incubating at different temperatures. The plate shown was incubated at 39°C for two days before this picture was taken. The diagram on the left shows the position of each strain on the plate.

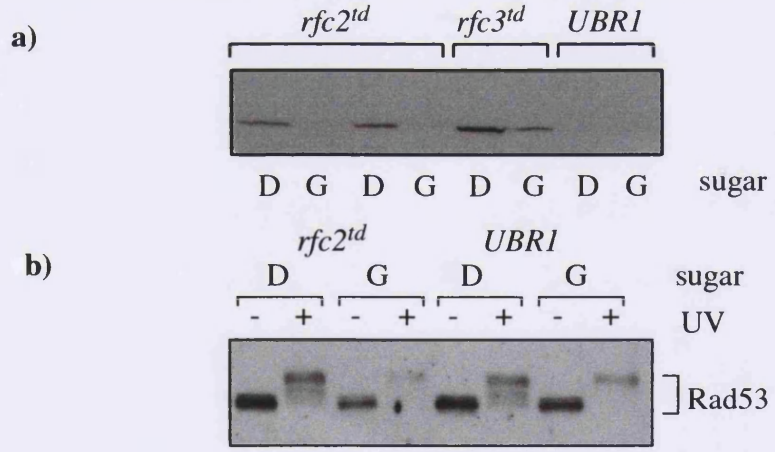

Figure 6.1.3. Analysis of RFC subunit degradation and UV dependent Rad53 phosphorylation in RFC^{td} strains. a) Western blot analysis using the 12CA5 monoclonal antibody of extracts from the strains indicated grown to mid-log phase in glucose (D) or galactose (G) at 30°C. b) Mid log cells from the strains indicated grown in glucose or galactose were UV irradiated (40J/m^2) or mock treated in saline then resuspended in prewarmed glucose or galactose media at 30°C. After 30 minutes the cells were harvested and extracts prepared for western blot analysis using the anti-Rad53 polyclonal antibody. The *UBR1* strain is W303 WT, except the endogenous *UBR1* promoter has been swapped for a galactose inducible promoter. *UBR1* encodes an E3 enzyme for the ubiquitin dependent proteosome pathway.

A further attempt to analyse checkpoint pathway activation in yeast strains with non functional RFC subunits was made using strains in which the normal *RFC2* or *RFC3* promoters were replaced by the *GAL1* promoter. These strains were kind gifts of Dr. Katsunori Sugimoto. The *GAL1* promoter is repressed by glucose and activated by galactose. It was hoped that transferring galactose grown culture to a glucose medium would prevent the expression of *RFC2* or *RFC3*, and hence lead to a reduction in the amount of functional protein in the cell and subsequent cell death. Indeed these cells are not viable on glucose containing plates (data not shown). However micro colony analysis showed that cells transferred from galactose media to glucose undergo at least 10 divisions, as the colonies formed contained approximately 1000 cells (data not shown). This delay between media shift and protein inactivation meant that experiments designed to analyse the checkpoint defect due to a lack of RFC subunits using these strains were unlikely to be successful.

Any attempt to analyse checkpoint defects in yeast with non-functional RFC subunits will be complicated by the essential requirement of these proteins for cell growth and division. It was therefore decided to try a slightly different approach. The aim was to produce a yeast strain which was specifically defective for the RFC-dependent checkpoint response, while the essential function of RFC was unaffected. In order to separate these two roles of the RFC subunits two overexpression constructs were created.

For these constructs the GAL promoter and adjacent HA tag was subcloned from YcpIF16 (Foreman and Davis, 1994), which was propagated in a *dam*$^-$ *E.coli* strain as the cloning required the use of the ClaI enzyme. This was inserted into pRS313 which is a centromeric yeast vector with the *HIS3* selective marker, using ClaI and ApaI enzymes. The *RFC1* ORF was amplified by PCR from genomic DNA in two fragments (oligonucleotide primers 897/8 with 901/2 see Appendix I) and these were cloned into the pRS313 based vector to give *GALHA-RFC1*. The hypothesis was that overexpression of *RFC1* would decrease the availability of the small RFC subunits for interaction with Rad24, and this might lead to a defect in the operation of the checkpoint pathway. A second approach was also tried, a 5' portion of the *RAD24* ORF containing the RFC homology domains was amplified by PCR from genomic DNA

(oligonucleotide primers 891/2 see Appendix I). This was also cloned into the pRS313 based GAL promoter vector to give *GALHA-RAD24N*. Here, the hypothesis was that because this fragment contained the RFC homology domains, it was likely to be able to interact normally with the small RFC subunits. The fragment was however, lacking the carboxyl terminal domain which is unique to Rad24. This novel domain may be required for the checkpoint function of the protein, for example for the predicted Rad17 complex interaction. This truncated fragment was therefore predicted to act as a dominant negative, sequestering the small RFC subunits from their normal interaction with functional Rad24.

These constructs were transformed into the W303 WT strain, and their sensitivity to UV analysed on galactose containing media. Ten fold dilution series were prepared from cells cultures grown to mid-logarithmic growth phase in galactose containing media. These were transferred to minimal media plates containing galactose and irradiated at the doses shown in Figure 6.1.4. Photographs were taken after three days growth at 30°C. The correct overexpression of the two constructs was checked by western blot analysis of extracts from the starter cultures using the 12CA5 monoclonal antibody (data not shown). The survival of the *GAL-HARAD24* strain was not different from the WT, suggesting that this fragment did not act as a dominant negative Rad24. The survival of the *GALHA-RFC1* appeared to be reduced when compared to WT (Figure 6.1.4). However, quantitative survival analysis of this strain after UV irradiation (Figure 6.1.5) demonstrated that this strains was as WT with respect to UV sensitivity. The apparent defect in survival observed by drop test analysis was due to a growth defect, *GALHARFC1* cells grow significantly more slowly than WT on galactose medium (data not shown).

6.2 – INVESTIGATING BIOCHEMICAL ACTIVITIES OF THE RAD24 COMPLEX

The identification of the Rad24 complex as being highly structurally similar to RFC immediately suggested that these two protein complexes might have related biochemical functions. RFC is a well studied protein complex, it is relatively easy to purify from budding yeast or human cell extracts (Tsurimoto and Stillman, 1989; Yoder and Burgers, 1991; Fien and Stillman, 1992), and recombinant systems have also been

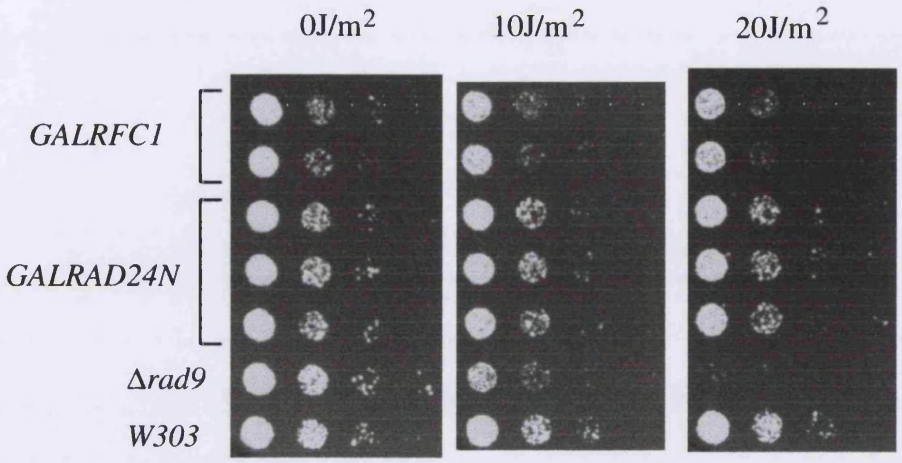

Figure 6.1.4. Survival after UV irradiation of strains over-expressing *RFC1* or a truncated *RAD24*. Ten fold dilution series were prepared from the strains indicated in a sterile 96 well plate with the highest concentration being $5x10^6$ cells/ml. The series were spotted onto YPD plates using a replica plater. Plates were irradiated with the doses shown above then incubated at 30°C for two days and photographed.

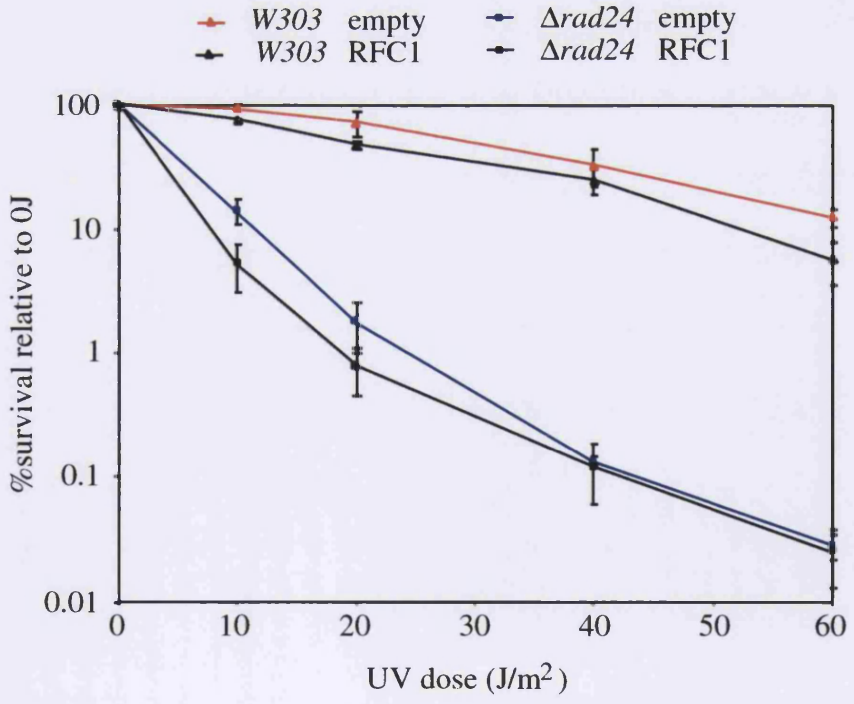

Figure 6.1.5. Survival after UV irradiation of strains over-expressing RFC1. Known numbers of cells of the strains indicated were plated onto YPD plates and UV irradiated at the doses shown. The % survival at each dose was calculated and corrected to the survival at 0J which was taken to be 100%. Each point is the mean value from three experiments, error bars are +/- 1 standard deviation.

designed for its production (Podust and Fanning, 1997; Gomes *et al.*, 2000). RFC has well characterised ATPase activity *in vitro* which is stimulated by DNA, and also binds DNA *in vitro* in a structure specific manner. Therefore the purified Rad24 complex was included in similar activity assays.

In order to assess whether the purified Rad24 complex has any ATP hydrolysis activity, increasing amounts of the most purified fraction from a medium scale purification (fraction 15 from a superose 6 column, see Figure 5.5.2) were incubated with [γ^{32}P]ATP. Also included in the reaction was magnesium and DNA substrates of different structures (see Materials and Methods). The reactions were incubated at 30°C for 30 minutes then spotted onto TLC plates for analysis of the products (Figure 6.2.1). Under none of the conditions tested was there any detectable ATPase activity when compared to buffer alone. The conditions used for this analysis were that which would have resulted in the ready detection of free phosphate had RFC been included in the reaction (Yoder and Burgers, 1991). Many different conditions were also tested, varying the concentration of magnesium, DNA substrates, ATP, salt and also the temperature and time of incubation, but without stimulating any activity. However, because of the ease with which large quantities of RFC can be produced, generally a much higher concentration of RFC is used in activity assays than was possible for Rad24 in this case. It was therefore possible that the failure to detect Rad24-dependent ATP hydrolysis was due to use of incorrect reaction conditions, or insufficient material, or because the complex does not possess such an activity.

One method by which the DNA binding activity of human RFC has been investigated is gel mobility shift analysis. A DNA substrate which RFC will bind to in vitro, and which can be used as a bandshift probe is a hairpin structure, labelled with [^{32}P]phosphate at the 5' end (Tsurimoto and Stillman, 1991). The 96 base oligonucleotide (N805 – see Appendix I) was sythesised on a large scale, and purified by poly-acrylamide gel electrophoresis, then labelled using T4 polynucleotide kinase (NEB) and [γ^{32}P]ATP. The hairpin secondary structure was allowed to form by heating the probe to 100°C then allowing it to cool slowly to room temperature. The labelled probe was incubated with purified Rad24 complex, and varying conditions including combinations of the following: ATP, ATPγS and poly dI:dC. After the incubation a crosslinking agent, in

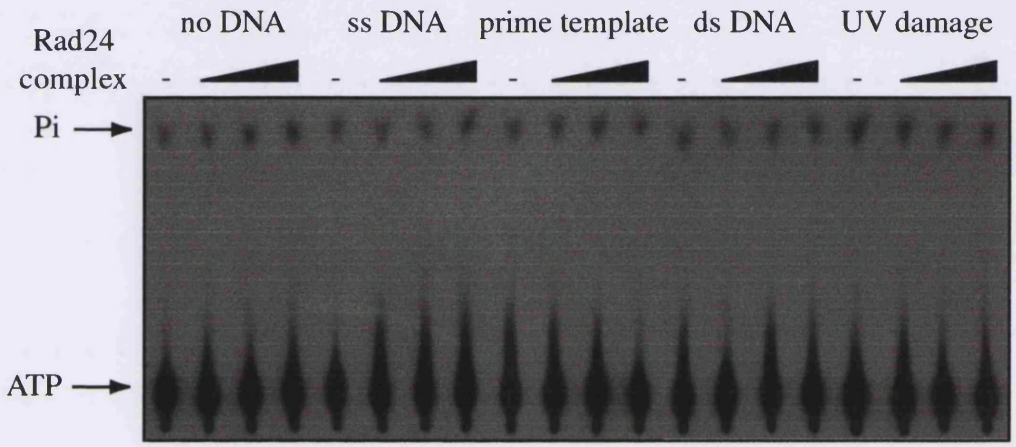

Figure 6.2.1. Analysis of ATPase activity associated with the purified HTH-Rad24 complex. 0, 1, 2 and 5 µl of the most pure fraction from a final stage superose 6 column (see Figure 5.5.2) were incubated with [γ-^{32}P]ATP and assorted DNA substrates as indicated. The products of the reaction were analysed by thin layer chromatography and autoradiography.

this case gluteraldehye was added, as this has been found to improve detection of RFC-DNA complexes (Tsurimoto and Stillman, 1991). The reaction products were separated on a 4.5% polyacrylamide gel, which was dried then exposed to Bio-Max MS film using an enhancing screen at –80°C for between 1 and 48 hours (Figure 6.2.2).

Using this method demonstrated that the preparation of purified Rad24 complex contains a DNA binding activity, as the mobility of the probe was altered in the rections containing this material, compared to buffer alone. This activity was more readily detected if a crosslinking reagent was added to the binding reactions, although is could be seen even in the absence of such treatment. The mobility shift of the probe was not altered in the presence of ATP or ATPγS, suggesting that the protein/DNA association that causes the shift is ATP independent. The mobility shift of the probe was also insensitive to the addition of the non-specific competitor poly (dI-dC)· poly (dI-dC), suggesting that this association is structure or sequence specific. It was possible that this mobility shift was a result of a contaminant in the Rad24 preparation, which has DNA binding activity, rather than to the DNA association of Rad24 itself. In order to address this possibility the experiment was repeated, including either anti-Rad24 polyclonal serum or 12CA5 monoclonal. The pre-immune serum from the anti-Rad24 rabbit or an unrelated monoclonal were also used as controls. Unfortunately it was found that the addition of any of these antibodies to the reaction resulted in a change in the mobility of the probe (data not shown). It was therefore not possible to determine whether the originally observed mobility shift of the probe upon addition of the Rad24 complex, was truly due to the DNA binding of Rad24. In a further attempt to address this question a bandshift western technique was employed. After the binding reaction the samples were loaded onto a polyacrylamide gel, as before. However, instead of drying the gel before autoradiography, the gel was submitted to a semi-dry transfer procedure in order to obtain the reaction products on a nitrocellulose filter. However, autoradiography of this filter demonstrated that the DNA had not been transmitted to it, and subsequent attempts to detect Rad24 using the polyclonal antibody were also unsuccessful. It is likely that the crosslinking procedure required for the detection of the mobility shift was inhibitory to optimal transfer of proteins and DNA from the gel. Due to time limitations these experiments were not pursued further, but this initial

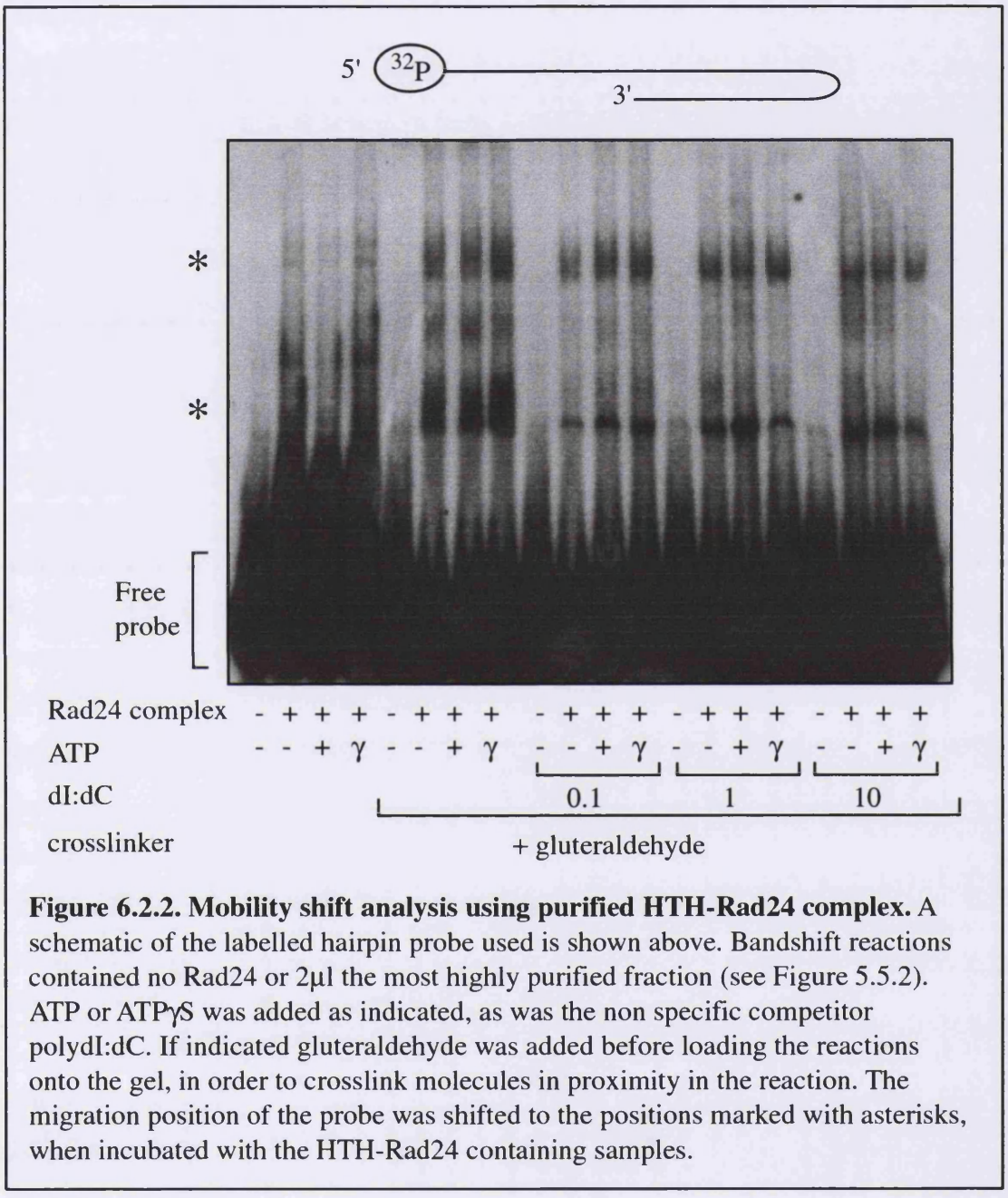

Figure 6.2.2. Mobility shift analysis using purified HTH-Rad24 complex. A schematic of the labelled hairpin probe used is shown above. Bandshift reactions contained no Rad24 or 2µl the most highly purified fraction (see Figure 5.5.2). ATP or ATPγS was added as indicated, as was the non specific competitor polydI:dC. If indicated gluteraldehyde was added before loading the reactions onto the gel, in order to crosslink molecules in proximity in the reaction. The migration position of the probe was shifted to the positions marked with asterisks, when incubated with the HTH-Rad24 containing samples.

demonstration of a DNA binding activity co-purifying with Rad24 certainly warrants further investigation.

Due to the difficulties in obtaining sufficient purified Rad24 complex for in vitro biochemical analysis, it was decided to attempt analysis of possible Rad24 DNA binding activity in cell free systems. We had previously initiated the development of a cell free system to analyse the activation of the Rad53 kinase upon addition of different DNA substrates to NER competent yeast whole cell extracts, and this system had given promising initial results (Murguia *et al.*, In preparation). Because plasmids have a high molecular weight, it should be possible to separate plasmid bound Rad24 complex from free Rad24 complex using a gel filtration procedure. High quality extracts were prepared from WT cells and aliqouts were incubated with no plasmid, plasmid, or UV irradiated plasmid at 4 or 30°C. These reactions were then fractionated by gel filtration using a superose 6 column, and the fractions analysed by western blot and ethidium staining of agarose gels, for the presence of Rad24 or plasmid respectively (Figure 6.2.3). When fractionated in this manner, the plasmid was always found to elute in, or very near to the void, with the peak in fraction 9. This elution position was independent of UV treatment or incubation temperature. In extracts incubated without plasmid Rad24 was detected in the expected fractions 14 and 15. This position was unchanged if the extracts were incubated with plasmid or UV treated plasmid, under all conditions tested (Figure 6.2.3). This suggests that the majority of the Rad24 complex was not associating with the DNA in this system. However it is still possible that some fraction of Rad24 was able to interact with this DNA substrate, which would not be detected by this method.

An improvement to this system was suggested by the work of K. Hartland, in the laboratory of Dr. John Diffley, who was analysing the association with DNA of proteins involved in replication origin recognition. They had developed a method for the coupling of plasmids to magnetic beads, in order to analyse the binding of proteins to DNA in a cell free system. Dr Diffley and Miss Hartland kindly allowed me to analyse Rad24 binding in this way, using their unpublished procedures. Either untreated or UV irradiated plasmids were attached to magnetic beads and incubated in high quality WT yeast whole cell extracts, in the presence of an ATP regenerating system. The beads

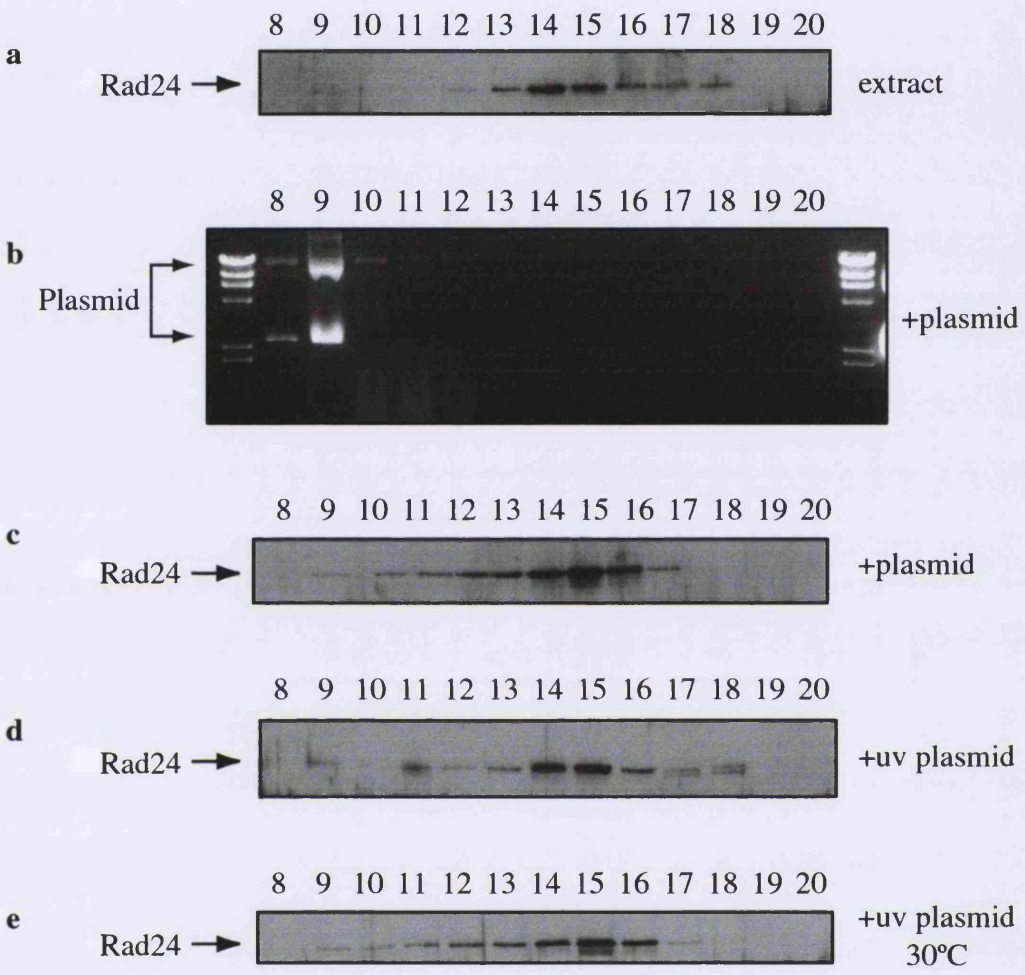

Figure 6.2.3. Analysis of HTH-Rad24 binding to plasmids in whole cell extracts. 250µg extract (a), or extract that had been incubated with untreated (c) or UV treated (d and e) plasmid was fractionated on a superose 6 gel filtration column. The fractions were analysed by western blot for the elution postion of Rad24, or ethidium bromide staining of agarose gels (b) for the elution position of the plasmid.

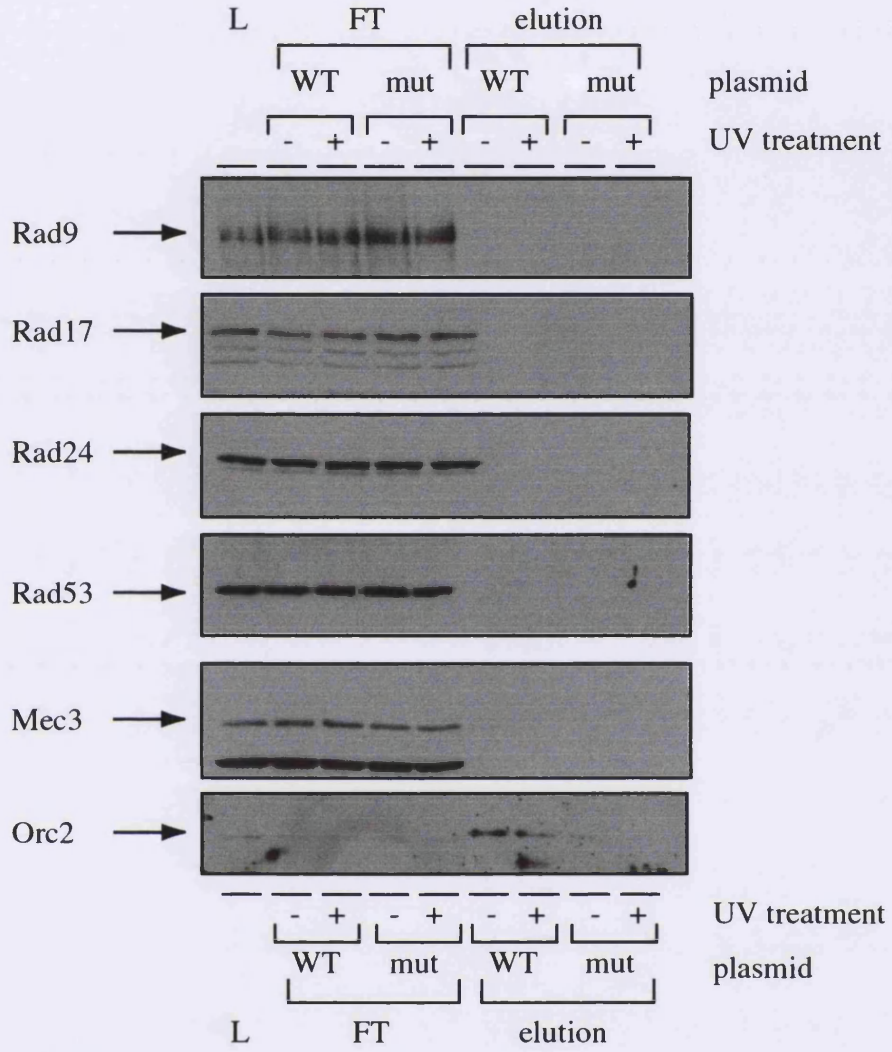

Figure 6.2.4. DNA pull down experiments using plasmids coupled to Dynabeads. Plasmids containing WT or mutant ARS306 (mut) replication origins were either UV irradiated with 450J/m^2 (+) or mock treated (-), and coupled to Photoprobe S-S biotin (Vector laboratories). These plasmids were bound to streptavidin coated Dynabeads (Dynal). The beads were incubated with extracts made by the liquid nitrogen method from undamaged WT cells (L) for 30 minutes at 24°C in the presence of an ATP regenerating system. After washing, the bound proteins were removed from the beads by heating at 95°C for 3 minutes in Laemmli buffer. The eluted proteins and the supernatants from the binding reaction (FT) were resolved by SDS-PAGE and visualised by western blotting using the polyclonal antibodies. A anti-Orc2 antibody was used as a control.

were then washed and associated proteins removed by boiling the beads in Laemmli buffer followed by western blot analysis (Figure 6.2.4). Because the plasmids used for these experiments contained yeast origin sequences, the binding of the Orc2 protein was used as a control for extract quality. Under the conditions tested no interaction of Rad24, or of any other checkpoint protein with the bead bound DNA was detected.

6.3 – DISCUSSION

The investigation into possible roles for the small RFC subunits in DNA damage dependent checkpoint activation outside of S phase has been hindered by the essential nature of the RFC genes. The slow growth phenotype of the *rfc2-1* strain used to address this issue created problems with the experimental design, which involved arrest of the cell cycle in G2 in order to analyse checkpoint pathway activation. One improvement to this experimental design would be to substitute the G2 arrest for arrest in G1 using alpha factor, as this pheromone dependent arrest can be prolonged. It would also be worth attempting an alpha factor block and release type checkpoint experiment after UV irradiation at permissive versus restrictive temperatures in this strain. Furthermore, the intra S checkpoint could be analysed by release into MMS containing media. It has been noted that rfc2-1 cells continue to divide for up to eight hours before arresting, suggesting that it takes this long for all the rfc2-1 protein to be inactivated. Hence all these experiments should incorporate an extended incubation at the restrictive temperature before checkpoint analyses are performed.

The analyses performed using the temperature dependent degron approach for *RFC2* and *RFC3* suggests that only a small fraction of the total cellular population of these proteins is required for the essential function of RFC, as a large reduction in protein levels does not affect growth (Figures 6.1.2 and 6.1.3). Analysis of the molecular sizes of protein complexes containing RFC subunits suggested that a large proportion of the small RFC subunits are not normally associated with Rfc1 in the RFC complex (Figure 5.5.1) It therefore seems likely that there is a significant amount of these small RFC subunits in a cell at any one time that are not performing an essential role. Also the *CUP1* promoter, from which $RFC2^{td}$ and $RFC3^{td}$ were expressed is not a repressible promoter. In non induced conditions it is therefore likely that there is basal transcription from this promoter. The resulting low level of continuous production of $Rfc2^{td}$ and

Rfc3^{td} proteins may be sufficient to perform the essential function of RFC, before these newly synthesised molecules are degraded. K. Labib has been devising a method to improve the degron strategy to reduce this problem. The *CUP1* promoter could be replaced with a more repressible promoter such as *GAL1*, in this case an alternative promoter would be used for the Ubr1 overproduction. This should reduce the background expression under the restrictive conditions, and will hopefully resolve this problem. However, it is possible that the Rfc2^{td} and Rfc3^{td} are refractory to degradation when incorporated into RFC, in which case not even the modified method will produce a functional conditional mutant of Rfc2 or Rfc3.

A very recent paper from the laboratory of K. Sugimoto (Naiki *et al.*, 2000) has demonstrated a role for the Rfc5 protein in the DNA damage-dependent checkpoint response in G2. *rfc5-1* is proficient for the G1 and G2 checkpoints. A stain carrying a mutation in the putative ATP binding site of Rad24, *rad24-K115R*, is also proficient for these checkpoint responses. However strains carrying both of these mutations are as deficient in the checkpoint responses as a *rad24Δ* strain. Moreover although rad24^{K115R} interacts normally with Rfc3, in an *rfc5-1* background this interaction is abolished. This demonstrates clearly the requirement for the intact Rad24/Rfc2-5 complex for the checkpoint function of *RAD24*, and validates the model presented here.

The attempt to separate the essential and checkpoint roles of the RFC subunits by the overexpression of *RFC1* was not successful (Figure 6.1.5). There could be multiple reasons for this: As discussed earlier there appears to be an excess of the small RFC subunits compared to Rad24 or Rfc1. Hence the extra Rfc1 protein produced by overexpression might all asociate with otherwise inactive small RFC subunits, and fail to titrate them from the Rad24 complex. Alternatively, if the interaction of Rad24 with Rfc2,3,4 and 5 is of a higher affinity than the equivalent interaction with Rfc1, excess Rfc1 will not remove the small RFC subunits from the Rad24 complex. The preliminary attempt to create a dominant negative Rad24 protein also failed (Figure 6.1.4). The rational production of such a dominant negative protein could be achieved if the interaction between Rad24 and the small RFC subunits was better mapped, alternatively a series of truncated Rad24 proteins could be produced, in order to pursue this line of investigation further.

One of the initial reasons for attempting a purification of a checkpoint protein complex was to identify a biochemical activity that could explain the mechanism of signal transduction within the checkpoint pathway. The purified Rad24 complex has indeed allowed us to initiate such studies. Unexpectedly no ATP hydrolysis activity was detected in the preparation of highly purified Rad24 (Figure 6.2.1). The most likely explanation for this is that very small quantities of the complex were used in these reactions, approximately 1ng. In comparison an ATPase assay using purified RFC would generally use 20ng protein (Yoder and Burgers, 1991). Also the conditions which were selected for the reactions may not have been optimal for Rad24 complex activity, for example the ATPase activity of RFC is stimulated by SSB and this was not included in these attempts, further decreasing the probability of detecting hydrolysis. Although initial analysis of Rad24 DNA binding activity using the gel mobility shift technique demonstrated that the complex was associated with DNA binding activity (Figure 6.2.2), a conclusive demonstration that this activity was due to the Rad24 complex was not achieved. Again, these experiments were hindered by the lack of available material, which is due to the low abundance of Rad24. In order to obtain greater quantities of the Rad24 complex a yeast strain was engineered to overproduce the HTH-Rad24 protein by replacing the endogenous promoter with a galactose inducible promoter. Because the small RFC subunits appear to be in excess in the cell, it seemed feasible that increasing the amount of Rad24 would consequently increase the amount of the Rad24 complex. However when extracts from this strain grown in media containing either glucose or galactose were analysed by western blotting, it was apparent that the quantity of Rad24 produced in this strain under galactose induing condition was not higher than in WT cells (data not shown). Hence it is possible that there is a regulatory mechanism which prevents the accumulation of an excess of Rad24 or the Rad24 complex. To date this phenomenon has not been investigated further. It therefore seems that in order to obtain sufficient Rad24 material recombinant methods will have to be employed. An E. coli vector which expresses all five yeast RFC subunits is available (Gomes *et al.*, 2000), and the re-engineering of this construct to produce the Rad24 complex would be worthwhile. Alternatively, because baculovirus systems are available for the production of human RFC (Podust and Fanning, 1997), it would be

possible express and characterise a hRad17/RFC complex. A readily available source of the Rad24 complex would greatly enhance the speed with which biochemical analysis of this complex can be performed.

Although initial attempts to analyse the association of Rad24 with plasmid substrates in cell free extracts has been initially unsuccessful (Figures 6.2.3 and 6.2.4), this is a promising strategy for investigation of checkpoint pathway function. Due to time limitations, only a very limited set of conditions was used in both plasmid binding assays. In particular it would be of interest to pursue the magnetic bead linked plasmid system further as it represents a very powerful technique due to the specific increase in concentration of the DNA bound proteins. It should be possible to create beads coupled to a variety of specific DNA structures, and the dependence of any binding upon ATP and other conditions could be readily investigated. If such a system was developed, the use of extracts produced from different mutant yeast strains would allow analysis of, for example, whether Mec1 or Rad24 are required for the association of Rad17 with DNA.

CHAPTER 7 – CONCLUSIONS AND FUTURE DIRECTIONS

The work presented in this thesis forms a preliminary analysis of some of the more upstream protein components of the *S. cerevisiae* DNA damage-dependent checkpoint pathway. These proteins have been little studied until very recently and the results shown here raise a number of questions for further study. The production of high quality immunological reagents for the detection of Rad24, Mec3, Rad17 and Rad53 was one of the achievements of this work (Section 3.1). These reagents permitted the study of these previously uncharacterised proteins, in terms of their regulation throughout the cell cycle and after DNA damage (Sections 3.2 and 3.3), their abundance in the cell (Section 3.4), their interactions with each other (Section 3.5) and the native molecular mass of the protein complexes in which they exist (Chapter 4).

The demonstration that the Rad24 protein exists as part of a large molecular mass complex, which does not include the other checkpoint proteins, led to the development of a purification system for the identification of this complex (Sections 5.1 and 5.3). The composition of this novel Rad24 complex (Section 5.4) immediately suggested a model for the operation of this complex, as a DNA structure sensor during DNA damage-dependent checkpoint pathway activation (Section 5.6). However, the direct testing of this model has proven to be extremely difficult, mainly because of the essential nature of the genes involved (Section 6.1), and the difficulties in obtaining sufficient purified material for biochemical analysis (Section 6.2).

Although the work presented here has furthered the understanding of the molecular nature of the Rad24 checkpoint protein complex, the over-riding conclusion to be drawn from this, or any of the other recent advances in this field is that there are many questions that remain to be answered regarding the operation of this pathway. As previously speculated it is by no means certain that all the components of this pathway have been identified, and it currently seems that each new publication raises more questions than it answers. This next section will raise some questions relating to this checkpoint pathway, and hypothesise as to possible answers, or at least methods by which such answers may be obtained.

One of the most prominent gaps in our understanding if the DNA damage-dependent checkpoint pathway in *S. cerevisiae* is that left by the lack of information pertaining to the Mec1 protein. The unresolved difficulties with placing *MEC1* function either upstream or downstream of *RAD9* and the *RAD24* group of genes is merely one manifestation of this. The recent works analysing the Rad26 protein in *S. pombe* (Edwards *et al.*, 1999) and Ddc2 protein in *S. cerevisiae* (Paciotti *et al.*, 2000) both support a model in which Mec1 is the most upstream component of the DNA damage sensing machinery, as these proteins undergo phosphorylation in a Mec1-dependent manner that is independent of the function of other checkpoint genes (Michelson and Weinert, 1999). Studies of the human homologues of Mec1, ATM and ATR have also lead to the conclusion that these proteins are direct sensors of DNA damage, indeed both ATM and ATR have protein kinase activity that is stimulated by DNA association (Hall-Jackson *et al.*, 1999; Lakin *et al.*, 1999; Smith *et al.*, 1999). Therefore it is likely that the initial models proposed for the order of function of the checkpoint pathway (see Figure 1.7) were not correct, and that *MEC1* function is upstream of, or perhaps required in concert with, *RAD9* and *RAD24*. If the biochemical functions of Rad9 and Rad24 are absolutely dependent upon Mec1 activity, this could account for the fact that *RAD9* or *RAD24* overexpression does not rescue the checkpoint defect observed in *mec1-1* (de la Torre-Ruiz *et al.*, 1998). If the situation in the human system for checkpoint pathway activation does resemble that in yeast, there are some obvious questions raised regarding the biochemistry of Mec1. Does Mec1 associate with damaged DNA or ssDNA and if so does this association require Ddc2? This association might activate a kinase activity within the Mec1/Ddc2 complex. What are the substrate of such a kinase activity, does Mec1 phosphorylate Ddc2, Ddc1 or Rad9 directly? Are these phosphorylation events required for activation of the checkpoint pathway, amplification or negative feedback regulation? Initial progress in the answer to some of these questions is likely to be soon forthcoming. We have recently produced a polyclonal antisera that is capable of recognising Mec1 in western blots from crude yeast extracts and which is capable of causing immunoprecipitation of Mec1 (C. Gilbert and J. Downs, personal communication). This reagent will be used in immunoprecipitation based analyses of Mec1 associated kinase activity, and its dependence the presence of different DNA substrates. Production of recombinant Ddc2, Ddc1 and Rad9, or portions of these proteins should identify whether these proteins are

direct substrates for a Mec1 kinase activity, at least *in vitro*. Purification of Mec1, perhaps utilising methods similar to the purification here described for Rad24, would allow analysis of the biochemistry of Mec1, and possible associated proteins.

Very recently progress has been made towards understanding the role of Rad9 in checkpoint pathway activation, a protein for which a biochemical function could not be inferred, due to the lack of sequence homology with other, characterised proteins. A recent study from our laboratory (Gilbert *et al.*, 2000) presents data which supports a solid phase catalytic role for Rad9 in the activation of Rad53 (see Figure 1.10). It had previously been noted that Rad53 expressed in *E. coli* became phosphorylated as the cellular concentration of Rad53 increased during the expression period (C. Santocanale and J. Diffley, personal communication). Our purification of Rad9, in a complex containing chaperone proteins, and the observation that this complex undergoes a conformational change and recruits Rad53 upon treatment of cells with DNA damaging agents, led us to investigate further the role of Rad9 in Rad53 activation. Rad9 exists as a BRCT-domain mediated oligomer after DNA damage (Soulier and Lowndes, 1999), which from our hydrodynamic analysis is likely to be a dimer. Each molecule of Rad9 in this dimer will have an equivalent binding site for FHA domain-mediated association of Rad53. This interaction will therefore bring two Rad53 molecule in close proximity to each other, effectively increasing the local concentration of Rad53 and mediating Rad53 *in trans* autophosphorylation. This phosphorylation of Rad53, and the subsequent release of activated Rad53 from the Rad9 complex, as well as the initial phosphorylation of Rad9 to produce Rad53 binding sites, is likely to be dependent of the chaperone activity of the Ssa proteins associated with Rad9 (Gilbert *et al.*, 2000). This is the first biochemical explanation for how the checkpoint pathway signal might be transmitted.

Even a detailed model such as that described above leaves questions still to be answered. For example, Rad53 can clearly still be modified in the absence of Rad9 (de la Torre-Ruiz *et al.*, 1998). This is due to the operation of the parallel branch of the checkpoint pathway that involves Rad24. It possible that Mec1 can directly phosphorylate and activate Rad53, indeed mutant Rad53 protein, with an amino acid substitution in the kinase domain that severely impairs kinase activity is still

phosphorylated after DNA damage. One mechanism by which the *RAD24* branch could activate Rad53 in the absence of Rad9 would therefore be via the enhancement of Mec1 kinase activity. Another kinase involved in the pathway is Chk1, it is also conceivable that Chk1 activity could contribute to the activation of Rad53 in the absence of Rad9. Such hypotheses have yet to be tested.

Although the elucidation of the structure of the Rad24 complex represents a major advance in our understanding of the likely biochemical function of this protein, it still remains to be determined how biochemical activities resembling RFC can be utilised to activate a signal transduction cascade. The prediction that the Rad17/Ddc1/Mec3 complex resembles PCNA strongly supports a model in which an interaction between this complex and Rad24 is a constituent part of the signal transduction process. However it should be noted that the true structure of the Rad17 complex has not been determined, and at present too much reliance on a PCNA based model may be premature. It should be relatively easy to determine if the Rad17 complex does have such a structure, for example using electron microscopic methods of purified, or recombinant complexes, of either the yeast or human homologues. If the structural predictions are correct then it seems highly likely that the Rad24 and Rad17 complex will associate in order to produce a DNA bound form of the Rad17 complex. How does this lead to activation of Rad53 and Chk1? It is possible that Rad17 in a DNA bound form can associate specifically with a downstream transducer such as Rad53, leading to conformational change and activation of that transducer. However, it seems clear that activation of Rad53 requires phosphorylation, and this is more difficult to explain by this mechanism, unless one postulates the existence of a novel kinase in the pathway. Alternatively phospho-residue docking site within the Rad17 complex could allow the Rad17 complex function in an analogous manner to Rad9 for the catalysis of Rad53 autophosphorylation, but to date no interaction has been reported between Rad53 and phosphorylated Ddc1. The only enzymatic activity likely to be associated with the Rad17 complex is that of an exonuclease, at least from inspection of primary sequence. Although no such activity has been demonstrated for the Rad17 protein, both hRad1 and hHus1 have been reported to possess exonuclease activity. Importantly these studies were performed using recombinant single proteins, although these proteins function as a trimeric complex in both human and yeast cells. Therefore it is essential to produce or

purify the entire Rad17 complex in order to address the existence of any enzymatic activities. If the Rad17 complex can be shown to have such an activity, then this would provide the basis for a model of Rad24/Rad17 complex involvement in signal transduction. One such model is depicted in Figure 7. In this proposed scheme for checkpoint pathway activation DNA damage is initially recognised and processed to a single stranded DNA region by repair processes such as NER or the Rad50/Xrs2/Mre11 complex. The Mec1 protein has affinity for this structure and binds, which induces conformational change of Mec1 and activation of Mec1 kinase activity. This step may be dependent on Ddc2. Mec1 phosphorylates Chk1 which leads to stabilisation of Pds1 and inhibition of anaphase. Mec1 phosphorylates Rad9, leading to Rad53 activation and hence downstream responses as described above. Mec1 also phosphorylates Ddc1. This allows the Rad24 dependent loading of the Rad17 complex at the Mec1 associated site. The exonuclease activity of the Rad17 complex then extends the single stranded region, producing more binding sites for Mec1 and hence amplification of the signal. Alternatively it is possible that the Rad17 complex acts as a processivity factor for a currently unidentified exonuclease. In this model Mec1 acts both upstream and downstream of Rad24, initially to activate the exonuclease, and then to further amplify the signal. This is very much a working model, which will alter as further information becomes available. There are likely to be levels of complexity and feedback in operation within this pathway that are currently beyond our understanding.

In *S. cerevisiae* maintanence of the checkpoint arrest requires the continual presence of active Mec1 (Gardner *et al.*, 1999). It is therefore likely that mechanisms exist for the continued down regulation of the pathway, which has to be actively maintained by continued signalling from Mec1. This could easily be achieved if one of the downstream targets of the pathway was, for example, a phosphatase that removed the activating phosphorylation on Ddc1 and Rad9. However, the existence of such a mechanism has yet to be experimentally determined. The suggestion that the persistence of ssDNA in yeast with defective Ku protein leads to permanent arrest supports this model (Lee *et al.*, 1998), as Mec1 signalling would continue in the presence ssDNA. In fact this phenotype might be useful to design a genetic screen to identify down regulators of the checkpoint pathway. It is also noted that a defect in the ssDNA binding protein RPA can suppress this permanent arrest, suggesting that it may be the RPA

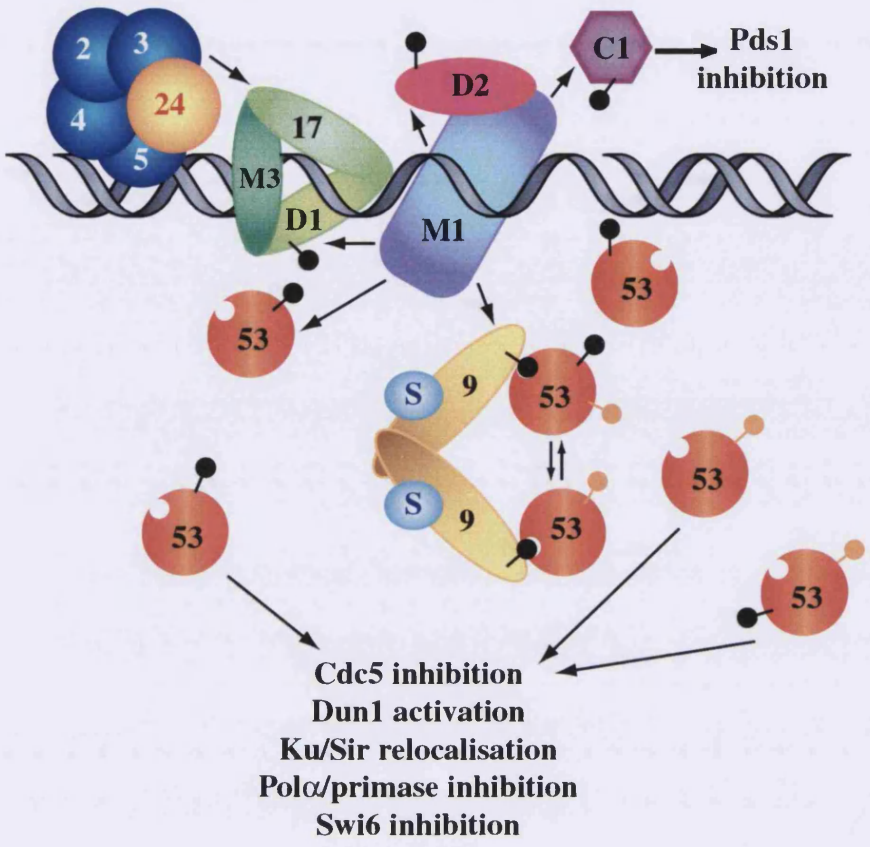

Figure 7. A model for events occurring during DNA damage-dependent checkpoint activation in *S. cerevisiae*. After damage, and initial lesion processing probably by repair pathways the situation may resemble that depicted above. Mec1 (M1) has associated with the ssDNA region, and achieved an active conformation. The Ddc2 (D2) has undergone Mec1 dependent phosphorylation. This Mec1/Ddc2 complex now phosphorylates Ddc1 (D1) which permits the Rad24/Rfc2-5 (24,2,3,4,5) dependent loading of the Rad17/Ddc1/Mec3 complex (17,D1,M3) onto the single stranded region. This Rad17 complex has exonuclease activity, which extends the ssDNA region, allowing more Mec1 to bind, and hence amplifying the signal. The Mec1/Ddc2 dependent phosphorylation of Chk1 (C1) leads to its activation, and the subsequent inhibition of mitosis via Pds1 inhibition. The Mec1/Ddc2 complex can directly phosphorylate and activate Rad53 (53), but Rad53 is also activated via the Rad9 branch of the pathway: The Mec1/Ddc2 dependent phosphorylation of Rad9 (9), causes a conformation shift in the Rad9/Ssa (S) complex, and dimerisation via the BRCT domains. This allows access of Rad53 FHA domains to phospho-peptide binding sites. This brings Rad53 molecules into close proximity, and an amplifying *in trans* autophosphorylation cascade is initiated, with Rad9 as a catalyst. The Rad53, activated via either method induces G2 arrest, transcriptional induction, repair, S-phase arrest and G1 arrest via the effectors shown.

associated with ssDNA, as opposed to the ssDNA *per se* that is the activating signal for Mec1 activation. Interestingly the association of RFC with DNA is enhanced by RPA, and RPA is indeed required for checkpoint function in G1 and intra-S (Longhese *et al.*, 1996). A further point of interest is the observation that RPA undergoes Mec1 dependent phosphorylation after DNA damage (Brush *et al.*, 1996). The affect of this phosphorylation has not been determined. If this phosphorylation was inhibitory for RPA binding, this could be a negative feedback mechanism by which the DNA damage dependent checkpoint pathway is down regulated.

During S phase *RAD9* and the *RAD24* group are much less involved in activation of the DNA damage dependent checkpoint pathway. This is presumably because there are proteins involved in replication that can perform analogous roles. Because replication proteins will be associated with the progressing replication fork, they will be in position to respond to the presence of DNA lesions. If the major role of Rad24 is to increase the availability of ssDNA for Mec1 activation (perhaps in an RPA dependent manner), this may well be redundant during S phase, as a helicase, advancing ahead of a polymerase which is stalled at a lesion site, might be expected to produce ssDNA. It is also possible that other S phase specific proteins may perform Rad9 like mediation of Rad53 activation. One possibility is the BRCT containing protein Dpb11.

Because of the extremely high level of conservation of this checkpoint pathway in many organisms, the future direction of this work is likely to have many parallel forms. In this way the strengths of one system may be utilised to address questions that have proved difficult to answer in another. This DNA damage-dependent checkpoint pathway is predicted by many to operate as a guardian of genomic stability. However, with the exception of ATM it has yet to be demonstrated that the human homologues of these yeast genes have tumour suppressor function. The increased cancer susceptibility of A-T patients may be due to the loss of repair function, rather than checkpoint defects. The investigation of the role of acquired mutations in the human DNA damage-dependent checkpoint genes in the onset of tumourigenesis is surely likely to be one of the much studies areas of checkpoint research in the near future.

REFERENCES

Aboussekhra, A., Vialard, J. E., Morrison, D. E., de la Torre-Ruiz, M. A., Cernakova, L., Fabre, F., and Lowndes, N. F. **(1996)**. A novel role for the budding yeast RAD9 checkpoint gene in DNA damage- dependent transcription, **Embo J** *15*, 3912-22.

al-Khodairy, F., and Carr, A. M. **(1992)**. DNA repair mutants defining G2 checkpoint pathways in Schizosaccharomyces pombe, **Embo J** *11*, 1343-50.

al-Khodairy, F., Fotou, E., Sheldrick, K. S., Griffiths, D. J., Lehmann, A. R., and Carr, A. M. **(1994)**. Identification and characterization of new elements involved in checkpoint and feedback controls in fission yeast, **Mol Biol Cell** *5*, 147-60.

Allen, J. B., Zhou, Z., Siede, W., Friedberg, E. C., and Elledge, S. J. **(1994)**. The SAD1/RAD53 protein kinase controls multiple checkpoints and DNA damage-induced transcription in yeast, **Genes Dev** *8*, 2401-15.

Aquilina, G., Crescenzi, M., and Bignami, M. **(1999)**. Mismatch repair, G(2)/M cell cycle arrest and lethality after DNA damage, **Carcinogenesis** *20*, 2317-26.

Araki, H., Leem, S. H., Phongdara, A., and Sugino, A. **(1995)**. Dpb11, which interacts with DNA polymerase II(epsilon) in Saccharomyces cerevisiae, has a dual role in S-phase progression and at a cell cycle checkpoint, **Proc Natl Acad Sci U S A** *92*, 11791-5.

Aravind, L., Walker, D. R., and Koonin, E. V. **(1999)**. Conserved domains in DNA repair proteins and evolution of repair systems, **Nucleic Acids Res** *27*, 1223-42.

Ashcroft, M., and Vousden, K. H. **(1999)**. Regulation of p53 stability, **Oncogene** *18*, 7637-43.

Bao, S., Shen, X., Shen, K., Liu, Y., and Wang, X. F. **(1998)**. The mammalian Rad24 homologous to yeast Saccharomyces cerevisiae Rad24 and Schizosaccharomyces pombe Rad17 is involved in DNA damage checkpoint, **Cell Growth Differ** *9*, 961-7.

Bashkirov, V. I., King, J. S., Bashkirova, E. V., Schmuckli-Maurer, J., and Heyer, W. D. **(2000)**. DNA repair protein rad55 is a terminal substrate of the DNA damage checkpoints [In Process Citation], **Mol Cell Biol** *20*, 4393-404.

Basrai, M. A., Velculescu, V. E., Kinzler, K. W., and Hieter, P. **(1999)**. NORF5/HUG1 is a component of the MEC1-mediated checkpoint response to DNA damage and replication arrest in Saccharomyces cerevisiae, **Mol Cell Biol** *19*, 7041-9.

Bates, S., and Vousden, K. H. **(1996)**. p53 in signaling checkpoint arrest or apoptosis, **Curr Opin Genet Dev** *6*, 12-8.

Bell, D. W., Varley, J. M., Szydlo, T. E., Kang, D. H., Wahrer, D. C., Shannon, K. E., Lubratovich, M., Verselis, S. J., Isselbacher, K. J., Fraumeni, J. F., *et al.* **(1999)**. Heterozygous germ line hCHK2 mutations in Li-Fraumeni syndrome, **Science** *286*, 2528-31.

Bessho, T., and Sancar, A. **(2000)**. Human DNA damage checkpoint protein hRAD9 is a 3' to 5' exonuclease, **J Biol Chem** *275*, 7451-4.

Blasina, A., de Weyer, I. V., Laus, M. C., Luyten, W. H., Parker, A. E., and McGowan, C. H. **(1999)**. A human homologue of the checkpoint kinase Cds1 directly inhibits Cdc25 phosphatase, **Curr Biol** *9*, 1-10.

Bluyssen, H. A., Naus, N. C., van Os, R. I., Jaspers, I., Hoeijmakers, J. H., and de Klein, A. **(1999)**. Human and mouse homologs of the Schizosaccharomyces pombe rad17+ cell cycle checkpoint control gene, **Genomics** *55*, 219-28.

Boddy, M. N., Furnari, B., Mondesert, O., and Russell, P. **(1998)**. Replication checkpoint enforced by kinases Cds1 and Chk1, **Science** *280*, 909-12.

Boddy, M. N., and Russell, P. **(1999)**. DNA replication checkpoint control, **Front Biosci** *4*, D841-8.

Bork, P., Hofmann, K., Bucher, P., Neuwald, A. F., Altschul, S. F., and Koonin, E. V. **(1997)**. A superfamily of conserved domains in DNA damage-responsive cell cycle checkpoint proteins, **Faseb J** *11*, 68-76.

Brush, G. S., Morrow, D. M., Hieter, P., and Kelly, T. J. **(1996)**. The ATM homologue MEC1 is required for phosphorylation of replication protein A in yeast, **Proc Natl Acad Sci U S A** *93*, 15075-80.

Burgers, P. M. **(1991)**. Saccharomyces cerevisiae replication factor C. II. Formation and activity of complexes with the proliferating cell nuclear antigen and with DNA polymerases delta and epsilon, **J Biol Chem** *266*, 22698-706.

Burke, D. J. **(2000)**. Complexity in the spindle checkpoint, **Curr Opin Genet Dev** *10*, 26-31.

Burns, V. W. **(1956)**. X-ray-induced division delay of individual yeast cells, **Radiat. Res** *4*, 394-412.

Cahill, D. P., Kinzler, K. W., Vogelstein, B., and Lengauer, C. **(1999)**. Genetic instability and darwinian selection in tumours, **Trends Cell Biol** *9*, M57-60.

Cahill, D. P., Lengauer, C., Yu, J., Riggins, G. J., Willson, J. K., Markowitz, S. D., Kinzler, K. W., and Vogelstein, B. **(1998)**. Mutations of mitotic checkpoint genes in human cancers [see comments], **Nature** *392*, 300-3.

Cai, J., Yao, N., Gibbs, E., Finkelstein, J., Phillips, B., O'Donnell, M., and Hurwitz, J. **(1998)**. ATP hydrolysis catalyzed by human replication factor C requires participation of multiple subunits, **Proc Natl Acad Sci U S A** *95*, 11607-12.

Callebaut, I., and Mornon, J. P. **(1997)**. From BRCA1 to RAP1: a widespread BRCT module closely associated with DNA repair, **FEBS Lett** *400*, 25-30.

Carney, J. P., Maser, R. S., Olivares, H., Davis, E. M., Le Beau, M., Yates, J. R., 3rd, Hays, L., Morgan, W. F., and Petrini, J. H. **(1998)**. The hMre11/hRad50 protein complex and Nijmegen breakage syndrome: linkage of double-strand break repair to the cellular DNA damage response, **Cell** *93*, 477-86.

Carr, A. M. **(1997)**. Control of cell cycle arrest by the Mec1sc/Rad3sp DNA structure checkpoint pathway, **Curr Opin Genet Dev** *7*, 93-8.

Caspari, T., and Carr, A. M. **(1999)**. DNA structure checkpoint pathways in Schizosaccharomyces pombe, **Biochimie** *81*, 173-81.

Caspari, T., Dahlen, M., Kanter-Smoler, G., Lindsay, H. D., Hofmann, K., Papadimitriou, K., Sunnerhagen, P., and Carr, A. M. **(2000)**. Characterization of Schizosaccharomyces pombe Hus1: a PCNA-related protein that associates with Rad1 and Rad9, **Mol Cell Biol** *20*, 1254-62.

Chan, T. A., Hermeking, H., Lengauer, C., Kinzler, K. W., and Vogelstein, B. **(1999)**. 14-3-3Sigma is required to prevent mitotic catastrophe after DNA damage [see comments], **Nature** *401*, 616-20.

Chan, T. A., Hwang, P. M., Hermeking, H., Kinzler, K. W., and Vogelstein, B. **(2000)**. Cooperative effects of genes controlling the G(2)/M checkpoint, **Genes Dev** *14*, 1584-8.

Chehab, N. H., Malikzay, A., Appel, M., and Halazonetis, T. D. **(2000)**. Chk2/hCds1 functions as a DNA damage checkpoint in G(1) by stabilizing p53, **Genes Dev** *14*, 278-88.

Chehab, N. H., Malikzay, A., Stavridi, E. S., and Halazonetis, T. D. **(1999)**. Phosphorylation of Ser-20 mediates stabilization of human p53 in response to DNA damage, **Proc Natl Acad Sci U S A** *96*, 13777-82.

Chen, L., Liu, T. H., and Walworth, N. C. **(1999)**. Association of Chk1 with 14-3-3 proteins is stimulated by DNA damage, **Genes Dev** *13*, 675-85.

Cheng, L., Hunke, L., and Hardy, C. F. J. **(1998)**. Cell cycle regulation of the Saccharomyces cerevisiae polo-like kinase cdc5p, **Mol Cell Biol** *18*, 7360-70.

Clarke, D. J., and Gimenez-Abian, J. F. **(2000)**. Checkpoints controlling mitosis [In Process Citation], **Bioessays** *22*, 351-63.

Cohen-Fix, O., and Koshland, D. **(1997)**. The anaphase inhibitor of Saccharomyces cerevisiae Pds1p is a target of the DNA damage checkpoint pathway, **Proc Natl Acad Sci U S A** *94*, 14361-6.

Corda, Y., Schramke, V., Longhese, M. P., Smokvina, T., Paciotti, V., Brevet, V., Gilson, E., and Geli, V. **(1999)**. Interaction between Set1p and checkpoint protein Mec3p in DNA repair and telomere functions, **Nat Genet** *21*, 204-8.

Cortez, D., Wang, Y., Qin, J., and Elledge, S. J. **(1999)**. Requirement of ATM-dependent phosphorylation of brca1 in the DNA damage response to double-strand breaks [see comments], **Science** *286*, 1162-6.

Craven, R. J., and Petes, T. D. **(2000)**. Involvement of the checkpoint protein Mec1p in silencing of gene expression at telomeres in Saccharomyces cerevisiae, **Mol Cell Biol** *20*, 2378-84.

Cullmann, G., Fien, K., Kobayashi, R., and Stillman, B. **(1995)**. Characterization of the five replication factor C genes of Saccharomyces cerevisiae, **Mol Cell Biol** *15*, 4661-71.

Dasika, G. K., Lin, S. C., Zhao, S., Sung, P., Tomkinson, A., and Lee, E. Y. **(1999)**. DNA damage-induced cell cycle checkpoints and DNA strand break repair in development and tumorigenesis, **Oncogene** *18*, 7883-99.

de la Torre-Ruiz, M., and Lowndes, N. F. **(2000)**. The Saccharomyces cerevisiae DNA damage checkpoint is required for efficient repair of double strand breaks by non-homologous end joining, **FEBS Lett** *467*, 311-5.

de la Torre-Ruiz, M. A., Green, C. M., and Lowndes, N. F. **(1998)**. RAD9 and RAD24 define two additive, interacting branches of the DNA damage checkpoint pathway in budding yeast normally required for Rad53 modification and activation, **Embo J** *17*, 2687-98.

Dean, F. B., Lian, L., and O'Donnell, M. **(1998)**. cDNA cloning and gene mapping of human homologs for Schizosaccharomyces pombe rad17, rad1, and hus1 and cloning of homologs from mouse, Caenorhabditis elegans, and Drosophila melanogaster, **Genomics** *54*, 424-36.

Degols, G., and Russell, P. **(1997)**. Discrete roles of the Spc1 kinase and the Atf1 transcription factor in the UV response of Schizosaccharomyces pombe, **Mol Cell Biol** *17*, 3356-63.

Desany, B. A., Alcasabas, A. A., Bachant, J. B., and Elledge, S. J. **(1998)**. Recovery from DNA replicational stress is the essential function of the S-phase checkpoint pathway, **Genes Dev** *12*, 2956-70.

Dohmen, R. J., Wu, P., and Varshavsky, A. **(1994)**. Heat-inducible degron: a method for constructing temperature-sensitive mutants, **Science** *263*, 1273-6.

Donjerkovic, D., and Scott, D. W. **(2000)**. Regulation of the G1 phase of the mammalian cell cycle, **Cell Res** *10*, 1-16.

Duckett, D. R., Bronstein, S. M., Taya, Y., and Modrich, P. **(1999)**. hMutSalpha- and hMutLalpha-dependent phosphorylation of p53 in response to DNA methylator damage, **Proc Natl Acad Sci U S A** *96*, 12384-8.

Durocher, D., Henckel, J., Fersht, A. R., and Jackson, S. P. **(1999)**. The FHA domain is a modular phosphopeptide recognition motif, **Mol Cell** *4*, 387-94.

Eckardt-Schupp, F., Siede, W., and Game, J. C. **(1987)**. The RAD24 (= Rs1) gene product of Saccharomyces cerevisiae participates in two different pathways of DNA repair, **Genetics** *115*, 83-90.

Edwards, R. J., Bentley, N. J., and Carr, A. M. **(1999)**. A Rad3-Rad26 complex responds to DNA damage independently of other checkpoint proteins, **Nat Cell Biol** *1*, 393-398.

Elledge, S. J. **(1996)**. Cell cycle checkpoints: preventing an identity crisis, **Science** *274*, 1664-72.

Emili, A. **(1998)**. MEC1-dependent phosphorylation of Rad9p in response to DNA damage, **Mol Cell** *2*, 183-9.

Enoch, T., Carr, A. M., and Nurse, P. **(1992)**. Fission yeast genes involved in coupling mitosis to completion of DNA replication, **Genes Dev** *6*, 2035-46.

Erdjument-Bromage, H., Lui, M., Lacomis, L., Grewal, A., Annan, R. S., McNulty, D. E., Carr, S. A., and Tempst, P. **(1998)**. Examination of micro-tip reversed-phase liquid chromatographic extraction of peptide pools for mass spectrometric analysis, **J Chromatogr A** *826*, 167-81.

Esashi, F., and Yanagida, M. **(1999)**. Cdc2 phosphorylation of Crb2 is required for reestablishing cell cycle progression after the damage checkpoint, **Mol Cell** *4*, 167-74.

Evan, G., and Littlewood, T. **(1998)**. A matter of life and cell death, **Science** *281*, 1317-22.

Fay, D. S., Sun, Z., and Stern, D. F. **(1997)**. Mutations in SPK1/RAD53 that specifically abolish checkpoint but not growth-related functions, **Curr Genet** *31*, 97-105.

Fien, K., and Stillman, B. **(1992)**. Identification of replication factor C from Saccharomyces cerevisiae: a component of the leading-strand DNA replication complex, **Mol Cell Biol** *12*, 155-63.

Flatt, P. M., Tang, L. J., Scatena, C. D., Szak, S. T., and Pietenpol, J. A. **(2000)**. p53 regulation of G(2) checkpoint is retinoblastoma protein dependent, **Mol Cell Biol** *20*, 4210-23.

Foiani, M., Liberi, G., Lucchini, G., and Plevani, P. **(1995)**. Cell cycle-dependent phosphorylation and dephosphorylation of the yeast DNA polymerase alpha-primase B subunit, **Mol Cell Biol** *15*, 883-91.

Foreman, P. K., and Davis, R. W. **(1994)**. Cloning vectors for the synthesis of epitope-tagged, truncated and chimeric proteins in Saccharomyces cerevisiae, **Gene** *144*, 63-8.

Francesconi, S., Grenon, M., Bouvier, D., and Baldacci, G. **(1997)**. p56(chk1) protein kinase is required for the DNA replication checkpoint at 37 degrees C in fission yeast, **Embo J** *16*, 1332-41.

Frei, C., and Gasser, S. M. **(2000)**. The yeast Sgs1p helicase acts upstream of Rad53p in the DNA replication checkpoint and colocalizes with Rad53p in S-phase-specific foci, **Genes Dev** *14*, 81-96.

Freire, R., Murguia, J. R., Tarsounas, M., Lowndes, N. F., Moens, P. B., and Jackson, S. P. **(1998)**. Human and mouse homologs of Schizosaccharomyces pombe rad1(+) and Saccharomyces cerevisiae RAD17: linkage to checkpoint control and mammalian meiosis, **Genes Dev** *12*, 2560-73.

Friedburg, E. C., Walker, G. C., and Siede, W. **(1995)**. DNA Repair and Mutagenesis (washington, D. C., ASM Press).

Furnari, B., Blasina, A., Boddy, M. N., McGowan, C. H., and Russell, P. **(1999)**. Cdc25 inhibited in vivo and in vitro by checkpoint kinases Cds1 and Chk1, **Mol Biol Cell** *10*, 833-45.

Furnari, B., Rhind, N., and Russell, P. **(1997)**. Cdc25 mitotic inducer targeted by chk1 DNA damage checkpoint kinase, **Science** *277*, 1495-7.

Gardner, R., Putnam, C. W., and Weinert, T. **(1999)**. RAD53, DUN1 and PDS1 define two parallel G2/M checkpoint pathways in budding yeast, **Embo J** *18*, 3173-85.

Garvik, B., Carson, M., and Hartwell, L. **(1995)**. Single-stranded DNA arising at telomeres in cdc13 mutants may constitute a specific signal for the RAD9 checkpoint [published erratum appears in Mol Cell Biol 1996 Jan;16(1):457], **Mol Cell Biol** *15*, 6128-38.

Gerik, K. J., Gary, S. L., and Burgers, P. M. **(1997)**. Overproduction and affinity purification of Saccharomyces cerevisiae replication factor C, **J Biol Chem** *272*, 1256-62.

Gilbert, C. S., Green, C. M., Vialard, J., Grenon, M., Erdjument-Bromage, H., Tempst, P., and Lowndes, N. F. **(2000)**. Budding yeast Rad9 requires chaperone proteins for its function as a catalyst of in trans autophosphorylation of Rad53, **Submitted**.

Gomes, X. V., Gary, S. L., and Burgers, P. M. **(2000)**. Overproduction in Escherichia coli and characterization of yeast replication factor C lacking the ligase homology domain, **J Biol Chem** *275*, 14541-9.

Gowen, L. C., Avrutskaya, A. V., Latour, A. M., Koller, B. H., and Leadon, S. A. **(1998)**. BRCA1 required for transcription-coupled repair of oxidative DNA damage, **Science** *281*, 1009-12.

Green, C. M., Erdjument-Bromage, H., Tempst, P., and Lowndes, N. F. **(2000)**. A novel Rad24 checkpoint protein complex closely related to replication factor C, **Curr Biol** *10*, 39-42.

Greenwell, P. W., Kronmal, S. L., Porter, S. E., Gassenhuber, J., Obermaier, B., and Petes, T. D. **(1995)**. TEL1, a gene involved in controlling telomere length in S. cerevisiae, is homologous to the human ataxia telangiectasia gene, **Cell** *82*, 823-9.

Grenon, M., Tillit, J., Piard, K., Baldacci, G., and Francesconi, S. **(1999)**. The S/M checkpoint at 37 degrees C and the recovery of viability of the mutant poldeltats3 require the crb2+/rhp9+ gene in fission yeast, **Mol Gen Genet** *260*, 522-34.

Griffiths, D., Uchiyama, M., Nurse, P., and Wang, T. S. **(2000)**. A novel mutant allele of the chromatin-bound fission yeast checkpoint protein Rad17 separates the DNA structure checkpoints, **J Cell Sci** *113*, 1075-88.

Griffiths, D. J., Barbet, N. C., McCready, S., Lehmann, A. R., and Carr, A. M. **(1995)**. Fission yeast rad17: a homologue of budding yeast RAD24 that shares regions of sequence similarity with DNA polymerase accessory proteins, **Embo J** *14*, 5812-23.

Grossman, L., Lin, C.-l., and Ahn, Y. (1998). Nucleotide Excision Repair in *Escherichia coli*. In DNA Damage and Repair: DNA Repair in Prokaryotes and Lower Eukaryotes, J. A. Nickoloff, and M. F. Hoekstra, eds. (Totowa, New Jersey, Humana Press), pp. 11-28.

Grushcow, J. M., Holzen, T. M., Park, K. J., Weinert, T., Lichten, M., and Bishop, D. K. **(1999)**. Saccharomyces cerevisiae checkpoint genes MEC1, RAD17 and RAD24 are required for normal meiotic recombination partner choice, **Genetics** *153*, 607-20.

Guan, J., DiBiase, S., and Iliakis, G. **(2000)**. The catalytic subunit DNA-dependent protein kinase (DNA-PKcs) facilitates recovery from radiation-induced inhibition of DNA replication, **Nucleic Acids Res** *28*, 1183-92.

Haber, J. E. **(1998)**. The many interfaces of Mre11, **Cell** *95*, 583-6.

Haber, J. E. **(1999)**. Sir-Ku-itous routes to make ends meet, **Cell** *97*, 829-32.

Hall-Jackson, C. A., Cross, D. A., Morrice, N., and Smythe, C. **(1999)**. ATR is a caffeine-sensitive, DNA-activated protein kinase with a substrate specificity distinct from DNA-PK, **Oncogene** *18*, 6707-13.

Hammet, A., Pike, B. L., Mitchelhill, K. I., Teh, T., Kobe, B., House, C. M., Kemp, B. E., and Heierhorst, J. **(2000)**. FHA domain boundaries of the dun1p and rad53p cell cycle checkpoint kinases, **FEBS Lett** *471*, 141-6.

Hang, H., and Lieberman, H. B. **(2000)**. Physical interactions among human checkpoint control proteins HUS1p, RAD1p, and RAD9p, and implications for the regulation of cell cycle progression, **Genomics** *65*, 24-33.

Hari, K. L., Santerre, A., Sekelsky, J. J., McKim, K. S., Boyd, J. B., and Hawley, R. S. **(1995)**. The mei-41 gene of D. melanogaster is a structural and functional homolog of the human ataxia telangiectasia gene, **Cell** *82*, 815-21.

Harlow E, and D., L. **(1988)**. Antibodies: A Laboratory Manual., Cold Spring Harbour).

Hartwell, L. H., and Kastan, M. B. **(1994)**. Cell cycle control and cancer, **Science** *266*, 1821-8.

Hartwell, L. H., and Weinert, T. A. **(1989)**. Checkpoints: controls that ensure the order of cell cycle events, **Science** *246*, 629-34.

Hawn, M. T., Umar, A., Carethers, J. M., Marra, G., Kunkel, T. A., Boland, C. R., and Koi, M. **(1995)**. Evidence for a connection between the mismatch repair system and the G2 cell cycle checkpoint, **Cancer Res** *55*, 3721-5.

Hellman, U., Wernstedt, C., Gonez, J., and Heldin, C. H. **(1995)**. Improvement of an "In-Gel" digestion procedure for the micropreparation of internal protein fragments for amino acid sequencing, **Anal Biochem** *224*, 451-5.

Hirao, A., Kong, Y. Y., Matsuoka, S., Wakeham, A., Ruland, J., Yoshida, H., Liu, D., Elledge, S. J., and Mak, T. W. **(2000)**. DNA damage-induced activation of p53 by the checkpoint kinase Chk2, **Science** *287*, 1824-7.

Hofmann, K., and Bucher, P. **(1995)**. The FHA domain: a putative nuclear signalling domain found in protein kinases and transcription factors, **Trends Biochem Sci** *20*, 347-9.

Howell, E. A., McAlear, M. A., Rose, D., and Holm, C. **(1994)**. CDC44: a putative nucleotide-binding protein required for cell cycle progression that has homology to subunits of replication factor C, **Mol Cell Biol** *14*, 255-67.

Huang, M., Zhou, Z., and Elledge, S. J. **(1998)**. The DNA replication and damage checkpoint pathways induce transcription by inhibition of the Crt1 repressor, **Cell** *94*, 595-605.

Hwang, B. J., Ford, J. M., Hanawalt, P. C., and Chu, G. **(1999)**. Expression of the p48 xeroderma pigmentosum gene is p53-dependent and is involved in global genomic repair, **Proc Natl Acad Sci U S A** *96*, 424-8.

Jimenez, G., Yucel, J., Rowley, R., and Subramani, S. **(1992)**. The rad3+ gene of Schizosaccharomyces pombe is involved in multiple checkpoint functions and in DNA repair, **Proc Natl Acad Sci U S A** *89*, 4952-6.

Jin, D. Y., Spencer, F., and Jeang, K. T. **(1998)**. Human T cell leukemia virus type 1 oncoprotein Tax targets the human mitotic checkpoint protein MAD1, **Cell** *93*, 81-91.

Jonsson, Z. O., and Hubscher, U. **(1997)**. Proliferating cell nuclear antigen: more than a clamp for DNA polymerases, **Bioessays** *19*, 967-75.

Kato, R., and Ogawa, H. **(1994)**. An essential gene, ESR1, is required for mitotic cell growth, DNA repair and meiotic recombination in Saccharomyces cerevisiae, **Nucleic Acids Res** *22*, 3104-12.

Keegan, K. S., Holtzman, D. A., Plug, A. W., Christenson, E. R., Brainerd, E. E., Flaggs, G., Bentley, N. J., Taylor, E. M., Meyn, M. S., Moss, S. B., *et al.* **(1996)**. The Atr and Atm protein kinases associate with different sites along meiotically pairing chromosomes, **Genes Dev** *10*, 2423-37.

Khanna, K., Gatti, R., Caoncannon, P., Weemaes, C. M. R., Hoekstra, M. F., Lavin, M., and D'Andrea, A. (1998a). Cellular Responses to DNA damage and the Human Chromosome Instability Syndromes. In DNA Damage and Repair: DNA Repair in Higher Eukaryotes, J. A. Nickoloff, and M. F. Hoekstra, eds. (Totowa, New Jersey, Humana Press), pp. 395-442.

Khanna, K. K., Keating, K. E., Kozlov, S., Scott, S., Gatei, M., Hobson, K., Taya, Y., Gabrielli, B., Chan, D., Lees-Miller, S. P., and Lavin, M. F. **(1998b)**. ATM associates with and phosphorylates p53: mapping the region of interaction, **Nat Genet** *20*, 398-400.

Kiser, G. L., and Weinert, T. A. **(1996)**. Distinct roles of yeast MEC and RAD checkpoint genes in transcriptional induction after DNA damage and implications for function, **Mol Biol Cell** *7*, 703-18.

Koch, W. H., and Woodgate, R. (1998). The SOS Response. In DNA Damage and Repair: DNA Repair in Prokaryotes and Lower Eukaryotes, J. A. Nickoloff, and M. F. Hoekstra, eds. (Totowa, New Jersey, Humana Press), pp. 107-134.

Kolodziej, P. A., and Young, R. A. **(1991)**. Epitope tagging and protein surveillance, **Methods Enzymol** *194*, 508-19.

Komatsu, K., Miyashita, T., Hang, H., Hopkins, K. M., Zheng, W., Cuddeback, S., Yamada, M., Lieberman, H. B., and Wang, H. G. **(2000)**. Human homologue of S. pombe Rad9 interacts with BCL-2/BCL-xL and promotes apoptosis, **Nat Cell Biol** *2*, 1-6.

Kondo, T., Matsumoto, K., and Sugimoto, K. **(1999)**. Role of a complex containing Rad17, Mec3, and Ddc1 in the yeast DNA damage checkpoint pathway, **Mol Cell Biol** *19*, 1136-43.

Kostrub, C. F., Knudsen, K., Subramani, S., and Enoch, T. **(1998)**. Hus1p, a conserved fission yeast checkpoint protein, interacts with Rad1p and is phosphorylated in response to DNA damage, **Embo J** *17*, 2055-66.

Kowalczykowski, S. C. **(2000)**. Initiation of genetic recombination and recombination-dependent replication, **Trends Biochem Sci** *25*, 156-65.

Lakin, N. D., Hann, B. C., and Jackson, S. P. **(1999)**. The ataxia-telangiectasia related protein ATR mediates DNA-dependent phosphorylation of p53, **Oncogene** *18*, 3989-95.

Lakin, N. D., and Jackson, S. P. **(1999)**. Regulation of p53 in response to DNA damage, **Oncogene** *18*, 7644-55.

Lambert, C., Couto, L. B., Weiss, W. A., Schultz, R. A., Thompson, L. H., and Friedberg, E. C. **(1988)**. A yeast DNA repair gene partially complements defective excision repair in mammalian cells, **Embo J** *7*, 3245-53.

Laurent, T. C., and Killander, J. **(1964)**. A theory of gel filtration and its experimental verification, **J. Chromatog.** *14*, 317-30.

Lee, J. S., Collins, K. M., Brown, A. L., Lee, C. H., and Chung, J. H. **(2000)**. hCds1-mediated phosphorylation of BRCA1 regulates the DNA damage response, **Nature** *404*, 201-4.

Lee, S. E., Moore, J. K., Holmes, A., Umezu, K., Kolodner, R. D., and Haber, J. E. **(1998)**. Saccharomyces Ku70, mre11/rad50 and RPA proteins regulate adaptation to G2/M arrest after DNA damage, **Cell** *94*, 399-409.

Lengauer, C., Kinzler, K. W., and Vogelstein, B. **(1998)**. Genetic instabilities in human cancers, **Nature** *396*, 643-9.

Levine, A. J. **(1997)**. p53, the cellular gatekeeper for growth and division, **Cell** *88*, 323-31.

Lew, D. J. **(2000)**. Cell-cycle checkpoints that ensure coordination between nuclear and cytoplasmic events in Saccharomyces cerevisiae, **Curr Opin Genet Dev** *10*, 47-53.

Lewis, L. K., Kirchner, J. M., and Resnick, M. A. **(1998)**. Requirement for end-joining and checkpoint functions, but not RAD52- mediated recombination, after EcoRI endonuclease cleavage of Saccharomyces cerevisiae DNA, **Mol Cell Biol** *18*, 1891-902.

Li, L., Peterson, C. A., Kanter-Smoler, G., Wei, Y. F., Ramagli, L. S., Sunnerhagen, P., Siciliano, M. J., and Legerski, R. J. **(1999)**. hRAD17, a structural homolog of the Schizosaccharomyces pombe RAD17 cell cycle checkpoint gene, stimulates p53 accumulation, **Oncogene** *18*, 1689-99.

Li, R., Waga, S., Hannon, G. J., Beach, D., and Stillman, B. **(1994)**. Differential effects by the p21 CDK inhibitor on PCNA-dependent DNA replication and repair, **Nature** *371*, 534-7.

Li, S., Ting, N. S., Zheng, L., Chen, P. L., Ziv, Y., Shiloh, Y., Lee, E. Y., and Lee, W. H. **(2000)**. Functional link of BRCA1 and ataxia telangiectasia gene product in DNA damage response, **Nature** *406*, 210-5.

Lim, D. S., Kim, S. T., Xu, B., Maser, R. S., Lin, J., Petrini, J. H., and Kastan, M. B. **(2000)**. ATM phosphorylates p95/nbs1 in an S-phase checkpoint pathway, **Nature** *404*, 613-7.

Lim, H. H., and Surana, U. **(1996)**. Cdc20, a beta-transducin homologue, links RAD9-mediated G2/M checkpoint control to mitosis in Saccharomyces cerevisiae, **Mol Gen Genet** *253*, 138-48.

Lindsay, H. D., Griffiths, D. J., Edwards, R. J., Christensen, P. U., Murray, J. M., Osman, F., Walworth, N., and Carr, A. M. **(1998)**. S-phase-specific activation of Cds1 kinase defines a subpathway of the checkpoint response in Schizosaccharomyces pombe, **Genes Dev** *12*, 382-95.

Liu, Q., Guntuku, S., Cui, X. S., Matsuoka, S., Cortez, D., Tamai, K., Luo, G., Carattini-Rivera, S., DeMayo, F., Bradley, A., *et al.* **(2000a)**. Chk1 is an essential kinase that is regulated by Atr and required for the G(2)/M DNA damage checkpoint, **Genes Dev** *14*, 1448-1459.

Liu, Y., Vidanes, G., Lin, Y. C., Mori, S., and Siede, W. **(2000b)**. Characterization of a Saccharomyces cerevisiae homologue of Schizosaccharomyces pombe Chk1 involved in DNA-damage-induced M-phase arrest, **Mol Gen Genet** *262*, 1132-46.

Longhese, M. P., Fraschini, R., Plevani, P., and Lucchini, G. **(1996a)**. Yeast pip3/mec3 mutants fail to delay entry into S phase and to slow DNA replication in response to DNA damage, and they define a functional link between Mec3 and DNA primase, **Mol Cell Biol** *16*, 3235-44.

Longhese, M. P., Neecke, H., Paciotti, V., Lucchini, G., and Plevani, P. **(1996b)**. The 70 kDa subunit of replication protein A is required for the G1/S and intra-S DNA damage checkpoints in budding yeast, **Nucleic Acids Res** *24*, 3533-7.

Longhese, M. P., Paciotti, V., Fraschini, R., Zaccarini, R., Plevani, P., and Lucchini, G. **(1997)**. The novel DNA damage checkpoint protein ddc1p is phosphorylated periodically during the cell cycle and in response to DNA damage in budding yeast, **Embo J** *16*, 5216-26.

Longhese, M. P., Paciotti, V., Neecke, H., and Lucchini, G. **(2000)**. Checkpoint proteins influence telomeric silencing and length maintenance in budding yeast, **Genetics** *155*, 1577-91.

Lowndes, N. F., and Murguia, J. R. **(2000)**. Sensing and responding to DNA damage, **Curr Opin Genet Dev** *10*, 17-25.

Lundgren, K., Walworth, N., Booher, R., Dembski, M., Kirschner, M., and Beach, D. **(1991)**. mik1 and wee1 cooperate in the inhibitory tyrosine phosphorylation of cdc2, **Cell** *64*, 1111-22.

Lustig, A. J., and Petes, T. D. **(1986)**. Identification of yeast mutants with altered telomere structure, **Proc Natl Acad Sci U S A** *83*, 1398-402.

Lydall, D., Nikolsky, Y., Bishop, D. K., and Weinert, T. **(1996)**. A meiotic recombination checkpoint controlled by mitotic checkpoint genes, **Nature** *383*, 840-3.

Lydall, D., and Weinert, T. **(1995)**. Yeast checkpoint genes in DNA damage processing: implications for repair and arrest, **Science** *270*, 1488-91.

Lydall, D., and Weinert, T. **(1997)**. G2/M checkpoint genes of Saccharomyces cerevisiae: further evidence for roles in DNA replication and/or repair, **Mol Gen Genet** *256*, 638-51.

Madeo, F., Frohlich, E., and Frohlich, K. U. **(1997)**. A yeast mutant showing diagnostic markers of early and late apoptosis, **J Cell Biol** *139*, 729-34.

Madeo, F., Frohlich, E., Ligr, M., Grey, M., Sigrist, S. J., Wolf, D. H., and Frohlich, K. U. **(1999)**. Oxygen stress: a regulator of apoptosis in yeast, **J Cell Biol** *145*, 757-67.

Mann, M., Hojrup, P., and Roepstorff, P. **(1993)**. Use of mass spectrometric molecular weight information to identify proteins in sequence databases, **Biol Mass Spectrom** *22*, 338-45.

Marini, F., Pellicioli, A., Paciotti, V., Lucchini, G., Plevani, P., Stern, D. F., and Foiani, M. **(1997)**. A role for DNA primase in coupling DNA replication to DNA damage response, **Embo J** *16*, 639-50.

Marsolier, M. C., Roussel, P., Leroy, C., and Mann, C. **(2000)**. Involvement of the PP2C-like phosphatase ptc2p in the DNA checkpoint pathways of saccharomyces cerevisiae [In Process Citation], **Genetics** *154*, 1523-32.

Martin, R. G., and Ames, B. N. **(1961)**. A Method for Determining the Sedimentation Behaviour of Enzymes: Application to Protein Mixtures, **J Biol Chem** *236*, 1372-79.

Martin, S. G., Laroche, T., Suka, N., Grunstein, M., and Gasser, S. M. **(1999)**. Relocalization of telomeric Ku and SIR proteins in response to DNA strand breaks in yeast, **Cell** *97*, 621-33.

Martinho, R. G., Lindsay, H. D., Flaggs, G., DeMaggio, A. J., Hoekstra, M. F., Carr, A. M., and Bentley, N. J. **(1998)**. Analysis of Rad3 and Chk1 protein kinases defines different checkpoint responses, **Embo J** *17*, 7239-49.

Matlashewski, G. **(1999)**. p53: Twenty years on, Meeting Review, **Oncogene** *18*, 7618-7620.

Matsumoto, T. **(1997)**. A fission yeast homolog of CDC20/p55CDC/Fizzy is required for recovery from DNA damage and genetically interacts with p34cdc2, **Mol Cell Biol** *17*, 742-50.

May, P., and May, E. **(1999)**. Twenty years of p53 research: structural and functional aspects of the p53 protein, **Oncogene** *18*, 7621-36.

McAinsh, A. D., Scott-Drew, S., Murray, J. A., and Jackson, S. P. **(1999)**. DNA damage triggers disruption of telomeric silencing and Mec1p- dependent relocation of Sir3p, **Curr Biol** *9*, 963-6.

McFarlane, R. J., Carr, A. M., and Price, C. **(1997)**. Characterisation of the Schizosaccharomyces pombe rad4/cut5 mutant phenotypes: dissection of DNA replication and G2 checkpoint control function, **Mol Gen Genet** *255*, 332-40.

McMillan, J. N., Longtine, M. S., Sia, R. A., Theesfeld, C. L., Bardes, E. S., Pringle, J. R., and Lew, D. J. **(1999)**. The morphogenesis checkpoint in Saccharomyces cerevisiae: cell cycle control of Swe1p degradation by Hsl1p and Hsl7p, **Mol Cell Biol** *19*, 6929-39.

Merrill, B. J., and Holm, C. **(1999)**. A requirement for recombinational repair in Saccharomyces cerevisiae is caused by DNA replication defects of mec1 mutants, **Genetics** *153*, 595-605.

Meyn, M. S. **(1999)**. Ataxia-telangiectasia, cancer and the pathobiology of the ATM gene, **Clin Genet** *55*, 289-304.

Michelson, R., and Weinert, T. **(1999)**. Sensor-less checkpoint activation?, **Nat Cell Biol** *1*, E177-E179.

Miki, Y., Swensen, J., Shattuck-Eidens, D., Futreal, P. A., Harshman, K., Tavtigian, S., Liu, Q., Cochran, C., Bennett, L. M., Ding, W., and et al. **(1994)**. A strong candidate for the breast and ovarian cancer susceptibility gene BRCA1, **Science** *266*, 66-71.

Millar, J. B., and Russell, P. **(1992)**. The cdc25 M-phase inducer: an unconventional protein phosphatase, **Cell** *68*, 407-10.

Mills, K. D., Sinclair, D. A., and Guarente, L. **(1999)**. MEC1-dependent redistribution of the Sir3 silencing protein from telomeres to DNA double-strand breaks, **Cell** *97*, 609-20.

Morrow, D. M., Tagle, D. A., Shiloh, Y., Collins, F. S., and Hieter, P. **(1995)**. TEL1, an S. cerevisiae homolog of the human gene mutated in ataxia telangiectasia, is functionally related to the yeast checkpoint gene MEC1, **Cell** *82*, 831-40.

Mossi, R., and Hubscher, U. **(1998)**. Clamping down on clamps and clamp loaders--the eukaryotic replication factor C, **Eur J Biochem** *254*, 209-16.

Murakami, H., and Nurse, P. **(1999)**. Meiotic DNA replication checkpoint control in fission yeast, **Genes Dev** *13*, 2581-93.

Murakami, H., and Nurse, P. **(2000)**. DNA replication and damage checkpoints and meiotic cell cycle controls in the fission and budding yeasts, **Biochem J** *349*, 1-12.

Murakami, H., and Okayama, H. **(1995)**. A kinase from fission yeast responsible for blocking mitosis in S phase, **Nature** *374*, 817-9.

Murguia, J. R., Grenon, M., Gilbert, C. S., Green, C. M., and Lowndes, N. F. **(In preparation)**. In vitro analysis of DNA damage-dependent checkpoint activation.

Naiki, T., Shimomura, T., Kondo, T., Matsumoto, K., and Sugimoto, K. **(2000)**. Rfc5, in cooperation with rad24, controls DNA damage checkpoints throughout the cell cycle in saccharomyces cerevisiae [In Process Citation], **Mol Cell Biol** *20*, 5888-96.

Navas, T. A., Sanchez, Y., and Elledge, S. J. **(1996)**. RAD9 and DNA polymerase epsilon form parallel sensory branches for transducing the DNA damage checkpoint signal in Saccharomyces cerevisiae, **Genes Dev** *10*, 2632-43.

Navas, T. A., Zhou, Z., and Elledge, S. J. **(1995)**. DNA polymerase epsilon links the DNA replication machinery to the S phase checkpoint, **Cell** *80*, 29-39.

Neecke, H., Lucchini, G., and Longhese, M. P. **(1999)**. Cell cycle progression in the presence of irreparable DNA damage is controlled by a Mec1- and Rad53-dependent checkpoint in budding yeast, **Embo J** *18*, 4485-97.

Nelson, W. G., and Kastan, M. B. **(1994)**. DNA strand breaks: the DNA template alterations that trigger p53- dependent DNA damage response pathways, **Mol Cell Biol** *14*, 1815-23.

Noskov, V. N., Araki, H., and Sugino, A. **(1998)**. The RFC2 gene, encoding the third-largest subunit of the replication factor C complex, is required for an S-phase checkpoint in Saccharomyces cerevisiae, **Mol Cell Biol** *18*, 4914-23.

Nurse, P. **(1990)**. Universal control mechanism regulating onset of M-phase, **Nature** *344*, 503-8.

Nurse, P., and Bissett, Y. **(1981)**. Gene required in G1 for commitment to cell cycle and in G2 for control of mitosis in fission yeast, **Nature** *292*, 558-60.

O'Connell, M. J., Raleigh, J. M., Verkade, H. M., and Nurse, P. **(1997)**. Chk1 is a wee1 kinase in the G2 DNA damage checkpoint inhibiting cdc2 by Y15 phosphorylation, **Embo J** *16*, 545-54.

O'Connell, M. J., Walworth, N. C., and Carr, A. M. **(2000)**. The G2-phase DNA-damage checkpoint, **Trends Cell Biol** *10*, 296-303.

Onel, K., Koff, A., Bennett, R. L., Unrau, P., and Holloman, W. K. **(1996)**. The REC1 gene of Ustilago maydis, which encodes a 3'-->5' exonuclease, couples DNA repair and completion of DNA synthesis to a mitotic checkpoint, **Genetics** *143*, 165-74.

Paciotti, V., Clerici, M., Lucchini, G., and Longhese, M. P. **(2000)**. The checkpoint protein Ddc2, functionally related to S. pombe Rad26, interacts with Mec1 and is regulated by Mec1-dependent phosphorylation in budding yeast, **Genes Dev** *14*, 2046-2059.

Paciotti, V., Lucchini, G., Plevani, P., and Longhese, M. P. **(1998)**. Mec1p is essential for phosphorylation of the yeast DNA damage checkpoint protein Ddc1p, which physically interacts with Mec3p, **Embo J** *17*, 4199-209.

Parker, A. E., Van de Weyer, I., Laus, M. C., Oostveen, I., Yon, J., Verhasselt, P., and Luyten, W. H. **(1998a)**. A human homologue of the Schizosaccharomyces pombe rad1+ checkpoint gene encodes an exonuclease, **J Biol Chem** *273*, 18332-9.

Parker, A. E., Van de Weyer, I., Laus, M. C., Verhasselt, P., and Luyten, W. H. **(1998b)**. Identification of a human homologue of the Schizosaccharomyces pombe rad17+ checkpoint gene, **J Biol Chem** *273*, 18340-6.

Parks, T. D., Leuther, K. K., Howard, E. D., Johnston, S. A., and Dougherty, W. G. **(1994)**. Release of proteins and peptides from fusion proteins using a recombinant plant virus proteinase, **Anal Biochem** *216*, 413-7.

Pati, D., Keller, C., Groudine, M., and Plon, S. E. **(1997)**. Reconstitution of a MEC1-independent checkpoint in yeast by expression of a novel human fork head cDNA, **Mol Cell Biol** *17*, 3037-46.

Paulovich, A. G., Armour, C. D., and Hartwell, L. H. **(1998)**. The Saccharomyces cerevisiae RAD9, RAD17, RAD24 and MEC3 genes are required for tolerating irreparable, ultraviolet-induced DNA damage, **Genetics** *150*, 75-93.

Paulovich, A. G., and Hartwell, L. H. **(1995)**. A checkpoint regulates the rate of progression through S phase in S. cerevisiae in response to DNA damage, **Cell** *82*, 841-7.

Paulovich, A. G., Margulies, R. U., Garvik, B. M., and Hartwell, L. H. **(1997)**. RAD9, RAD17, and RAD24 are required for S phase regulation in Saccharomyces cerevisiae in response to DNA damage, **Genetics** *145*, 45-62.

Pellicioli, A., Lucca, C., Liberi, G., Marini, F., Lopes, M., Plevani, P., Romano, A., Di Fiore, P. P., and Foiani, M. **(1999)**. Activation of Rad53 kinase in response to DNA damage and its effect in modulating phosphorylation of the lagging strand DNA polymerase, **Embo J** *18*, 6561-72.

Peng, C. Y., Graves, P. R., Thoma, R. S., Wu, Z., Shaw, A. S., and Piwnica-Worms, H. **(1997)**. Mitotic and G2 checkpoint control: regulation of 14-3-3 protein binding by phosphorylation of Cdc25C on serine-216, **Science** *277*, 1501-5.

Petrini, J. H. **(1999)**. The mammalian Mre11-Rad50-nbs1 protein complex: integration of functions in the cellular DNA-damage response, **Am J Hum Genet** *64*, 1264-9.

Piette, J., and Munoz, P. **(2000)**. Implication of the G2 checkpoint in the maintenance of genome integrity, **Pathol Biol (Paris)** *48*, 174-81.

Podust, V. N., and Fanning, E. **(1997)**. Assembly of functional replication factor C expressed using recombinant baculoviruses, **J Biol Chem** *272*, 6303-10.

Prolla, T., Baker, S., and Liskay, R. M. (1998). Genetics of Mismatch Repair, Microsatellite Instability, and Cancer. In DNA Damage and Repair: DNA Repair in Higher Eukaryotes, J. A. Nickoloff, and M. F. Hoekstra, eds. (Totowa, New Jersey, Humana Press), pp. 443-465.

Raleigh, J. M., and O'Connell, M. J. **(2000)**. The G(2) DNA damage checkpoint targets both wee1 and cdc25, **J Cell Sci** *113*, 1727-36.

Rasmussen, L. J., Samson, L., and Marinus, M. G. (1998). Dam-Directed DNA Mismatch Repair. In DNA Damage and Repair: DNA Repair in Prokaryotes and Lower Eukaryotes, J. A. Nickoloff, and M. F. Hoekstra, eds. (Totowa, New Jersey, Humana Press), pp. 205-228.

Rauen, M., Burtelow, M. A., Dufault, V. M., and Karnitz, L. M. **(2000)**. The human checkpoint protein hRad17 interacts with the PCNA-like proteins hRad1, hHus1, and hRad9, **J Biol Chem**.

Reynolds, N., Fantes, P. A., and MacNeill, S. A. **(1999)**. A key role for replication factor C in DNA replication checkpoint function in fission yeast, **Nucleic Acids Res** *27*, 462-9.

Rhind, N., Furnari, B., and Russell, P. **(1997)**. Cdc2 tyrosine phosphorylation is required for the DNA damage checkpoint in fission yeast, **Genes Dev** *11*, 504-11.

Rhind, N., and Russell, P. **(1998a)**. Mitotic DNA damage and replication checkpoints in yeast, **Curr Opin Cell Biol** *10*, 749-58.

Rhind, N., and Russell, P. **(1998b)**. The Schizosaccharomyces pombe S-phase checkpoint differentiates between different types of DNA damage, **Genetics** *149*, 1729-37.

Rhind, N., and Russell, P. **(1998c)**. Tyrosine phosphorylation of cdc2 is required for the replication checkpoint in Schizosaccharomyces pombe, **Mol Cell Biol** *18*, 3782-7.

Ritchie, K. B., Mallory, J. C., and Petes, T. D. **(1999)**. Interactions of TLC1 (which encodes the RNA subunit of telomerase), TEL1, and MEC1 in regulating telomere length in the yeast Saccharomyces cerevisiae, **Mol Cell Biol** *19*, 6065-75.

Rothstein, R. **(1991)**. Targeting, disruption, replacement, and allele rescue: integrative DNA transformation in yeast, **Methods Enzymol** *194*, 281-301.

Rowley, R., Subramani, S., and Young, P. G. **(1992)**. Checkpoint controls in Schizosaccharomyces pombe: rad1, **Embo J** *11*, 1335-42.

Saka, Y., Esashi, F., Matsusaka, T., Mochida, S., and Yanagida, M. **(1997)**. Damage and replication checkpoint control in fission yeast is ensured by interactions of Crb2, a protein with BRCT motif, with Cut5 and Chk1, **Genes Dev** *11*, 3387-400.

Saka, Y., Fantes, P., Sutani, T., McInerny, C., Creanor, J., and Yanagida, M. **(1994)**. Fission yeast cut5 links nuclear chromatin and M phase regulator in the replication checkpoint control, **Embo J** *13*, 5319-29.

Saka, Y., and Yanagida, M. **(1993)**. Fission yeast cut5+, required for S phase onset and M phase restraint, is identical to the radiation-damage repair gene rad4+, **Cell** *74*, 383-93.

Sambrook J, Fritsch EF, and T., M. **(1989)**. Molecular: Cloning a Laboratory Manual, second edn (New York, Cold Spring Harbour).

Sanchez, Y., Bachant, J., Wang, H., Hu, F., Liu, D., Tetzlaff, M., and Elledge, S. J. **(1999)**. Control of the DNA damage checkpoint by chk1 and rad53 protein kinases through distinct mechanisms, **Science** *286*, 1166-71.

Sanchez, Y., Desany, B. A., Jones, W. J., Liu, Q., Wang, B., and Elledge, S. J. **(1996)**. Regulation of RAD53 by the ATM-like kinases MEC1 and TEL1 in yeast cell cycle checkpoint pathways, **Science** *271*, 357-60.

Sanchez, Y., Wong, C., Thoma, R. S., Richman, R., Wu, Z., Piwnica-Worms, H., and Elledge, S. J. **(1997)**. Conservation of the Chk1 checkpoint pathway in mammals: linkage of DNA damage to Cdk regulation through Cdc25, **Science** *277*, 1497-501.

Sandell, L. L., and Zakian, V. A. **(1993)**. Loss of a yeast telomere: arrest, recovery, and chromosome loss, **Cell** *75*, 729-39.

Santocanale, C., and Diffley, J. F. **(1998)**. A Mec1- and Rad53-dependent checkpoint controls late-firing origins of DNA replication, **Nature** *395*, 615-8.

Savitsky, K., Bar-Shira, A., Gilad, S., Rotman, G., Ziv, Y., Vanagaite, L., Tagle, D. A., Smith, S., Uziel, T., Sfez, S., and et al. **(1995)**. A single ataxia telangiectasia gene with a product similar to PI-3 kinase, **Science** *268*, 1749-53.

Schiestl, R. H., Reynolds, P., Prakash, S., and Prakash, L. **(1989)**. Cloning and sequence analysis of the Saccharomyces cerevisiae RAD9 gene and further evidence that its product is required for cell cycle arrest induced by DNA damage, **Mol Cell Biol** *9*, 1882-96.

Schneider, C., Newman, R. A., Sutherland, D. R., Asser, U., and Greaves, M. F. **(1982)**. A one-step purification of membrane proteins using a high efficiency immunomatrix, **J Biol Chem** *257*, 10766-9.

Schultz, M. C. **(1999)**. Chromatin assembly in yeast cell-free extracts, **Methods** *17*, 161-72.

Scopes, R. K. **(1993)**. Protein Purification Principles and Practice (New York, Springer-Verlag).

Scully, R., Chen, J., Plug, A., Xiao, Y., Weaver, D., Feunteun, J., Ashley, T., and Livingston, D. M. **(1997)**. Association of BRCA1 with Rad51 in mitotic and meiotic cells, **Cell** *88*, 265-75.

Shackelford, R. E., Kaufmann, W. K., and Paules, R. S. **(2000)**. Oxidative stress and cell cycle checkpoint function(1), **Free Radic Biol Med** *28*, 1387-404.

Shieh, S. Y., Ahn, J., Tamai, K., Taya, Y., and Prives, C. **(2000)**. The human homologs of checkpoint kinases Chk1 and Cds1 (Chk2) phosphorylate p53 at multiple DNA damage-inducible sites, **Genes Dev** *14*, 289-300.

Shimada, M., Okuzaki, D., Tanaka, S., Tougan, T., Tamai, K. K., Shimoda, C., and Nojima, H. **(1999)**. Replication factor C3 of Schizosaccharomyces pombe, a small

subunit of replication factor C complex, plays a role in both replication and damage checkpoints, **Mol Biol Cell** *10*, 3991-4003.

Shimomura, T., Ando, S., Matsumoto, K., and Sugimoto, K. **(1998)**. Functional and physical interaction between Rad24 and Rfc5 in the yeast checkpoint pathways, **Mol Cell Biol** *18*, 5485-91.

Shirahige, K., Hori, Y., Shiraishi, K., Yamashita, M., Takahashi, K., Obuse, C., Tsurimoto, T., and Yoshikawa, H. **(1998)**. Regulation of DNA-replication origins during cell-cycle progression, **Nature** *395*, 618-21.

Sidorova, J. M., and Breeden, L. L. **(1997)**. Rad53-dependent phosphorylation of Swi6 and down-regulation of CLN1 and CLN2 transcription occur in response to DNA damage in Saccharomyces cerevisiae, **Genes Dev** *11*, 3032-45.

Siede, W., Friedberg, A. S., Dianova, I., and Friedberg, E. C. **(1994)**. Characterization of G1 checkpoint control in the yeast Saccharomyces cerevisiae following exposure to DNA-damaging agents, **Genetics** *138*, 271-81.

Siede, W., Friedberg, A. S., and Friedberg, E. C. **(1993)**. RAD9-dependent G1 arrest defines a second checkpoint for damaged DNA in the cell cycle of Saccharomyces cerevisiae, **Proc Natl Acad Sci U S A** *90*, 7985-9.

Siede, W., Nusspaumer, G., Portillo, V., Rodriguez, R., and Friedberg, E. C. **(1996)**. Cloning and characterization of RAD17, a gene controlling cell cycle responses to DNA damage in Saccharomyces cerevisiae, **Nucleic Acids Res** *24*, 1669-75.

Siegel, L. M., and Monty, K. J. **(1966)**. Determination of molecular weights and frictional ratios of proteins in impure systems by use of gel filtration and density gradient centrifugation. Application to crude preparations of sulfite and hydroxylamine reductases, **Biochim Biophys Acta** *112*, 346-62.

Sikorski, R. S., and Hieter, P. **(1989)**. A system of shuttle vectors and yeast host strains designed for efficient manipulation of DNA in Saccharomyces cerevisiae, **Genetics** *122*, 19-27.

Smith, B. T., and Walker, G. C. **(1998)**. Mutagenesis and more: umuDC and the Escherichia coli SOS response, **Genetics** *148*, 1599-610.

Smith, G. C., Cary, R. B., Lakin, N. D., Hann, B. C., Teo, S. H., Chen, D. J., and Jackson, S. P. **(1999)**. Purification and DNA binding properties of the ataxia-telangiectasia gene product ATM, **Proc Natl Acad Sci U S A** *96*, 11134-9.

Smith, G. R. (1998). DNA Double-Strand Break Repair and Recombination in *Escherichia coli*. In DNA Damage and Repair: DNA Repair in Prokaryotes and Lower Eukaryotes, J. A. Nickoloff, and M. F. Hoekstra, eds. (Totowa, New Jersey, Humana Press), pp. 135-162.

Smith, M. L., Chen, I. T., Zhan, Q., Bae, I., Chen, C. Y., Gilmer, T. M., Kastan, M. B., O'Connor, P. M., and Fornace, A. J., Jr. **(1994)**. Interaction of the p53-regulated protein Gadd45 with proliferating cell nuclear antigen, **Science** *266*, 1376-80.

Smits, V. A., Klompmaker, R., Vallenius, T., Rijksen, G., Makela, T. P., and Medema, R. H. **(2000)**. p21 inhibits Thr161-phosphorylation of cdc2 to enforce the G2 DNA damage checkpoint, **J Biol Chem**.

Song, Z., and Steller, H. **(1999)**. Death by design: mechanism and control of apoptosis, **Trends Cell Biol** *9*, M49-52.

Soulier, J., and Lowndes, N. F. **(1999)**. The BRCT domain of the S. cerevisiae checkpoint protein Rad9 mediates a Rad9-Rad9 interaction after DNA damage, **Curr Biol** *9*, 551-4.

Sprules, T., Green, N., Featherstone, M., and Gehring, K. **(1998)**. Nickel-induced oligomerization of proteins containing 10-histidine tags, **Biotechniques** *25*, 20-2.

St. Onge, R. P., Udell, C. M., Casselman, R., and Davey, S. **(1999)**. The human G2 checkpoint control protein hRAD9 is a nuclear phosphoprotein that forms complexes with hRAD1 and hHUS1, **Mol Biol Cell** *10*, 1985-95.

Steensgaard, J., Humphries, S., and Spragg, S. P. (1992). Measurements of sedimentation coefficients. In Preparative Centrifugation: A Practical Approach, D. Rickwood, ed. (Oxford, Oxford University Press), pp. 187-232.

Stern, D. F., Zheng, P., Beidler, D. R., and Zerillo, C. **(1991)**. Spk1, a new kinase from Saccharomyces cerevisiae, phosphorylates proteins on serine, threonine, and tyrosine, **Mol Cell Biol** *11*, 987-1001.

Stewart, G. S., Maser, R. S., Stankovic, T., Bressan, D. A., Kaplan, M. I., Jaspers, N. G., Raams, A., Byrd, P. J., Petrini, J. H., and Taylor, A. M. **(1999)**. The DNA double-strand break repair gene hMRE11 is mutated in individuals with an ataxia-telangiectasia-like disorder, **Cell** *99*, 577-87.

Sugimoto, K., Ando, S., Shimomura, T., and Matsumoto, K. **(1997)**. Rfc5, a replication factor C component, is required for regulation of Rad53 protein kinase in the yeast checkpoint pathway, **Mol Cell Biol** *17*, 5905-14.

Sugimoto, K., Shimomura, T., Hashimoto, K., Araki, H., Sugino, A., and Matsumoto, K. **(1996)**. Rfc5, a small subunit of replication factor C complex, couples DNA replication and mitosis in budding yeast, **Proc Natl Acad Sci U S A** *93*, 7048-52.

Sun, Z., Fay, D. S., Marini, F., Foiani, M., and Stern, D. F. **(1996)**. Spk1/Rad53 is regulated by Mec1-dependent protein phosphorylation in DNA replication and damage checkpoint pathways, **Genes Dev** *10*, 395-406.

Sun, Z., Hsiao, J., Fay, D. S., and Stern, D. F. **(1998)**. Rad53 FHA domain associated with phosphorylated Rad9 in the DNA damage checkpoint, **Science** *281*, 272-4.

Sung, P., Bailly, V., Weber, C., Thompson, L. H., Prakash, L., and Prakash, S. **(1993)**. Human xeroderma pigmentosum group D gene encodes a DNA helicase, **Nature** *365*, 852-5.

Tanaka, H., Arakawa, H., Yamaguchi, T., Shiraishi, K., Fukuda, S., Matsui, K., Takei, Y., and Nakamura, Y. **(2000)**. A ribonucleotide reductase gene involved in a p53-dependent cell-cycle checkpoint for DNA damage, **Nature** *404*, 42-9.

Terleth, C., Schenk, P., Poot, R., Brouwer, J., and van de Putte, P. **(1990)**. Differential repair of UV damage in rad mutants of Saccharomyces cerevisiae: a possible function of G2 arrest upon UV, **Mol Cell Biol** *10*, 4678-84.

Thelen, M. P., Onel, K., and Holloman, W. K. **(1994)**. The REC1 gene of Ustilago maydis involved in the cellular response to DNA damage encodes an exonuclease, **J Biol Chem** *269*, 747-54.

Thelen, M. P., Venclovas, C., and Fidelis, K. **(1999)**. A sliding clamp model for the Rad1 family of cell cycle checkpoint proteins, **Cell** *96*, 769-70.

Thompson, L. H. (1998). Nucleotide Excision Repair: Its Relation to Human Disease. In DNA Damage and Repair: DNA Repair in Higher Eukaryotes, J. A. Nickoloff, and M. F. Hoekstra, eds. (Totowa, New Jersey, Humana Press), pp. 335-394.

Tobey, R. A. **(1975)**. Different drugs arrest cells at a number of distinct stages in G2, **Nature** *254*, 245-7.

Toczyski, D. P., Galgoczy, D. J., and Hartwell, L. H. **(1997)**. CDC5 and CKII control adaptation to the yeast DNA damage checkpoint, **Cell** *90*, 1097-106.

Tominaga, K., Morisaki, H., Kaneko, Y., Fujimoto, A., Tanaka, T., Ohtsubo, M., Hirai, M., Okayama, H., Ikeda, K., and Nakanishi, M. **(1999)**. Role of human Cds1 (Chk2) kinase in DNA damage checkpoint and its regulation by p53, **J Biol Chem** *274*, 31463-7.

Tsurimoto, T., and Stillman, B. **(1989)**. Purification of a cellular replication factor, RF-C, that is required for coordinated synthesis of leading and lagging strands during simian virus 40 DNA replication in vitro, **Mol Cell Biol** *9*, 609-19.

Tsurimoto, T., and Stillman, B. **(1991)**. Replication factors required for SV40 DNA replication in vitro. I. DNA structure-specific recognition of a primer-template junction by eukaryotic DNA polymerases and their accessory proteins, **J Biol Chem** *266*, 1950-60.

Udell, C. M., Lee, S. K., and Davey, S. **(1998)**. HRAD1 and MRAD1 encode mammalian homologues of the fission yeast rad1(+) cell cycle checkpoint control gene, **Nucleic Acids Res** *26*, 3971-6.

Varon, R., Vissinga, C., Platzer, M., Cerosaletti, K. M., Chrzanowska, K. H., Saar, K., Beckmann, G., Seemanova, E., Cooper, P. R., Nowak, N. J., *et al.* **(1998)**. Nibrin, a novel DNA double-strand break repair protein, is mutated in Nijmegen breakage syndrome, **Cell** *93*, 467-76.

Venclovas, C., and Thelen, M. P. **(2000)**. Structure-based predictions of Rad1, Rad9, Hus1 and Rad17 participation in sliding clamp and clamp-loading complexes, **Nucleic Acids Res** *28*, 2481-2493.

Verkade, H. M., Bugg, S. J., Lindsay, H. D., Carr, A. M., and O'Connell, M. J. **(1999)**. Rad18 is required for DNA repair and checkpoint responses in fission yeast, **Mol Biol Cell** *10*, 2905-18.

Vialard, J. E., Gilbert, C. S., Green, C. M., and Lowndes, N. F. **(1998)**. The budding yeast Rad9 checkpoint protein is subjected to Mec1/Tel1- dependent hyperphosphorylation and interacts with Rad53 after DNA damage, **Embo J** *17*, 5679-88.

Vogelstein, B., and Kinzler, K. W. **(1993)**. The multistep nature of cancer, **Trends Genet** *9*, 138-41.

Volkmer, E., and Karnitz, L. M. **(1999)**. Human homologs of Schizosaccharomyces pombe rad1, hus1, and rad9 form a DNA damage-responsive protein complex, **J Biol Chem** *274*, 567-70.

von Deimling, F., Scharf, J. M., Liehr, T., Rothe, M., Kelter, A. R., Albers, P., Dietrich, W. F., Kunkel, L. M., Wernert, N., and Wirth, B. **(1999)**. Human and mouse RAD17 genes: identification, localization, genomic structure and histological expression pattern in normal testis and seminoma, **Hum Genet** *105*, 17-27.

Waga, S., Hannon, G. J., Beach, D., and Stillman, B. **(1994)**. The p21 inhibitor of cyclin-dependent kinases controls DNA replication by interaction with PCNA, **Nature** *369*, 574-8.

Walworth, N., Davey, S., and Beach, D. **(1993)**. Fission yeast chk1 protein kinase links the rad checkpoint pathway to cdc2, **Nature** *363*, 368-71.

Wang, H., and Elledge, S. J. **(1999)**. DRC1, DNA replication and checkpoint protein 1, functions with DPB11 to control DNA replication and the S-phase checkpoint in Saccharomyces cerevisiae, **Proc Natl Acad Sci U S A** *96*, 3824-9.

Wang, Y., Cortez, D., Yazdi, P., Neff, N., Elledge, S. J., and Qin, J. **(2000)**. BASC, a super complex of BRCA1-associated proteins involved in the recognition and repair of aberrant DNA structures, **Genes Dev** *14*, 927-39.

Ward, J. F. (1998). The Nature of Lesions formed by Ionizing Radiation. In DNA Damage and Repair: DNA Repair in Higher Eukaryotes, J. A. Nickoloff, and M. F. Hoekstra, eds. (Totowa, New Jersey, Humana Press), pp. 65-84.

Webb, Y., Zhou, X., Ngo, L., Cornish, V., Stahl, J., Erdjument-Bromage, H., Tempst, P., Rifkind, R. A., Marks, P. A., Breslow, R., and Richon, V. M. **(1999)**. Photoaffinity

labeling and mass spectrometry identify ribosomal protein S3 as a potential target for hybrid polar cytodifferentiation agents, **J Biol Chem** *274*, 14280-7.

Weinert, T. **(1997)**. A DNA damage checkpoint meets the cell cycle engine [comment], **Science** *277*, 1450-1.

Weinert, T. A., and Hartwell, L. H. **(1988)**. The RAD9 gene controls the cell cycle response to DNA damage in Saccharomyces cerevisiae, **Science** *241*, 317-22.

Weinert, T. A., and Hartwell, L. H. **(1993)**. Cell cycle arrest of cdc mutants and specificity of the RAD9 checkpoint, **Genetics** *134*, 63-80.

Weinert, T. A., Kiser, G. L., and Hartwell, L. H. **(1994)**. Mitotic checkpoint genes in budding yeast and the dependence of mitosis on DNA replication and repair, **Genes Dev** *8*, 652-65.

Weinreich, M., and Stillman, B. **(1999)**. Cdc7p-Dbf4p kinase binds to chromatin during S phase and is regulated by both the APC and the RAD53 checkpoint pathway, **Embo J** *18*, 5334-46.

Welcsh, P. L., Owens, K. N., and King, M. C. **(2000)**. Insights into the functions of BRCA1 and BRCA2, **Trends Genet** *16*, 69-74.

Willson, J., Wilson, S., Warr, N., and Watts, F. Z. **(1997)**. Isolation and characterization of the Schizosaccharomyces pombe rhp9 gene: a gene required for the DNA damage checkpoint but not the replication checkpoint, **Nucleic Acids Res** *25*, 2138-46.

Wilson, D. M., Engelward, B. P., and Samson, L. (1998). Prokaryotic Base Excision Repair. In DNA Damage and Repair: DNA Repair in Prokaryotes and Lower Eukaryotes, J. A. Nickoloff, and M. F. Hoekstra, eds. (Totowa, New Jersey, Humana Press), pp. 29-64.

Wisniewski, D., Strife, A., Swendeman, S., Erdjument-Bromage, H., Geromanos, S., Kavanaugh, W. M., Tempst, P., and Clarkson, B. **(1999)**. A novel SH2-containing phosphatidylinositol 3,4,5-trisphosphate 5- phosphatase (SHIP2) is constitutively tyrosine phosphorylated and associated with src homologous and collagen gene (SHC) in chronic myelogenous leukemia progenitor cells, **Blood** *93*, 2707-20.

Wu, X., Bayle, J. H., Olson, D., and Levine, A. J. **(1993)**. The p53-mdm-2 autoregulatory feedback loop, **Genes Dev** *7*, 1126-32.

Wu, X., Ranganathan, V., Weisman, D. S., Heine, W. F., Ciccone, D. N., O'Neill, T. B., Crick, K. E., Pierce, K. A., Lane, W. S., Rathbun, G., *et al.* **(2000)**. ATM phosphorylation of Nijmegen breakage syndrome protein is required in a DNA damage response, **Nature** *405*, 477-82.

Xu, X., Weaver, Z., Linke, S. P., Li, C., Gotay, J., Wang, X. W., Harris, C. C., Ried, T., and Deng, C. X. **(1999)**. Centrosome amplification and a defective G2-M cell cycle checkpoint induce genetic instability in BRCA1 exon 11 isoform-deficient cells, **Mol Cell** *3*, 389-95.

Yamamoto, A., Guacci, V., and Koshland, D. **(1996)**. Pds1p, an inhibitor of anaphase in budding yeast, plays a critical role in the APC and checkpoint pathway(s), **J Cell Biol** *133*, 99-110.

Yasui, A., and Eker, A. P. M. (1998). DNA Photolyases. In DNA Damage and Repair: DNA Repair in Higher Eukaryotes, J. A. Nickoloff, and M. F. Hoekstra, eds. (Totowa, New Jersey, Humana Press), pp. 9-32.

Yoder, B. L., and Burgers, P. M. **(1991)**. Saccharomyces cerevisiae replication factor C. I. Purification and characterization of its ATPase activity, **J Biol Chem** *266*, 22689-97.

Zeng, Y., Forbes, K. C., Wu, Z., Moreno, S., Piwnica-Worms, H., and Enoch, T. **(1998)**. Replication checkpoint requires phosphorylation of the phosphatase Cdc25 by Cds1 or Chk1, **Nature** *395*, 507-10.

Zeng, Y., and Piwnica-Worms, H. **(1999)**. DNA damage and replication checkpoints in fission yeast require nuclear exclusion of the Cdc25 phosphatase via 14-3-3 binding, **Mol Cell Biol** *19*, 7410-9.

Zhao, S., Weng, Y. C., Yuan, S. S., Lin, Y. T., Hsu, H. C., Lin, S. C., Gerbino, E., Song, M. H., Zdzienicka, M. Z., Gatti, R. A., *et al.* **(2000)**. Functional link between ataxia-telangiectasia and Nijmegen breakage syndrome gene, **Nature** *405*, 473-7.

Zhao, X., Muller, E. G., and Rothstein, R. **(1998)**. A suppressor of two essential checkpoint genes identifies a novel protein that negatively affects dNTP pools, **Mol Cell** *2*, 329-40.

Zheng, P., Fay, D. S., Burton, J., Xiao, H., Pinkham, J. L., and Stern, D. F. **(1993)**. SPK1 is an essential S-phase-specific gene of Saccharomyces cerevisiae that encodes a nuclear serine/threonine/tyrosine kinase, **Molecular & Cellular Biology** *13*, 5829-5842.

Zhong, Q., Chen, C. F., Li, S., Chen, Y., Wang, C. C., Xiao, J., Chen, P. L., Sharp, Z. D., and Lee, W. H. **(1999)**. Association of BRCA1 with the hRad50-hMre11-p95 complex and the DNA damage response, **Science** *285*, 747-50.

Zhou, B. B., Chaturvedi, P., Spring, K., Scott, S. P., Johanson, R. A., Mishra, R., Mattern, M. R., Winkler, J. D., and Khanna, K. K. **(2000)**. Caffeine abolishes the mammalian G(2)/M DNA damage checkpoint by inhibiting ataxia-telangiectasia-mutated kinase activity, **J Biol Chem** *275*, 10342-8.

Zhou, Z., and Elledge, S. J. **(1993)**. DUN1 encodes a protein kinase that controls the DNA damage response in yeast, **Cell** *75*, 1119-27.

APPENDIX I

OLIGONUCLEOTIDES

NUMBER	NAME	SEQUENCE
358	RAD17T1	CGTCAGGATCCGCGAATAAACAGTGAGCTAGCG
360	RAD53T1	CGTCAGCAAGCTTGAAAATATTACACAACCC
361	RAD53B1	GCTGACGAAGCTTCGAAAATTGCAAATTCTCGGGG CC
362	MEC3T1	CGTCAGGATCCGAAATTAAAATTGATAGTAAATGG
363	MEC3B1	CCAGTGGATCCGCCAAGCCCTTCGATCTTGC
441	RAD17B1	CCAGTCCATCCGTAAAAAATATAGGAATATCCTTTG TTGG
442	RAD24T	GCATAGGATCCCAGCAACGGAACGTCCTTTCG
443	RAD24B	CGTACGGATCCTCCAGATCTGAATCTGAAAGGG
487	RAD53NKT	CGTCAGCAAGCTTAGGTCGACAGCTGCAAAAGCC
488	RAD53NB	GCTGACGAAGCTTCCTATTATTTGGATCCACC
509	RAD17T2	CGTCAGGATCCGTATGCAAAGACCGAGGCG
510	RAD17B2	GCAGTGGATCCGTTGCATATACATAGCACTCTTTGC ATCC
564	10HIST	TCTAGAATGCATCACCATCATCACCATCATCACCAC CATG
566	9PROMT	GCATGGAGCTCGTGCAAGTAGAACACTTGGGAATC C
567	9PROMB	GTACGTCTAGACCTGATGTTGAAGATTTTCTCACTA TGC
592	M3PROMT	GCATGCCGCGGTGTCTGAGCACAAATAACC
593	M3PROMB	GTACGTCTAGATTAACTGAATTAAGACACACC
594	M3ORFT	GCATGGGATCCAAATTAAAATTGATAGTAAATGG
595	M3ORFB	GTACGATCGATTAATCGGAAGAGATCCTTCC
596	17PROMT	GCATGCCGCGGGCATTATAGTTGTAACATATGC
597	17PROMB	GTACGTCTAGAAGTTGAAATCCTTCAACTACTTTGT TTCC
598	17ORFT	GCATGGGATCCCGAATCAACAGTGAGCTAGCG
599	17ORFB	GTACGATCGATCAAGTTCATTAGTCTCCATCAGG

NUMBER	NAME	SEQUENCE
600	24PROMT	GCATGCCGCGGCATTATCATTGATTTCTCCCCC
601	24PROMB	GTACGTCTAGAATCATTCAGACAGG
602	24ORFT	GCATGCCCGGGGATAGTACGAATTTGAACAAACGG
603	24ORFB	GTACGATCGATCTCGGGTTGAAATCGGC
605	10HISB	GATCCATGGTGGTGATGATGGTGATGATGGTGATG CATT
651	TEVHAT	CATGGGGAAAACTTGTACTTCCAAGGTTACCCATAC GACGTCCCAGACTA
652	TEVHAB	CATGGCCAGCGTAGTCTGGGACGTCGTATGGGTAA CCTTGGAAGTACAAG
720	LTEVT	CCCACATGTGGATTACGATATCCCAACTACCGAAA ACTTGTACTTCCAAGGTGGCGGCCGCCATGGAGTCG AC
721	LTEVB	GTCGACTCCATGGCGGCCGCCACCTTGGAAGTACA AGTTTTCGGTAGTTGGGATATCGTAATCCACATGTG GG
733	HAT	GACGACGGCCGCTACCCATACGATGTTCCAGATTAC GCCCATGGAGTCGAC
734	HAB	GTCGACTCCATGGGCGTAATCTGGAACATCGTATGG GTAGCGGCCGTCGTC
792	RFC2DEGT	ATCGTGAAGCTTCCGGAGGCATGTTTGAAGGGTTTG GTCC
793	RFC2DEGB	ATCGTGATCGATTTAAATGATCTTATACGGTGGGCA CGG
805	PROBE	CACACACACACACACACACACACACACAGATCCCC GGGTACCGAGCTCGAATTCGTAATCATATGATTACG AATTCGAGCTCGGTACCCGGGGATC
810	RFC3DEGT	GGAGGGCAAGCTTCCGGAGGCATGTCGACAAGTAC AGAGAAGAGGAGCAAAGAAAACC
811	RFC3DEGB	CGGCATCGATATCCGACGCTCAATGGCCTCTTGGGG C

NUMBER	NAME	SEQUENCE
812	FLAG3T	TAGTGGATCCATGGATTATAAAGATGATGACGATA AAGATTATAAAGATGATGACGATAAAGATTATAAA GATGATGACGATAAATCGCGATAACCCGGGCTGC
813	FLAG3B	GCAGCCCGGGTTATCGCGATTTATCGTCATCATCTT TATAATCTTTATCGTCATCATCTTTATAATCTTTATC GTCATCATCTTTATAATCCATGGATCCACTA
829	RFC15'T	CCCGGAGCTCGGTCCTGATGTGACCACAGCC
830	RFC15'B	CCGGGGATCCTGCTTTCGTTTTCCTTTTTTTGC
831	RFC25'T	CCCGGAGCTCGGGGGCGCAATACTTGG
832	RFC25'B	CCGGGGATCCGAGTTGGGATATTTTAACC
833	RFC35'T	CCCGGAGCTCTGCTGTGGGGCACCCAGACC
834	RFC35'B	CCGGGGATCCTACGTTGGATTTAACAGTTTCG
835	RFC45'T	CCCGGAGCTCGTACAGTAGCAGGACACG
836	RFC45'B	CCGGGGATCCGGCTTTATTATTTAGTTTATGAATTTT CG
837	RFC55'T	CCCGGAGCTCGCATTGAAAAGCAGTAGC
838	RFC55'B	CCGGGGATCCATCTAGACAGCACATAACTTTTGC
891	RAD24NT	CCATCGATTGATAGTACGAATTTGAACAAACGG
892	RAD24NB	TCCCCCCGGTTAAAAGTAGTATATGGTGGATTCTCG GG
897	RFC1NT	CCATCGATGGTCAATATTTCTGATTTCTTTGG
898	RFC1CT	CCATCGATAGCCACTAGAGTTTCTGGTGGCC
901	RFC1NB	TCCCCCCGGGTTAATCAAAGTCATCAAAATATAATG CG
902	RFC1CB	TCCCCCCGGGTCATGCTTTCGTTTTCCTTTTTTTGC

APPENDIX II

This CD-ROM contains the following:

DNA Strider 3.1 Application program for Macintosh

DNA Strider files for the genes *RAD9*, *RAD24*, *RAD17*, *MEC3*, *DDC1*, *MEC1*, *RAD53*, *RFC1*, *RFC2*, *RFC3*, *RFC4*, *RFC5*, including each ORF and 1kb sequence upstream.

DNA Strider files for the plasmids used in this work.

Text files of all the above for import into PC compatible sequence analysis software.

A Microsoft excel spreadsheet for the calculation of the partial specific volume of a protein of known sequence (Mac and PC versions).

The Endnote library used in preparation of this thesis (including abstracts of all references).

PDF files of the references used here (where available).